Ae/APh/CE/ME 101 Notes

Bradford Sturtevant

Hans W. Liepmann Professor of Aeronautics

Graduate Aeronautical Laboratories

California Institute of Technology

April 23, 2001

Ae101 Notes

Contents

Ae/APh/CE/ME 101 Notes

1 The Conservation Equations in Integral Form

Inertial frame of reference.

1.1 Material Volume V^* (Surface S^*)
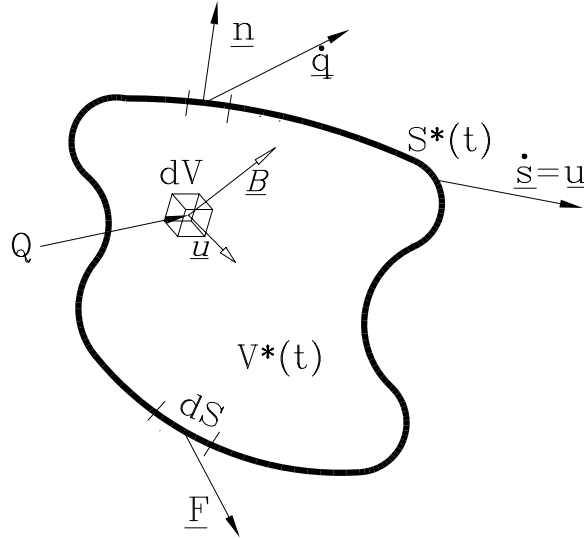
Figure 1. Notation for a material volume

$$
\begin{aligned}
\text{Mass :} \qquad & \frac{d}{dt} \int_{V^*} \rho \, dV = 0 \\[2mm]
\text{Momentum :} \qquad & \frac{d}{dt} \int_{V^*} \rho \, \underline{u} \, dV = \int_{V^*} \rho \underline{B} \, dV + \int_{S^*} \underline{F} \, dS \\[2mm]
\text{Energy :} \qquad & \frac{d}{dt} \int_{V^*} \rho \left(e + \frac{u^2}{2} \right) dV = \int_{V^*} \rho \underline{B} \cdot \underline{u} \, dV + \int_{S^*} \underline{F} \cdot \underline{u} \, dS - \int_{S^*} \underline{\dot{q}} \cdot \underline{n} \, dS + \int_{V^*} \rho Q \, dV \\[2mm]
\text{Entropy :} \qquad & \frac{d}{dt} \int_{V^*} \rho s \, dV + \int_{S^*} \frac{\underline{q}}{T} \cdot \underline{n} \, dS - \int_{V^*} \rho \frac{Q}{T} \, dV \geq 0
\end{aligned}
\tag{1.1}
$$

These equations are forms of the conservation of mass, Newton's laws of motion, the first law of thermodynamics and the second law of thermodynamics, respectively.

1.1.1 Variables and dimensions

The units of every term in each of these equations are as follows,

$$
\begin{aligned}
\textbf{Mass}: &\quad \frac{\text{M}}{\text{T}} \\[4pt]
\textbf{Momentum}: &\quad \frac{\text{ML}}{\text{T}^2} = \text{F} \\[4pt]
\textbf{Energy}: &\quad \frac{\text{ML}^2}{\text{T}^3} \\[4pt]
\textbf{Entropy}: &\quad \frac{\text{ML}^2}{\text{T}^3\theta}
\end{aligned}
\tag{1.2}
$$

Thus the units of $\underline{B}$ are acceleration, and of $\underline{F}$ are pressure. The units of $\underline{q}$ are energy per unit area per unit time. In particular,

ρ	density	$\dfrac{\text{M}}{\text{L}^3}$	$\underline{u}$	velocity	$\dfrac{\text{L}}{\text{T}}$
$\underline{B}$	specific body force	$\dfrac{\text{L}}{\text{T}^2}$	$\underline{F}$	traction force	$\dfrac{\text{M}}{\text{LT}^2}$
e	specific internal energy	$\dfrac{\text{L}^2}{\text{T}^2}$	$\underline{q}$	heat flux vector	$\dfrac{\text{M}}{\text{T}^3}\left(\dfrac{\text{watts}}{\text{m}^2}\right)$
s	specific entropy	$\dfrac{\text{L}^2}{\theta\text{T}^2}$	Q	specific volumetric energy addition	$\dfrac{\text{L}^2}{\text{T}^3}$

1.2 Reynolds Transport Theorem

For a control volume V moving relative to material (Surface S, $\underline{\dot{s}} \neq \underline{u}$), the Reynolds Transport Theorem is

$$
\frac{d}{dt}\int_V f \, dV = \int_V \frac{\partial f}{\partial t} \, dV + \int_S f\,\underline{\dot{s}} \cdot \underline{n} \, dS \ ,
\tag{1.3}
$$

where $\underline{\dot{s}} =$ velocity of surface S. In general, the conservation laws are of the form

$$
\frac{d}{dt}\int_{V^*} f \, dV = \int_{V^*} g \, dV + \int_{S^*} h \, dS \ ,
\tag{1.4}
$$

which, using Eq. 1.3, is

$$
\int_{V^*} \frac{\partial f}{\partial t} \, dV + \int_{S^*} f\underline{u} \cdot \underline{n} \, dS = \int_{V^*} g \, dV + \int_{S^*} h \, dS \ ,
\tag{1.5}
$$

Taking V^* and V to instantaneously coincide and adding Eqs. 1.3 and 1.5,

$$
\boxed{\ \frac{d}{dt}\int_V f \, dV + \int_S f(\underline{u} - \underline{\dot{s}}) \cdot \underline{n} \, dS = \int_V g \, dV + \int_S h \, dS\ }
\tag{1.6}
$$

1.3 Moving (Non-Material) Control Volume V (Surface S, $\underline{\dot{s}} \neq \underline{u}$)

$$
\begin{aligned}
\textbf{Mass}: \quad & \frac{d}{dt}\int_V \rho\, dV + \int_S \rho(\underline{u}-\underline{\dot{s}})\cdot \underline{n}\, dS \;=\; 0 \\[1mm]
\textbf{Momentum}: \quad & \frac{d}{dt}\int_V \rho\,\underline{u}\, dV + \int_S \rho\underline{u}\,(\underline{u}-\underline{\dot{s}})\cdot \underline{n}\, dS \;=\; \int_V \rho\underline{B}\, dV + \int_S \underline{F}\, dS \\[1mm]
\textbf{Energy}: \quad & \frac{d}{dt}\int_V \rho\left(e+\frac{u^2}{2}\right) dV + \int_S \rho\left(e+\frac{u^2}{2}\right)(\underline{u}-\underline{\dot{s}})\cdot \underline{n}\, dS \;= \\
& \int_V \rho\underline{B}\cdot\underline{u}\, dV + \int_S \underline{F}\cdot\underline{u}\, dS - \int_S \underline{q}\cdot\underline{n}\, dS
\end{aligned}
\tag{1.7}
$$

1.4 Fixed Control Volume V (Surface S, $\underline{\dot{s}}=0$)

$$
\begin{aligned}
\textbf{Mass}: \quad & \frac{d}{dt}\int_V \rho\, dV + \int_S \rho\underline{u}\cdot \underline{n}\, dS \;=\; 0 \\[1mm]
\textbf{Momentum}: \quad & \frac{d}{dt}\int_V \rho\,\underline{u}\, dV + \int_S \rho\underline{u}\,\underline{u}\cdot \underline{n}\, dS \;=\; \int_V \rho\underline{B}\, dV + \int_S \underline{F}\, dS \\[1mm]
\textbf{Energy}: \quad & \frac{d}{dt}\int_V \rho\left(e+\frac{u^2}{2}\right) dV + \int_S \rho\left(e+\frac{u^2}{2}\right)\underline{u}\cdot \underline{n}\, dS \;= \\
& \int_V \rho\underline{B}\cdot\underline{u}\, dV + \int_S \underline{F}\cdot\underline{u}\, dS - \int_S \underline{q}\cdot\underline{n}\, dS \\[1mm]
\textbf{Entropy}: \quad & \frac{d}{dt}\int_V \rho s\, dV + \int_S \rho s\,\underline{u}\cdot \underline{n}\, dS + \int_S \frac{\underline{q}}{T}\cdot\underline{n}\, dS - \int_V \rho\frac{Q}{T}\, dV \;\geq\; 0
\end{aligned}
\tag{1.8}
$$

1.5 Scaling: Non-dimensional numbers

It is useful to be able to compare the magnitude of terms in an equation. This is done by *scaling*. Because of the equality expressed by an equation, at least two terms must be of the same order of magnitude (unless there is only one term, in which case it is trivially equal to zero). The order of magnitude of the size of terms in Eqs. 1.8 are expressed by characteristic quantities (L, T, ρ, U, *etc*). The body force term is scaled by the acceleration of gravity g. The traction force has a pressure contribution which scales with pressure changes Δp through the flow, and a viscous contribution scaled by $\mu\frac{U}{L}$, where μ is a viscosity and the scaling is patterned after the Newtonian viscous shear model. In the energy equation the characteristic internal energy is denoted by e, which in turn is scaled by a specific heat c_p and temperature θ and also an acoustic speed squared c^2,

$$
e \;\sim\; c_p\theta \;\sim\; c^2 \;.
\tag{1.9}
$$

The heat flux is modeled by the Fourier heat conduction law, $k\frac{\theta}{L}$, where k is the thermal conductivity.

The equations of motion then suggest the following balances:

$$
\begin{aligned}
\textbf{Mass}: \quad & \underbrace{\frac{\rho L^3}{T}}_{\boxed{1}} \quad \underbrace{\rho U L^2}_{\boxed{2}} \;=\; 0 \\[3mm]
& \frac{\boxed{2}}{\boxed{1}} \;=\; \frac{UT}{L}
\end{aligned}
\tag{1.10}
$$

April 23, 2001

$$\textbf{Momentum}: \quad \underbrace{\frac{\rho U L^3}{T}}_{\boxed{3}} \quad \underbrace{\rho U^2 L^2}_{\boxed{4}} \quad = \quad \underbrace{\rho g L^3}_{\boxed{5}} \quad \underbrace{\Delta p L^2}_{\boxed{6}} \quad \underbrace{\mu U L}_{\boxed{7}}$$

$$\frac{\boxed{4}}{\boxed{5}} \;=\; \frac{U^2}{gL} \;=\; Fr$$

$$\frac{\boxed{4}}{\boxed{7}} \;=\; \frac{UL}{\nu} \;=\; Re$$

$$Re \cdot \frac{\boxed{5}}{\boxed{7}} \;=\; \frac{Re^2}{Fr} \;=\; \frac{gL^3}{\nu^2} \;=\; Gr$$

$$(1.11)$$

$$\textbf{Energy}: \quad \underbrace{\frac{\rho e L^3}{T}}_{\boxed{8}} \quad \underbrace{\frac{\rho U^2 L^3}{T}}_{\boxed{9}} \quad \underbrace{\rho e U L^2}_{\boxed{10}} \quad \underbrace{\rho U^3 L^2}_{\boxed{11}} \quad = \quad \underbrace{\rho g U L^3}_{\boxed{12}} \quad \underbrace{\Delta p U L^2}_{\boxed{13}} \quad \underbrace{\mu U^2 L}_{\boxed{14}} \quad \underbrace{k\theta L}_{\boxed{15}}$$

$$\frac{\boxed{8}}{\boxed{9}} \;=\; \frac{e}{U^2} \overset{\text{gases}}{\sim} \frac{1}{M^2}$$

$$\frac{\boxed{14}}{\boxed{15}} \;=\; \frac{\mu U^2}{k\theta} \;\sim\; Pr \frac{U^2}{e}$$

$$\frac{\boxed{10}}{\boxed{15}} \;=\; \frac{\rho e U L}{k\theta} \;\sim\; \frac{UL}{\kappa} \;=\; Pe \;=\; Re\,Pr \;,$$

$$(1.12)$$

where we have taken

$$e \;\sim\; c_p \theta \;; \qquad \nu = \frac{\mu}{\rho} \;; \qquad \kappa = \frac{k}{c_p \rho} \;; \qquad Pr = \frac{\nu}{\kappa} \tag{1.13}$$

The pressure may balance with one other term. For example,

$$\frac{\boxed{6}}{\boxed{4}} \;=\; \frac{\Delta p}{\rho U^2} \overset{\text{gases}}{\sim} \frac{\Delta \rho}{\rho} \frac{1}{M^2}$$

$$\frac{\boxed{6}}{\boxed{5}} \;=\; \frac{\Delta p}{\rho g L}$$

$$\frac{\boxed{6}}{\boxed{7}} \;=\; \frac{\Delta p\, L}{\mu U}$$

$$(1.14)$$

ρU^2 is the *dynamic* pressure, $\rho g L$ is the *hydrostatic* pressure and $\mu U/L$ is the *viscous pressure drop*. From the last, it follows that *viscous drag* must be of order $\mu U L$.

We have not accounted for the fact that the fluid may be a mixture of substances, the conservation of each one of which may have to be accounted for. In this case each component satisfies an equation like the first of Eqs. 1.1, say, for its concentration C (same units as ρ), except that there will be source terms on the right hand side. Chemical reactions cause volumetric changes and diffusion causes flux across the boundaries,

$$\frac{d}{dt} \int_{V^*} C \, dV \;=\; \int_{V^*} C k_c \, dV + \int_{S^*} C \underline{u_d} \, dS \;, \tag{1.15}$$

April 23, 2001

where k_c is the chemical reaction rate with units $1/\mathrm{T}$, and u_d is the diffusive flux velocity. The latter is modeled to order of magnitude by (see Fick's Law)

$$C\underline{u_d} \;=\; D\frac{C}{L} \;, \tag{1.16}$$

where D is the diffusion coefficient, $[D] = \mathrm{L}^2/\mathrm{T}$. This leads to two more nondimensional numbers,

$$Le \;=\; \frac{D}{\kappa} \tag{1.17}$$

$$Sc \;=\; \frac{\nu}{D} \;. \tag{1.18}$$

1.6 Control Volume Analysis – Mass and Momentum

In this section we illustrate how the above ideas can be used to solve even rather difficult problems. Usually, the control volume boundary in internal (channel) flows is placed at locations where the flow conditions can be assumed uniform, so the surface integrals reduce to algebraic expressions.

The rocket equation. A rocket accelerates vertically upward in a vertical gravitational field. We write the equations of motion in the inertial frame fixed with the earth (Fig. 2). In that coordinate system the fluid
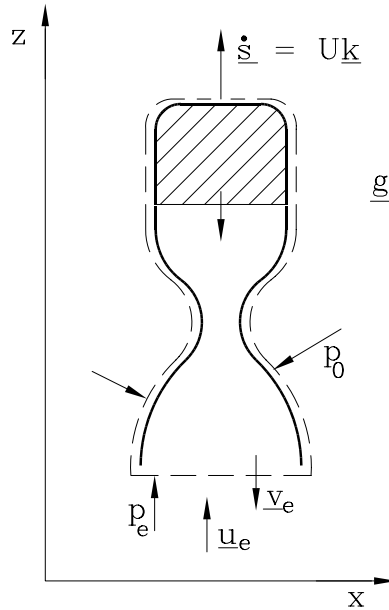
Figure 2. Schematic of a rocket moving parallel to the gravity vector

velocity is $\underline{u}$ and the velocity of the control volume is $\underline{\dot{s}}$, while the velocity relative to the rocket is $\underline{v}$. That is,

$$\underline{v} \;=\; \underline{u} - \underline{\dot{s}} \;. \tag{1.19}$$

The integral equation for the conservation of mass is

$$\frac{d}{dt}\int_V \rho \, dV \;=\; -\int_{S_e} \rho(\underline{u} - \underline{\dot{s}}) \cdot \underline{n} \, dS \;. \tag{1.20}$$

Defining the total mass of the rocket M, and evaluating the integrals gives

$$\boxed{\frac{dM}{dt} \;=\; -\rho_e v_e S_e}\;, \tag{1.21}$$

where S_e is the nozzle exit area.

The momentum equation is

$$\frac{d}{dt}\int_V \rho \underline{u}\, dV + \int_{S_e} \rho \underline{u}(\underline{u} - \underline{\dot{s}})\cdot\underline{n}\, dS \;=\; \int_V \rho \underline{g}\, dV + \int_S \underline{F}\, dS \tag{1.22}$$

By symmetry the net contribution from the pressure acting on the solid body to the last term is a vertical force downward of magnitude $p_0 S_e$. Writing the equation for the vertical momentum, and splitting the first term into the momenta of the masses moving (combustion products) and fixed (*e.g.*, the unburned propellant) with respect to the rocket casing, respectively,

$$\frac{d}{dt}\int_{V_{fix}} (\rho\dot{s})_{fix}\, dV + \frac{d}{dt}\int_{V_{move}} (\rho v)_{move}\, dV + \rho_e(v_e + \dot{s})v_e S_e \;=\; -Mg + (p_e - p_0)S_e - D\,, \tag{1.23}$$

where D is the contribution of the vicous traction forces. Throughout most of the trajectory the momentum of the gases in the rocket chamber and nozzle (the second term) is small compared to the momentum of the solid components of the rocket. With the definition of M,

$$\frac{dM\dot{s}}{dt} - \dot{M}(v_e + \dot{s}) \;=\; -Mg + (p_e - p_0)S_e - D\,. \tag{1.24}$$

Partially differentiating the fist term and cancelling results in the so-called *rocket equation*

$$\boxed{M\frac{dU}{dt} \;=\; \dot{M}v_e - Mg - (p_0 - p_e)S_e - D\,.} \tag{1.25}$$

The thrust is defined by

$$T \;\equiv\; \dot{M}v_e\,. \tag{1.26}$$

Optimal performance results when the exit pressure is matched to the ambient, $p_e = p_0$, typically at high altutude. At sea level $(p_0 > p_e)$, there is a performance penalty. At very high altitude, where the atmosphere is rarefied,

$$M\frac{dU}{dt} \;=\; T - Mg + p_e S_e\,. \tag{1.27}$$

Losses at area changes in pipes – pressure recovery. Control surface analysis can be used to analyze the effects of losses on pressure recovery across a sudden enlargement of a pipe in the flow of an incompressible fluid, as shown in Fig. 3. It is assumed that the incoming stream is uniform and the control volume is long
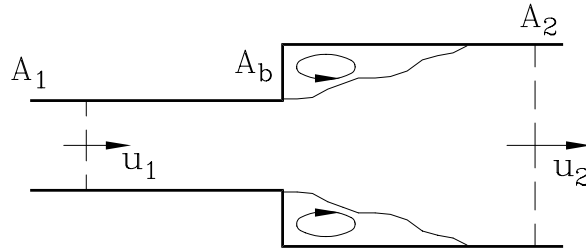
Figure 3. Control surface for area expansion in a pipe

enough that the flow across station 1 is also uniform. For simplicity, viscous forces are neglected. The flow is steady. That means that, though there may be large fluctuations internally, the flows in and out are

steady, so the integral quantities do not vary in time, $d/dt = 0$. It will emerge that one further piece of information is required to close the problem. We use the fact that the fluid by the vertical section at the area change can communicate very well with the region on the left (1), so the pressure p_b on the vertical section at the area change is constant and equal to p_1.

The control volume is fixed, so the mass equation gives that

$$u_2 A_2 \;=\; u_1 A_1 \;. \tag{1.28}$$

The flow slows down. The integral momentum equation in the horizontal direction states that the change of momentum flux between 1 and 2, $\rho u_2^2 A_2 - \rho u_1^2 A_1$, is balanced by the pressure forces acting in the downstream direction. Using the continuity equation and $p_b = p_1$,

$$\rho u_2 A_2 (u_2 - u_1) \;=\; p_1 A_1 + p_1 (A_2 - A_1) - p_2 A_2 \;. \tag{1.29}$$

Thus the pressure increase is

$$
\begin{aligned}
p_2 - p_1 &= \rho u_2 (u_1 - u_2) \,, \\
C_p &= 2\frac{A_1}{A_2}\left(1 - \frac{A_1}{A_2}\right)
\end{aligned}
\tag{1.30}
$$

where $C_p \equiv (p_2 - p_1)/\frac{1}{2}\rho u_1^2$.

If the area change were very gradual, so there were no losses, the flow would satisfy the Bernoulli equation, $p + \frac{1}{2}\rho u^2 = \text{const}$, with the result

$$C_p \;=\; 1 - \left(\frac{A_1}{A_2}\right)^2 \tag{1.31}$$

These two results are compared in Fig. 4. The estimate based on $p_b = p_1$ gives considerably lower pressure recovery, but they both agree for very small changes of area, where in any case the process is nearly ideal.

1.7   The Stress Tensor

The force $\underline{F}$ depends on the orientation of the surface S. This means that in order to express the force, we need 3 components for each component of the outward normal, *i.e.*, a tensor of rank 2, called the stress tensor σ (see figure, drawn for 2 dimensions). In terms of the stress tensor the traction force is expressed

$$\underline{F} \;=\; \sigma\,\underline{n}\,; \qquad F_i \;=\; \sigma_{ij}\,n_j \ \text{(Cartesian tensor notation)} \tag{1.32}$$

Splitting the Stress Tensor:
The concept of the stress tensor is very general, and applies to all substances. The stress and strain δ experienced by a general substance can be thought of as divided into two parts

$$
\begin{aligned}
\sigma \;=\;\ &\sigma_{\text{elastic}} &+&\quad &\sigma_{\text{plastic}}\\
&\text{cold part+} & & &\text{fluid-like+}\\
&\text{thermal part} & & &\text{memory, hysteresis}\\[6pt]
\delta \;=\;\ &\delta_{\text{elastic}} &+& &\delta_{\text{plastic}} \;.
\end{aligned}
\tag{1.33}
$$
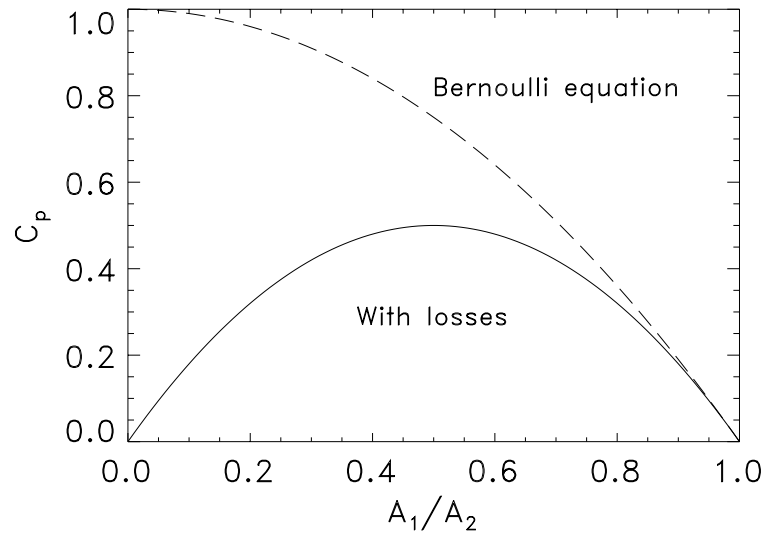
Figure 4. Comparison of Bernoulli flow with model flow with losses
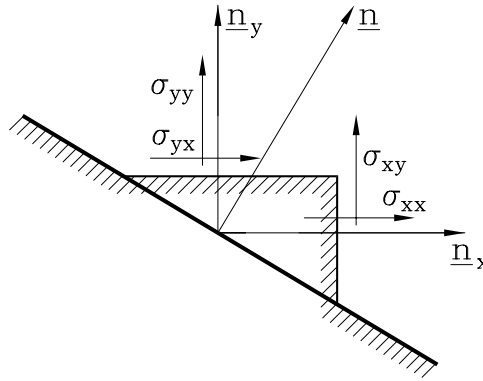
Figure 5. Components of the stress in 2D

We consider only the simplest fluids and solids at stresses greater than about 1 Mbar = 100 GPa, in which case the stress can be split into the isotropic normal contribution which is finite when there is no motion (the *pressure p*), and a viscous contribution (the *viscous stress tensor* τ).

$$\sigma = -pI + \tau \; ; \qquad \sigma_{ij} = -p \, \delta_{ij} + \tau_{ij} \; , \qquad (1.34)$$

where δ_{ij} is the Kronecker delta; $\delta_{ij} = \begin{cases} 1 \text{ if } i = j \\ 0 \text{ if } i \neq j \end{cases}$. Here, the pressure is taken to be the thermodynamic pressure, *i.e.*, it is a thermal quantity. The traction force is thus expressed in terms of the stress tensor as

$$\underline{F} = -p\underline{n} + \tau\underline{n} \; ; \qquad F_i = -pn_i + \tau_{ij}n_j \; . \qquad (1.35)$$

April 23, 2001

1.8   The Flux of Momentum Tensor $\rho \underline{u}\, \underline{u}$

Where a vector multiplies a scalar dot product in the equations, it can be replaced by a tensor multiplying a vector, as justified by the Catresian tensor form. For example,

$$\rho \underline{u}\, (\underline{u} \cdot \underline{n}) \;=\; (\rho \underline{u}\, \underline{u})\underline{n} \,; \qquad \rho u_i \,(u_j n_j) \;=\; (\rho u_i u_j)\, n_j \tag{1.36}$$

1.9   Summary of Equations

Thus, summarizing for a stationary control volume ($\underline{\dot{s}} = 0$),

$$
\begin{aligned}
\textbf{Mass}: \quad & \frac{d}{dt} \int_V \rho \, dV + \int_S \rho \underline{u} \cdot \underline{n} \, dS \;=\; 0 \\[2mm]
\textbf{Momentum}: \quad & \frac{d}{dt} \int_V \rho \underline{u} \, dV + \int_S (\rho \underline{uu}) \underline{n} \, dS \;=\; -\int_S p\, \underline{n} \, dS + \int_V \rho \underline{B} \, dV + \int_S \tau \underline{n} \, dS \\[2mm]
\textbf{Energy}: \quad & \frac{d}{dt} \int_V \rho \left(e + \frac{u^2}{2} \right) dV + \int_S \rho \left(e + \frac{u^2}{2} \right) \underline{u} \cdot \underline{n} \, dS \;= \\[2mm]
& \quad -\int_S p \underline{u} \cdot \underline{n} \, dS + \int_V \rho \underline{B} \cdot \underline{u} \, dV + \int_S \tau \underline{u} \cdot \underline{n} \, dS - \int_S \underline{q} \cdot \underline{n} \, dS + \int_V \rho Q \, dV \\[2mm]
\textbf{Entropy}: \quad & \frac{d}{dt} \int_V \rho s \, dV + \int_S \rho s \, \underline{u} \cdot \underline{n} \, dS + \int_S \frac{\underline{q}}{T} \cdot \underline{n} \, dS - \int_V \rho \frac{Q}{T} \, dV \;\geq\; 0
\end{aligned}
\tag{1.37}
$$

April 23, 2001

2   The Equations of Motion in Differential Form

The surface integrals in the conservation equations (Eqs. 1.8) can be transformed to volume integrals by using the Divergence (Gauss') Theorem. Then the limit $\lim\limits_{V\to 0}$ can be taken, with some corresponding constraints, to transform the equations into differential form.

2.1   The Divergence Theorem

The definition of the divergence is, for any "density" variable,

$$\nabla \cdot f \;=\; \lim_{V\to 0} \frac{1}{V} \int_S f\underline{n}\, dS \tag{2.1}$$

This forms the basis for the Divergence Theorem,

$$\int_S f\underline{n}\, dS \;=\; \int_V \nabla \cdot f \, dV \tag{2.2}$$

f can be a scalar, vector or tensor, because any operation on a vector $\underline{f}$ can be written in terms of the equivalent skew-symmetric tensor

$$f \;=\; \begin{pmatrix} 0 & -f_3 & f_2 \\ f_3 & 0 & -f_1 \\ -f_2 & f_1 & 0 \end{pmatrix}. \tag{2.3}$$

Writing the various surface integrals that appear in the equations of motion in terms of the divergence theorem illustrates how it applies to scalars, vectors and tensors:

$$
\begin{aligned}
&I. & \int_S \rho\underline{u}\cdot\underline{n}\,dS \;\;&=\;\; \int_V \nabla\cdot(\rho\underline{u})\,dV & & & &\\[2mm]
&II. & \int_S \rho\underline{u}(\underline{u}\cdot\underline{n})\,dS \;\;&=\;\; \int_S(\rho\underline{u}\,\underline{u})\underline{n}\,dS \;\;&=\;\; \int_V \nabla\cdot(\rho\underline{u}\,\underline{u})\,dV & & &\\[2mm]
&III. & \int_S \underline{F}\,dS \;\;&=\;\; \int_S \sigma\underline{n}\,dS \;\;&=\;\; \int_V \nabla\cdot\sigma\,dV & & &\\[2mm]
&IV. & \int_S \underline{F}\cdot\underline{u}\,dS \;\;&=\;\; \int_S(\sigma\underline{n})\cdot\underline{u}\,dS \;\;&=\;\; \int_S(\sigma\underline{u})\cdot\underline{n}\,dS \;\;&=\;\; \int_V \nabla\cdot(\sigma\underline{u})\,dV &\\[2mm]
&V. & \int_S \underline{q}\cdot\underline{n}\,dS \;\;&=\;\; \int_V \nabla\cdot\underline{q}\,dV\,. & & & &
\end{aligned}
\tag{2.4}
$$

2.2   The Equations of Motion

Eqs. 2.4 transform the equations of motion to a form which contains only volume integrals. Then, with the definition of the partial with respect to time,

$$\frac{\partial f}{\partial t} \;\equiv\; \lim_{V\to 0} \frac{1}{V}\frac{d}{dt} \int_V f\,dV\,, \tag{2.5}$$

April 23, 2001

we can take the limit $V \to 0$, yielding the *equations of motion in differential form*.

$$\textbf{Mass}: \qquad \frac{\partial \rho}{\partial t} + \nabla \cdot \rho \underline{u} = 0$$

$$\frac{\partial \rho}{\partial t} + \frac{\partial \rho u_j}{\partial x_j} = 0$$

$$\textbf{Momentum}: \qquad \frac{\partial \rho \underline{u}}{\partial t} + \nabla \cdot (\rho \underline{u}\,\underline{u}) = \rho \underline{B} + \nabla \cdot \sigma$$

$$\frac{\partial \rho u_i}{\partial t} + \frac{\partial \rho u_i u_j}{\partial x_j} = \rho B_i + \frac{\partial \sigma_{ij}}{\partial x_j} \tag{2.6}$$

$$\textbf{Energy}: \qquad \frac{\partial \rho \left(e + \frac{u^2}{2}\right)}{\partial t} + \nabla \cdot \rho \left(e + \frac{u^2}{2}\right)\underline{u} = \rho \underline{B} \cdot \underline{u} + \nabla \cdot (\sigma \underline{u}) - \nabla \cdot \underline{q} + \rho Q$$

$$\frac{\partial \rho \left(e + \frac{u^2}{2}\right)}{\partial t} + \frac{\partial \rho \left(e + \frac{u^2}{2}\right) u_j}{\partial x_j} = \rho B_j u_j + \frac{\partial \sigma_{ij} u_i}{\partial x_j} - \frac{\partial q_j}{\partial x_j} + \rho Q$$

Splitting the stress tensor according to Eq. 1.34 and using $\nabla \cdot (pI) = \nabla p$, *i.e.*, $\frac{\partial p \delta_{ij}}{\partial x_j} = \frac{\partial p}{\partial x_j}$, gives for the momentum and energy equations

$$\frac{\partial \rho \underline{u}}{\partial t} + \nabla \cdot (\rho \underline{u}\,\underline{u}) = -\nabla p + \rho \underline{B} + \nabla \cdot \tau \tag{2.7}$$

$$\frac{\partial \rho u_i}{\partial t} + \frac{\partial \rho u_i u_j}{\partial x_j} = -\frac{\partial p}{\partial x_i} + \rho B_i + \frac{\partial \tau_{ij}}{\partial x_j}$$

$$\frac{\partial \rho \left(e + \frac{u^2}{2}\right)}{\partial t} + \nabla \cdot \rho \left(e + \frac{u^2}{2}\right)\underline{u} = -\nabla \cdot (p\underline{u}) + \rho \underline{B} \cdot \underline{u} + \nabla \cdot (\tau \underline{u}) - \nabla \cdot \underline{q} + \rho Q \tag{2.8}$$

$$\frac{\partial \rho \left(e + \frac{u^2}{2}\right)}{\partial t} + \frac{\partial \rho \left(e + \frac{u^2}{2}\right) u_j}{\partial x_j} = -\frac{\partial p u_i}{\partial x_i} + \rho B_j u_j + \frac{\partial \tau_{ij} u_i}{\partial x_j} - \frac{\partial q_j}{\partial x_j} + \rho Q$$

2.3 The Convective Derivative

The convective derivative expresses the changes in time of a density quantity f following a fluid particle. The location $\underline{x}(\underline{\xi}, t)$ of any fluid particle at time t in a given flow is uniquely defined by its initial position $\underline{\xi}$ and t. The local velocity at the point is $\underline{u} = \frac{\partial \underline{x}(\underline{\xi}, t)}{\partial t}$. Thus, the convective derivative of f is

$$\frac{Df}{Dt} \equiv \frac{\partial f(\underline{x}(\underline{\xi}, t), t)}{\partial t} = \frac{\partial f}{\partial t} + \frac{\partial f}{\partial \underline{x}} \frac{\partial \underline{x}}{\partial t} = \frac{\partial f}{\partial t} + \underline{u} \nabla f$$

$$\frac{Df}{Dt} = u_j \frac{\partial f}{\partial x_j} . \tag{2.9}$$

For scalars:

$$\frac{Df}{Dt} = \frac{\partial f}{\partial t} + \underline{u} \cdot \nabla f \ ; \qquad \frac{Df}{Dt} = \frac{\partial f}{\partial t} + u_j \frac{\partial f}{\partial x_j} \tag{2.10}$$

For vectors:

$$\frac{D\underline{f}}{Dt} = \frac{\partial \underline{f}}{\partial t} + \underline{u} \nabla \underline{f} \ ; \qquad \frac{Df_i}{Dt} = \frac{\partial f_i}{\partial t} + u_j \frac{\partial f_i}{\partial x_j} \tag{2.11}$$

April 23, 2001

The latter is usually expressed with the vector notation

$$\frac{D\underline{f}}{Dt} = \frac{\partial \underline{f}}{\partial t} + (\underline{u} \cdot \nabla)\,\underline{f} \tag{2.12}$$

The convective derivative (sometimes called *substantial* or *total* derivative) expresses how quantities change following a fluid particle, *i.e., along a streamline.*

2.4 Convective Form of the Equations of Motion

A new form of the continuity equation is obtained by partially differentiating it and using Eq. 2.9,

$$\frac{D\rho}{Dt} + \rho \nabla \cdot \underline{u} = 0$$
$$\frac{D\rho}{Dt} + \rho \frac{\partial u_j}{\partial x_j} = 0 \tag{2.13}$$

This expresses the fact that, necessarily, any change of fluid density in a fluid particle must be accompanied by a divergence of the velocity field. In a flowing incompressible fluid the velocity is divergence free,

$$\boxed{\frac{D\rho}{Dt} = 0\,; \qquad \nabla \cdot \underline{u} = 0\,.} \tag{2.14}$$

A further operation on the convective derivative is necessary to treat the remaining equations of motion. Multiplying Eq. 2.9 by ρ and adding the continuity equation times f ($= 0$) gives

$$\rho \frac{Df}{Dt} = \frac{\partial \rho f}{\partial t} + \nabla \cdot (\rho \underline{u} f)\,; \qquad \rho \frac{D\underline{f}}{Dt} = \frac{\partial \rho \underline{f}}{\partial t} + \nabla \cdot (\rho \underline{u}\,\underline{f})\,. \tag{2.15}$$

This directly transforms the LHS of the momentum, energy and entropy equations to convective form.

$$\rho \frac{D\underline{u}}{Dt} = -\nabla p + \rho \underline{B} + \nabla \cdot \tau \tag{2.16}$$
$$\rho \frac{D u_i}{Dt} = -\frac{\partial p}{\partial x_i} + \rho B_i + \frac{\partial \tau_{ij}}{\partial x_j}$$

$$\rho \frac{D\left(e + \frac{u^2}{2}\right)}{Dt} = -\nabla \cdot p\underline{u} + \rho \underline{B} \cdot \underline{u} + \nabla \cdot (\tau \underline{u} - \underline{q}) + \rho\,Q \tag{2.17}$$
$$\rho \frac{D\left(e + \frac{u_j u_j}{2}\right)}{Dt} = -\frac{\partial p u_j}{\partial x_j} + \rho B_j u_j + \frac{\partial}{\partial x_j}\left(\tau_{ij} u_i - q_j\right) + \rho\,Q$$

$$\rho \frac{Ds}{Dt} + \nabla \cdot \left(\frac{\underline{q}}{T}\right) - \rho \frac{Q}{T} \geq 0 \tag{2.18}$$
$$\rho \frac{Ds}{Dt} + \frac{\partial q_j/T}{\partial x_j} - \rho \frac{Q}{T} \geq 0$$

2.5 Alternative Forms of the Conservation Equations

2.5.1 Mechanical Energy Equation

The mechanical energy equation is derived by dotting the momentum equation into $\underline{u}$.

$$\rho \frac{D\frac{u^2}{2}}{Dt} = -\nabla p \cdot \underline{u} + \rho \underline{B} \cdot \underline{u} + (\nabla \cdot \tau) \cdot \underline{u} \tag{2.19}$$

April 23, 2001

2.5.2 Internal Energy Equation

The internal energy equation is derived by subtracting the mechanical energy equation (2.19) from the energy equation (2.17).

$$\rho\frac{De}{Dt} = -p\nabla\cdot\underline{u} + \Phi - \nabla\cdot\underline{q} + \rho Q \tag{2.20}$$
$$\Phi \equiv \tau\,\nabla\underline{u}$$

$\nabla\underline{u}$ is the velocity gradient tensor, which, for example, appears in the definition 2.9 of $D\underline{u}/Dt$, and Φ is the *dissipation*. Eq. 2.20 is valid even when body forces $\underline{B}$ are present.

2.5.3 Equation for Total Enthalpy – The Bernoulli Equation

Other forms of the energy equation can be derived by substituting

$$-\nabla p\cdot\underline{u} = -\frac{Dp}{Dt} + \frac{\partial p}{\partial t} \tag{2.21}$$

and, from Eq. 2.13,

$$-p\nabla\cdot\underline{u} = \frac{p}{\rho}\frac{D\rho}{Dt} \ , \tag{2.22}$$

and combining into $D(p/\rho)/Dt$. Similarly, for body forces that are conservative, that is, work done by the force on a body is independent of path, a potential G can be defined such that

$$\rho\underline{B}\cdot\underline{u} = -\rho\nabla G\cdot\underline{u} = -\rho\frac{DG}{Dt} + \rho\frac{\partial G}{\partial t} \ . \tag{2.23}$$

We take $\partial G/\partial t = 0$ (neglect gravity waves).

In the total energy equation Eq. 2.17, letting $h = e + p/\rho$ gives

$$\boxed{\rho\frac{D\left(h + \frac{u^2}{2} + G\right)}{Dt} = \frac{\partial p}{\partial t} + \nabla\cdot(\tau\underline{u} - \underline{q}) + \rho Q \ .} \tag{2.24}$$

For steady flow ($\partial/\partial t = 0$), and if the fluid is inviscid and nonheatconducting,

$$\frac{D(h + \frac{u^2}{2} + G)}{Dt} = Q \ , \tag{2.25}$$

and for $Q = 0$,

$$h + \frac{u^2}{2} + G \equiv H = \text{const along a streamline.} \tag{2.26}$$

This is the form of the Bernoulli equation for steady compressible flow. In this sense the Bernoulli "constant" H is a generalized total enthalpy. The potential G includes the effects of gravity and rotation. For incompressible flow, by Eq. 2.20 $De/Dt = 0$. Therefore,

$$\boxed{p + \tfrac{1}{2}\rho u^2 + \rho G = \text{const along a streamline,}} \tag{2.27}$$

the incompressible form of the Bernoulli equation for steady flow. Here the Bernoulli equation has been derived from the enrgy equation. Later, in the Crocco Theorem (Eq. 3.21) we will see how it also comes from the momentum equation, establishing a connection between vorticity and entropy.

April 23, 2001

2.5.4 Entropy Equation

The internal energy equation Eq. 2.20 provides a form independent of the body forces, since they only increase mechanical energy. Using the relation (2.21) gives immediately

$$\rho\left(\frac{De}{Dt} + p\frac{D1/\rho}{Dt}\right) = \Phi - \nabla \cdot \underline{q} + \rho Q . \tag{2.28}$$

With the thermodynamic identity

$$T\,ds = de + p\,d\frac{1}{\rho} , \tag{2.29}$$

(2.28) becomes

$$\boxed{\rho T\frac{Ds}{Dt} = \Phi - \nabla \cdot \underline{q} + \rho Q .} \tag{2.30}$$

This equation is valid even when body forces $\underline{B}$ are present, because they do not serve to increase the entropy. In order for it to be consistent with the second law Eq. 2.18, it must be that $\Phi - \dfrac{q}{T}\nabla T > 0$. We will come back to this question later.

Gases: The potential temperature. From thermodynamics, variations of the entropy can be expressed in terms of p and T, *i.e.*, $s(p,T)$,

$$ds = \left(\frac{\partial s}{\partial T}\right)_p dT + \left(\frac{\partial s}{\partial p}\right)_T dp . \tag{2.31}$$

Using $c_p \equiv T(\partial s/\partial T)_p$ and the Maxwell relation

$$\left(\frac{\partial s}{\partial p}\right)_T = -\left(\frac{\partial v}{\partial T}\right)_p = -\alpha v , \tag{2.32}$$

derived from the differential $dg = v\,dp - s\,dT$ of the Gibbs free energy, $g = h - Ts$, where α is the thermal coefficient of expansion, gives

$$ds = \frac{c_p}{T}\,dT - \frac{\alpha}{\rho}\,dp , \tag{2.33}$$

or

$$\frac{ds}{c_p} = \frac{dT}{T} - \frac{\alpha p}{c_p\rho}\frac{dp}{p} . \tag{2.34}$$

For a perfect gas, $\alpha = 1/T$ and $p = \rho RT$, so

$$\frac{\alpha p}{c_p\rho} = \frac{\gamma - 1}{\gamma} , \tag{2.35}$$

where $\gamma = c_p/c_v = \text{const}$. Thus the logarithmic derivatives in Eq. 2.34 combine to form the *potential temperature* θ,

$$\frac{ds}{c_p} = \frac{d\theta}{\theta}, \tag{2.36}$$

where

$$\theta \equiv \left(\frac{p}{p_0}\right)^{-\frac{\gamma-1}{\gamma}} T , \tag{2.37}$$

with the result that

$$\frac{\theta}{\theta_0} = e^{\frac{s-s_0}{c_p}} . \tag{2.38}$$

So the potential temperature is really just the entropy. θ is the temperature which a fluid particle, initially at T, aquires when the pressure changes from p to p_0 isentropically. Correspondingly, there is the *potential density*,

$$\rho_\theta \equiv \left(\frac{p}{p_0}\right)^{-\frac{1}{\gamma}} \rho .$$ (2.39)

In terms of θ the entropy equation (2.30) becomes

$$\boxed{\frac{D\theta}{Dt} = \frac{\theta}{c_p T}\left(\frac{\Phi}{\rho} - \frac{1}{\rho}\nabla\cdot\underline{q} + Q\right) .}$$ (2.40)

As would be expected from the definition of θ, it changes along a particle path only if entropy-altering processes, indicated on the right hand side, are active. In particular, the potential temperature of a fluid particle is constant in an isentropic flow.

A stationary atmosphere ($\underline{u} = 0$), for which the z-momentum equation gives

$$\frac{dp}{dz} = \rho\,g ,$$ (2.41)

gives for the temperature gradient (2.34)

$$\frac{1}{T}\frac{dT}{dz} = \frac{\gamma-1}{\gamma}\frac{1}{p}\frac{dp}{dz} = -\frac{\gamma-1}{\gamma}\frac{\rho g}{p} .$$ (2.42)

That is,

$$\boxed{\left(\frac{dT}{dz}\right)_{ad} = -\frac{g}{c_p} .}$$ (2.43)

This is so-called *the adiabatic lapse rate* for a stationary atmosphere. It describes the temperatures acquired by the reversible adiabatic (isentropic) motion of a fluid particle. Such a motion is used to test the stability of an atmosphere. If such a fluid particle finds itself at the same density as its surroundings, then the atmospher is *neutrally stable*. If, upon being elevated, it finds itself lighter than the surroundings because $dT/dz > (dT/dz)_{ad}$ then the atmosphere is unstable, while if it is heavier because $dT/dz < (dT/dz)_{ad}$, the atmosphere is stable. In summary, if $d\theta/dz = 0$ the atmosphere is neutrally stable.

Temperature energy equation.   Now, finally, an equation can be derived for how the temperature varies in a flow. From Eq. 2.34, the entropy equation Eq. 2.30 can be written

$$\boxed{\rho c_p \frac{DT}{Dt} = \alpha T \frac{Dp}{Dt} + \Phi - \nabla\cdot\underline{q} + \rho\,Q .}$$ (2.44)

The energy equation for liquids.   With the flow of liquids at modest velocities the changes of entropy (density) by heating $\left(\frac{\partial s}{\partial T}\right)_p dT$ may be large compared to the changes due to dynamical changes of pressure $\left(\frac{\partial s}{\partial p}\right)_T dp$. That is,

$$\alpha T \frac{Dp}{Dt} \ll \rho c_p \frac{DT}{Dt} .$$ (2.45)

With $\Delta p \sim \rho U^2$, and to order of magnitude $\Delta T \sim T$, the condition becomes

$$\frac{\alpha U^2}{c_p} = \alpha T \frac{U^2}{c_p T} \ll 1 .$$ (2.46)

For water, this requires that $U \ll 2000$ m/s. Then, changes of density are due to heating, that is $\rho = \rho(T)$, and the energy equation becomes

$$\frac{DT}{Dt} = \frac{1}{c_p} \left(\frac{\Phi}{\rho} - \frac{1}{\rho} \nabla \cdot \underline{q} + Q \right) , \qquad (2.47)$$

or

$$\frac{D\rho}{Dt} = -\frac{\alpha \rho_0}{c_p} \left(\frac{\Phi}{\rho} - \frac{1}{\rho} \nabla \cdot \underline{q} + Q \right) . \qquad (2.48)$$

For constant α, $\rho(T)$ is given by the familiar formula

$$\frac{\rho}{\rho_0} = 1 - \alpha(T - T_0) , \qquad (2.49)$$

but, near 4C in water, α actually changes sign.

Again, note that all these equations apply when there are body forces, even though they don't appear in these forms.

2.6 Control Volume Analysis – Energy

A global form of Bernoulli's equation can be derived by control-volume analysis of the energy equation, Eq. 1.37. Consider a volume V contained in surface S (see Fig. 6) containing a steady flow subject to drag elements D, heat addition $\dot{Q}$ from the external system, work $\dot{W}$ powered from an external source, and a body force $\underline{g}$ which can be expressed in terms of a potential $-\underline{g} = -\nabla G$. One effect of viscosity,
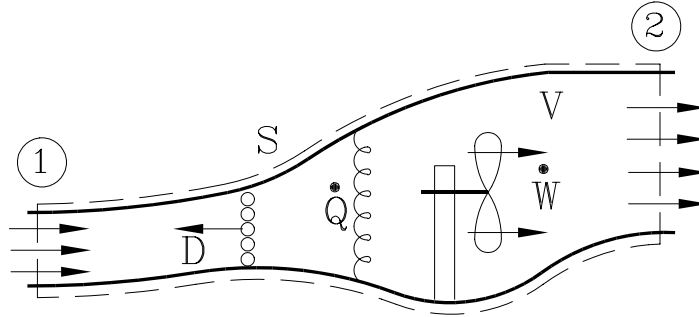
Figure 6. Schematic diagram of possible processes affecting energy in a control volume.

namely the no-slip boundary condition at solid surfaces, is explicitly invoked. This "lumped parameter" approach is used to simplify an otherwise complicated problem. All of the viscous and pressure traction forces on fixed surfaces which depend on the configuration of the flow, and thus on its detailed solution, are represented by D, which we won't calculate, but assume is given. Those acting on moving surfaces, which do work, are represented by $\dot{W}$, which we won't calculate, but assume is given. Energy addition by heat flux accross boundaries and by volumetric heat addition are represented by $\dot{Q}$, also assumed given. The drag contribution D disappears from the energy equation because of the no-slip condition. This means that the only surviving surface area term on the right hand side of Eq. 1.37 is the contribution of pressure on surfaces $S_{1,2}$. Similarly, the lhs has nonzero velocity contributions only from $S_{1,2}$. Thus, the energy equation is

$$\int_{S_{1,2}} \rho \left(e + \frac{u^2}{2} \right) \underline{u} \cdot \underline{n} \, dS = -\int_{S_{1,2}} p\underline{u} \cdot \underline{n} \, dS - \int_V \nabla G \cdot \rho \underline{u} \, dV + \dot{W} + \dot{Q} . \qquad (2.50)$$

April 23, 2001

Now, $\nabla G \cdot \rho \underline{u} = \nabla \cdot (\rho G \underline{u}) - G \nabla \cdot \rho \underline{u}$, and the continuity equation for steady flow says that $\nabla \cdot \rho \underline{u} = 0$ everywhere in the volume. The consequence of the resulting form of the body-force term is that the volume integral can be converted to a surface integral by the divergence theorem. Thus, grouping terms,

$$\int_{S_{1,2}} \rho \left(e + \frac{u^2}{2} + \frac{p}{\rho} + G \right) \underline{u} \cdot \underline{n} \, dS \;=\; \dot{W} + \dot{Q} \,. \tag{2.51}$$

Defining the control volume so that flow quantities are uniform across $S_{1,2}$ gives

$$\boxed{\dot{M} \left[h + \frac{u^2}{2} + G \right]_1^2 \;=\; \dot{W} + \dot{Q} \,,} \tag{2.52}$$

where $\dot{M} \equiv \rho_2 u_2 S_2 = \rho_1 u_1 S_1$ and $[\;]_1^2 \equiv (\;)_2 - (\;)_1$. This is a general form of the energy equation. It yields an integral form of the Bernoulli Equation when $\dot{W} = \dot{Q} = 0$. Subject to the assumptions made here, the actual Bernoulli Equation, as derived earlier, may be obtained by letting the control volume become a stream tube.

2.7 The Rate of Deformation Tensor and Vorticity

$$
\begin{array}{ccccc}
\underbrace{\dfrac{\partial u_i}{\partial x_j}}_{\substack{\text{velocity} \\ \text{gradient} \\ \text{tensor}}} & = & \dfrac{1}{2} \underbrace{\left(\dfrac{\partial u_i}{\partial x_j} + \dfrac{\partial u_j}{\partial x_i} \right)}_{\text{rate of deformation tensor}} & + & \dfrac{1}{2} \underbrace{\left(\dfrac{\partial u_i}{\partial x_j} - \dfrac{\partial u_j}{\partial x_i} \right)}_{\text{vorticity tensor}}
\end{array}
$$

$$
\equiv \qquad \tfrac{1}{2} \epsilon_{ij} \qquad + \qquad \tfrac{1}{2} \omega_{ij} \tag{2.53}
$$

$$
= \quad \frac{1}{2} \begin{pmatrix} \epsilon_{11} & \epsilon_{12} & \epsilon_{13} \\ \epsilon_{12} & \epsilon_{22} & \epsilon_{23} \\ \epsilon_{13} & \epsilon_{23} & \epsilon_{33} \end{pmatrix} + \frac{1}{2} \begin{pmatrix} 0 & \omega_{12} & \omega_{13} \\ -\omega_{12} & 0 & \omega_{23} \\ -\omega_{13} & -\omega_{23} & 0 \end{pmatrix}
$$

$$
= \frac{1}{2} \begin{pmatrix} 2\dfrac{\partial u}{\partial x} & \dfrac{\partial u}{\partial y} + \dfrac{\partial v}{\partial x} & \dfrac{\partial u}{\partial z} + \dfrac{\partial w}{\partial x} \\ \dfrac{\partial v}{\partial x} + \dfrac{\partial u}{\partial y} & 2\dfrac{\partial v}{\partial y} & \dfrac{\partial v}{\partial z} + \dfrac{\partial v}{\partial y} \\ \dfrac{\partial w}{\partial x} + \dfrac{\partial u}{\partial z} & \dfrac{\partial w}{\partial y} + \dfrac{\partial v}{\partial z} & 2\dfrac{\partial w}{\partial z} \end{pmatrix} + \frac{1}{2} \begin{pmatrix} 0 & \dfrac{\partial u}{\partial y} - \dfrac{\partial v}{\partial x} & \dfrac{\partial u}{\partial z} - \dfrac{\partial w}{\partial x} \\ \dfrac{\partial v}{\partial x} - \dfrac{\partial u}{\partial y} & 0 & \dfrac{\partial v}{\partial z} - \dfrac{\partial w}{\partial y} \\ \dfrac{\partial w}{\partial x} - \dfrac{\partial u}{\partial z} & \dfrac{\partial w}{\partial y} - \dfrac{\partial v}{\partial z} & 0 \end{pmatrix}
$$

$$
\nabla \underline{u} \quad = \qquad\qquad \tfrac{1}{2} \operatorname{def} \underline{u} \qquad\qquad + \qquad\qquad \tfrac{1}{2} \, \omega
$$

2.8 Vorticity

A second order skew symmetric tensor has 3 independent components and so represents a vector in three dimensions. In particular, the vorticity vector $\underline{\omega}$ is defined by

$$\omega_1 \;=\; \omega_{32} \,; \qquad \omega_2 \;=\; \omega_{13} \,; \qquad \omega_3 \;=\; \omega_{21} \,. \tag{2.54}$$

April 23, 2001

That is,

$$\omega_{ij} = -\epsilon_{ijk}\,\omega_k\,;\qquad \omega_i = -\frac{1}{2}\epsilon_{ijk}\,\omega_{jk} = -\frac{1}{2}\epsilon_{ijk}\left(\frac{\partial u_j}{\partial x_k} - \frac{\partial u_k}{\partial x_j}\right)\,,\tag{2.55}$$

where ϵ_{ijk} is the permutation operator[1]. From the last relation,

$$\underline{\omega} = \left(\frac{\partial w}{\partial y} - \frac{\partial v}{\partial z}\right)\underline{e}_x + \left(\frac{\partial u}{\partial z} + \frac{\partial w}{\partial x}\right)\underline{e}_y + \left(\frac{\partial v}{\partial x} - \frac{\partial u}{\partial y}\right)\underline{e}_z = \begin{vmatrix} \underline{e}_x & \underline{e}_y & \underline{e}_z \\ \dfrac{\partial}{\partial x} & \dfrac{\partial}{\partial y} & \dfrac{\partial}{\partial z} \\ u & v & w \end{vmatrix} = \operatorname{curl}\underline{u}\tag{2.56}$$

Thus the vorticity vector $\underline{\omega}$ is normal to the velocity $\underline{u}$. In view of the second of Eqs. 2.55,

$$\omega_i = \epsilon_{ijk}\frac{\partial u_k}{\partial x_j}\,.\tag{2.57}$$

As we will see later, because

$$\nabla\cdot(\nabla\times\underline{u}) = \nabla\cdot\underline{\omega} = 0\tag{2.58}$$

there is no such thing as a point source of vorticity.

2.8.1 The vorticity equation

The vorticity equation is derived by taking the curl of the momentum equation, Eq. 2.16. First, the convective derivative is modified by using the vector identity

$$\underline{u}\cdot\nabla\underline{u} = (\nabla\times\underline{u})\times\underline{u} + \nabla\frac{u^2}{2}\,,\tag{2.59}$$

so,

$$\frac{\partial\underline{u}}{\partial t} + \underline{u}\cdot\nabla\underline{u} = \frac{\partial\underline{u}}{\partial t} + \nabla\frac{u^2}{2} + \underline{\omega}\times\underline{u}\tag{2.60}$$

When the curl is taken and the identities $\operatorname{curl\,grad} = 0$, $\operatorname{div\,curl} = 0$ and

$$\nabla\times(\underline{u}\times\underline{v}) = (\underline{v}\cdot\nabla)\underline{u} - \underline{v}\nabla\cdot\underline{u} + \underline{u}\nabla\cdot\underline{v} - (\underline{u}\cdot\nabla)\underline{v}\tag{2.61}$$

are used, the result is

$$\frac{\partial\underline{\omega}}{\partial t} + (\underline{u}\cdot\nabla)\underline{\omega} + \underline{\omega}(\nabla\cdot\underline{u}) - (\underline{\omega}\cdot\nabla)\underline{u} = \tag{2.62}$$

$$\frac{D\underline{\omega}}{Dt} + \underline{\omega}(\nabla\cdot\underline{u}) - (\underline{\omega}\cdot\nabla)\underline{u} = -\nabla\times\left(\frac{1}{\rho}\nabla p\right) + \nabla\times\left(\frac{1}{\rho}\nabla\cdot\tau\right)$$

Now, rewriting in terms of the specific vorticity, $\underline{\xi} = \underline{\omega}/\rho$

$$\rho\frac{D\underline{\xi}}{Dt} + \underline{\xi}\frac{D\rho}{Dt} + \rho\,\underline{\xi}(\nabla\cdot\underline{u}) - (\underline{\omega}\cdot\nabla)\underline{u} = -\nabla\times\left(\frac{1}{\rho}\nabla p\right) + \nabla\times\left(\frac{1}{\rho}\nabla\cdot\tau\right)\tag{2.63}$$

---

[1] $\epsilon_{ijk} = \begin{cases} 0 & \text{if 2 of the indices }(ijk)\text{ are equal} \\ 1 & \text{if }(ijk)\text{ is an even permutation of }(123) \\ -1 & \text{if }(ijk)\text{ is an odd permutation of }(123) \end{cases}$. The cross product is given by $(\underline{a}\times\underline{b})_i = \epsilon_{ijk}a_jb_k$.

Vector identities are easily proven in this notation, with the help of the identity $\epsilon_{ijk}\epsilon_{ilm} = \delta_{jl}\delta_{km} - \delta_{jm}\delta_{kl}$.

April 23, 2001

Using the continuity equation and expanding the pressure and viscous terms leads finally to

$$\rho\frac{D\underline{\omega}/\rho}{Dt} \;=\; \underbrace{\underline{\omega}\cdot\nabla\underline{u}}_{\substack{\text{vortex}\\\text{stretching}}} \;-\; \underbrace{\left(\nabla\frac{1}{\rho}\right)\times\nabla p}_{\substack{\text{baroclinic}\\\text{generation}}} \;+\; \underbrace{\frac{1}{\rho}\nabla\times\nabla\cdot\tau}_{\substack{\text{viscous}\\\text{decay}}} \;+\; \underbrace{\left(\nabla\frac{1}{\rho}\right)\times\nabla\cdot\tau}_{\substack{\text{variable density}\\\text{viscous decay}}} \;.$$
(2.64)

With $dh = T\,ds + \frac{1}{\rho}\,dp$, the baroclinic generation term can be written in alternative form,

$$-\left(\nabla\frac{1}{\rho}\right)\times\nabla p \;=\; -\nabla\times\left(\frac{1}{\rho}\nabla p\right) \;=\; \nabla\times(T\nabla s) \;=\; \nabla T\times\nabla s\,,$$
(2.65)

so

$$\rho\frac{D\underline{\omega}/\rho}{Dt} \;=\; \underline{\omega}\cdot\nabla\underline{u} \;+\; \nabla T\times\nabla s \;+\; \nabla\times\left(\frac{1}{\rho}\nabla\cdot\tau\right)\,.$$
(2.66)

For an <u>inviscid, constant-density fluid</u>,

$$\frac{D\underline{\omega}}{Dt} \;=\; \underline{\omega}\cdot\nabla\underline{u} \qquad \text{Helmholtz Equation}$$
(2.67)

In <u>2D flow</u> there are no velocity gradients parallel to the vorticity vector, so there is no vortex stretching, and

$$\frac{D\underline{\omega}}{Dt} \;=\; 0\,.$$
(2.68)

3   Viscous Stresses and Heat Flux

3.1   Newtonian fluid

In establishing a constitutive law relating stress to strain, it is first hypothesized that the viscous stress τ depends on *changes of velocity*. The simplest Gallilean invariant measure of changes is $\nabla \underline{u}$. The Newtonian approximation is that the relationship is linear,

$$
\begin{aligned}
\tau_{ij} &= \mu_{ijkl} \frac{\partial u_k}{\partial x_l} \\
&= \mu_{ijkl}(\epsilon_{kl} + \omega_{kl}) \,,
\end{aligned}
\tag{3.1}
$$

where μ_{ijkl} are the (89) viscosity coefficients. The complexity of the material properties is drastically reduced when the fluid behaves isotropically (there is no preferred direction), i.e., both the stress and the strain are isotropic. Therefore, necessarily so is μ_{ijkl}. The basic isotropic tensor is the Kronecker delta, so a 4th-order isotropic tensor can be constructed from products of pairs of deltas,

$$
\mu_{ijkl} = \mu_1 \, \delta_{ij}\delta_{kl} + \mu_2 \, \delta_{ik}\delta_{jl} + \mu_3 \, \delta_{il}\delta_{jk} \,.
\tag{3.2}
$$

So the 89 coefficients are reduced to 3! There are many non-isotropic fluids, so beware. However, τ is symmetric, so, from Eq. 3.1 μ_{ijkl} is symmetric in (i, j). Thus,

$$
\mu_{ijkl} = \mu_1 \, \delta_{ij}\delta_{kl} + 2\mu_2 \, \delta_{ik}\delta_{jl} \,.
\tag{3.3}
$$

Furthermore, from this result it can be seen that μ_{ijkl} is also symmetric in (k, l), which eliminates the ω_{kl} term, which is antisymmetric, from Eq. 3.1. Thus,

$$
\begin{aligned}
\tau_{ij} &= \mu_1 \, \delta_{ij}\delta_{kl} \, \epsilon_{kl} + 2\mu_2 \, \delta_{ik}\delta_{jl} \, \epsilon_{kl} \\
&= \mu_1 \delta_{ij} \, \epsilon_{kk} + 2\mu_2 \, \epsilon_{ij} \,.
\end{aligned}
\tag{3.4}
$$

ϵ_{kk} is $2\frac{\partial u_k}{\partial x_k}$, so we redefine the two viscosities $(\mu_1, \mu_2) \to (\lambda, \mu)$, such that

$$
\begin{aligned}
\tau_{ij} &= \lambda \frac{\partial u_k}{\partial x_k} \delta_{ij} &+ \mu \left(\frac{\partial u_i}{\partial x_j} + \frac{\partial u_j}{\partial x_i} \right) \\
\tau &= \lambda \, \nabla \cdot \underline{u} \, I &+ \mu \operatorname{def} \underline{u} \\
\Phi &= \tau \, \nabla \underline{u} = \tfrac{1}{2}\tau\epsilon
\end{aligned}
\tag{3.5}
$$

The last equality is true because the stress tensor is symmetric. λ is called the *compressive viscosity* and μ the *shear viscosity*, but note that there are not only shear stress terms but also normal-stress terms in $\operatorname{def}\underline{u}$. The compressive viscosity has effect only in compressible flow.

3.2   Bulk viscosity

The average normal viscous stress is given by the $1/3$ of the trace of the stress tensor. (Note: $\delta_{ii} = 3$.)

$$
\tau_{ii} = (3\lambda + 2\mu)\frac{\partial u_i}{\partial x_i}
\tag{3.6}
$$

April 23, 2001

The average stress is taken to be proportional to the *bulk viscosity*

$$\frac{\operatorname{tr}\tau}{3} \;=\; \eta\,\nabla\cdot\underline{u} \tag{3.7}$$

$$\eta \;=\; \lambda + \frac{2}{3}\mu \tag{3.8}$$

so,

$$\begin{aligned}
\tau &= \eta\nabla\cdot\underline{u}\,I + \mu(\operatorname{def}\underline{u} - \frac{2}{3}\nabla\cdot\underline{u})\\[4pt]
\tau_{ij} &= \eta\frac{\partial u_k}{\partial x_k}\delta_{ij} + \mu\left(\frac{\partial u_i}{\partial x_j} + \frac{\partial u_j}{\partial x_i} - \frac{2}{3}\frac{\partial u_k}{\partial x_k}\delta_{ij}\right)
\end{aligned} \tag{3.9}$$

3.3 Heat flux vector (Fourier's law)

$$\underline{q} \;=\; -k\,\nabla T \tag{3.10}$$

3.4 The Equations of Motion - Newtonian Fluid

In the equations of motion $\nabla\cdot\tau$ becomes

$$\nabla\cdot\tau \;=\; \nabla(\lambda\,\nabla\cdot\underline{u}) + \nabla\cdot(\mu\,\operatorname{def}\underline{u})\;, \tag{3.11}$$

so

$$\mathbf{Momentum}:\;\; \rho\frac{D\underline{u}}{Dt} \;=\; -\nabla p + \rho\underline{B} + \nabla(\lambda\,\nabla\cdot\underline{u}) + \nabla\cdot(\mu\,\operatorname{def}\underline{u})$$

$$\rho\frac{Du_i}{Dt} \;=\; -\frac{\partial p}{\partial x_i} + \rho B_i + \frac{\partial}{\partial x_i}\left(\lambda\frac{\partial u_k}{\partial x_k}\right) + \frac{\partial}{\partial x_j}\left[\mu\left(\frac{\partial u_i}{\partial x_j} + \frac{\partial u_j}{\partial x_i}\right)\right] \tag{3.12}$$

$$\mathbf{Energy}:\;\; \rho\frac{De}{Dt} \;=\; -p\nabla\cdot\underline{u} + \Phi + \nabla\cdot(k\nabla T)$$

$$\Phi = \lambda(\nabla\cdot\underline{u})^2 + \frac{\mu}{2}\,(\operatorname{def}\underline{u})^2$$

$$\rho\frac{De}{Dt} \;=\; -p\frac{\partial u_j}{\partial x_j} + \Phi + \frac{\partial}{\partial x_j}k\frac{\partial T}{\partial x_j}$$

$$\begin{aligned}
\Phi &= \lambda\frac{\partial u_k}{\partial x_k}\delta_{ij}\frac{\partial u_i}{\partial x_j} + \mu\left(\frac{\partial u_i}{\partial x_j} + \frac{\partial u_j}{\partial x_i}\right)\frac{\partial u_i}{\partial x_j}\\[6pt]
&= \left(\eta - \frac{2}{3}\mu\right)\left(\frac{\partial u_j}{\partial x_j}\right)^2 + \frac{\mu}{2}\left(\frac{\partial u_i}{\partial x_j} + \frac{\partial u_j}{\partial x_i}\right)^2\\[6pt]
&= \frac{1}{4}\left[\left(\eta - \frac{2}{3}\mu\right)\epsilon_{ii}^2 + 2\mu\,\epsilon_{ij}^2\right]
\end{aligned} \tag{3.13}$$

From Eq. 2.44,

$$\rho\,c_p\frac{DT}{Dt} \;=\; \alpha T\,\frac{Dp}{Dt} + \Phi + \nabla\cdot(k\nabla T) \tag{3.14}$$

3.4.1 Vorticity equation - Isothermal fluid

If the temperature is constant $p = p(\rho)$, so the pressure and density gradients are parallel. This is called *barotropic* flow. It holds when *any single* thermodynamic variable is constant throughout. An added side benefit of the isothermal case is that $\mu(T) = $ const. Then Eq. 2.64 becomes

$$\rho \frac{D\underline{\omega}/\rho}{Dt} \;=\; \underline{\omega} \cdot \nabla \underline{u} \;+\; \nu \nabla \times (\nabla \cdot \mathrm{def}\underline{u}) + \mu \nabla \frac{1}{\rho} \times \nabla \cdot \mathrm{def}\underline{u} + \lambda \nabla \frac{1}{\rho} \times \nabla(\nabla \cdot \underline{u}) \;, \tag{3.15}$$

where $\nu = \mu/\rho$ is the kinematic viscosity and the fact that $\mathrm{curl\,grad} = 0$ has been used. From the vector identity $\mathrm{curl\,div\,def} = \mathrm{div\,grad\,curl}$,

$$\rho \frac{D\underline{\omega}/\rho}{Dt} \;=\; \underline{\omega} \cdot \nabla \underline{u} \;+\; \nu \nabla^2 \underline{\omega} + \mu \nabla \frac{1}{\rho} \times \nabla \cdot \mathrm{def}\underline{u} + \lambda \nabla \frac{1}{\rho} \times \nabla(\nabla \cdot \underline{u}) \;, \tag{3.16}$$

The last 3 terms are all second order derivatives and so act to diffuse vorticity. This can be most easily seen in constant-density, two-dimensional plane flow, where there are no velocity gradients parallel to the vorticity and so there is no vortex stretching, and where the density gradient terms vanish,

$$\frac{D\underline{\omega}}{Dt} \;=\; \nu \nabla^2 \underline{\omega} \;. \tag{3.17}$$

Viscosity is a "diffusion coefficient" that diffuses vorticity. In order to preclude pathological behavior overall diffusion must be *down* the vorticity gradient. In the simple case where there is only one diffusive term (Eq. 3.17) the viscosity had better be positive to insure this, $\mu > 0$.

3.4.2 Constant viscosity and heat conductivity

For constant viscosity and heat conductivity, from Eq. 3.12, since $\nabla \cdot \mathrm{def}\underline{u} = \nabla(\nabla \cdot \underline{u}) + \nabla^2 \underline{u}$

$$\nabla \cdot \tau \;=\; (\lambda + \mu)\nabla(\nabla \cdot \underline{u}) + \mu \nabla^2 \underline{u} \;, \tag{3.18}$$

so,

$$\frac{D\underline{u}}{Dt} \;=\; -\frac{1}{\rho}\nabla p + \underline{B} + \nu \nabla^2 \underline{u} + \left(\frac{\eta}{\rho} + \tfrac{1}{3}\nu \right) \nabla(\nabla \cdot \underline{u}) \;. \tag{3.19}$$

From Eq. 2.44

$$\rho\, c_p \frac{DT}{Dt} \;=\; \alpha T \frac{Dp}{Dt} + \Phi + k \nabla^2 T \;; \quad \Phi \;=\; \tau \cdot \nabla \underline{u} \tag{3.20}$$

3.5 Crocco's Theorem

Another form of the momentum equation Eq. 2.16 can be derived by using the modified form of the convective derivative given in Eq. 2.60. Using the form (3.11) for $\nabla \cdot \tau$, and taking $\underline{B} = -\nabla G$, $dh = T\,ds + \frac{1}{\rho}\,dp$ and $\lambda = \eta - \frac{2}{3}\mu$ gives

$$\rho \left(\frac{\partial \underline{u}}{\partial t} + \underline{\omega} \times \underline{u} + \nabla H \right) \;=\; \rho T \nabla s + \nabla \left[\left(\eta - \tfrac{2}{3}\mu\right) \nabla \cdot \underline{u} \right] + \nabla \cdot (\mu\, \mathrm{def}\underline{u}) \tag{3.21}$$

where H was defined in Eq. 2.26. For steady, inviscid flow

$$\underline{\omega} \times \underline{u} + \nabla H \;=\; T \nabla s \;. \tag{3.22}$$

April 23, 2001

a. If $s = \text{constant everywhere}$ (homentropic), then $H = \text{constant everywhere}$ if

$$\underline{\omega} \times \underline{u} = 0 . \tag{3.23}$$

In this case either the flow must be irrotational ($\underline{\omega} = 0$) or $\underline{\omega}$ and $\underline{u}$ must be parallel, which is a very limited class of flows called Beltrami flow.

b. On the other hand, if the flow is irrotational, then

$$\nabla H = T \nabla s . \tag{3.24}$$

While Eq. 2.25 deals with behavior along a streamline, these results apply throughout the flow, and are valid in general for steady inviscid irrotational flow.

For constant viscosity, using the form (3.18) for $\nabla \cdot \tau$ permits use of the vector identity

$$\nabla^2 \underline{u} = \nabla(\nabla \cdot \underline{u}) - \nabla \times \underline{\omega} , \tag{3.25}$$

to give

$$\frac{\partial \underline{u}}{\partial t} + \underline{\omega} \times \underline{u} + \nabla H = T \nabla s + \left(\frac{\eta}{\rho} + \tfrac{4}{3}\nu \right) \nabla(\nabla \cdot \underline{u}) - \nu \nabla \times \underline{\omega} . \tag{3.26}$$

In irrotational flow only the dilatational contributions to viscous stress act. Note that nowhere in this paragraph has constant density been assumed.

3.6 Incompressible fluid

$D\rho/Dt = 0$ and $\alpha = 0$:

$$\nabla \cdot \underline{u} = 0 \tag{3.27}$$

$$\rho \frac{D\underline{u}}{Dt} = -\nabla p + \rho \underline{B} + \mu \nabla^2 \underline{u} \tag{3.28}$$

$$\rho \, c_p \frac{DT}{Dt} = \Phi + k \nabla^2 T ; \quad \Phi = \tau \cdot \nabla \underline{u} \tag{3.29}$$

Again, with the vector identities Eqs. 3.25 and 2.59, and taking $\underline{B} = -\nabla G$, another form of the momentum equation is

$$\frac{\partial \underline{u}}{\partial t} + \underline{\omega} \times \underline{u} + \nabla H = -\nu \nabla \times \omega , \tag{3.30}$$

where H now is of the incompressible form

$$H = \frac{u^2}{2} + \frac{p}{\rho} + G \tag{3.31}$$

and the ρ has been brought inside the ∇p because it is constant. Compare with Eqs. 3.26 and 2.27.

For irrotational flow ($\omega = 0$), this is the Bernoulli equation for nonsteady incompressible flow.

The term $\underline{u} \times \underline{\omega}$ in the momentum equation is analogous to the Coriolis force and is related to the so-called Magnus effect, in which a normal velocity imposed upon a vortex line is resisted by a force, the "lift". On airfoils this is the Kutta-Joukowski theorem.

4 Summary: Other Forms of the Equations of Motion

4.1 Cartesian Tensor Notation

Momentum equation.

$$\rho\frac{\partial u_i}{\partial t} + \rho u_j\frac{\partial u_i}{\partial x_j} = -\frac{\partial p}{\partial x_i} + \frac{\partial}{\partial x_i}\left(\eta - \frac{2}{3}\mu\right)\frac{\partial u_j}{\partial x_j} + \frac{\partial}{\partial x_j}\mu\left(\frac{\partial u_i}{\partial x_j} + \frac{\partial u_j}{\partial x_i}\right) \tag{4.1}$$

Energy Equation.

$$\rho\, c_p\left(\frac{\partial T}{\partial t} + u_j\frac{\partial T}{\partial x_j}\right) = \alpha T\frac{Dp}{Dt} + \Phi + \frac{\partial}{\partial x_j}k\frac{\partial T}{\partial x_j} \tag{4.2}$$

$$\Phi = \left(\eta - \frac{2}{3}\mu\right)\left(\frac{\partial u_j}{\partial x_j}\right)^2 + \mu\left(\frac{\partial u_i}{\partial x_j} + \frac{\partial u_j}{\partial x_i}\right)\frac{\partial u_i}{\partial x_j} \tag{4.3}$$

4.2 2 Dimensional Plane Flow: Cartesian Coordinates

Continuity equation:

$$\frac{\partial \rho u}{\partial x} + \frac{\partial \rho v}{\partial y} = 0 \tag{4.4}$$

x-momentum equation:

$$\rho\frac{\partial u}{\partial t} + \rho u\frac{\partial u}{\partial x} + \rho v\frac{\partial u}{\partial y} = -\frac{\partial p}{\partial x} + \frac{\partial}{\partial x}\left(\eta - \frac{2}{3}\mu\right)\left(\frac{\partial u}{\partial x} + \frac{\partial v}{\partial y}\right) + 2\frac{\partial}{\partial x}\left(\mu\frac{\partial u}{\partial x}\right) + \frac{\partial}{\partial y}\mu\left(\frac{\partial u}{\partial y} + \frac{\partial v}{\partial x}\right) \tag{4.5}$$

y-momentum equation:

$$\rho\frac{\partial v}{\partial t} + \rho u\frac{\partial v}{\partial x} + \rho v\frac{\partial v}{\partial y} = -\frac{\partial p}{\partial y} + \frac{\partial}{\partial y}\left(\eta - \frac{2}{3}\mu\right)\left(\frac{\partial u}{\partial x} + \frac{\partial v}{\partial y}\right) + 2\frac{\partial}{\partial y}\left(\mu\frac{\partial v}{\partial y}\right) + \frac{\partial}{\partial x}\mu\left(\frac{\partial u}{\partial y} + \frac{\partial v}{\partial x}\right) \tag{4.6}$$

Energy equation:

$$\rho\, c_p\left(\frac{\partial T}{\partial t} + u\frac{\partial T}{\partial x} + v\frac{\partial T}{\partial y}\right) = \alpha T\left(\frac{\partial p}{\partial t} + u\frac{\partial p}{\partial x} + v\frac{\partial p}{\partial y}\right) + \Phi + \frac{\partial}{\partial x}\left(k\frac{\partial T}{\partial x}\right) + \frac{\partial}{\partial y}\left(k\frac{\partial T}{\partial y}\right) \tag{4.7}$$

$$\Phi = \left(\eta - \frac{2}{3}\mu\right)\left(\frac{\partial u}{\partial x} + \frac{\partial v}{\partial y}\right)^2 + \mu\left[2\left(\frac{\partial u}{\partial x}\right)^2 + 2\left(\frac{\partial v}{\partial y}\right)^2 + \left(\frac{\partial u}{\partial y} + \frac{\partial v}{\partial x}\right)^2\right] \tag{4.8}$$

4.3 Cylindrical Coordinates

$(r,\theta)(u,v)\ (\frac{\partial}{\partial z} = 0)$
Continuity equation:

$$\frac{\partial \rho}{\partial t} + \frac{1}{r}\frac{\partial\, \rho u r}{\partial r} + \frac{1}{r}\frac{\partial\, \rho v}{\partial \theta} = 0 \tag{4.9}$$

r-momentum equation:

$$\rho\left(\frac{Du}{Dt} - \frac{v^2}{r}\right) = -\frac{\partial p}{\partial r} + \frac{1}{r}\frac{\partial\, r\tau_{rr}}{\partial r} + \frac{1}{r}\frac{\partial \tau_{r\theta}}{\partial \theta} - \frac{\tau_{\theta\theta}}{r} \tag{4.10}$$

θ-momentum equation:

$$\rho\left(\frac{Dv}{Dt} + \frac{uv}{r}\right) = -\frac{1}{r}\frac{\partial p}{\partial \theta} + \frac{1}{r^2}\frac{\partial\, r^2\tau_{r\theta}}{\partial r} + \frac{\partial \tau_{\theta\theta}}{\partial \theta} \tag{4.11}$$

April 23, 2001

$$\tau_{rr} = 2\mu\frac{\partial u}{\partial r} + \eta\,\nabla\cdot\underline{u} \tag{4.12}$$

$$\tau_{r\theta} = \mu\left(\frac{1}{r}\frac{\partial u}{\partial\theta} + r\frac{\partial v/r}{\partial r}\right) \tag{4.13}$$

$$\tau_{\theta\theta} = 2\mu\left(\frac{1}{r}\frac{\partial v}{\partial\theta} + \frac{u}{r}\right) + \eta\,\nabla\cdot\underline{u} \tag{4.14}$$

$$\nabla\cdot\underline{u} = \frac{1}{r}\frac{\partial ru}{\partial r} + \frac{1}{r}\frac{\partial v}{\partial\theta} \tag{4.15}$$

$$\frac{D}{Dt} = \frac{\partial}{\partial t} + u\frac{\partial}{\partial r} + \frac{v}{r}\frac{\partial}{\partial\theta} \tag{4.16}$$

Energy equation:

$$\rho c_v\frac{DT}{Dt} = -p\left(\frac{1}{r}\frac{\partial ru}{\partial r} + \frac{1}{r}\frac{\partial v}{\partial\theta}\right) + \Phi + \frac{1}{r}\frac{\partial}{\partial r}\left(kr\frac{\partial T}{\partial r}\right) + \frac{1}{r^2}\frac{\partial}{\partial\theta}\left(k\frac{\partial T}{\partial\theta}\right) \tag{4.17}$$

$$\Phi = \frac{1}{4}\left(\eta - \frac{2}{3}\mu\right)(\nabla\cdot\underline{u})^2 + 2\mu\left[\left(\frac{\partial u}{\partial r}\right)^2 + \frac{1}{2}\left(\frac{1}{r}\frac{\partial u}{\partial\theta} + r\frac{\partial}{\partial r}\frac{v}{r}\right)^2 + \left(\frac{1}{r}\frac{\partial v}{\partial\theta} + \frac{u}{r}\right)^2\right] \tag{4.18}$$

4.4 2 Dimensional Axisymmetric Flow: Cylindrical Polar Coordinates

$(z, r)(u, v)\ (\frac{\partial}{\partial\theta} = 0)$

Continuity equation:

$$\frac{\partial\rho}{\partial t} + \frac{\partial\rho u}{\partial z} + \frac{1}{r}\frac{\partial\,\rho vr}{\partial r} = 0 \tag{4.19}$$

z-momentum equation:

$$\rho\frac{Du}{Dt} = -\frac{\partial p}{\partial z} + \frac{\partial\tau_{zz}}{\partial z} + \frac{1}{r}\frac{\partial\,r\tau_{zr}}{\partial r} \tag{4.20}$$

r-momentum equation:

$$\rho\frac{Dv}{Dt} = -\frac{\partial p}{\partial r} + \frac{1}{r}\frac{\partial\,r\tau_{rr}}{\partial r} + \frac{\partial\tau_{zz}}{\partial z} \tag{4.21}$$

$$\tau_{zz} = 2\mu\frac{\partial u}{\partial z} + \eta\,\nabla\cdot\underline{u} \tag{4.22}$$

$$\tau_{rr} = 2\mu\frac{\partial v}{\partial r} + \eta\,\nabla\cdot\underline{u} \tag{4.23}$$

$$\tau_{rz} = \mu\left(\frac{\partial u}{\partial r} + \frac{\partial v}{\partial z}\right) \tag{4.24}$$

$$\nabla\cdot\underline{u} = \frac{\partial u}{\partial z} + \frac{1}{r}\frac{\partial\,rv}{\partial r} \tag{4.25}$$

$$\frac{D}{Dt} = \frac{\partial}{\partial t} + u\frac{\partial}{\partial z} + v\frac{\partial}{\partial r} \tag{4.26}$$

Energy equation:

$$\rho c_v\frac{DT}{Dt} = -p\left(\frac{\partial u}{\partial z} + \frac{1}{r}\frac{\partial\,rv}{\partial r}\right) + \Phi + \frac{\partial}{\partial z}\left(k\frac{\partial T}{\partial z}\right) + \frac{1}{r}\frac{\partial}{\partial r}\left(kr\frac{\partial T}{\partial r}\right) \tag{4.27}$$

$$\Phi = \frac{1}{4}\left(\eta - \frac{2}{3}\mu\right)(\nabla\cdot\underline{u})^2 + 2\mu\left[\left(\frac{\partial u}{\partial z}\right)^2 + \frac{1}{2}\left(\frac{\partial u}{\partial z} + \frac{\partial v}{\partial r}\right)^2 + \left(\frac{\partial v}{\partial r}\right)^2\right] \tag{4.28}$$

Vorticity:

$$\nabla\times\underline{u} = \omega_\theta = \frac{\partial v}{\partial z} - \frac{\partial u}{\partial r} \tag{4.29}$$

April 23, 2001

4.5   2 Dimensional Flow: Spherical Polar Coordinates

$(r, \phi)(u, v)$ $\left(\frac{\partial}{\partial \theta} = 0\right)$

r-momentum equation:

$$\rho \left(\frac{Du}{Dt} - \frac{v^2}{r} \right) = -\frac{\partial p}{\partial r} + \frac{1}{r^2} \frac{\partial}{\partial r} \left(r^2 \tau_{rr} \right) + \frac{1}{r \sin \phi} \frac{\partial}{\partial \phi} \left(\tau_{r\phi} \sin \phi \right) - \frac{\tau_{\phi\phi}}{r} \tag{4.30}$$

ϕ-momentum equation:

$$\rho \left(\frac{Dv}{Dt} + \frac{uv}{r} \right) = -\frac{\partial p}{\partial \phi} + \frac{1}{r^2} \frac{\partial}{\partial r} \left(r^2 \tau_{r\phi} \right) + \frac{1}{r \sin \phi} \frac{\partial}{\partial \phi} \left(\tau_{\phi\phi} \sin \phi \right) + \frac{\tau_{r\phi}}{r} \tag{4.31}$$

$$\tau_{rr} = 2\mu \frac{\partial u}{\partial r} + \eta \, \nabla \cdot \underline{u} \tag{4.32}$$

$$\tau_{\phi\phi} = 2\mu \left(\frac{1}{r} \frac{\partial v}{\partial \phi} + \frac{u}{r} \right) + \eta \, \nabla \cdot \underline{u} \tag{4.33}$$

$$\tau_{r\phi} = \mu \left(\frac{1}{r} \frac{\partial u}{\partial \phi} + r \frac{\partial}{\partial r} \frac{v}{r} \right) \tag{4.34}$$

$$\nabla \cdot \underline{u} = \frac{1}{r^2} \frac{\partial \, r^2 u}{\partial r} + \frac{1}{r \sin \phi} \frac{\partial}{\partial \phi} (v \sin \phi) \tag{4.35}$$

$$\frac{D}{Dt} = \frac{\partial}{\partial t} + u \frac{\partial}{\partial r} + \frac{v}{r} \frac{\partial}{\partial \phi} \tag{4.36}$$

Vorticity:

$$\nabla \times \underline{u} = \omega_\theta = \frac{1}{r} \frac{\partial r v}{\partial r} - \frac{1}{r} \frac{\partial u}{\partial \phi} \tag{4.37}$$

4.5.1   Stream Function

$$u = \frac{1}{r^2 \sin \phi} \frac{\partial \Psi}{\partial \phi}, \qquad v = -\frac{1}{r \sin \phi} \frac{\partial \Psi}{\partial r} \tag{4.38}$$

April 23, 2001

5 Dimensions

L	length	meter (m)
M	mass	kilogram (kg)
T	time	second (s)
θ	temperature	Kelvin (K)
I	current	Ampere (A)

5.1 Some derived dimensional units

force	Newton (N)	MLT^{-2}
pressure	Pascal (Pa)	$ML^{-1}T^{-2}$
	bar $= 10^5$ Pa	
energy	Joule (J)	ML^2T^{-2}
frequency	Hertz (Hz)	T^{-1}
power	Watt (W)	ML^2T^{-3}
viscosity (μ)	Pa s	$ML^{-1}T^{-1}$

5.2 Conventional Dimensionless Numbers

Reynolds	Re	$\rho U L / \mu$
Mach	Ma	U/c
Prandtl	Pr	$\mu c_P / k = \nu / \kappa$
Strouhal	St	fL/U
Knudsen	Kn	Λ/L
Peclet	Pe	UL/κ
Schmidt	Sc	ν/D
Lewis	Le	D/κ
Rayleigh	Ra	$\dfrac{gL^3}{\nu\kappa}$

Reference conditions: U, velocity; μ, vicosity; D, mass diffusivity; k, thermal conductivity; L, length scale; f, frequency; c, sound speed; Λ, mean free path; c_P, specific heat at constant pressure.

5.3 Parameters for Air and Water

Values given for nominal standard conditions 20 C and 1 bar.

			Air	Water
dynamic viscosity	μ	(kg/ms)	1.8×10^{-5}	1.00×10^{-3}
kinematic viscosity	ν	(m^2/s)	1.5×10^{-5}	1.0×10^{-6}
thermal conductivity	k	(W/mK)	2.54×10^{-2}	0.589
thermal diffusivity	κ	(m^2/s)	2.1×10^{-5}	1.4×10^{-7}
specific heat	c_p	(J/kgK)	1004.	4182.
sound speed	c	(m/s)	343.3	1484
density	ρ	(kg/m^3)	1.2	998.
gas constant	R	(m^2/s^{2}K)	287	462.
thermal expansion	α	(K^{-1})	3.3×10^{-4}	2.1×10^{-4}
isentropic compressibility	κ_s	(Pa^{-1})	7.01×10^{-6}	4.5×10^{-10}
Prandtl number	Pr		.72	7.1
Fundamental derivative	Γ		1.205	4.4
ratio of specific heats	γ		1.4	1.007
Grüneisen coefficient	G		0.40	0.11

April 23, 2001

6 Thermodynamics

6.1 Thermodynamic potentials and fundamental relations

The first thermodynamic potential derives from the first law

$$
\begin{aligned}
dq &= de + dw \\
&= de + p\,dv
\end{aligned}
\tag{6.1}
$$

and the definition of entropy

$$
dq = T\,ds \,,
\tag{6.2}
$$

namely,

energy $e(s,v)$

$$
de = T\,ds - p\,dv
\tag{6.3}
$$

$$
\left(\frac{\partial e}{\partial s}\right)_v = T \,; \qquad \left(\frac{\partial e}{\partial v}\right)_s = -p
\tag{6.4}
$$

Then, others follow from the definitions of new state variables,

enthalpy, $\quad h(s,p) = e + pv$

$$
dh = T\,ds + v\,dp
\tag{6.5}
$$

$$
\left(\frac{\partial h}{\partial s}\right)_p = T \,; \qquad \left(\frac{\partial h}{\partial p}\right)_s = v
\tag{6.6}
$$

Helmholtz free energy, $\quad f(T,v) = e - Ts$

$$
df = -s\,dT - p\,dv
\tag{6.7}
$$

$$
\left(\frac{\partial f}{\partial T}\right)_v = -s \,; \qquad \left(\frac{\partial f}{\partial v}\right)_T = -p
\tag{6.8}
$$

Gibbs free energy, $\quad g(T,p) = h - Ts$

$$
dg = -s\,dT + v\,dp
\tag{6.9}
$$

$$
\left(\frac{\partial g}{\partial T}\right)_p = -s \,; \qquad \left(\frac{\partial g}{\partial p}\right)_T = v
\tag{6.10}
$$

6.2 Maxwell relations

$$
\left(\frac{\partial T}{\partial v}\right)_s = -\left(\frac{\partial p}{\partial s}\right)_v
\tag{6.11}
$$

$$
\left(\frac{\partial T}{\partial p}\right)_s = \left(\frac{\partial v}{\partial s}\right)_p
\tag{6.12}
$$

$$
\left(\frac{\partial s}{\partial v}\right)_T = \left(\frac{\partial p}{\partial T}\right)_v
\tag{6.13}
$$

$$
\left(\frac{\partial s}{\partial p}\right)_T = -\left(\frac{\partial v}{\partial T}\right)_p
\tag{6.14}
$$

Thermodynamic differentials:

Given that $f(x, y, z) = 0$, then

$$x(y, z): \qquad dx = \left(\frac{\partial x}{\partial y} \right)_z dy + \left(\frac{\partial x}{\partial z} \right)_y dz \tag{6.15}$$

$$y(x, z): \qquad dy = \left(\frac{\partial y}{\partial x} \right)_z dx + \left(\frac{\partial y}{\partial z} \right)_x dz \tag{6.16}$$

Eliminating dy,

$$dx \left(1 - \left(\frac{\partial x}{\partial y} \right)_z \left(\frac{\partial y}{\partial x} \right)_z \right) = dz \left(\left(\frac{\partial x}{\partial z} \right)_y + \left(\frac{\partial x}{\partial y} \right)_z \left(\frac{\partial y}{\partial z} \right)_x \right) \tag{6.17}$$

so

$$\left(\frac{\partial x}{\partial y} \right)_z = \frac{1}{\left(\frac{\partial y}{\partial x} \right)_z} \tag{6.18}$$

$$\left(\frac{\partial x}{\partial z} \right)_y = - \left(\frac{\partial x}{\partial y} \right)_z \left(\frac{\partial y}{\partial z} \right)_x \tag{6.19}$$

6.3   Reciprocity relations and the equations of state

The thermal equation of state is a relation $\mathrm{fnc}(p, v, T) = 0$. The caloric equation of state is a relation $\mathrm{fnc}(e, v, T) = 0$ or $\mathrm{fnc}(h, p, T) = 0$. From the thermodynamic identity Eq. 6.5,

$$ds = \frac{1}{T} dh - \frac{v}{T} dp. \tag{6.20}$$

Considering h to be $h(p, T)$, expanding the differential dh in terms of partials and substituting, gives

$$ds = \frac{1}{T} \left(\frac{\partial h}{\partial T} \right)_p dT + \frac{1}{T} \left[\left(\frac{\partial h}{\partial p} \right)_T - v \right] dp. \tag{6.21}$$

Now, treating $s(p, T)$ and expanding, we can identify

$$\left(\frac{\partial s}{\partial T} \right)_p = \frac{1}{T} \left(\frac{\partial h}{\partial T} \right)_p \tag{6.22}$$

$$\left(\frac{\partial s}{\partial p} \right)_T = \frac{1}{T} \left[\left(\frac{\partial h}{\partial p} \right)_T - v \right]. \tag{6.23}$$

Performing the same steps on Eq. 6.3 with $e(v, T)$, $s(v, T)$ gives

$$\left(\frac{\partial s}{\partial T} \right)_v = \frac{1}{T} \left(\frac{\partial e}{\partial T} \right)_v \tag{6.24}$$

$$\left(\frac{\partial s}{\partial v} \right)_T = \frac{1}{T} \left[\left(\frac{\partial e}{\partial v} \right)_T + p \right]. \tag{6.25}$$

Eqs. 6.22 – 6.25 are the reciprocity relations. Cross differentiating the LHS of Eqs. 6.22 and 6.23 and Eqs. 6.24 and 6.25, respectively, permits the elimination of s, resulting in relations between the thermal and caloric equations of state,

$$\left(\frac{\partial h}{\partial p} \right)_T = v - T \left(\frac{\partial v}{\partial T} \right)_p \tag{6.26}$$

$$\left(\frac{\partial e}{\partial v} \right)_T = T \left(\frac{\partial p}{\partial T} \right)_v - p \tag{6.27}$$

Given an empirical determination of the (p, v, T) behavior of a substance, these equations permit the construction of the caloric EOS by integration along appropriate paths.

6.4 Various defined quantities

The specific heat is defined as

$$c \equiv \frac{dq}{dt} \, . \tag{6.28}$$

At constant pressure,

$$c_p = T \left(\frac{\partial s}{\partial T} \right)_p = \left(\frac{\partial h}{\partial T} \right)_p \, . \tag{6.29}$$

where Eq. 6.5 has been used for for the second step. Similarly,

$$c_v = T \left(\frac{\partial s}{\partial T} \right)_v = \left(\frac{\partial e}{\partial T} \right)_v \, . \tag{6.30}$$

Thus,

$$\text{specific heat at constant volume} \quad c_v \equiv \left(\frac{\partial e}{\partial T} \right)_v \tag{6.31}$$

$$\text{specific heat at constant pressure} \quad c_p \equiv \left(\frac{\partial h}{\partial T} \right)_p \tag{6.32}$$

$$\text{ratio of specific heats} \quad \gamma \equiv \frac{c_p}{c_v} \tag{6.33}$$

$$\text{sound speed} \quad c \equiv \sqrt{\left(\frac{\partial p}{\partial \rho} \right)_s} \tag{6.34}$$

$$\text{coefficient of thermal expansion} \quad \alpha \equiv \frac{1}{v} \left(\frac{\partial v}{\partial T} \right)_p \tag{6.35}$$

$$\text{isothermal compressibility} \quad k_T \equiv -\frac{1}{v} \left(\frac{\partial v}{\partial p} \right)_T \tag{6.36}$$

$$\text{isentropic compressibility} \quad k_s \equiv -\frac{1}{v} \left(\frac{\partial v}{\partial p} \right)_s = \frac{1}{\rho a^2} \tag{6.37}$$

Specific heat relationships

$$k_T = \gamma k_s \quad \text{or} \quad \left(\frac{\partial p}{\partial v} \right)_s = \gamma \left(\frac{\partial p}{\partial v} \right)_T \tag{6.38}$$

$$c_p - c_v = -T \left(\frac{\partial p}{\partial v} \right)_T \left(\frac{\partial v}{\partial T} \right)_p^2 \tag{6.39}$$

Sound speed (squared)

$$a^2 \equiv \left(\frac{\partial p}{\partial \rho} \right)_s \tag{6.40}$$

$$= -v^2 \left(\frac{\partial p}{\partial v} \right)_s \tag{6.41}$$

$$= \frac{v}{k_s} \tag{6.42}$$

$$= \gamma \frac{v}{k_T} \tag{6.43}$$

Fundamental derivative

$$\Gamma \equiv \frac{v^3}{2a^2}\left(\frac{\partial^2 p}{\partial v^2}\right)_s \tag{6.44}$$

$$= \frac{a^4}{2v^3}\left(\frac{\partial^2 v}{\partial p^2}\right)_s \tag{6.45}$$

$$= 1 + \frac{\rho}{2a^2}\left(\frac{\partial^2 p}{\partial \rho^2}\right)_s \tag{6.46}$$

$$= 1 + \frac{\rho}{a}\left(\frac{\partial a}{\partial \rho}\right)_s = \frac{\rho}{a}\left(\frac{\partial \rho a}{\partial \rho}\right)_s \tag{6.47}$$

$$= 1 + \rho a \left(\frac{\partial a}{\partial p}\right)_s \tag{6.48}$$

$$= \frac{1}{2}\left(\frac{v^2}{a^2}\left(\frac{\partial^2 h}{\partial v^2}\right)_s + 1\right) \tag{6.49}$$

$$\equiv \beta + 1 \tag{6.50}$$

Grüneisen Coefficient

$$G \equiv v\left(\frac{\partial p}{\partial e}\right)_v \tag{6.51}$$

$$= \frac{v}{T}\left(\frac{\partial p}{\partial s}\right)_v \tag{6.52}$$

$$= -\frac{v}{T}\left(\frac{\partial T}{\partial v}\right)_s \tag{6.53}$$

$$= \frac{v\alpha}{c_p k_s} = \frac{\alpha a^2}{c_p} \tag{6.54}$$

$$= \frac{v\alpha}{c_v k_T} \tag{6.55}$$

6.5 Perfect Gas Equations of State

Thermally perfect gas:

$$p = \rho R T \tag{6.56}$$

Calorically perfect gas:

$$c_p, \; c_v = \text{const} \tag{6.57}$$

so,

$$\gamma = \frac{c_p}{c_v} = \text{const} \tag{6.58}$$

$$R = c_p - c_v = \text{const} \tag{6.59}$$

Therefore,

$$h = c_p T + \text{const} \tag{6.60}$$

$$e = c_v + \text{const} \tag{6.61}$$

April 23, 2001

Entropy:

$$ds \;=\; \frac{de + p\,dv}{T} \;=\; c_v \frac{dT}{T} + R\frac{dv}{v} \tag{6.62}$$

$$s - s_0 \;=\; c_v \, \ln\frac{T}{T_0} + R \, \ln\frac{v}{v_0} \;, \tag{6.63}$$

and, from the *dh* identity,

$$s - s_0 \;=\; c_p \, \ln\frac{T}{T_0} - R \, \ln\frac{p}{p_0} \;. \tag{6.64}$$

For constant entropy

$$\frac{dT}{T} \;=\; -\frac{R}{c_v}\frac{dv}{v} \;=\; \frac{R}{c_p}\frac{dp}{p} \;, \tag{6.65}$$

so

$$\frac{dp}{p} \;=\; \gamma\frac{d\rho}{\rho} \;; \qquad p \;\sim\; \rho^{\gamma} \tag{6.66}$$

Canonical Equation of State
From the last equation

$$s \;\sim\; c_p \, \ln\left(T\,p^{-\frac{R}{c_p}}\right) \tag{6.67}$$

$$e^{\frac{s}{c_p}} \;\sim\; T\,p^{-\frac{R}{c_p}} \tag{6.68}$$

With

$$h \;=\; c_p\,T \tag{6.69}$$

we get

$$h(s,p) \;=\; \text{const } c_p \, e^{\frac{s}{c_p}} \, p^{\frac{R}{c_p}} \tag{6.70}$$

$$e(s,v) \;=\; \text{const } c_v \, e^{\frac{s}{c_v}} \, v^{\frac{R}{c_v}} \tag{6.71}$$

Other equations

$$\left(\frac{\partial p}{\partial \rho}\right)_s \;=\; \gamma\left(\frac{\partial p}{\partial \rho}\right)_T \;=\; \gamma RT \tag{6.72}$$

$$a^2 \;=\; \gamma RT \;=\; \gamma\frac{p}{\rho} \tag{6.73}$$

$$\Gamma \;=\; \frac{\gamma + 1}{2} \;; \qquad \beta \;=\; \frac{\gamma - 1}{2} \tag{6.74}$$

$$G \;=\; \gamma - 1 \;. \tag{6.75}$$

7 Quasi-onedimensional flow

The quasi-1D model is a useful approximation for describing many fluid flows. The flow is taken to be "mostly" in the x direction, and gradients in the y direction are assumed much smaller than those in the x direction. A control volume is shown in Fig. 7. A is the cross-sectional area and S is the area of the
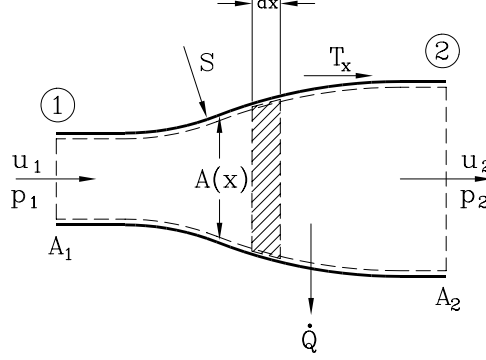
Figure 7. Control volume for quasi-1D flow.

control volume. T_x is the viscous traction force, and $\dot{Q}$ is the energy loss per unit area per unit time.

The equations are

$$\frac{d}{dt} \int_V \rho \, dV - \rho_1 u_1 A_1 + \rho_2 u_2 A_2 \;=\; 0 \tag{7.1}$$

$$\frac{d}{dt} \int_V \rho \underline{u} \, dV - \rho_1 u_1^2 A_1 + \rho_2 u_2^2 A_2 \;=\; p_1 A_1 - p_2 A_2 + \int p \, dA + T_x dS \tag{7.2}$$

$$\frac{d}{dt} \int_V \rho \left(e + \frac{u^2}{2} \right) dV - \rho_1 \left(e_1 + \frac{u_1^2}{2} \right) u_1 A_1 + \rho_2 \left(e_2 + \frac{u_2^2}{2} \right) u_2 A_2 \;=\; p_1 u_1 A_1 - p_2 u_2 A_2 - \int \dot{Q} \, dS \tag{7.3}$$

From the definitions of the areas,

$$dV \;=\; A \, dx \tag{7.4}$$

$$dS \;=\; P \, dx \tag{7.5}$$

$$dA \;=\; \frac{dA}{dx} \, dx \;, \tag{7.6}$$

where P is the perimeter of the channel. To get the equations in differential form the volume is shrunk in a limiting process to the one shown hatched. The various integrals and differences become,

$$\int f \, dV \;\longrightarrow\; f \, dV \;=\; f A \, dx \tag{7.7}$$

$$\frac{d}{dt} \int f \, dV \;\longrightarrow\; \frac{\partial}{\partial f A} t \, dx \tag{7.8}$$

$$f_2 - f_1 \;\longrightarrow\; df \;=\; \frac{\partial f}{\partial x} dx \tag{7.9}$$

$$\int f \, dA \;\longrightarrow\; f \frac{dA}{dx} dx \tag{7.10}$$

$$\int f \, dS \;\longrightarrow\; f P \, dx \;, \tag{7.11}$$

with the result

$$\frac{\partial \rho A}{\partial t} + \frac{\partial \rho u A}{\partial x} = 0 \tag{7.12}$$

$$\frac{\partial \rho u A}{\partial t} + \frac{\partial \rho u^2 A}{\partial x} + \frac{\partial p A}{\partial x} - p\frac{dA}{dx} = PT_x \tag{7.13}$$

$$\frac{\partial \rho \left(e + \frac{u^2}{2}\right) A}{\partial t} + \frac{\partial \rho \left(e + \frac{u^2}{2}\right) uA}{\partial x} + \frac{\partial puA}{\partial x} = -\dot{Q}P \tag{7.14}$$

Differentiate the nonsteady and convective terms on the left hand side of all equations and use the continuity equation in the momentum and energy equations. But, first, in the energy equation combine the *pua* term with the first x derivative, setting $h_t = e + p/rho + u^2/2$, and arrange to get the same form in the time derivative by adding and subtracting $A\partial p/\partial t$. Further, assume that the area does not vary in time, $A = A(x)$. Then, there results,

$$\frac{\partial \rho}{\partial t} + \frac{\partial \rho u}{\partial x} = -\frac{\rho u}{A}\frac{dA}{dx} \tag{7.15}$$

$$\frac{Du}{Dt} = \frac{\partial u}{\partial t} + u\frac{\partial u}{\partial x} = -\frac{1}{\rho}\frac{\partial p}{\partial x} + f \tag{7.16}$$

$$\frac{Dh_t}{Dt} = \frac{\partial h_t}{\partial t} + u\frac{\partial h_t}{\partial x} = \frac{1}{\rho}\frac{\partial p}{\partial t} - \frac{\dot{Q}P}{\rho A} , \tag{7.17}$$

where $f = PT_x/\rho A$ is the friction force per unit mass.

These equations apply to general substances. The continuity equation now contains a source term, induced by changes of area.

7.1 The Euler equations

Strictly 1D flow ($dA/dx = 0$) with $f = \dot{Q} = 0$ is governed by Euler's equations for an inviscid, nonheatconducting fluid in 1D flow. In convective form,

$$\frac{\partial \rho}{\partial t} + \frac{\partial \rho u}{\partial x} = 0 \tag{7.18}$$

$$\frac{Du}{Dt} = -\frac{1}{\rho}\frac{\partial p}{\partial x} \tag{7.19}$$

$$\frac{Dh_t}{Dt} = \frac{1}{\rho}\frac{\partial p}{\partial t} . \tag{7.20}$$

7.2 Steady flow

$$\frac{d\rho u A}{dx} = 0 \tag{7.21}$$

$$u\frac{du}{dx} + \frac{1}{\rho}\frac{dp}{dx} = f \tag{7.22}$$

$$\frac{dh}{dx} + u\frac{du}{dx} = -\dot{q} , \tag{7.23}$$

where $\dot{q} = P\dot{Q}/\rho u A$, the energy loss per unit mass per unit length of channel.

April 23, 2001

7.2.1 Quasi-1D Steady Euler flow

$f = \dot{q} = 0$.

$$d(\rho u A) \;=\; 0 \tag{7.24}$$

$$dp + \rho u\, du \;=\; 0 \tag{7.25}$$

$$dh + u\, du \;=\; 0 \tag{7.26}$$

$$ds \;=\; 0\,. \tag{7.27}$$

The continuity and energy equations integrate immediately

$$\rho u A \;=\; \dot{m} \;=\; \text{const} \tag{7.28}$$

$$h + \frac{u^2}{2} \;=\; h_t \;=\; \text{const}\,, \tag{7.29}$$

but the momentum equation doesn't. Note that the energy integral is actually more general than this and applies in the steady flow of an inviscid nonheatconducting fluid in any dimensionality along a streamline (Eq. 2.26).

The momentum equation says

$$\boxed{dp \;=\; -\rho u\, du\,,} \tag{7.30}$$

so ρu is a form of *impedance*.

With

$$T\,ds \;=\; dh - \frac{1}{\rho}dp \tag{7.31}$$

and Eq. 7.25, Eq. 7.26 gives

$$ds \;=\; 0, \tag{7.32}$$

so Euler flow is isentropic. Then, the definition $(\partial p/\partial \rho)_s = a^2$ gives

$$\boxed{dp \;=\; a^2\, d\rho\,.} \tag{7.33}$$

Using this in the momentum equation gives

$$\boxed{\frac{d\rho}{\rho} \;=\; -M^2\frac{du}{u}} \tag{7.34}$$

Dependence on the area is introduced by considering the continuity equation. Differentiating the continuity equation logarithmically and eliminating ρ from Eq. 7.34 yields,

$$\boxed{\frac{du}{u} \;=\; \frac{1}{M^2-1}\frac{dA}{A}\,.} \tag{7.35}$$

This shows that in subsonic flow a fluid acclerates in a converging channel, while in supersonic flow it accelerates in a diverging channel.

The material property β is (Eq. 6.50)

$$\left(\frac{\partial a}{\partial p}\right)_s \;\equiv\; \frac{\beta}{\rho a}\,. \tag{7.36}$$

Thus,

$$\boxed{\frac{da}{a} \;=\; \beta \frac{dp}{\rho a^2} \;=\; \beta \frac{d\rho}{\rho} \;.}$$
(7.37)

Then, from the momentum equation, for this isentropic flow

$$\boxed{\frac{da}{a} \;=\; -\beta \, M^2 \, \frac{du}{u} \;.}$$
(7.38)

Note the significance of $\beta = 0$. From the logarithmic differentiation of the definition of Mach number, there results,

$$\frac{dM}{M} \;=\; (1 + \beta M^2)\frac{du}{u}$$
(7.39)

and, with (7.35),

$$\boxed{\frac{dA}{A} \;=\; \frac{M^2 - 1}{1 + \beta M^2}\frac{dM}{M} \;=\; \frac{M^2 - 1}{\Gamma M^2 - (M^2 - 1)}\frac{dM}{M} \;.}$$
(7.40)

With monatonically changing M, dA must change sign at $M = 1$. Whether A is minimum or maximum depends on the derivative of Eq. 7.40 at $M = 1$,

$$\frac{1}{A}\left(\frac{d^2 A}{dx^2}\right)_{M=1} \;=\; \frac{2}{\Gamma}\left(\frac{dM}{dx}\right)^2 \;,$$
(7.41)

where $\Gamma = \beta + 1$ is the "fundamental derivative" (Eq. 6.44). Thus, whether the throat is convergent or divergent depends on the sign of Γ.

Eq. 7.40 can be used in the above relations to show how (u, ρ, h) depend on M,

$$\boxed{\frac{du}{u} \;=\; \frac{1}{1 + \beta M^2}\frac{dM}{M}}$$
(7.42)

$$\boxed{\frac{d\rho}{\rho} \;=\; -\frac{M^2}{1 + \beta M^2}\frac{dM}{M}}$$
(7.43)

$$\boxed{\frac{dh}{2(h - h_t)} \;=\; \frac{1}{1 + \beta M^2}\frac{dM}{M} \;,}$$
(7.44)

where the last expression is obtained from the energy equation

$$dh \;=\; -u \, du \;=\; -u^2 \, \frac{du}{u} \;=\; 2(h - h_t)\frac{du}{u} \;,$$
(7.45)

where $h_t = h + u^2/2$. Also, from $dh = T \, ds + v \, dp$ we have

$$\left(\frac{\partial h}{\partial p}\right)_s \;=\; \frac{1}{\rho} \;,$$
(7.46)

so, from the definition of β,

$$\boxed{dh \;=\; \frac{1}{\beta} \, a \, da}$$
(7.47)

7.3 Constant β (or Γ) fluid

So far, differential relations have been written for a general fluid in terms of the material properties β and Γ. If they are constant, the equations may be integrated. This approximation holds for local regions in p-v space far from a zero of Γ. Integrating Eq. 7.47 gives,

$$a^2 = 2\beta h , \tag{7.48}$$

which may be compared to $a^2 = \gamma RT$ for a perfect gas.

With constant β, Eq. 7.37 integrates to give

$$\frac{a}{a_t} = \left(\frac{\rho}{\rho_t}\right)^{\beta} , \tag{7.49}$$

Eq. 7.43 to give

$$\frac{\rho_t}{\rho} = \left(1 + \beta M^2\right)^{\frac{1}{2\beta}} , \tag{7.50}$$

and Eq. 7.40 to give

$$\left(\frac{A}{A^*}\right)^2 = \frac{1}{M^2}\left(\frac{1 + \beta M^2}{1 + \beta}\right)^{\frac{1+\beta}{\beta}} . \tag{7.51}$$

With Eq. 7.49,

$$\frac{a_t}{a} = \left(1 + \beta M^2\right)^{\frac{1}{2}} , \tag{7.52}$$

and with Eq. 7.48,

$$\frac{h_t}{h} = 1 + \beta M^2 . \tag{7.53}$$

Finally, we get the pressure from the definition of sound speed,

$$\frac{dp}{\rho_t a_t^2} = \frac{\rho a^2}{\rho_t a_t^2}\frac{d\rho}{\rho} . \tag{7.54}$$

Substituting Eq. 7.43 and integrating gives

$$\frac{p - p_t}{\rho_t a_t^2} = \frac{1}{2\beta + 1}\left\{\left(1 + \beta M^2\right)^{-\frac{2\beta+1}{2\beta}} - 1\right\} \tag{7.55}$$

If outside of the region $-\frac{1}{2} < \beta < 0$ where the exponent $(2\beta + 1)/2\beta$ is negative, we require that $\lim_{M\to+\infty} p = 0$, then from that limit Eq. 7.55 gives

$$p_t = \frac{1}{2\beta + 1}\rho_t a_t^2 , \tag{7.56}$$

so,

$$\frac{p_t}{p} = \left(1 + \beta M^2\right)^{\frac{2\beta+1}{2\beta}} \tag{7.57}$$

7.4 Perfect Gas

Relations for Quasi-1D flow of a perfect gas are directly obtained by substituting $\beta = (\gamma - 1)/2$,

$$\frac{h_t}{h} = 1 + \frac{\gamma - 1}{2} M^2 . \tag{7.58}$$

$$\frac{a_t}{a} = \left(1 + \frac{\gamma - 1}{2} M^2\right)^{\frac{1}{2}} , \tag{7.59}$$

$$\frac{\rho_t}{\rho} = \left(1 + \frac{\gamma - 1}{2} M^2\right)^{\frac{1}{\gamma - 1}} , \tag{7.60}$$

$$\frac{p_t}{p} = \left(1 + \frac{\gamma - 1}{2} M^2\right)^{\frac{\gamma}{\gamma - 1}} \tag{7.61}$$

$$\frac{u}{a_t} = \frac{u}{a} \frac{a}{a_t} = \left\{\frac{M^2}{1 + \frac{\gamma - 1}{2} M^2}\right\}^{\frac{1}{2}} \tag{7.62}$$

$$\frac{A}{A^*} = \frac{1}{M} \left\{\frac{2}{\gamma + 1}\left(1 + \frac{\gamma - 1}{2} M^2\right)\right\}^{\frac{\gamma + 1}{2(\gamma - 1)}} . \tag{7.63}$$

For high Mach number flow ($M \longrightarrow \infty$) and fixed stagnation conditions,

$$h, \; a, \; \rho, \; p \; \longrightarrow \; 0 \tag{7.64}$$

$$u \longrightarrow \sqrt{\frac{2}{\gamma - 1}} \, a_t = \sqrt{2 \, h_t} \equiv u_m \tag{7.65}$$

$$\frac{A}{A^*} \longrightarrow \infty \tag{7.66}$$

At sonic conditions ($M = 1$),

$$\frac{h_t}{h^*} = \frac{\gamma + 1}{2} \tag{7.67}$$

$$\frac{a_t}{a^*} = \left(\frac{\gamma + 1}{2}\right)^{\frac{1}{2}} \tag{7.68}$$

$$\frac{\rho_t}{\rho^*} = \left(\frac{\gamma + 1}{2}\right)^{\frac{1}{\gamma - 1}} \tag{7.69}$$

$$\frac{p_t}{p^*} = \left(\frac{\gamma + 1}{2}\right)^{\frac{\gamma}{\gamma - 1}} = 1.893 = \frac{1}{0.528} \text{ for } \gamma = \frac{7}{5} \tag{7.70}$$

$$\frac{u^*}{a_t} = \frac{a^*}{a_t} = \sqrt{\frac{2}{\gamma + 1}} < 1 \tag{7.71}$$

$$u_m = \sqrt{\frac{\gamma + 1}{\gamma - 1}} \, a^* \tag{7.72}$$

$$\dot{m}^* = \rho^* u^* A^* = \left(\frac{2}{\gamma + 1}\right)^{\frac{\gamma + 1}{2(\gamma - 1)}} \rho_t \, a_t \, A^* \tag{7.73}$$

April 23, 2001

From Eqs. 7.59and 7.68,

$$\frac{a^*}{a} = \left[1 + \frac{\gamma - 1}{\gamma + 1}\left(M^2 - 1\right)\right]^{\frac{1}{2}} . \tag{7.74}$$

Dynamic pressure.

$$q \equiv \frac{1}{2}\rho u^2 \tag{7.75}$$

$$= \frac{\gamma}{2}M^2 p , \tag{7.76}$$

$$\frac{q}{p_t} = \frac{\gamma}{2}M^2\left(1 + \frac{\gamma - 1}{2}M^2\right)^{-\frac{\gamma}{\gamma - 1}} \tag{7.77}$$

Note:

$$\frac{p + q}{p_t} = \frac{1 + \frac{\gamma}{2}M^2}{\left(1 + \frac{\gamma - 1}{2}M^2\right)^{\frac{\gamma}{\gamma - 1}}} \neq 1 \tag{7.78}$$

Fig. 8 shows the progression A⟶B⟶C that takes place as the exit pressure p_e is decreased, starting
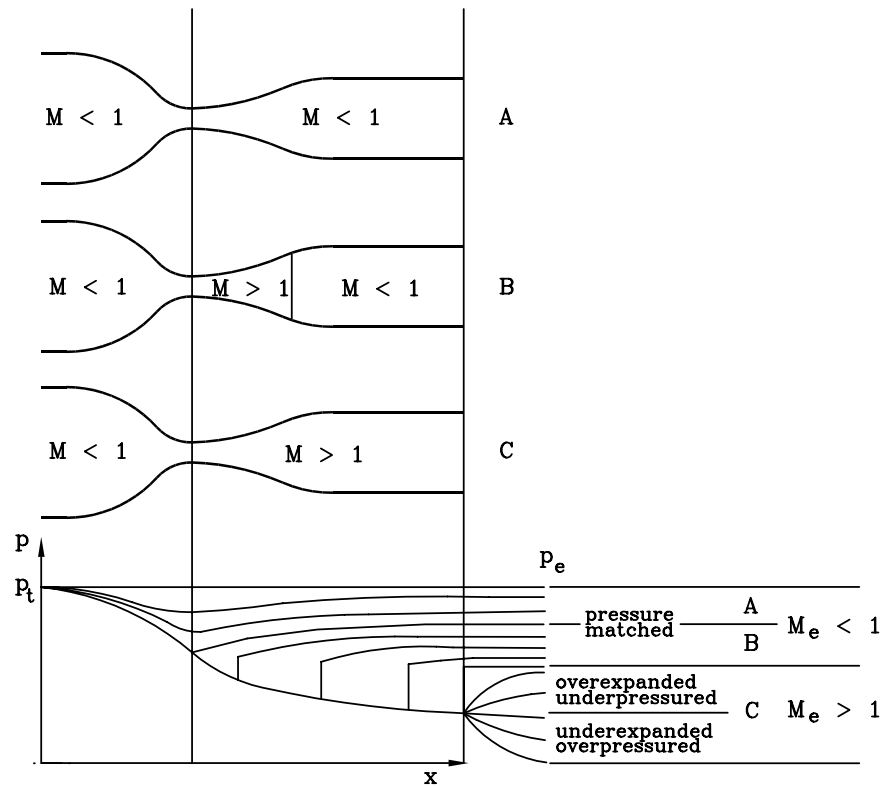
Figure 8. Pressure profiles in compressible channel flow as the exit pressure is reduced.

at $p_e = p_t$, with p_t held constant. Condition B is called the shock-in-nozzle configuration.

8   Normal Shock Waves

8.1   Steady Frame

Constant area, adiabatic, frictionless flow.

Shock waves are discontinuities, so we must use an integral formulation to see how they behave. The control volume shown in Fig. 9 yields the following equations for the conservation of mass, momentum,
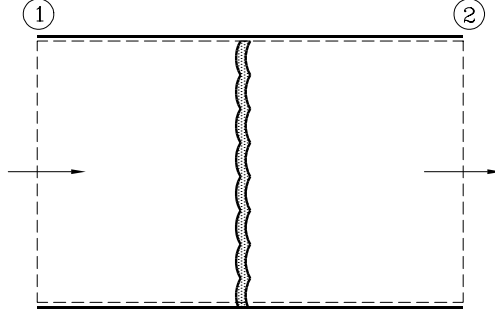
Figure 9. Control volume for calculating the shock jump conditions.

energy and entropy,

$$\rho_2 \, u_2 \;=\; \rho_1 \, u_1 \;=\; \dot{m} \tag{8.1}$$

$$p_2 - p_1 \;=\; \rho_1 \, u_1^2 - \rho_2 \, u_2^2 \tag{8.2}$$

$$h_2 - h_1 \;=\; \frac{u_1^2}{2} - \frac{u_2^2}{2} \tag{8.3}$$

$$s_2 - s_1 \;>\; 0 \tag{8.4}$$

Other forms of the continuity equation are

$$\frac{\Delta u}{u_1} \;=\; -\frac{\Delta \rho}{\rho_2} \;=\; \frac{\Delta v}{v_1} \; . \tag{8.5}$$

Combining mass and momentum,

$$p_2 - p_1 \;=\; \rho_1 \, u_1 (u_1 - u_2) \tag{8.6}$$

$$\Delta p \;=\; -\dot{m} \, \Delta u \; . \tag{8.7}$$

The following useful forms result,

$$\frac{\Delta p}{\Delta \rho} \;=\; u_1 \, u_2 \tag{8.8}$$

$$\frac{\Delta p}{\Delta v} \;=\; -\dot{m}^2 \tag{8.9}$$

$$\Delta p \Delta v \;=\; -(\Delta u)^2 \; , \tag{8.10}$$

Compare Eq. 8.9 with

$$\left(\frac{\partial p}{\partial v} \right)_s \;=\; -\rho^2 \, a^2 \tag{8.11}$$

Combining with the energy equation gives,

$$\Delta h \;=\; \bar{v} \Delta p \tag{8.12}$$

$$\Delta e \;=\; -\bar{p} \Delta v \; , \tag{8.13}$$

April 23, 2001

where $\overline{(\ )} \equiv [(\ )_2 + (\ )_1]/2$. Compare with

$$\left(\frac{\partial h}{\partial p}\right)_s = v \tag{8.14}$$

$$\left(\frac{\partial e}{\partial p}\right)_s = -p \tag{8.15}$$

Fig. 10 shows the graphical interpretation of some of these results. The chord between the upstream and
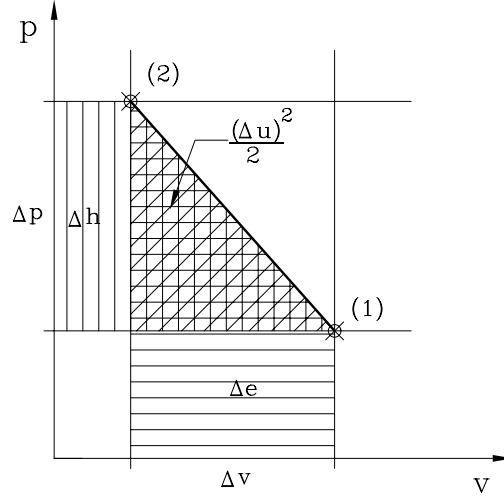
Figure 10. Graphical interpretation of the shock jump conditions.

downstream states is known as the Rayleigh Line.

8.1.1   Calculating Shock Conditions for Real Fluids

Useful forms of the equations for use in iterative numerical calculations on substances with complex equations of state are,

$$p_2 = p_1 + \rho_1 u_1 \left(1 - \frac{\rho_1}{\rho_2}\right) \tag{8.16}$$

$$h_2 = h_1 + \frac{u_1^2}{2}\left[1 - \left(\frac{\rho_1}{\rho_2}\right)^2\right]. \tag{8.17}$$

The approach is to guess ρ_1/ρ_2, calculate p_2 and h_2 and then calculate a new value of ρ_1/ρ_2 from the equations of state.

8.1.2   Expansion about the upstream state (weak shocks)

General fluid.
An important constraint on the entropy can be obtained by expanding

$$\Delta e = -\overline{p}\Delta v = -\frac{\Delta p}{2}\Delta v - p_1 \Delta v \tag{8.18}$$

about the upstream state $(\ )_1$. Taking $e(s,v)$,

$$\Delta e = \left(\frac{\partial e}{\partial v}\right)_s \Delta v + \left(\frac{\partial^2 e}{\partial v^2}\right)_s \frac{\Delta v^2}{2} + \left(\frac{\partial^3 e}{\partial v^3}\right)_s \frac{\Delta v^3}{6} + \cdots + \left(\frac{\partial e}{\partial s}\right)_v \Delta s + \cdots \tag{8.19}$$

April 23, 2001

$$\doteq \ -p\Delta v \ - \ \left(\frac{\partial p}{\partial v}\right)_s \frac{\Delta v^2}{2} \ - \ \left(\frac{\partial^2 p}{\partial v^2}\right)_s \frac{\Delta v^3}{6} \ + \ T\Delta s \ , \tag{8.20}$$

the substitutions for the thermodynamic derivatives being derived from Eq. 6.3. Similarly, with $p(s,v)$,

$$\Delta p \ = \ \left(\frac{\partial p}{\partial v}\right)_s \Delta v \ + \ \left(\frac{\partial^2 p}{\partial v^2}\right)_s \frac{\Delta v^2}{2} + \cdots \ , \tag{8.21}$$

so,

$$\frac{\Delta p}{2}\Delta v \doteq \ \left(\frac{\partial p}{\partial v}\right)_s \frac{\Delta v^2}{2} \ + \ \left(\frac{\partial^2 p}{\partial v^2}\right)_s \frac{\Delta v^3}{4} \ . \tag{8.22}$$

Using Eqs. 8.20 and 8.22 in 8.18 yields

$$T\Delta s \ = \ -\frac{1}{12}\left(\frac{\partial^2 p}{\partial v^2}\right)_s \Delta v^3 \ + \cdots \ . \tag{8.23}$$

Therefore,

$$T_1\Delta s \doteq \ - \ \frac{\Gamma_1}{6} \, a_1^2 \, \frac{\Delta v^3}{v_1^3} \ . \tag{8.24}$$

The entropy increase is third order in the shock strength. For $\Gamma > 0$ ("normal" fluids) the second law requires that shock waves be compression shocks, for $\Gamma < 0$, expansion shocks.

With this information, we can now qualitatively construct the *locus of downstream states* ② for shocks, known as the *shock adiabat*, or the *Hugoniot*. The shock adiabat has the same slope and curvature as the isentrope through the upstream state ① . When isentropes are concave up (normal fluids), the Hugoniot near the upstream state (weak shocks) must also be concave up, and *vice versa*. Fig. 11 shows how the Hugoniot looks compared to the isentropes and the Rayleigh line for 4 different cases, depending on the signs of Γ (Eq. 6.44) and G (Eq. 6.52).

8.1.3   Perfect gas

For a perfect gas the enthalpy h in terms of p and v is

$$h \ = \ \frac{\gamma}{\gamma - 1} \, pv \ , \tag{8.25}$$

so eliminating h from Eq. 8.12 gives the Hugoniot explicity,

$$\frac{p_2}{p_1} \ = \ \frac{\dfrac{\gamma+1}{\gamma-1} - \dfrac{v_2}{v_1}}{\dfrac{\gamma+1}{\gamma-1}\dfrac{v_2}{v_1} - 1} \tag{8.26}$$

Fig. 12 shows its behavior. Note the intercept $v_{int} = (\gamma+1)/(\gamma-1)$ on the x-axis and the asymptote $v_{min} = (\gamma-1)/(\gamma+1)$ for large p_2/p_1. The isentrope, $p \sim v^{-\gamma}$, through (1,1) is the long-dashed line.

Another form of (8.26) is

$$\frac{\Delta v}{v_1} \ = \ -\frac{2\dfrac{\Delta p}{p_1}}{2\gamma + (\gamma+1)\dfrac{\Delta p}{p_1}} \ , \tag{8.27}$$

which, with

$$\frac{\Delta p}{p_1} \ = \ -\gamma \, M_1^2 \, \frac{\Delta v}{v_1} \ , \tag{8.28}$$
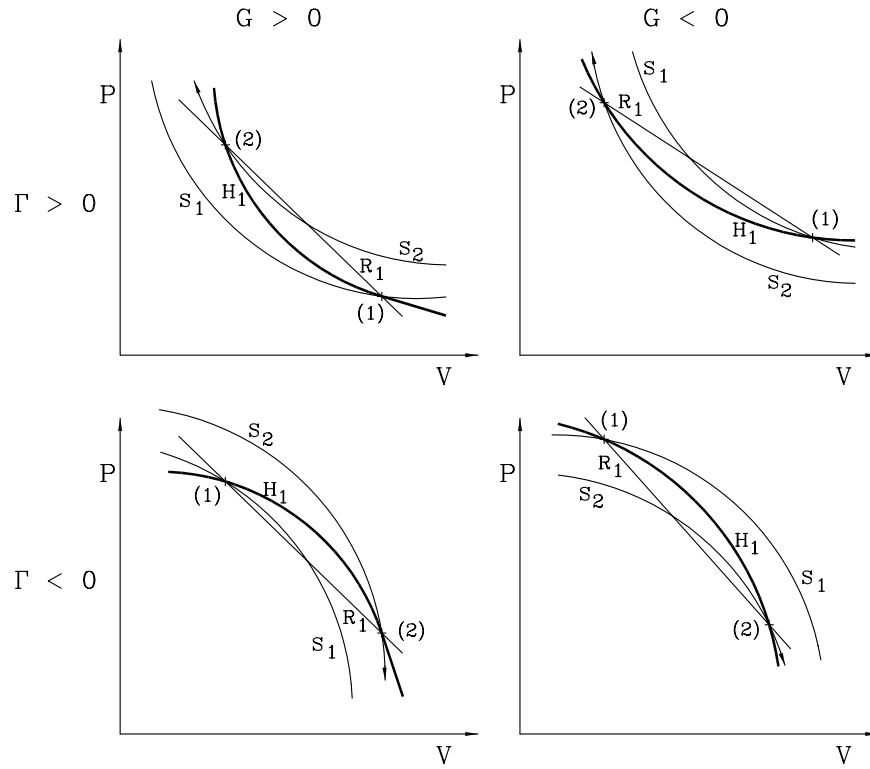
Figure 11. Qualitative behavior of the shock adiabat for general fluids.
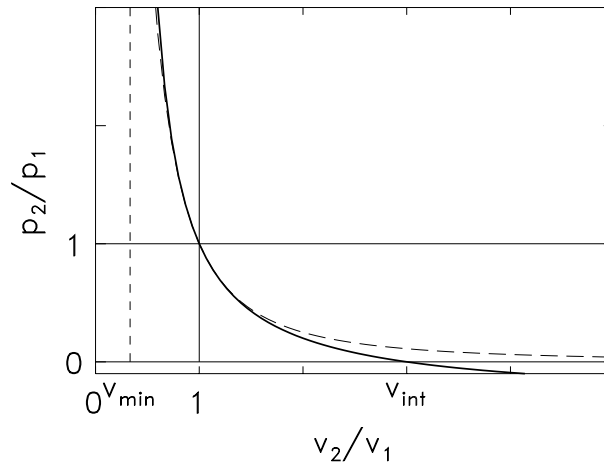
Figure 12. The shock Hugoniot for a perfect gas.

gives

$$\frac{p_2}{p_1} \;=\; 1 \;+\; \frac{2\gamma}{\gamma+1}\,(M_1^2 - 1) \tag{8.29}$$

From the other equations of this section, there follows a series of relations for the important parameters

for perfect gases in terms of M_1^2,

$$\frac{\Delta u}{a_1} = -\frac{2}{\gamma+1}\frac{M_1^2-1}{M_1} \tag{8.30}$$

$$\frac{\rho_2}{\rho_1} = \frac{M_1^2}{1+\frac{\gamma-1}{\gamma+1}(M_1^2-1)} \tag{8.31}$$

$$\frac{h_2}{h_1} = \frac{T_2}{T_1} = 1 + \frac{2(\gamma-1)}{(\gamma+1)^2}\frac{(M_1^2-1)(1+\gamma M_1^2)}{M_1^2} \tag{8.32}$$

$$M_2^2 = \frac{1+\frac{\gamma-1}{\gamma+1}(M_1^2-1)}{1+\frac{2\gamma}{\gamma+1}(M_1^2-1)} \tag{8.33}$$

For strong shocks ($M_1^2 \gg 1$),

$$\frac{p_2}{p_1} \longrightarrow \frac{2\gamma}{\gamma+1}M_1^2 \tag{8.34}$$

$$\frac{u_2}{a_1} \longrightarrow \frac{\gamma-1}{\gamma+1}M_1 \tag{8.35}$$

$$\frac{\rho_2}{\rho_1} \longrightarrow \frac{\gamma+1}{\gamma-1} \tag{8.36}$$

$$\frac{h_2}{h_1} \longrightarrow \frac{2\gamma(\gamma-1)}{(\gamma+1)^2}M_1^2 \tag{8.37}$$

$$M_2^2 \longrightarrow \frac{\gamma-1}{2\gamma} \tag{8.38}$$

For weak shocks ($M_1^2 - 1 \ll 1$),

$$\frac{\Delta p}{p_1} \doteq \frac{2\gamma}{\gamma+1}(M_1^2-1) \tag{8.39}$$

$$\frac{\Delta u}{a_1} \doteq -\frac{2}{\gamma+1}(M_1^2-1) \tag{8.40}$$

$$\frac{\Delta \rho}{\rho_1} \doteq \frac{2}{\gamma+1}(M_1^2-1) \tag{8.41}$$

$$\frac{\Delta T}{T_1} \doteq \frac{2(\gamma-1)}{\gamma+1}(M_1^2-1) \tag{8.42}$$

$$1 - M_2^2 \doteq M_1^2 - 1 \tag{8.43}$$

Prandtl's relation. For a perfect gas

$$h = \frac{a^2}{\gamma-1}. \tag{8.44}$$

Thus the energy equation can be written

$$\frac{u_1^2}{2} + \frac{a_1^2}{\gamma-1} = \frac{u_2^2}{2} + \frac{a_2^2}{\gamma-1} = h_t. \tag{8.45}$$

With

$$\frac{h_t}{h^*} = \frac{\gamma+1}{2} \quad \text{and} \quad \frac{h^*}{a^{*2}} = \frac{1}{\gamma-1}, \tag{8.46}$$

h_t can be written

$$h_t = \frac{\gamma + 1}{2(\gamma - 1)} a^{*2} . \tag{8.47}$$

Thus

$$
\begin{aligned}
a_1^2 &= \frac{\gamma + 1}{2} a^{*2} - \frac{\gamma - 1}{2} u_1^2 \\
a_2^2 &= \frac{\gamma + 1}{2} a^{*2} - \frac{\gamma - 1}{2} u_2^2 .
\end{aligned}
\tag{8.48}
$$

Here $(\ )^*$ is the fictitious state that is arrived at by compressing (expanding) state 1 (2) *isentropically* to sonic conditions. The momentum equation

$$p_2 - p_1 = \rho_1 u_1^2 - \rho_2 u_2^2 \tag{8.49}$$

can be rewritten

$$u_1 - u_2 = \frac{p_2}{\rho_2 u_2} - \frac{p_1}{\rho_1 u_1} = \frac{a_2^2}{\gamma u_2} - \frac{a_1^2}{\gamma u_1} \tag{8.50}$$

Substituting (8.48) into (8.50) gives, after cancelation,

$$u_1 u_2 = a^{*2} \tag{8.51}$$

For weak shock waves, a^* is very close to $a_1 = a_2$, so the left hand side must be also. Thus weak shocks move at the speed of sound and in the limit are acoustic waves. It follows that for shocks of finite strength, one of the velocities must be supersonic and the other must be subsonic. For perfect gases we have seen that only compression shocks satisfy the second law, **so u_1 is supersonic and u_2 is subsonic**. It can be shown that the supersonic-subsonic relation is required by basic considerations of causality, for all materials.

8.2 Nonsteady Frame

General fluid.
'Til now, we have treated shocks in a steady frame. However, by a Galilean transformation the shock jump conditions can be expressed in a general, nonsteady frame. The conserved velocities are:

1. Δu the change of fluid (particle) velocity across the shock.

2. u_S the velocity of the shock *relative to the fluid ahead.*

The correspondence between the notation in the two frames is:

Steady	Nonsteady
u_1	u_S
$u_1 - u_2$	Δu

For the "shock-tube" frame, in which the fluid ahead of the shock is at rest (see Fig. 13), $\Delta u = u_2$. Convenient forms of the equations of motion for a general nonsteady frame are,

$$\frac{\Delta u}{u_S} = \frac{\Delta \rho}{\rho_2} = -\frac{\Delta v}{v_1} ; \qquad (\Delta u)^2 = -\Delta p\, \Delta v \tag{8.52}$$

$$\Delta p = \rho_1 u_S\, \Delta u \tag{8.53}$$

$$\Delta h = \bar{v}\, \Delta p , \tag{8.54}$$

where $(\ )_1$ and $(\ )_2$ refer to the thermodynamic states ahead of and behind the wave, respectively.

April 23, 2001

8.2.1 Reflected shock waves

When a shock reflects from the solid end of a tube, the interaction is shown in space-time in Fig. 13. The important result implied by the boundary condition $u_5 = 0$ imposed by the presence of the wall is
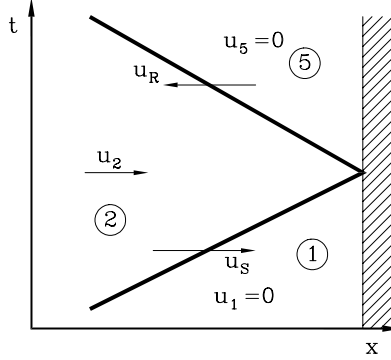
Figure 13. Schematic of a shock wave reflecting from a solid wall

that the fluid velocity jump across both waves is the same, $\Delta u_R = \Delta u_S = u_2$. For the incident wave, from Eq. 8.52,

$$\frac{u_2}{u_S} = \frac{\rho_2 - \rho_1}{\rho_2} \tag{8.55}$$

and for the reflected wave

$$\frac{u_2}{u_R + u_2} = \frac{\rho_5 - \rho_2}{\rho_5} . \tag{8.56}$$

From the last equation, we get u_R in terms of the unknown ρ_5,

$$u_R = \frac{u_2}{\dfrac{\rho_5}{\rho_2} - 1} . \tag{8.57}$$

From the momentum equation for the reflected shock

$$p_5 - p_2 = \rho_2(u_R + u_2)u_2 \tag{8.58}$$

Using continuity,

$$p_5 = p_2 + \frac{\rho_5\, u_2^2}{\dfrac{\rho_5}{\rho_2} - 1} , \tag{8.59}$$

and, from the energy equation,

$$h_5 - h_2 = \frac{v_2 + v_5}{2}(p_5 - p_2) \tag{8.60}$$

$$= \frac{\rho_5 + \rho_2}{2\rho_2} \frac{u_2^2}{\dfrac{\rho_5}{\rho_2} - 1} , \tag{8.61}$$

so,

$$h_5 = h_2 + \frac{u_2^2}{2} \frac{\dfrac{\rho_5}{\rho_2} + 1}{\dfrac{\rho_5}{\rho_2} - 1} \tag{8.62}$$

These relations can be used to calculate the reflected shock jump conditions for any equation of state.

April 23, 2001

Perfect gas. From the last form of Eq. 8.52 a *p-v* relation can be derived,

$$(p_5 - p_2)(v_5 - v_2) = (p_2 - p_1)(v_2 - v_1) , \tag{8.63}$$

or, in terms of pressure ratios $P_R = p_5/p_2$ and $P_S = p_2/p_1$,

$$(P_R - 1)\frac{\Delta v_R}{v_2} = \frac{(P_S - 1)\dfrac{\Delta v_S}{v_1}}{P_S\left(\dfrac{\Delta v_S}{v_1} + 1\right)} , \tag{8.64}$$

with the introduction of obvious temporary notation. With use of Eq. 8.27 Δv for both the incident and reflected waves can be eliminated to yield a remarkably simple relationship between pressure ratios,

$$\frac{p_5}{p_2} = \frac{(3\gamma - 1)\dfrac{p_2}{p_1} - (\gamma - 1)}{(\gamma - 1)\dfrac{p_2}{p_1} + (\gamma + 1)} . \tag{8.65}$$

Other simple results include

$$\frac{M_{1R}^2 - 1}{M_{1R}} = \frac{a_1}{a_2}\frac{M_S^2 - 1}{M_S} \tag{8.66}$$

$$\frac{u_R + u_2}{u_S} = M_S^{-2}\frac{p_2}{p_1} \tag{8.67}$$

$$\frac{p_5 - p_2}{p_2} = \gamma\frac{\rho_2 - \rho_1}{\rho_1} \tag{8.68}$$

$$\frac{u_S - u_2}{a_2} = \frac{a_2}{u_S + u_R} \tag{8.69}$$

$$\frac{u_R}{a_1} = \frac{1 + 2\frac{\gamma - 1}{\gamma + 1}(M_S^2 - 1)}{M_S} \tag{8.70}$$

$$\frac{p_5 - p_1}{p_1} = 2\frac{p_2 - p_1}{p_1}\frac{1 + \left(\frac{1}{2} + \frac{\gamma - 1}{\gamma + 1}\right)(M_S^2 - 1)}{1 + \frac{\gamma - 1}{\gamma + 1}(M_S^2 - 1)} \tag{8.71}$$

$$\frac{T_5 - T_1}{T_1} = 4\frac{\gamma - 1}{\gamma + 1}\frac{M_S^2 - 1}{M_S}\left[1 + \left(\frac{1}{2} + \frac{\gamma - 1}{\gamma + 1}\right)(M_S^2 - 1)\right] \tag{8.72}$$

where $M_{1R} = (u_R + u_2)/a_2$.

9   Frictional Flow – Fanno Flow

Constant area, one-dimensional adiabatic flow.   This treatment can be taken as a model for compressible flow in a pipe when the pipe is small enough that viscous friction becomes important.

The equations of motion are

$$d(\rho u) = 0 \tag{9.1}$$

$$u\,du + \frac{1}{\rho}\,dp = f\,dx \tag{9.2}$$

$$dh + u\,du = 0 \tag{9.3}$$

$f = PT_x/\rho A$ is the force per unit mass. The Fanning skin friction coefficient C_f is defined by $T_x = \frac{1}{2}\rho u^2 C_f$, so another form for f is

$$f = 2\,C_f\,\frac{u^2}{D} \;, \tag{9.4}$$

where D is the hydraulic diameter. The Darcy friction factor is

$$\lambda = 4\,C_f \;. \tag{9.5}$$

To analize Fanno flow, the "good" equations, mass and energy, are used to write a relation between thermodynamic variables. They may be integrated to yield

$$\rho u = \dot{m} \tag{9.6}$$

$$h + \frac{u^2}{2} = h_t \;, \tag{9.7}$$

or,

$$\boxed{h + \frac{\dot{m}^2 v^2}{2} = h_t \;.} \tag{9.8}$$

Thus, for frictional flow we are interested in the h-v plane. Eq. 9.8 is sketched in Fig. 14.
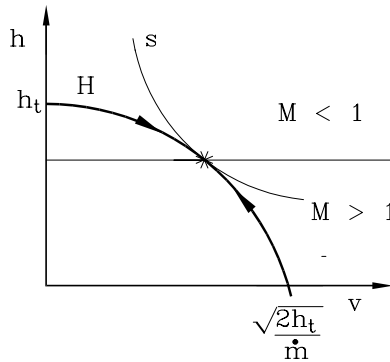
Figure 14. The h-v plane for a Fanno Flow, $\dot{m}, h_t = \text{const.}$

From the dh thermodynamic identity we can obtain an expression for ds,

$$T\,ds = dh - v\,dp \tag{9.9}$$

$$= -u\,du + u\,du - f\,dx \tag{9.10}$$

April 23, 2001

The second law says that the entropy must increase. Therefore,

$$\frac{ds}{dx} = -\frac{f}{T} \geq 0 . \tag{9.11}$$

Thus, $\boxed{f < 0}$. In order to satisfy the 2nd law, the traction force must act as a drag.

9.1 dh/dv and tangency

Combining the continuity and energy equation gives a relation for dh/dv, the slope of the Fanno process on the h-v plane.

$$\frac{du}{u} = \frac{dv}{v} \tag{9.12}$$

$$dh = -u^2 \frac{du}{u} , \tag{9.13}$$

so,

$$\frac{dh}{dv} = -\frac{u^2}{v} . \tag{9.14}$$

Compare with

$$\left(\frac{\partial h}{\partial v}\right)_s = \left(\frac{\partial h}{\partial p}\right)_s \left(\frac{\partial p}{\partial v}\right)_s = -\frac{a^2}{v} . \tag{9.15}$$

Thus, if an isentrope is tangent to $h(v)$ for a Fanno flow, as indicated in Fig. 14. the flow must be sonic there. This point is indicated by the star in Fig. 14.

9.2 Curvature of the isentropes in the h-v plane

The criterion for isentrope curvature is of course different in (h, v) than in (p, v),

$$\left(\frac{\partial^2 h}{\partial v^2}\right)_s = \frac{\partial}{\partial v}\left(v \frac{\partial p}{\partial v}\right) \tag{9.16}$$

$$= \left(\frac{\partial p}{\partial v}\right)_s + v \left(\frac{\partial^2 p}{\partial v^2}\right)_s . \tag{9.17}$$

Therefore,

$$\frac{v^2}{2a^2}\left(\frac{\partial^2 h}{\partial v^2}\right)_s = \frac{v^3}{2a^2}\left(\frac{\partial^2 p}{\partial v^2}\right)_s - \frac{1}{2} \tag{9.18}$$

$$= \Gamma - \frac{1}{2} \tag{9.19}$$

$$= \beta + \frac{1}{2} . \tag{9.20}$$

Thus, the isentrope shown in Fig. 14 is for $\Gamma > \frac{1}{2}$. A straight-line isentrope tangent at $*$ would have $\Gamma = \frac{1}{2}$.

9.3 Entropy

In order to see what direction the flow moves with positive dx on the h-v plane, we obtain a relevant expression for the entropy and use the 2nd law. From

$$T \, ds = dh + v \, dp \tag{9.21}$$

and

$$dp = \left(\frac{\partial p}{\partial v}\right)_s dv + \left(\frac{\partial p}{\partial s}\right)_v ds \qquad (9.22)$$

we get

$$\left[T + v \left(\frac{\partial p}{\partial s}\right)_v\right] ds = -(u^2 - a^2)\frac{dv}{v} . \qquad (9.23)$$

With

$$\left(\frac{\partial p}{\partial s}\right)_v = -\left(\frac{\partial p}{\partial v}\right)_s \left(\frac{\partial v}{\partial T}\right)_v \left(\frac{\partial T}{\partial s}\right)_p \qquad (9.24)$$

$$= \frac{T}{v}\frac{\alpha a^2}{c_p} = \frac{T}{v}G , \qquad (9.25)$$

where G is the Grüneisen parameter, (9.23) becomes

$$\boxed{T\,ds = -\frac{u^2 - a^2}{1 + G}\frac{dv}{v}} \qquad (9.26)$$

Thus, for $\alpha > 0$, in order to have $ds/dx > 0$ in the subsonic region $dv > 0$, and in the supersonic region $dv < 0$. This result is indicated schematically in Fig. 14 by the arrows. Friction in a pipe flow forces the flow toward choking, either from the subsonic or the supersonic side.

April 23, 2001

10   Flow with Heat Addition – Rayleigh Flow

Constant area, one-dimensional frictionless nonadiabatic flow.
Now the equations of motion are

$$d(\rho u) = 0 \tag{10.1}$$

$$u\,du + \frac{1}{\rho}\,dp = 0 \tag{10.2}$$

$$dh + u\,du = -q\,dx \tag{10.3}$$

$q = P\dot{Q}/\rho u A$ is the heat lost per unit mass per unit length of channel. The Stanton number St is defined by

$$St \equiv -\frac{\dot{Q}}{\rho u h} = \frac{Aq}{hP} = \frac{D}{4h}\,q\,, \tag{10.4}$$

where, again, D is the hydraulic diameter.

The "good" equations are now mass and momentum. Integrating,

$$\rho u = \dot{m}\,; \qquad u = \dot{m}\,v \tag{10.5}$$

$$(\rho u)\,u + p = I\,, \tag{10.6}$$

so

$$p = I - \dot{m}^2\,v\,. \tag{10.7}$$

The Rayleigh flow executes a straight line in the p-v plane, the Rayleigh line, indicated in Fig. 15.
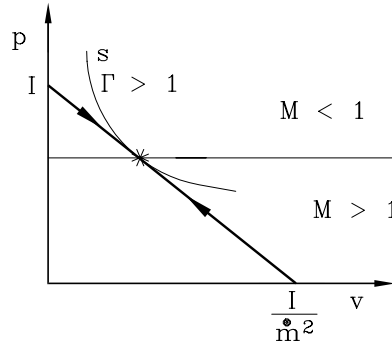
Figure 15. p-v plane for a Rayleigh process

10.1   Tangency

Differential relations given by continuity and momentum are

$$\frac{du}{u} = -\frac{d\rho}{\rho} \tag{10.8}$$

$$dp = -\rho u^1 \frac{du}{u}\,. \tag{10.9}$$

Therefore,

$$\frac{dp}{d\rho} = u^2\,; \qquad \frac{dp}{dv} = -\frac{u^2}{v^2} \tag{10.10}$$

April 23, 2001

Compare with

$$\left(\frac{\partial p}{\partial \rho}\right)_s = a^2 . \tag{10.11}$$

Thus, again, where an isentrope is tangent to the Rayleigh line, there is a sonic point, indicated by the $*$.

10.2 Entropy

Taking $s(p, v)$,

$$ds = \left(\frac{\partial s}{\partial p}\right)_v dp + \left(\frac{\partial s}{\partial v}\right)_p dv . \tag{10.12}$$

With the chain rule for $(\partial s/\partial p)_v$, $dp/dv = -u^2/v^2$ and $(\partial p/\partial v)_s = -a^2/v^2$, we get

$$ds = -\left(\frac{\partial s}{\partial v}\right)_p (M^2 - 1) \, dv . \tag{10.13}$$

Now

$$\left(\frac{\partial s}{\partial v}\right)_p = \left(\frac{\partial s}{\partial T}\right)_p \left(\frac{\partial T}{\partial v}\right)_p = \frac{c_p}{\alpha v T} , \tag{10.14}$$

so finally

$$\boxed{T \, ds = \frac{a^2 - u^2}{G} \frac{dv}{v} .} \tag{10.15}$$

Increasing entropy causes the flow to progress in the direction on the p-v plane indicated by the arrows. That is, increasing entropy tends to choke a nonadiabtic pipe flow.

Whether the entropy is actually increasing or decreasing in the flow direction is determined by the sign of the heat flow in this problem. We have

$$T \, ds = dh - v \, dp = -q \, dx \tag{10.16}$$

$$\frac{ds}{dx} = -\frac{q}{T} . \tag{10.17}$$

With heat addition ($q < 0$), $ds/dx > 0$, and vice versa. As with friction, heat *addition* tends to choke a flow in a pipe.

10.3 The Mollier Diagram

Both Fanno flow and Rayleigh flow flow toward a maximum entropy in (h, s) space (see Fig. 16).
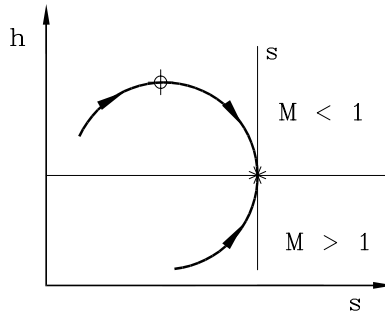
Figure 16. Rayleigh process on a Mollier Diagram

However, in a Rayleigh process there may also be a maximum in enthalpy. From the energy and mass equations,

$$dh = -u\,du - q\,dx \tag{10.18}$$

$$= -u^2\frac{dv}{v} - q\,dx \tag{10.19}$$

Substituting from Eq. 10.15,

$$dh = u^2\frac{\alpha T}{c_p}\frac{ds}{M^2 - 1} - q\,dx \tag{10.20}$$

With $\alpha > 0$, for large enough heat addition ($q < 0$), or M close enough to unity, $dh > 0$. At the maximum, $dh/ds = 0$; after a little algebra,

$$M^2 = \frac{1}{1 + \frac{a^2\alpha}{c_p}}\,. \tag{10.21}$$

For a *perfect gas*, $\alpha = 1/T$, so the enthalpy is maximum at

$$M^2 = \frac{1}{\gamma}\,. \tag{10.22}$$

11   Detonation Waves in One Dimension

Detonation waves are driven by the release of chemical energy in a combustion process at a sharp front. They move supersonically into a combustible mixture and self ignite. As a consequence, the uspstream substance is thermodynamically distinct from the combustion products downstream, so the Hugoniot does not pass smoothly through the initial point. The two possible cases are shown in the sketch. Note that
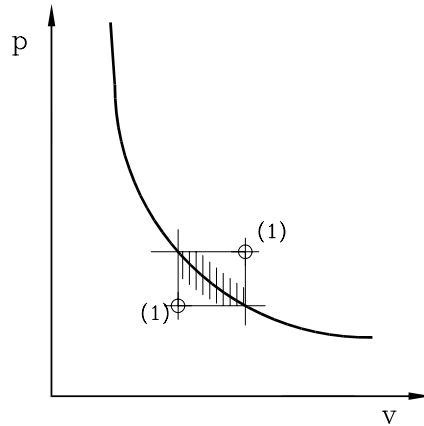
by Eq. 8.9 the cross-hatched portion of the Hugoniot is not possible. The equations of motion for this discontinuity are Eqs. 8.52 – 8.54. Here we consider the case when the Hugoniot falls above the initial state.

It is useful to study differential changes of the downstream state. Differentiating the momentum equation Eq. 8.9,

$$\frac{dp_2}{\Delta p} - \frac{dv_2}{\Delta v} \;=\; 2\frac{d\dot{m}}{\dot{m}} \;, \tag{11.1}$$

or,

$$\frac{d\dot{m}}{dv} \;=\; \frac{\dot{m}}{2\Delta p}\left(\frac{dp_2}{dv_2} - \frac{\Delta p}{\Delta v}\right) \;. \tag{11.2}$$

This shows that a tangency condition may arise; namely, the Rayleigh line may be tangent to the Hugoniot, at which point the mass flux is stationary, $d\dot{m} = 0$. This is shown on the sketch below.

April 23, 2001
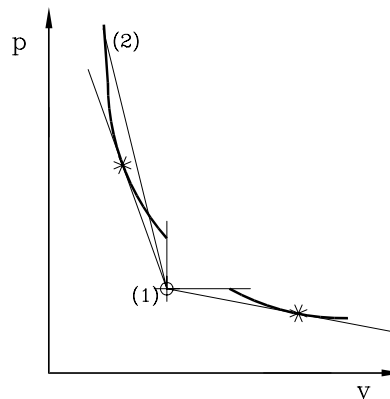
Differentiating the energy equation Eq. 8.54 and using it again to eliminate Δh,

$$dh_2 \;=\; \overline{v}\,dp_2 + \frac{\Delta p}{2}\,dv_2 \;.$$

(11.3)

Substituting this into the dh_2 thermodynamic identity gives

$$T_2\,\frac{ds_2}{dv_2} \;=\; \frac{\Delta v}{2}\left(\frac{\Delta p}{\Delta v} - \frac{dp_2}{dv_2}\right) \;.$$

(11.4)

Therefore, at the same tangency the entropy is stationary, so the isentrope is also tangent there! A consequence of this fact is that the downstream flow is sonic relative to the wave; in the steady frame,

$$\frac{\Delta p}{\Delta v} \;=\; -\frac{u_2^2}{v_2^2} \;; \qquad \left(\frac{\partial p}{\partial v}\right)_s \;=\; -\frac{a_2^2}{v_2^2} \;,$$

(11.5)

so,

$$M_2 \;=\; 1 \;.$$

(11.6)

This is indicated by the $*$ on the sketch. This important state is called the Chapman-Jouget (C-J) point.

By inspecting the geometry at the point indicated by (2), it can be seen that $M_2 < 1$ there; detonations falling above the $*$ are called *strong* detonations. Correspondingly, final states below the $*$ have supersonic downstream states, $M_2 > 1$, and are called weak detonations. Because of the supersonic condition they violate causality and are not dynamically realizable states.

Waves that expand and depressurize the flow are called deflagrations, and are not discussed here.

11.1 2-γ model of detonation waves

Perfect gas.
We assume that the upstream and downstream fluids are different perfect gases, such that

$$
\begin{aligned}
h_1 &= c_{p_1}T_1 + q \;; & h_2 &= c_{p_2}T_2 \\
p_1 &= \rho_1 R_1 T_1 \;; & p_2 &= \rho_2 R_2 T_2 \\
c_{p_1} &= \frac{\gamma_1}{\gamma_1 - 1}R_1 \;; & c_{p_2} &= \frac{\gamma_2}{\gamma_2 - 1}R_2 \;,
\end{aligned}
$$

(11.7)

where q is the heat of reaction. Using

$$h_1 \;=\; \frac{\gamma_1}{\gamma_1 - 1}\,p_1 v_1 + q$$

(11.8)

$$h_2 \;=\; \frac{\gamma_2}{\gamma_2 - 1}\,p_2 v_2$$

(11.9)

in Eq. 8.12 in the same manner as for deriving Eq. 8.26, gives the detonation Hugoniot

$$\frac{p_2}{p_1} \;=\; \frac{\dfrac{\gamma_1 + 1}{\gamma_1 - 1} - \dfrac{v_2}{v_1} + 2\gamma_1\dfrac{q}{a_1^2}}{\dfrac{\gamma_2 + 1}{\gamma_2 - 1}\dfrac{v_2}{v_1} - 1} \;.$$

(11.10)

Evaluating at $v_2/v_1 = 1$,

$$\frac{p_2}{p_1} \;=\; \frac{\gamma_2 - 1}{\gamma_1 - 1}\left[1 + \gamma_1(\gamma_1 - 1)\frac{q}{a_1^2}\right]$$

(11.11)

shows that for $\gamma_2 < \gamma_1$, which is usually the case, the Hugoniot is *below* the upstream state, while for $q > 0$, appropriate for the necessary exothermic reaction to make a detonation wave, it is *above*. It turns out that with real fuels the latter effect always dominates, *i.e.*,

$$\frac{q}{a_1^2} > \frac{\gamma_1 - \gamma_2}{\gamma_1(\gamma_1 - 1)(\gamma_2 - 1)} \ . \tag{11.12}$$

11.2   Equations in the steady frame

The momentum equation Eq. 8.2 can be written

$$p_2 \left(1 + \frac{\rho_2}{p_2} u_2^2 \right) \ = \ p_1 \left(1 + \frac{\rho_1}{p_1} u_1^2 \right) \ , \tag{11.13}$$

so,

$$\frac{p_2}{p_1} \ = \ \frac{1 + \gamma_1 M_1^2}{1 + \gamma_2 M_2^2} \ . \tag{11.14}$$

The continuity equation Eq. 8.1 can be written

$$\frac{\rho_2}{p_2} u_2 \ = \ \frac{\rho_1}{p_1} u_1 \frac{p_1}{p_2} \tag{11.15}$$

$$\frac{\gamma_2 M_2^2}{u_2} \ = \ \frac{\gamma_1 M_1^2}{u_1} \frac{p_1}{p_2} \ , \tag{11.16}$$

so,

$$\frac{u_2}{u_1} \ = \ \frac{v_2}{v_1} \ = \ \frac{\gamma_2 M_2^2}{\gamma_1 M_1^2} \frac{1 + \gamma_1 M_1^2}{1 + \gamma_2 M_2^2} \ . \tag{11.17}$$

The energy equation Eq. 8.3 becomes

$$\frac{\gamma_2}{\gamma_1 - 1} R_2 T_2 \left(1 + \frac{\gamma_2 - 1}{2} M_2^2 \right) \ = \ \frac{\gamma_1}{\gamma_1 - 1} R_1 T_1 \left(1 + \frac{\gamma_1 - 1}{2} M_1^2 \right) + q \ , \tag{11.18}$$

so,

$$\frac{T_2}{T_1} \ = \ \frac{R_1}{R_2} \frac{\gamma_1}{\gamma_2} \frac{\gamma_2 - 1}{\gamma_1 - 1} \frac{1 + \dfrac{\gamma_1 - 1}{2} M_1^2 + (\gamma_1 - 1)\dfrac{q}{a_1^2}}{1 + \dfrac{\gamma_2 - 1}{2} M_2^2} \tag{11.19}$$

Finally, from the thermal EOS

$$\frac{p_2}{p_1} \frac{v_2}{v_1} \ = \ \frac{R_2}{R_1} \frac{T_2}{T_1} \ . \tag{11.20}$$

Using this to combine all the equations gives

$$\frac{M_2^2 \left(1 + \dfrac{\gamma_2 - 1}{2} M_2^2 \right)}{\left(1 + \gamma_2 M_2^2 \right)^2} \ = \ \left(\frac{\gamma_1}{\gamma_2} \right)^2 \frac{\gamma_2 - 1}{\gamma_1 - 1} \frac{M_1^2 \left(1 + \dfrac{\gamma_1 - 1}{2} M_1^2 + (\gamma_1 - 1)\dfrac{q}{a_1^2} \right)}{\left(1 + \gamma_1 M_1^2 \right)^2} \ . \tag{11.21}$$

This is a quadratic equation for M_2^2. The two real roots give the weak and strong detonation waves. A quantitative plot of the solution for $\gamma_2 = \gamma_1$ is shown in the sketch below. The 45° line is the trivial solution $M_2 = M_1$ and applies for $q = 0$. The hyperbola passing through (1,1) for $q = 0$ is the shock wave solution. To the right of (1,1) in the 4th quadrant it is a compression shock ($M_1 > 1, M_2 < 1$), while to

April 23, 2001

$$\gamma_1 = 1.10 \qquad \gamma_2 = 1.10$$
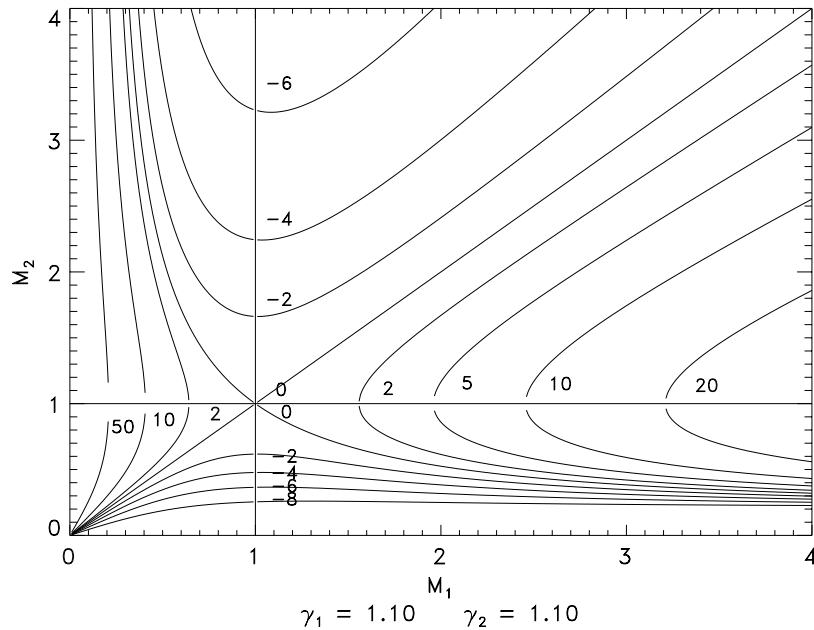
the left in the 2nd quadrant it is an expansion shock, impossible for these perfect gases. In the first and third quadrants are the weak solutions, bordering on $M_2 = M_1$, and in the 2nd and 4th quadrants are the strong solutions, bordering on the shock. In the 1st quadrant, below the 45° line $q > 0$ (detonation waves) and above $q < 0$ (refrigeration waves?), *etc.*

A case for $\gamma_2 < \gamma_1$ is shown in the last sketch. Note that $q/a_1^2 \simeq 2$ gives essentially the adiabatic shock conditions for a single-γ gas.

$$\gamma_1 = 1.40 \qquad \gamma_2 = 1.20$$

April 23, 2001
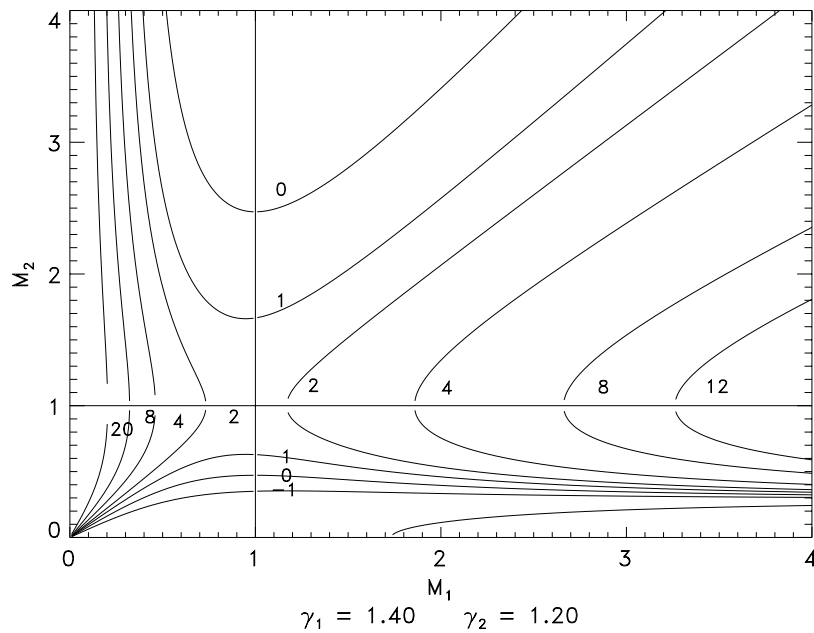
12 Nonsteady Flows

12.1 One-dimensional inviscid nonheatconducting flow

Eqs. 7.18 and 7.19, with

$$\frac{Ds}{Dt} = 0 \quad \text{or} \quad \frac{D\rho}{Dt} = \frac{1}{a^2}\frac{Dp}{Dt} \tag{12.1}$$

(see Eq. 2.30) apply to these flows. Rewriting the continuity and momentum equations, taking the continuity equation in terms of pressure,

$$\frac{\partial p}{\partial t} + u\frac{\partial p}{\partial x} + \rho a^2 \frac{\partial u}{\partial x} = 0 \tag{12.2}$$

$$\rho\frac{\partial u}{\partial t} + \rho u\frac{\partial u}{\partial x} + \frac{\partial p}{\partial x} = 0 \,. \tag{12.3}$$

Multiplying the momentum equation by a and adding and subtracting the two equations gives two more equations, in so-called characteristic form, plus the entropy equation,

$$\left[\frac{\partial}{\partial t} + (u \pm a)\frac{\partial}{\partial x}\right] p \pm \rho a \left[\frac{\partial}{\partial t} + (u \pm a)\frac{\partial}{\partial x}\right] u = 0 \tag{12.4}$$

$$\left(\frac{\partial}{\partial t} + u\frac{\partial}{\partial x}\right) s = 0 \tag{12.5}$$

The operators in square brackets are wave operators and define curves of constant phase (α, β),

$$\frac{\partial}{\partial \alpha} = \frac{\partial}{\partial t} + (u + a)\frac{\partial}{\partial x} \quad ; \quad \frac{\partial}{\partial x} = \frac{1}{2a}\left(\frac{\partial}{\partial \alpha} - \frac{\partial}{\partial \beta}\right) \tag{12.6}$$

$$\frac{\partial}{\partial \beta} = \frac{\partial}{\partial t} + (u - a)\frac{\partial}{\partial x} \quad ; \quad \frac{\partial}{\partial t} = \frac{1}{2a}\left[-(u - a)\frac{\partial}{\partial \alpha} + (u + a)\frac{\partial}{\partial \beta}\right] \,, \tag{12.7}$$

or, with $\alpha(x,t), \beta(x,t)$ and $x(\alpha,\beta), t(\alpha,\beta)$,

$$d\alpha = \frac{1}{2a}\left(dx - (u - a)dt\right) \quad ; \quad dx = (u + a)d\alpha + (u - a)d\beta \tag{12.8}$$

$$d\beta = \frac{1}{2a}\left(-dx + (u + a)dt\right) \quad ; \quad dt = d\alpha + d\beta \,. \tag{12.9}$$

Constant phase means

$$\beta = \text{const along} \quad \frac{dx}{dt} = u + a \tag{12.10}$$

$$\alpha = \text{const along} \quad \frac{dx}{dt} = u - a \,. \tag{12.11}$$

Eqs. 12.4 and 12.5 state that

$$dp \pm \rho a\, du = 0 \quad \text{along} \quad \frac{dx}{dt} = u \pm a \tag{12.12}$$

$$ds = 0 \quad \text{along} \quad \frac{dx}{dt} = u \,. \tag{12.13}$$

Compare Eq. 12.12 with Eq. 7.25, the momentum equation in quasi-1D steady flow. The difference between the two is in the "impedance," ρa *vs.* ρu. The two flows in some sense trade behavior between subsonic

April 23, 2001

and supersonic flow. Expressed in this way, the relation between dp and du, and the geometry on which they occur are transparent. However, u and a are unknowns, so, though the mathematical approach to getting a solution is evident, a closed form analytical solution is not possible.

Formally integrating,

$$\int \frac{dp}{\rho a} \pm u = \begin{matrix} P \\ Q \end{matrix} \quad \text{along} \quad \frac{dx}{dt} = u \pm a \,. \tag{12.14}$$

P and Q are the Riemann invariants.

12.2   Homentropic flow

If the entropy is the same everywhere,

$$s = s_0 \,, \tag{12.15}$$

then the number of variables is reduced by one, and we can write

$$\frac{dp}{\rho a} = \left(\frac{\partial p}{\partial a}\right)_s \frac{da}{\rho a} \,. \tag{12.16}$$

With Eq. 6.48, Eq. 12.14 becomes

$$\int \frac{da}{\Gamma(a)-1} \pm u = \begin{matrix} P \\ Q \end{matrix} \quad \text{along} \quad \frac{dx}{dt} = u \pm a \tag{12.17}$$

There are now 2 unknowns (u, a) and 2 equations.

Uniform Flow.   In uniform flow the characteristics are straight, $dx/dt = u \pm a = \text{const.}$

12.3   Simple waves

A nonuniform flow bordered on one side in (x, t) space by a uniform flow is a "simple wave." Fig. 17 shows a simple wave bordered on the left by a uniform flow, a "left-facing simple wave." The simplifying
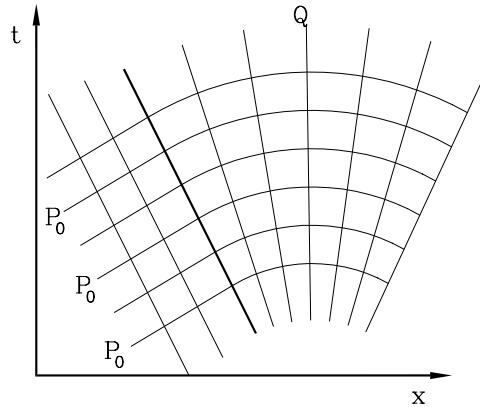
Figure 17. A nonsteady wave flow with unifom conditions on its left

thing here is that all of the P characteristics carry the same value of the P Riemann invariant, say, P_0. Thus,

$$\int \frac{da}{\Gamma(a)-1} + u = P_0 \quad \text{everywhere} \tag{12.18}$$

$$\int \frac{da}{\Gamma(a)-1} - u = Q \quad \text{along} \quad \frac{dx}{dt} = u - a \,. \tag{12.19}$$

April 23, 2001

Therefore,

$$\left.\begin{array}{rcl} \displaystyle\int \frac{da}{\Gamma(a)-1} &=& \dfrac{P_0+Q}{2} \\[2mm] u &=& \dfrac{P_0-Q}{2} \end{array}\right\} \quad \text{along} \quad \frac{dx}{dt} = u - a \,, \tag{12.20}$$

which proves that

$$u, a = \text{const} \quad \text{along} \quad \frac{dx}{dt} = u - a \,, \tag{12.21}$$

in turn showing that the Q characteristics are straight lines, as shown in Fig. 17.

We have, then, that

$$du = \mp \frac{da}{\Gamma - 1} \,; \qquad \begin{array}{c}\text{left}\\\text{right}\end{array} \text{ facing wave} \tag{12.22}$$

$$\frac{dx}{dt} = u \mp a \,; \qquad \begin{array}{c}Q\\P\end{array} \text{ straight characteristic} \tag{12.23}$$

$$\left.\begin{array}{rcl} d\left(\dfrac{dx}{dt}\right) &=& du \mp da \\[2mm] &=& \mp\dfrac{\Gamma}{\Gamma-1}\, da \end{array}\right\} \,; \qquad \begin{array}{c}Q\\P\end{array} \text{ straight characteristic} \,, \tag{12.24}$$

the last expression indicating how the slope of the straight set of characteristics changes from the head to the tail of the wave. Using these relations, we can build up Table 1 to describe the behavior of all the different cases: Cases 1 and 2 are representative of the behavior of perfect gases. In cases 3 and 4, even though the fluid is "normal," the sound speed varies oppositely to what we are used to in fluids with positive β; it increases in expansion waves and decreases in compression waves. Cases 2 and 3 give compression shocks after a certain propagation distance and case 6 gives expansion shocks because of the convergence of the characteristics.

12.4 Perfect gas

In a perfect gas $\Gamma = (\gamma + 1)/2$, so Eq. 12.17 can be integrated to give

$$a \pm \frac{\gamma - 1}{2} u = \begin{array}{c}P\\Q\end{array} \quad \text{along} \quad \frac{dx}{dt} = u \pm a \tag{12.25}$$

12.4.1 Simple Waves
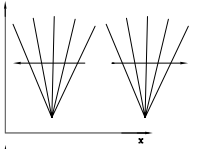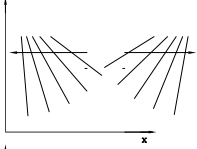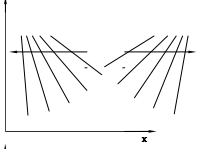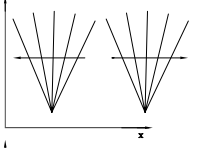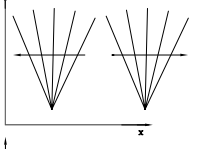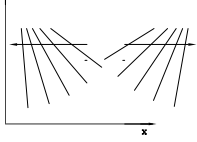
For $\begin{array}{c}\text{left}\\\text{right}\end{array}$ waves propagating into a fluid at rest $(u_1 = 0)$,

$$a \pm \frac{\gamma - 1}{2} u = a_1 \,; \quad \frac{1}{a_1}\frac{dx}{dt} = \mp 1 + \frac{\gamma + 1}{2}\frac{u}{a_1} \tag{12.26}$$

$$\frac{a}{a_1} = 1 \mp \frac{\gamma - 1}{2}\frac{u}{a_1} = \frac{1}{1 \pm \frac{\gamma-1}{2}M} \tag{12.27}$$

$$\frac{T}{T_1} = \left(1 \mp \frac{\gamma - 1}{2}\frac{u}{a_1}\right)^2 = \frac{1}{\left(1 \pm \frac{\gamma-1}{2}M\right)^2} \tag{12.28}$$

April 23, 2001

Table 1. Twelve cases for continuous nonsteady flow

		da	$\dfrac{dp}{d\rho}$	du	$d\left(\dfrac{dx}{dt}\right)$	
1.	$\begin{array}{c}\Gamma > 1 \\ \beta > 0\end{array}$	< 0	< 0 (expansion)	$\begin{array}{c}> 0 \\ < 0\end{array}$	$\begin{array}{c}> 0 \\ < 0\end{array}$	
2.		> 0	> 0 (compression)	$\begin{array}{c}< 0 \\ > 0\end{array}$	$\begin{array}{c}< 0 \\ > 0\end{array}$	
3.	$\begin{array}{c}0 < \Gamma < 1 \\ \beta < 0\end{array}$	< 0	> 0 (compression)	$\begin{array}{c}< 0 \\ > 0\end{array}$	$\begin{array}{c}< 0 \\ > 0\end{array}$	
4.		> 0	< 0 (expansion)	$\begin{array}{c}> 0 \\ < 0\end{array}$	$\begin{array}{c}> 0 \\ < 0\end{array}$	
5.	$\begin{array}{c}\Gamma < 0 \\ \beta < 0\end{array}$	< 0	> 0 (compression)	$\begin{array}{c}< 0 \\ > 0\end{array}$	$\begin{array}{c}> 0 \\ < 0\end{array}$	
6.		> 0	< 0 (expansion)	$\begin{array}{c}> 0 \\ < 0\end{array}$	$\begin{array}{c}< 0 \\ > 0\end{array}$	

$$\frac{\rho}{\rho_1} = \left(1 \mp \frac{\gamma - 1}{2}\frac{u}{a_1}\right)^{\frac{2}{\gamma - 1}} = \frac{1}{\left(1 \pm \frac{\gamma - 1}{2}M\right)^{\frac{2}{\gamma - 1}}} \qquad (12.29)$$

$$\frac{p}{p_1} = \left(1 \mp \frac{\gamma - 1}{2}\frac{u}{a_1}\right)^{\frac{2\gamma}{\gamma - 1}} = \frac{1}{\left(1 \pm \frac{\gamma - 1}{2}M\right)^{\frac{2\gamma}{\gamma - 1}}} \qquad (12.30)$$

12.4.2 Centered Waves

Impulsive expansion of a fluid, *e.g.* by the impulsive acceleration of a piston, produces a centered wave, as in the Fig. 18.   It is possible for compression waves to be centered, also. In the former case, the discontinuity in flow properties at $t = 0$ immediately disintegrates and the flow becomes continuous. The flow shown in Fig. 18 is a centered left-facing simple wave with straight Q characteristics. In centered waves the flow properties have a simple "conical" dependence on space and time (x, t). The equation for

April 23, 2001
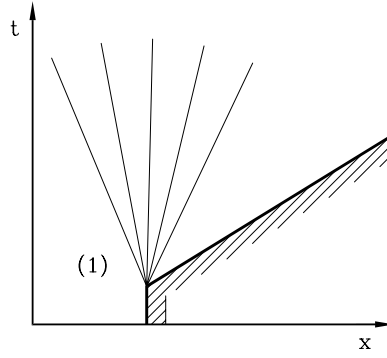
Figure 18. A left-facing centered wave

the Q characteristics is

$$
\begin{aligned}
\frac{x}{a_1 t} &= \frac{u - a}{a_1} \\
&= \frac{2}{\gamma - 1}\left(1 - \frac{\gamma + 1}{2}\frac{a}{a_1}\right) \\
&= \frac{1 - M}{1 \pm \frac{\gamma - 1}{2}M} ,
\end{aligned}
\tag{12.31}
$$

or,

$$
\frac{a}{a_1} = \frac{2}{\gamma + 1}\left(1 - \frac{\gamma - 1}{2}\frac{x}{a_1 t}\right) .
\tag{12.32}
$$

Centered waves have the interesting property that, if the flow has a vertical characteristic through the origin, then the flow is sonic there, $u = a$, $a = 2/(\gamma + 1)a_1$. Thus, the time axis in a centered nonsteady wave plays the role of the throat in a quasi-1D steady flow. However because of the difference in the impedances (see above) the flow behavior is different. For example,

$$
\begin{array}{cc}
\textbf{Nonsteady} & \textbf{Steady} \\
\frac{T_1}{T} = \left(1 + \frac{\gamma - 1}{2}M\right)^2 & \frac{T_t}{T} = 1 + \frac{\gamma - 1}{2}M^2 .
\end{array}
\tag{12.33}
$$

In fact, since the total temperature is defined for every flow, including these nonsteady flows, we can combine the two Eqs. 12.33 and compare the local total temperature T_t with the "reservoir temperature" T_1,

$$
\frac{T_t}{T_1} = \frac{1 + \frac{\gamma - 1}{2}M^2}{\left(1 + \frac{\gamma - 1}{2}M\right)^2} .
\tag{12.34}
$$

This function is plotted *vs.* the local Mach number M in Fig. 19. For large enough M, T_t can be substantially greater than the reservoir temperature, a useful feature of nonsteady flow resulting from nonsteady pressure work (see Eq. 7.20).

April 23, 2001
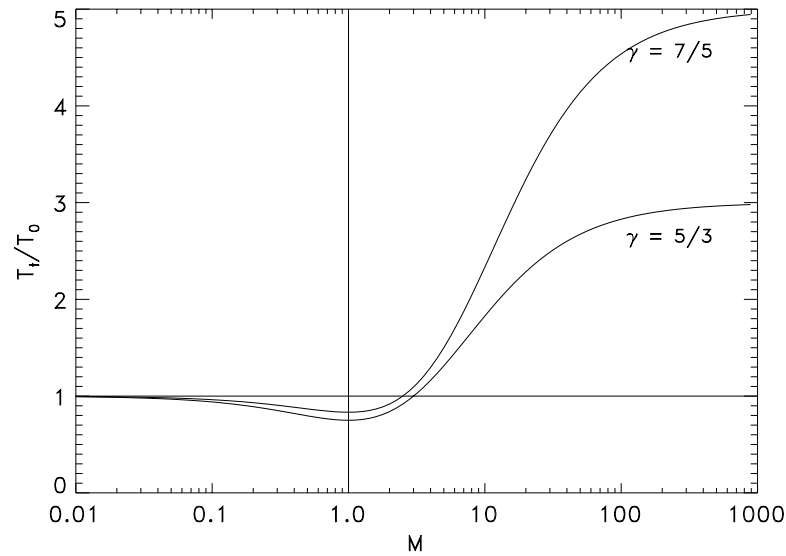
Figure 19. Total temperature in nonsteady flow

12.4.3 Complete expansion

If the piston recedes fast enough, the flow thermal energy can be converted entirely to kinetic energy, when $a, \rho, p = 0$. Then,

$$
\begin{array}{cc}
\textbf{Nonsteady} & \textbf{Steady} \\[2mm]
\dfrac{u_e}{a_1} = \dfrac{2}{\gamma - 1} & \dfrac{u_m}{a_t} = \sqrt{\dfrac{2}{\gamma - 1}} \; .
\end{array}
\tag{12.35}
$$

u_e is known as the *escape velocity*. The steady result shown above is Eq. 7.65, an analogous result from the same conversion of thermal energy to kinetic energy. However, owing to the effects of nonsteady pressure work, it is not as large as for nonsteady flow.

12.5 Wave interactions – The shock-tube equation

The shock jump conditions, in particular Eq. 8.29 and Eq. 8.30, can be plotted together with the corresponding relation for expansion waves, Eq. 12.30, in a form useful for the graphical solution of wave interaction problems (see Fig. 20).

For example, the solution of the classic problem of gasdynamics called the shock tube problem, is shown in Fig. 21. At time $t = 0$ a partition dividing a high-pressure region (4, the driver) from a low pressure chamber (1, the driven section) is instantaneously removed, generating a shock wave moving to the right and an expansion (rarefaction) wave moving to the left. The moving boundary (dashed line) between the shock-processed fluid and the expanded fluid is called a "contact surface," and it supports no waves. Thus, $p_3 = p_2$ and $u_3 = u_2$. The solution to this problem is shown graphically in Fig. 22. The pressure between the two waves is intermediate between the initial high and low pressures. The gas between is moving to the right.
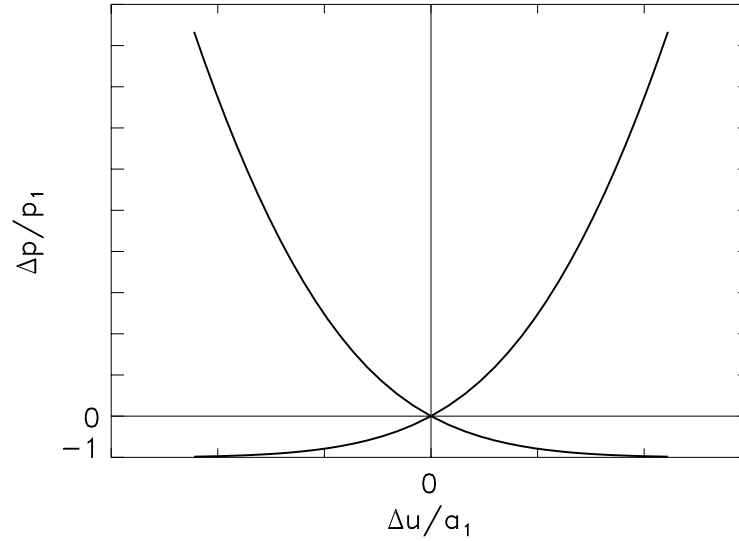
Figure 20. $\Delta p/p_1$ *vs.* $\Delta u/a_1$ for shocks ($\Delta p/p_1 > 0$) and for expansion waves ($\Delta p/p_1 < 0$).
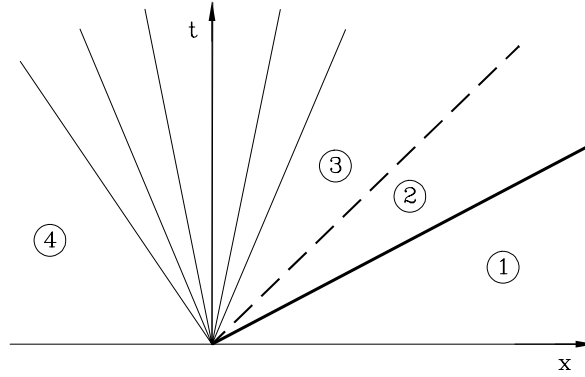
Figure 21. The shock-tube problem

We obtain an analytical expression for the solution as follows. Expanding the pressure ratio p_4/p_1,

$$\frac{p_4}{p_1} = \frac{p_4}{p_3}\frac{p_3}{p_2}\frac{p_2}{p_1} \ , \tag{12.36}$$

and substituting Eq. 12.30 for p_3/p_4, Eq. 8.29 for p_2/p_1, with $p_3 = p_2$ and $u_3 = u_2$, and then substituting Eq. 8.30 for u_2/a_1, gives

$$\frac{p_4}{p_1} = \frac{1 + \dfrac{2\gamma_1}{\gamma_1+1}(M_s^2 - 1)}{\left(1 - \dfrac{\gamma_4 - 1}{\gamma_1 + 1}\dfrac{a_1}{a_4}\dfrac{M_s^2 - 1}{M_s}\right)^{\frac{2\gamma_4}{\gamma_4 - 1}}} \tag{12.37}$$

The γ's have been subscripted to allow for the fact that different gases may initially occupy the driver and driven regions. This result shows that even with an infinite pressure ratio p_4/p_1 only a finite strength shock will be generated, owing to the finite escape velocity when the driver gas has been expanded to zero

April 23, 2001
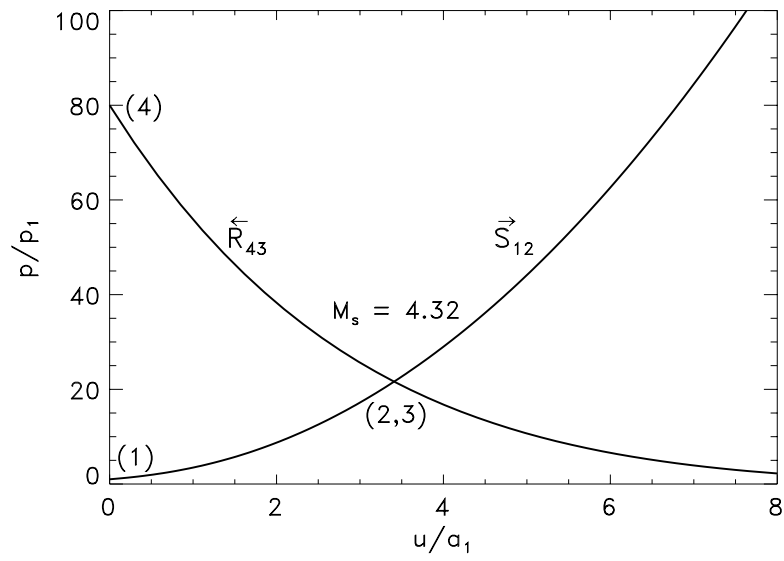
Figure 22. The shock tube problem solved in p-u space, for $\gamma_1 = \gamma_4 = 1.4$, $p_4/p_1 = 80$ and $a_4/a_1 = 4$.

pressure. u_e is greater for high-sound-speed gases, so the limiting Mach number is larger for large a_4,

$$\frac{M_s^2 - 1}{M_s} \longrightarrow \frac{a_4}{a_1} \frac{\gamma_1 + 1}{\gamma_4 - 1} \tag{12.38}$$

April 23, 2001

13 Steady Two-Dimensional Flow

Ray tracing has demonstrated that, in general, wave fronts become curved by reflection, refraction and diffraction. Therefore, the study of shock waves and their interactions in two or three dimensions is an important endeavor. A propagating shock which encounters a sloping wall may reflect regularly, as shown in the sketch. The problem may be transformed to a locally steady one by superimposing a negative
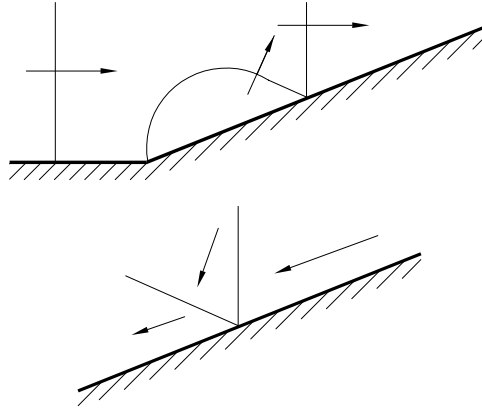
Figure 23. Nonsteady and steady shock reflection.

velocity parallel to the wall, to stop the reflection point, as shown at the bottom of the sketch. Then the flow behind the incident shock is pointing down toward the wall and the refelcted shock is required to bend it back parallel to the wall. Both of these waves are therefore oblique to the incoming flow, and are called "oblique waves."

13.1 Oblique shock waves

When a supersonic stream encounters a sharp obstacle, such as a wedge (Fig. 24), it is observed that an *oblique* shock wave emanates from the leading edge, and the flow behind is usually supersonic. Thus, the supersonic-subsonic relation of normal shocks does not generally hold for oblique shocks. The reason is that the oblique shock wave has the added feature that there is a flow commponent parallel to the shock front, that is not altered upon passing through the shock. In fact, all properties of normal shocks must hold for the *normal* component of the velocity. Thus, to analyze these flows we decompose the velocity into normal and tangential components. The notation is shown in Fig. 24. The flow is deflected through
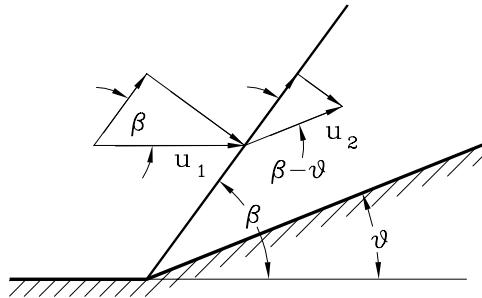
Figure 24. Notation for oblique shock waves.

the angle θ, and the shock angle *with the upstream flow* is β.

For the infinite wedge there is no characteristic length, so the flow is *conical*. Conditions are constant

along radii centered at the tip of the cone.

The preservation of the parallel flow component is expressed by

$$u_1 \cos \beta \ = \ u_2 \cos(\beta - \theta) \,. \tag{13.1}$$

The continuity, momentum and energy equations are Eqs. 8.1–8.3 applied to the *normal* component of the velocities,

$$\rho_1 u_1 \sin \beta \ = \ \rho_2 u_2 \sin(\beta - \theta) \tag{13.2}$$

$$p_2 - p_1 \ = \ \rho_1 u_1^2 \sin^2 \beta - \rho_2 u_2^2 \sin^2(\beta - \theta) \tag{13.3}$$

$$h_2 - h_1 \ = \ \frac{u_1^2 \sin^2 \beta}{2} - \frac{u_2^2 \sin^2(\beta - \theta)}{2} \tag{13.4}$$

Because the equations are fundamentally the same, we can pass immediately to the perfect gas case, Eqs. 8.29, 8.31 and 8.32. Substituting the correct form for the normal component gives

$$\begin{aligned} \frac{p_2}{p_1} \ &= \ 1 + \frac{2\gamma}{\gamma + 1} \left(M_1^2 \sin^2 \beta - 1 \right) \\ \frac{\rho_2}{\rho_1} \ &= \ \frac{M_1^2 \sin^2 \beta}{1 + \frac{\gamma - 1}{\gamma + 1}(M_1^2 \sin^2 \beta - 1)} \\ \frac{h_2}{h_1} \ &= \ 1 + \frac{2(\gamma - 1)}{(\gamma + 1)^2} \frac{(M_1^2 \sin^2 \beta - 1)(1 + \gamma M_1^2 \sin^2 \beta)}{M_1^2 \sin^2 \beta} \,. \end{aligned} \tag{13.5}$$

These equations determine the unknowns p_2, ρ_2 and h_2 in terms of the unknown β and the knowns θ, p_1, ρ_1 and h_1. An equation for M_2 is given by Eq. 13.2,

$$M_2^2 \sin^2(\beta - \theta) \ = \ \frac{M_1^2 \sin^2 \beta}{\dfrac{\rho_2}{\rho_1} \dfrac{p_2}{p_1}} \,, \tag{13.6}$$

so that,

$$M_2^2 \sin^2(\beta - \theta) \ = \ \frac{1 + \frac{\gamma - 1}{\gamma + 1}(M_1^2 \sin^2 \beta - 1)}{1 + \frac{2\gamma}{\gamma + 1}(M_1^2 \sin^2 \beta - 1)} \,. \tag{13.7}$$

Finally, Eq. 13.1 can be used to determine β. Dividing it into (13.2),

$$\rho_1 \tan \beta \ = \ \rho_2 \tan(\beta - \theta) \tag{13.8}$$

and expanding the tangent of the difference between two angles gives

$$\tan \theta \ = \ \frac{1}{\tan \beta} \frac{M_1^2 \sin^2 \beta - 1}{\frac{\gamma + 1}{2} M_1^2 - (M_1^2 \sin^2 \beta - 1)} \,. \tag{13.9}$$

Eq. 13.9 shows that θ can be 0 if $\beta = \sin^{-1} \frac{1}{M_1} \equiv \mu$, the Mach angle, or $\beta = \frac{\pi}{2}$. In the latter case $\sin \beta = 1$, and all the above equations reduce to those for normal shocks (Sec. 8). θ carries the sign of β, which can be either positive (for shocks of the + family) or negative (− family).

Fig. 25 shows the "shock polar", p_2/p_1 *vs.* θ (the first of Eqs. 13.5 with 13.9) for several different upstream Mach numbers M_1. For given wedge angle θ there are *two solutions*, known as the weak

April 23, 2001
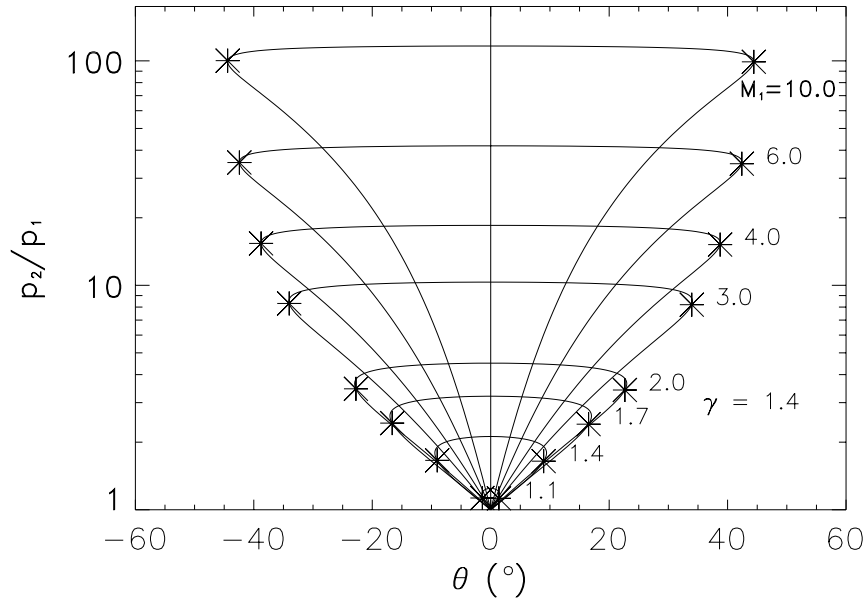
Figure 25. The shock polar, shown for several different upstream Mach numbers M_1. ✳, sonic condition.

solution and the strong solution. The asterisks mark the "sonic condition," below which the downstream flow is supersonic (the *weak* solution) and above which it is subsonic (the *strong* solution). Thus, for $\theta = 0$ there is either no disturbance or a normal shock wave. There is a maximum θ, beyond which there is no solution at all for each upstream Mach number. This is the "maximum deflection angle" or the "detachment angle," beyond which the shock detaches from the wedge. The sonic condition happens to occur very close to the maximum deflection angle, but not precisely at it.

When the wedge angle increases beyond the maximum deflection angle, the body becomes a *bluff body*, and experiments show that the fact that the body must really be of finite transverse size controls the flow. That is, there is a characteristic length, the body diameter D. The shock jumps out to a distance of order D ahead of the body, and is normal on the axis of symmetry, the stagnation streamline, as is shown in the sketches of Fig. 26. The figure shows a compilation of shock standoff distance for several different body shapes (Liepmann & Roshko 1957). The standoff distance gets very large as the upstream Mach number $M_1 \to 1$.

13.2   Weak shocks

For small θ and $\Delta p = p_2 - p_1$, $M_1^2 \sin^2 \beta - 1 \ll 1$, and the shocks are weak, though the Mach number itself might be large. Then,

$$\sin \beta \;\doteq\; \frac{1}{M_1} \tag{13.10}$$

$$\tan \beta \;\doteq\; \frac{1}{\sqrt{M_1^2 - 1}} \;, \tag{13.11}$$

FIG. 4-15 Shock wave detachment distance for plane and axially symmetric flow. Sources of experimental data: G. F. Solomon, *N.A.C.A. Tech. Note* 3213; W. Griffith, *J. Aeronaut. Sci., 19* (1952); Heberle, Wood, and Gooderum, *N.A.C.A. Tech. Note* 2000; C. S. Kim, *J. Phys. Soc. Japan, 11* (1956); U. S. Naval Ordnance Lab., unpublished data; California Institute of Technology, various unpublished data (Alperin, Hartwig, Kubota, Oliver, Puckett). Data are for air, with constant specific heat.

Figure 26. Experimental measurements of shock stand off for several different body shapes, as compiled by Liepmann & Roshko (1957).

so,

$$\theta \doteq \sqrt{M_1^2 - 1}\, \frac{2}{\gamma + 1} \frac{M_1^2 \sin^2 \beta - 1}{M_1^2} \tag{13.12}$$

$$\frac{\Delta p}{p} \doteq \frac{2\gamma}{\gamma + 1} (M_1^2 \sin^2 \beta - 1) . \tag{13.13}$$

Thus,

$$\boxed{\frac{\Delta p}{p} \doteq \frac{\gamma M_1^2}{\sqrt{M_1^2 - 1}} \theta} \tag{13.14}$$

This function of M_1 is large for both small and large M_1, and is minimum for $M_1 = \sqrt{2}$, independent of γ. This behavior explains why the shock polars in the above sketch first expand and then get thinner as $M - 1$ increases.

Another important weak shock relation is obtained from Eq. 13.1; expanding the cosine of the difference of two angles, and using the above approximation for $\tan \beta$ gives

$$\boxed{\frac{\Delta u}{u_1} \doteq -\frac{\theta}{\sqrt{M_1^2 - 1}} .} \tag{13.15}$$

69

The change of Mach number can be obtained by multiplying the approximate velocity ratio by the sound speed ratio, and substituting for the latter,

$$\frac{M_2}{M_1} \doteq \frac{a_1}{a_2} \left(1 - \frac{\theta}{\sqrt{M_1^2 - 1}} \right) \tag{13.16}$$

$$\frac{a_2}{a_1} \doteq 1 + \frac{\gamma - 1}{2} \frac{M_1^2}{\sqrt{M_1^2 - 1}} \theta \, , \tag{13.17}$$

with the result

$$\boxed{\frac{\Delta M}{M_1} \doteq -\left(1 + \frac{\gamma - 1}{2} M_1^2 \right) \frac{\theta}{\sqrt{M_1^2 - 1}} \, .} \tag{13.18}$$

13.3   Continuous flows – Prandtl-Meyer expansion

The weak-shock relations can be generalized to describe local changes in continuous 2-dimensional isentropic flow. In particular, for a continuous process Eq. 13.18 can be written

$$d\theta = -\frac{\sqrt{M^2 - 1}}{1 + \frac{\gamma - 1}{2} M^2} \frac{dM}{M} \, , \tag{13.19}$$

and integrated to give

$$-\theta + \text{const} = \nu(M) \, , \tag{13.20}$$

where

$$\nu(M) = \sqrt{\frac{\gamma + 1}{\gamma - 1}} \tan^{-1} \sqrt{\frac{\gamma - 1}{\gamma + 1}(M^2 - 1)} - \tan^{-1} \sqrt{M^2 - 1} \tag{13.21}$$

is the Prandtl-Meyer function, shown in Fig. 27 It gives the Mach number change with the flow deflection
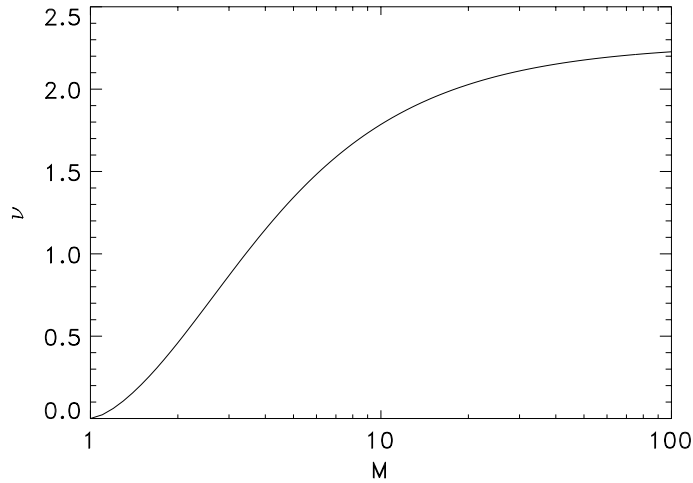
Figure 27. The Prandtl-Meyer Function $\nu(M)$.

angle. The thermodynamic variables follow from Eqs. 7.58–7.62. As with shock waves, the Mach number decreases with either increasing or decreasing θ, depending on which family of waves is present. Similarly for expansions. (See below.)

April 23, 2001

Note that $\nu(1) = 0$ and $\nu(\infty) = \frac{\pi}{2}\left(\sqrt{\frac{\gamma+1}{\gamma-1}} - 1\right)$; the maximum turning angle results from expanding from $M = 1$ to $M = \infty$, and is predicted to be greater than $180°$ for $\gamma < 5/4$!

In the (p, θ) plane, Prandtl-Meyer expansion waves $(\Delta p/p_0 < 0)$ join smoothly with the shock polar, as shown in Fig. 28. The compressive branch $(\Delta p/p_0 > 0)$ falls nearly on the shock polar, for weak
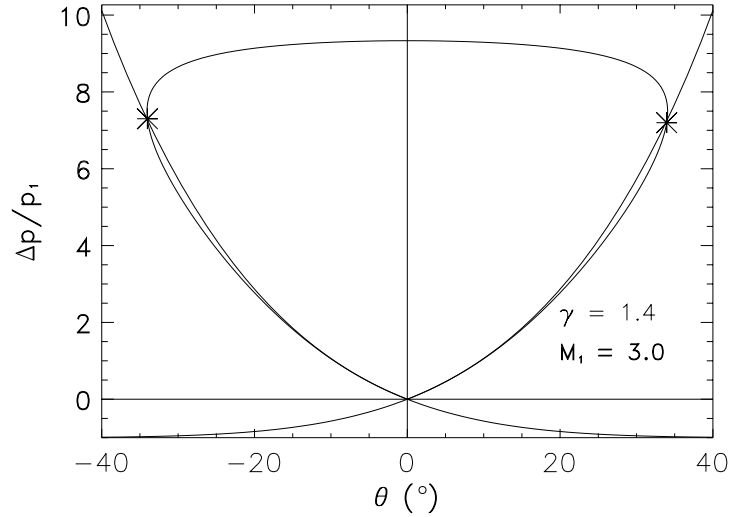
Figure 28. Comparison of compression $(\Delta p/p_0 > 0)$ and expansion $(\Delta p/p_0 < 0)$ Prandtl-Meyer flows with the shock polar for one upstream Mach number.

shocks. The Prandtl-Meyer curve with positive slope represents the positive family of waves, and the one with negative slope the negative. Compression members of the positive family increase the flow defelction angle, while the opposite is true of the opposite family.

13.4 The hodograph

Useful geometrical insight can be obtained by examining solutions in the hodograph plane (u_x, u_y).

Oblique shocks. The sketch below shows the shock polar for oblique waves. The tigonometry of the similar
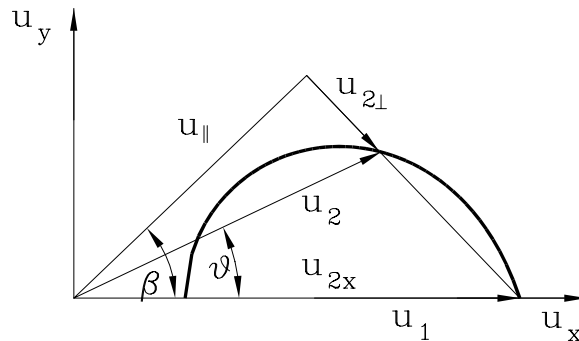
triangles establishes the following relations,

$$\frac{u_\parallel}{u_{1\perp}} = \frac{u_{2y}}{u_1 - u_{2x}} \tag{13.22}$$

$$\frac{u_\parallel}{u_1} = \frac{u_{2y}}{u_{1\perp} - u_{2\perp}} \tag{13.23}$$

$$u_1^2 = u_{1\perp}^2 + u_\parallel^2 \tag{13.24}$$

$$u_2^2 = u_{2\perp}^2 + u_\parallel^2 . \tag{13.25}$$

The Prandtl relation, Eq. 8.51, was derived using the energy equation, and so doesn't transform trivially to the oblique flow. The energy equations Eq. 8.48 now becomes

$$u_{1\perp}^2 + \frac{2}{\gamma - 1} a_1^2 = u_{2\perp}^2 + \frac{2}{\gamma - 1} a_2^2 = \frac{\gamma + 1}{\gamma - 1} a^{*2} - u_\parallel^2 , \tag{13.26}$$

with the consequence that, after incorporating the momentum equation, the Prandtl relation becomes

$$\boxed{u_{1\perp} u_{2\perp} = a^{*2} - \frac{\gamma - 1}{\gamma + 1} u_\parallel^2 .} \tag{13.27}$$

It is convenient to normalize all velocities with a^*, $M^* \equiv u/a^*$, because, for example, when $M \to \infty$, M^* is finite,

$$M^{*2} = \frac{M^2}{1 + \frac{\gamma-1}{\gamma+1}(M^2 - 1)} . \tag{13.28}$$

Eliminating the perpendicular and parallel velocities from the Prandtl relation using Eqs. 13.22–13.25 gives the shock polar in the hodograph plane,

$$\boxed{M_{2y}^{*2} = \frac{(M_1^* - u_{2x})^2 (M_1^* M_{2x}^* - 1)}{\frac{2}{\gamma+1} M_1^{*2} - (M_1^* M_{2x}^* - 1)} .} \tag{13.29}$$

This result is the epicycloid curve plotted in the sketch above (for $M_1^* = 2$).

Prandtl-Meyer function. Written in terms of M^*, the Prandtl-Meyer function, Eq. 13.21 becomes

$$\nu(M^*) = \sqrt{\frac{\gamma+1}{\gamma-1}} \tan^{-1} \sqrt{\frac{M^{*2} - 1}{\frac{\gamma+1}{\gamma-1} - M^{*2}}} - \tan^{-1} \sqrt{\frac{\gamma+1}{\gamma-1}} \sqrt{\frac{M^{*2} - 1}{\frac{\gamma+1}{\gamma-1} - M^{*2}}} \tag{13.30}$$

This function plots onto the hodograph as shown below. M^* continuously increases from $M^* = 1$ to
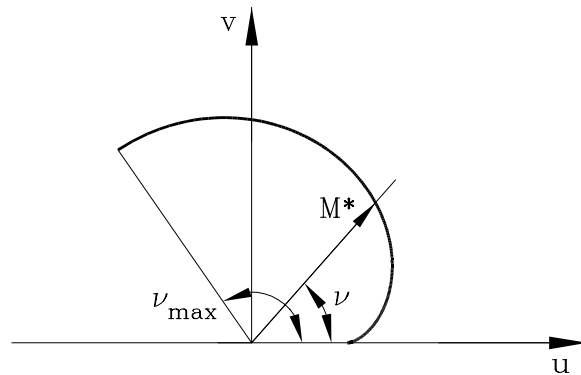
$M \to \infty$ at ν_{max}, which depends on γ. The above sketch is for $\gamma = 1.4$ and the sketch below shows the strophoid for several values of γ. It shows turning angles greater than $180°$ for small γ. For flows with $M_1 > 1$, the strophoid is rotated so that the initial M^* coincides with the initial θ, and changes from the initial state are then followed in the direction appropriate for compressions or expansions.
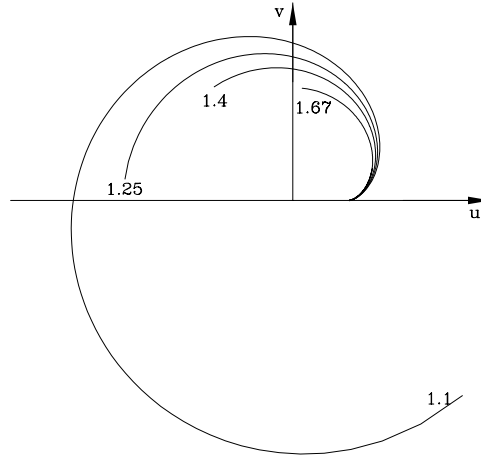
13.5 Wave interactions

With the tools developed in this section, arbitrarily complex wave interactions can be solved. First, we treat the simplest reflection problem, the reflection of an incident oblique shock from a plane wall. Fig. 29 illustrates a quantitative case in which the upstream Mach number is $M_1 = 5$, and θ is measured relative to the upstream flow direction. The lowest polar shows the incident shock, and the point
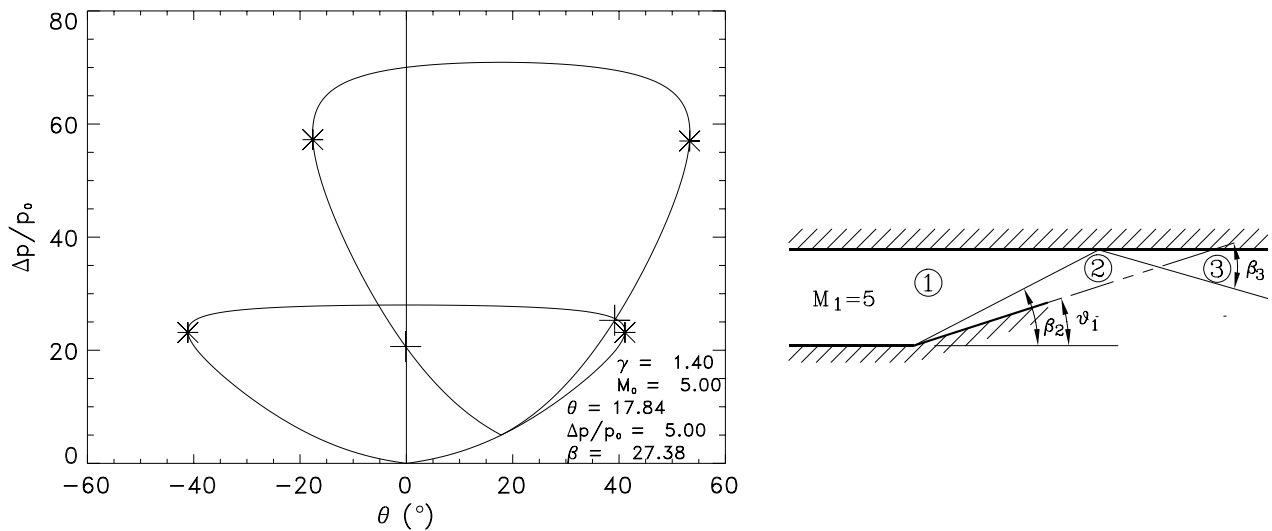
Figure 29. p-θ diagram and quantitative sketch of a regular reflection. $\theta_1 = 17.84°$. $\beta_2 = 27.38°$. $\beta_3 = -33.88°$.

$\Delta p/p_1 = 5.0, \theta = 17.84°$ depicts the downstream state, from which the reflected shock polar begins. Two solution points are marked by the pluses. The one of interest here is the left one where the flow deflection angle is 0.

Often the reflection is such that the point of maximum flow deflection falls to the right of the $\theta = 0$ axis, as in Fig. 30. In this case there is no solution with $\theta = 0$. Experiments show that, in fact, Mach reflection occurs, such that the solution indicated by the $+$ is realized locally, in a configuration indicated in the sketch on the right. The p-θ curve originationg at conditions ① gives the two waves 1–2 and 1–3,
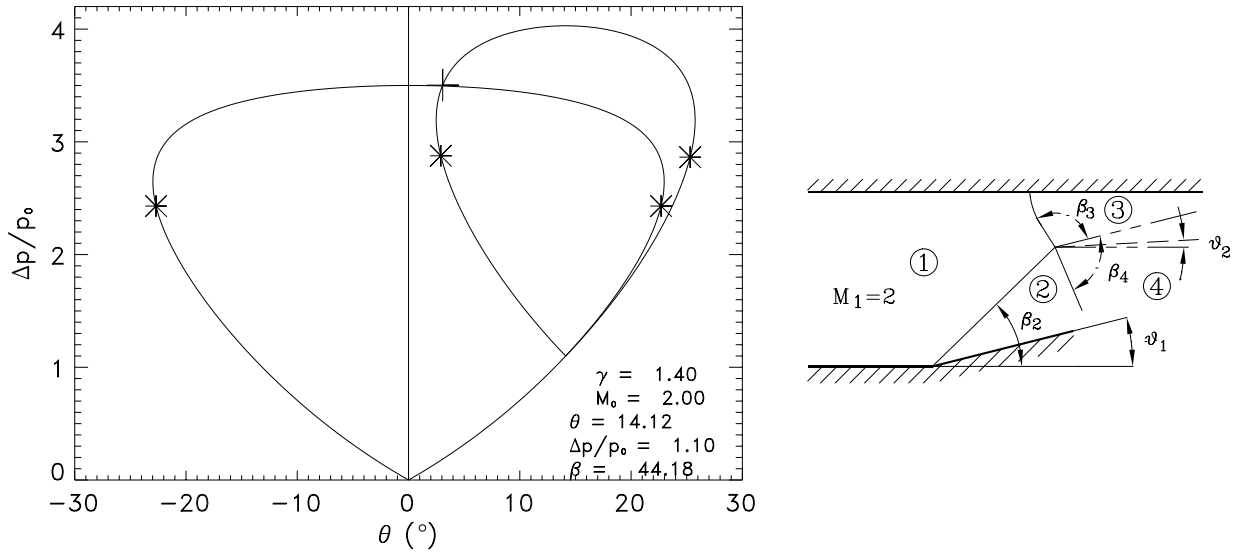
Figure 30. p-θ diagram and quantitative sketch of a Mach reflection. $\theta_1 = 14.12°$. $\beta_2 = 44.18°$. $\theta_2 = 3.07°$. $\beta_3 = -71.8°$. $\beta_4 = -81.1°$.

and the one originating at condition ② gives 1–4.

13.6 Natural Coordinates

We now make a slight diversion in order to simplify the general treatment of supersonic flow in two dimensions. We rederive the equations of motion in terms of motions down streamtubes, the "natural" coordinate system of Crocco. Fig. 31 shows the geometry. s is in the streamwise direction, n is normal to s.
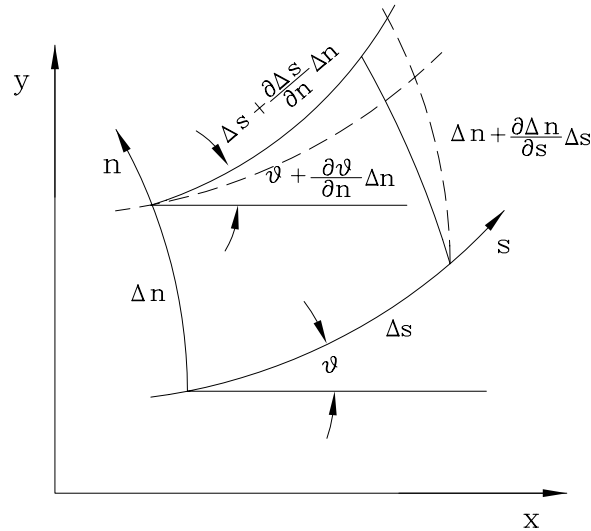
Figure 31. Definition of the natural coordinate system

We use the notation Δn and Δs temporarily, and, later, pass to the limit where they become differentials.

From the geometry of the figure (*viz.* dashed lines)

$$\tan\frac{\partial\theta}{\partial n}\,\Delta n \;\doteq\; \frac{\partial\theta}{\partial n}\,\Delta n \;=\; \frac{\partial\Delta n}{\partial s} \tag{13.31}$$

$$\tan\frac{\partial\theta}{\partial s}\,\Delta s \;\doteq\; \frac{\partial\theta}{\partial s}\,\Delta s \;=\; \frac{\partial\Delta s}{\partial n}\;. \tag{13.32}$$

By definition, since the volume is infinitesimal, the equations of quasi-onedimensional flow apply exactly. However, they must be improved to account for the fact that fluid tends to slosh outward on a curve, *i.e.*, they must be augmented for transverse curvature effects.

The continuity equation is

$$\rho\,u\,\Delta n \;=\; \text{const}\;, \tag{13.33}$$

which, differentiated logarithmically becomes

$$\frac{1}{\rho}\frac{\partial\rho}{\partial s} + \frac{1}{u}\frac{\partial u}{\partial s} + \frac{1}{\Delta n}\frac{\partial\Delta n}{\partial s} \;=\; 0\;. \tag{13.34}$$

Using Eq. 13.31,

$$\boxed{\frac{1}{\rho}\frac{\partial\rho}{\partial s} + \frac{1}{u}\frac{\partial u}{\partial s} + \frac{\partial\theta}{\partial n} \;=\; 0\;.} \tag{13.35}$$

The *s*-momentum equation is

$$\boxed{\rho u\frac{\partial u}{\partial s} + \frac{\partial p}{\partial s} \;=\; 0\;.} \tag{13.36}$$

The *new* equation required is derived from the fact that the infinitesimal volume of Fig. 31 is not an inertial system, but is rotating. There are no velocities in the transverse direction, so the normal momentum equation is simply a hydrostatic force balance between a pressure gradient and a "body force" resulting from the centripetal acceleration $\Omega^2 R$, where $R = \frac{\Delta s}{\Delta\theta}$ is the radius of curvature. Here,

$$\Omega \;=\; \frac{\Delta\theta}{\Delta t} \;=\; u\,\frac{\Delta\theta}{\Delta s} \;\longrightarrow\; u\,\frac{\partial\theta}{\partial s}\;. \tag{13.37}$$

The last equality is obtained by expressing $\Delta\theta$ and Δs as differentials. With reference to Eq. 2.16, the *n*-momentum equation is

$$-\rho\Omega^2 R - \frac{\partial p}{\partial n} \;=\; 0\;, \tag{13.38}$$

or,

$$\boxed{\rho u^2\frac{\partial\theta}{\partial s} + \frac{\partial p}{\partial n} \;=\; 0\;.} \tag{13.39}$$

The energy equation will give a useful condition for ensuring isentropic flow. We begin by making the minimum assumption, namely, adiabatic flow.

$$h + \frac{u^2}{2} \;=\; h_t(n)\;; \qquad dh \;=\; dh_t - u\,du\;. \tag{13.40}$$

April 23, 2001

The total enthalpy can vary normal to the streamlines because of upstream conditions. The following thermodynamic identity gives

$$T\, dS \;=\; dh - \frac{1}{\rho}\, dp \tag{13.41}$$

$$\;=\; dh_t - \left(u\, du + \frac{1}{\rho}\, dp \right)\;. \tag{13.42}$$

Decomposed into the two directions s and n, it gives,

$$T\frac{\partial S}{\partial s} \;=\; 0 \tag{13.43}$$

$$T\frac{\partial S}{\partial n} \;=\; -u\left(\frac{\partial u}{\partial n} - u\frac{\partial \theta}{\partial s} \right) + \frac{dh_t}{dn}\;, \tag{13.44}$$

where in each equation the corresponding momentum equation has been used to eliminate p. This can be put in terms of vorticity ω. The vorticity can be written down from its definition, or it can be derived from *Kelvin's Theorem*. The circulation Γ is defined as

$$\Gamma \;\equiv\; \oint \underline{u} \cdot d\underline{\ell} \;=\; \int_S \underline{\omega} \cdot d\underline{S}\;, \tag{13.45}$$

where the last equality follows from Stokes Theorem. Now, the circulation around the infinitesimal volume of Fig. 31 has contributions from only the bottom and top legs,

$$\Gamma \;=\; u\,\Delta s \;-\; (u + \frac{\partial u}{\partial n}\Delta n)(\Delta s + \frac{\partial \Delta s}{\partial n}\Delta n)$$

$$\;=\; \left(u\frac{\partial \theta}{\partial s} - \frac{\partial u}{\partial n} \right)\Delta s \Delta n\;, \tag{13.46}$$

where Eq. 13.32 has been used. Thus

$$\omega \;=\; u\frac{\partial \theta}{\partial s} - \frac{\partial u}{\partial n}\;, \tag{13.47}$$

so the energy equation is

$$\boxed{T\frac{\partial S}{\partial n} \;=\; u\omega + \frac{dh_t}{dn}\;.} \tag{13.48}$$

This is the inviscid 2D form of Crocco's theorem, Eq. 3.22.

13.7   The Equations in Characteristic Form

<u>Homentropic flow</u>, which we consider from here on, is obtained by the assumptions $\omega = 0$ and $h_t =$ const. The equations can be put in characteristic form in the same way as with nonsteady flow; multiply Eq. 13.35 by $a^2 = dp/d\rho$, eliminate $d\rho$ in favor of dp. However, here we prefer to write equations for (u, θ), so we eliminate p by subtracting Eq. 13.36 to obtain

$$\boxed{\begin{aligned} (M^2 - 1)\frac{1}{u}\frac{\partial u}{\partial s} - \frac{\partial \theta}{\partial n} &= 0 \\ \frac{\partial u}{\partial n} - u\frac{\partial \theta}{\partial s} &= 0\;. \end{aligned}} \tag{13.49}$$

The last equation is the irrotationality condition, $\omega = 0$.

These equations can be simplified by replacing u by $\nu(M)$ from Eq. 13.15,

$$d\theta \equiv -d\nu(M) = -\sqrt{M^2 - 1} \frac{du}{u} \tag{13.50}$$

or

$$d\nu = \cot\mu \frac{du}{u} . \tag{13.51}$$

Substituting into the above equations gives

$$\frac{\partial \nu}{\partial s} - \tan\mu \frac{\partial \theta}{\partial n} = 0 \tag{13.52}$$

$$\tan\mu \frac{\partial \nu}{\partial n} - \frac{\partial \theta}{\partial s} = 0 . \tag{13.53}$$

Now they can be put directly into charcteristic form by adding and subtracting,

$$\boxed{\frac{\partial}{\partial s}(\nu \mp \theta) \pm \tan\mu \frac{\partial}{\partial n}(\nu \mp \theta) = 0 ,} \tag{13.54}$$

or, in words,

$$\boxed{\theta \mp \nu = \frac{P}{Q} \quad \text{along} \quad \frac{dn}{ds} = \pm\tan\mu .} \tag{13.55}$$

13.7.1 The Method of Characteristics

These equations form the basis for numerical calculations by the method of characteristics. It can easily be extended to non-homentropic (but isentropic) flows, with some additional computational complexity. For this purpose, the equations can at this stage be transformed from natural coordinates back into (x, y) almost trivially, simply by inspection of Fig. 31,

$$\boxed{\theta \mp \nu = \frac{P}{Q} \quad \text{along} \quad \frac{dy}{dx} = \tan(\theta \pm \mu) .} \tag{13.56}$$

14   Acoustics

Acoustics is the small-amplitude approximation to gas-dynamics. Because entropy changes are third order in shock strength, acoustic fields are isentropic.

14.1   Plane Waves I

Uni-directional propagation.   One-way propagation (say, in the x-direction) can be derived from the shock relation Eq. 8.7 by approximating the changes as differentials,

$$dp = \rho a \, du \, , \tag{14.1}$$

where ρ and a are the values for the undisturbed ambient medium. This is of course the Riemann invariant for an infinitesimal right-facing wave.

Bidirectional propagation.   The equation for general one-dimensional acoustic fields can be derived by linearizing Eq. 12.4 with the substitution

$$p = p_0 + p' \tag{14.2}$$
$$\rho = \rho_0 + \rho' \tag{14.3}$$
$$a = a_0 + a' \tag{14.4}$$
$$\underline{u} = \underline{u}' \, . \tag{14.5}$$

( )$_0$ refers to the ambient medium. Dropping all but the first-order terms gives

$$\frac{\partial p}{\partial t} + a_0 \frac{\partial p}{\partial x} + \rho_0 a_0 \left(\frac{\partial u}{\partial t} + a_0 \frac{\partial u}{\partial x} \right) = 0 \tag{14.6}$$

$$\frac{\partial p}{\partial t} - a_0 \frac{\partial p}{\partial x} - \rho_0 a_0 \left(\frac{\partial u}{\partial t} - a_0 \frac{\partial u}{\partial x} \right) = 0 \, , \tag{14.7}$$

where the primes have been dropped from the perturbation quantities. Adding and subtracting the two equations recovers the original forms of the continuity and momentum equations,

$$\frac{\partial p}{\partial t} + \rho_0 a_0^2 \frac{\partial u}{\partial x} = 0 \tag{14.8}$$

$$\frac{\partial p}{\partial x} + \rho_0 \frac{\partial u}{\partial t} = 0 \, . \tag{14.9}$$

Differentiating the first with respect to t, multiplying the second by a_0^2 and differentiating with respect to x, and subtracting from the first gives the wave equation

$$\boxed{\frac{\partial^2 p}{\partial t^2} - a_0^2 \frac{\partial^2 p}{\partial x^2} = 0 \, .} \tag{14.10}$$

Factoring the operators exhibits again the bi-directional structure of the equation,

$$\boxed{\left(\frac{\partial}{\partial t} + a_0 \frac{\partial}{\partial x} \right) \left(\frac{\partial}{\partial t} - a_0 \frac{\partial}{\partial x} \right) p = 0 \, ,} \tag{14.11}$$

the solution to which is

$$\boxed{p = f(x - a_0 t) + g(x + a_0 t) \, .} \tag{14.12}$$

In a uniform medium ($a_0 = $ const) acoustic waves propagate along straight lines $dx/dt = \pm a_0$ in (x, t).

April 23, 2001

14.2   Acoustics in multi dimensions

The wave equation for multi-dimensional flow follows by applying the same procedure to Eqs. 2.13-2.17. The linearized continuity equation is

$$\frac{\partial \rho'}{\partial t} + \rho_0 \nabla \cdot \underline{u}' \; = \; 0 \; , \tag{14.13}$$

Substituting

$$a_0^2 \; = \; \left(\frac{\partial p}{\partial \rho} \right)_{s_0} \tag{14.14}$$

to eliminate $d\rho$ gives

$$\frac{\partial p}{\partial t} + \rho_0 a_0^2 \nabla \cdot \underline{u} \; = \; 0 \; , \tag{14.15}$$

where now the primes have been dropped. The linearized momentum equation is

$$\rho_0 \frac{\partial \underline{u}}{\partial t} + \nabla p \; = \; 0 \; . \tag{14.16}$$

Dividing Eq. 14.15 by a_0^2, differentiating it with respect to time and subtracting $\nabla \cdot$ times Eq. 14.16 gives

$$\boxed{\frac{\partial^2 p}{\partial t^2} - a_0^2 \nabla^2 p \; = \; 0 \; ,} \tag{14.17}$$

the multi-dimensional version of Eq. 14.10.

Likewise, a wave equation can be derived for $\underline{u}$. In fact, defining a velocity potential

$$\boxed{\underline{u} \; = \; \nabla \phi \; ,} \tag{14.18}$$

the momentum equation, Eq. 14.16, becomes

$$\nabla \left(\rho_0 \frac{\partial \phi}{\partial t} + p \right) \; = \; 0 \; , \tag{14.19}$$

which is solved by

$$\boxed{p \; = \; -\rho_0 \frac{\partial \phi}{\partial t} \; ,} \tag{14.20}$$

where the arbitrary time function from the integration has been absorbed into ϕ because it doesn't change $\underline{u} = \nabla \phi$. Conveniently, ϕ gives both the acoustic pressure and the acoustic velocity. Substituting Eqs. 14.18 and 14.20 into Eq. 14.15 results directly in a wave equation for ϕ,

$$\boxed{\frac{\partial^2 \phi}{\partial t^2} - a_0^2 \nabla^2 \phi \; = \; 0 \; ,} \tag{14.21}$$

Energy.   To linearize Eq. 2.17 express $e(s, v)$ and Taylor expand the perturbation,

$$e' \; = \; e - e_0 \; = \; \left(\frac{\partial e}{\partial v} \right)_{s_0} v' + \frac{1}{2} \left(\frac{\partial^2 e}{\partial v^2} \right)_{s_0} v'^2 + \cdots \; . \tag{14.22}$$

Using Eqs. 6.4, 6.41 and

$$v' \; = \; \left(\frac{\partial p}{\partial v} \right)_s p' \; , \tag{14.23}$$

April 23, 2001

gives

$$e + \frac{u^2}{2} \;=\; e_0 + e' + \frac{u'^2}{2} \;\dot=\; e_0 - p_0 v' + \frac{1}{2} \frac{p'^2}{\rho_0^2 a_0^2} + \frac{u'^2}{2} \;. \tag{14.24}$$

With linearization, the convective derivative becomes simply the time derivative. The first term on the right of Eq. 2.17 (all the rest are zero in this inviscid theory) linearizes to $p_0 \nabla \cdot \underline{u}' + \nabla \cdot p' \underline{u}'$, so the energy equation is

$$-p_0 \rho_0 \frac{\partial v'}{\partial t} + \rho_0 \frac{\partial}{\partial t}\left(\frac{1}{2} \frac{p'^2}{\rho_0^2 a_0^2} + \frac{u'^2}{2} \right) + p_0 \nabla \cdot \underline{u}' + \nabla \cdot p' \underline{u}' \;=\; 0 \;. \tag{14.25}$$

Eq. 14.13 can be written

$$-\frac{1}{v_0} \frac{\partial v'}{\partial t} + \nabla \cdot \underline{u}' \;=\; 0 \;, \tag{14.26}$$

so, combining with (14.25),

$$\boxed{\rho_0 \frac{\partial}{\partial t}\left(\frac{1}{2} \frac{p^2}{\rho_0^2 a_0^2} + \frac{u^2}{2} \right) + \nabla \cdot p\underline{u} \;=\; 0 \;,} \tag{14.27}$$

where now the primes have been dropped.

In a left- or right-facing wave,

$$p \;=\; \pm \rho_0 a_0 \, u \;, \tag{14.28}$$

so

$$\frac{1}{2} \frac{p^2}{\rho_0^2 a_0^2} \;=\; \frac{1}{2} \frac{pu}{\rho_0 a_0} \;=\; \frac{u^2}{2} \;. \tag{14.29}$$

That is, the acoustic energy is equi-partitioned between potential and kinetic energy. Eq. 14.27 can then be written

$$\boxed{\frac{1}{a_0} \frac{\partial pu}{\partial t} + \nabla \cdot p\underline{u} \;=\; 0 \;,} \tag{14.30}$$

which is an equation in conservative form,

$$\frac{\partial}{\partial t}\text{density} \;=\; \nabla \cdot \text{flux} \;. \tag{14.31}$$

We have,

$$\boxed{\begin{aligned} E &\equiv \text{ energy density } = & \frac{pu}{a_0} \\[2mm] \underline{F} &\equiv \quad \text{ energy flux } \quad = \; p\underline{u} \;=\; a_0 \, E \, \frac{u}{u} \end{aligned}} \tag{14.32}$$

The last equality shows that acoustic energy in this non-dispersive medium is carried with the sound speed a_0.

14.3 Plane waves II

For plane-waves the solution to Eq. 14.21 is

$$\phi \;=\; f\left(t - \frac{x \cdot \underline{n}}{a_0} \right) + g\left(t + \frac{x \cdot \underline{n}}{a_0} \right) \;, \tag{14.33}$$

where

$$\underline{n} \;=\; \frac{\underline{u}}{u} \tag{14.34}$$

is the unit vector in the direction of propagation. Thus

$$
\boxed{
\begin{aligned}
\underline{u} &= \nabla\phi &&= -\frac{1}{a_0}(f' - g')\,\underline{n} \\
p &= -\rho_0\frac{\partial\phi}{\partial t} &&= -\rho_0(f' + g')\,,
\end{aligned}
}
\tag{14.35}
$$

where here the primes denote differentiation with respect to the argument.

Harmonic plane waves. The velocity potential for harmonic plane waves is conventionally taken to be

$$
\phi = \operatorname{fnc}(\underline{x})\,e^{-i\omega t}\,.
\tag{14.36}
$$

Then the solution, (14.33), becomes

$$
\boxed{
\begin{aligned}
\phi &= \left(Ae^{i\underline{k}\cdot\underline{x}} + Be^{-i\underline{k}\cdot\underline{x}}\right)e^{-i\omega t} \\
&= A\,e^{i(\underline{k}\cdot\underline{x}-\omega t)} + B\,e^{-i(\underline{k}\cdot\underline{x}+\omega t)}\,,
\end{aligned}
}
\tag{14.37}
$$

where the wave vector $\underline{k}$ is

$$
\underline{k} = \frac{\omega}{a_0}\,\underline{n}\,.
\tag{14.38}
$$

Thus,

$$
\begin{aligned}
p &= -\rho_0\frac{\partial\phi}{\partial t} = \rho_0\,i\omega\left(Ae^{i\underline{k}\cdot\underline{x}} + Be^{-i\underline{k}\cdot\underline{x}}\right)e^{-i\omega t} \\
\underline{u} &= \nabla\phi = i\underline{k}\left(Ae^{i\underline{k}\cdot\underline{x}} - Be^{-i\underline{k}\cdot\underline{x}}\right)e^{-i\omega t}\,.
\end{aligned}
\tag{14.39}
$$

As with any plane-wave field, this solution can be rewritten to show that it is a summation of a standing wave and a travelling wave, either left-facing or right-facing,

$$
\begin{aligned}
\phi &= 2A\,\cos(\underline{k}\cdot\underline{x})\,e^{-i\omega t} - (A - B)\,e^{-i(\underline{k}\cdot\underline{x}+\omega t)} \tag{14.40} \\
&= 2B\,\cos(\underline{k}\cdot\underline{x})\,e^{-i\omega t} + (A - B)\,e^{i(\underline{k}\cdot\underline{x}-\omega t)} \tag{14.41}
\end{aligned}
$$

When $A = B$, it is a pure standing wave.

Energy. The magnitude of the energy flux for progressive harmonic waves, say, $B = 0$, is

$$
F = pu = \rho_0 a_0\,u^2 = \rho_0 a_0\,k^2\,A^2 = \frac{\rho_0}{a_0}\,\omega^2\,A^2\,,
\tag{14.42}
$$

where the last two equalities follow from Eq. 14.39. It follows from Eq. 14.32 that the energy density is

$$
E = \frac{\rho_0}{a_0^2}\,\omega^2\,A^2\,.
\tag{14.43}
$$

Measures of sound amplitude – Decibels. The sound pressure level is defined as

$$
\text{SPL} = 20\log_{10}\frac{|p|}{2\times10^{-5}\ \text{Pa}}\,,
\tag{14.44}
$$

where the units of SPL are called deciBels (dB). Roughly speaking, 0 dB is the limit of human hearing. The particle velocity in air induced by the least audible sound (2×10^{-5} Pa) is about 4×10^{-8} m/s, and the energy flux is approximately 10^{-12} w/m^2. An increase of SPL by 100 dB implies an increase of rms pressure by a factor of 10^5, so SPL $= 100$ dB is $p = 2$ Pa, and SPL $= 200$ dB is $p = 2\times10^5$ Pa $= 2$ bar!

14.4 Refraction

The refraction of plane waves $\phi = f(t - \frac{n \cdot x}{a})$ at a discontinuous interface is easy to work out, and applies locally to curved waves incident on curved interfaces, so long as the interface can be taken to be discontinuous. We take the wave incident from above ($y > 0$) onto an interface aligned with the x axis. The notation is defined in Fig. 32. The arrows are the normals to the phase fronts and are called *rays*. The
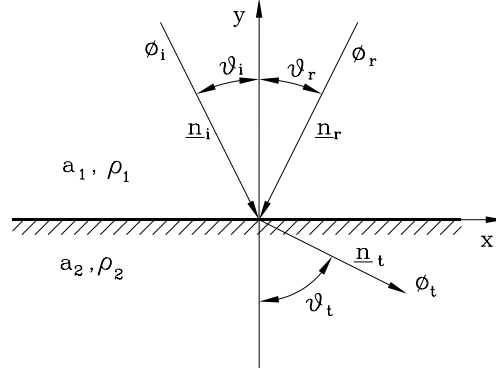
Figure 32. Refraction of plane waves.

potential function of the field in region ① is the superposition of the incident and reflected waves, while in region ② it is just the reflected wave,

$$\phi_1 = \phi_i + \phi_r \tag{14.45}$$
$$\phi_2 = \phi_t , \tag{14.46}$$

The boundary conditions are that the pressure and vertical component of the velocity be continuous across the interface, and that the phases of $\phi_{i,r,t}$ all be equal. The phase η is

$$\eta = t - \frac{n_x x + n_y y}{a} \tag{14.47}$$
$$= t - \frac{x \sin \theta \pm y \cos \theta}{a} , \tag{14.48}$$

where the sign expresses whether the wave is propagating in the positive or negative y direction. Thus, the phase condition at the interface is

$$t - \frac{x \sin \theta_i}{a_1} = t - \frac{x \sin \theta_r}{a_1} = t - \frac{x \sin \theta_t}{a_2} , \tag{14.49}$$

which give the familiar results

$$\begin{aligned} \theta_i &= \theta_r \\ \frac{\sin \theta_t}{a_2} &= \frac{\sin \theta_i}{a_1} . \end{aligned} \tag{14.50}$$

The last equation is Snell's Law. *Total reflection* occurs when $\theta_t = \pi/2$, *i.e.*, when

$$\sin \theta_i = \frac{a_1}{a_2} < 1 ; \qquad \text{Total reflection} \tag{14.51}$$

April 23, 2001

That is, total reflection can only occur in fast-slow refraction. The velocity v_{tr} along the interface of the intersection of a phase front with the interface is known as the trace velocity,

$$
\begin{aligned}
v_{tr} &= \frac{a_1}{\sin\theta_i} > a_1 \\
&= \frac{a_2}{\sin\theta_t} \; .
\end{aligned}
\tag{14.52}
$$

For real wave propagation the trace velocity must be supersonic. For total reflection v_{tr} becomes just sonic relative to region $\textcircled{2}$,

$$
v_{tr} = a_2 \; ; \qquad \text{Total reflection} ,
\tag{14.53}
$$

so wave propagation does not occur below the interface.

The wave amplitudes are determined by the dynamical boundary conditions at the interface,

$$
\begin{aligned}
u_{2y} &= u_{1y} & p_2 &= p_2 \\
\frac{\partial\phi_2}{\partial y} &= \frac{\partial\phi_1}{\partial y} & \rho_2\frac{\partial\phi_2}{\partial t} &= \rho_1\frac{\partial\phi_1}{\partial t} \\
\phi_t'\frac{\cos\theta_t}{a_2} &= \phi_i'\frac{\cos\theta_i}{a_1} - \phi_r'\frac{\cos\theta_r}{a_1} & \rho_2\phi_t' &= \rho_1(\phi_i' + \phi_r') ,
\end{aligned}
\tag{14.54}
$$

where the primes denote differentiation with respect to the argument. The last two equations determine ϕ_r'/ϕ_i' and ϕ_t'/ϕ_i',

$$
\frac{\phi_r'}{\phi_i'} = \frac{2\rho_1 a_2 \cos\theta_i}{\rho_2 a_2 \cos\theta_i + \rho_1 a_1 \cos\theta_t}
\tag{14.55}
$$

$$
\frac{\phi_t'}{\phi_i'} = \frac{\rho_2 a_2 \cos\theta_i - \rho_1 a_1 \cos\theta_t}{\rho_2 a_2 \cos\theta_i + \rho_1 a_1 \cos\theta_t} \; .
\tag{14.56}
$$

The pressures and velocities are

$$
\frac{p_r}{p_i} = \frac{\rho_2 a_2 \cos\theta_i - \rho_1 a_1 \cos\theta_t}{\rho_2 a_2 \cos\theta_i + \rho_1 a_1 \cos\theta_t} \quad ;
\tag{14.57}
$$

$$
\frac{p_t}{p_i} = \frac{2\rho_2 a_2 \cos\theta_i}{\rho_2 a_2 \cos\theta_i + \rho_1 a_1 \cos\theta_t} \quad ; \quad \frac{u_t}{u_i} = \frac{2\rho_1 a_1 \cos\theta_t}{\rho_2 a_2 \cos\theta_i + \rho_1 a_1 \cos\theta_t}
\tag{14.58}
$$

This gives an interesting case where there is no reflected pressure field, perhaps "total refraction,"

$$
\tan^2\theta_i = \frac{\left(\dfrac{\rho_2 a_2}{\rho_1 a_1}\right)^2 - 1}{1 - \left(\dfrac{a_2}{a_1}\right)^2} > 0 \; .
\tag{14.59}
$$

This condition can be realized in either slow-fast or fast-slow configurations, and is unique to acoustics.

14.5   Spherical waves

In spherical coordinates the wave equation is

$$
\frac{\partial^2\phi}{\partial t^2} - \frac{a_0^2}{r^2}\frac{\partial}{\partial r}\left(r^2\frac{\partial\phi}{\partial r}\right) = 0 \; .
\tag{14.60}
$$

The substitution

$$\phi = \frac{\kappa}{r} \tag{14.61}$$

reduces the wave equation to the one-dimensional form,

$$\frac{\partial^2 \kappa}{\partial t^2} - a_0^2 \frac{\partial^2 \kappa}{\partial r^2} = 0 , \tag{14.62}$$

so

$$\kappa = f(r - a_0 t) + g(r + a_0 t) , \tag{14.63}$$

or,

$$\boxed{\phi = \frac{f(r - a_0 t)}{r} + \frac{g(r + a_0 t)}{r} .} \tag{14.64}$$

The pressure disturbance is

$$p = -\rho_0 \frac{\partial \phi}{\partial t} = \frac{\rho_0 a_0}{r}(f' - g') , \tag{14.65}$$

and the velocity perturbation in the radial direction is

$$u = \frac{\partial \phi}{\partial r} = \frac{1}{r}(f' + g') - \frac{1}{r^2}(f + g) . \tag{14.66}$$

For the important case of a wave system propagating outward from a point source, $g = 0$, and

$$\boxed{\begin{aligned} p &= \rho_0 a_0 \frac{f'}{r} \\ u &= \frac{f'}{r} - \frac{f}{r^2} . \end{aligned}} \tag{14.67}$$

The fact that u now has two terms distinquishes a "far field" solution, $r \gg 0$,

$$u \doteq \frac{f'}{r} \tag{14.68}$$

$$p \doteq \rho_0 a_0 u , \tag{14.69}$$

for which (14.69) implies that the behavior in the far field is plane-wave-like, and a near field solution, $r \ll a_0 t$,

$$u \doteq -\frac{f(-a_0 t)}{r^2} . \tag{14.70}$$

The latter can be expressed in terms of the volume flux from the origin (source strength)

$$Q(t) = \lim_{r \to 0} 4\pi r^2 u = -4\pi f(-a_0 t) , \tag{14.71}$$

i.e.,

$$f(\eta) = -\frac{Q\left(-\frac{\eta}{a_0}\right)}{4\pi} ; \qquad f'(\eta) = \frac{Q'\left(-\frac{\eta}{a_0}\right)}{4\pi a_0} . \tag{14.72}$$

Thus, in terms of the source strength the outgoing wave is

$$
\begin{aligned}
\phi(r,t) &= -\frac{1}{4\pi} \frac{Q\left(t - \frac{r}{a_0}\right)}{r} \\
p(r,t) &= \frac{\rho_0}{4\pi} \frac{Q'\left(t - \frac{r}{a_0}\right)}{r} \\
u(r,t) &= \frac{1}{4\pi} \left[\frac{Q\left(t - \frac{r}{a_0}\right)}{r^2} + \frac{Q'\left(t - \frac{r}{a_0}\right)}{a_0 r} \right] .
\end{aligned}
\tag{14.73}
$$

The important properties of this solution are,

- $Q = \text{const} \longrightarrow$ no nonsteadiness, so no wave propagation.
  Incompressible, steady source.

- $(a \to \infty) \longrightarrow$ no delay, no distiction between near and far fields, *i.e.*, no wave propagation.
  Incompressible, non-steady source.

- In the far field p and u are *derivatives* of the source strength.
  In the absence of attenuation, high frequencies are enhanced.
  Acoustics is a differentiator (analog computer).

- The source strength attenuated by $1/r^2$ measures the departure of the wave field from plane waves,

$$
u(r,t) - \frac{p(r,t)}{\rho_0 a_0} = \frac{Q\left(t - \frac{r}{a_0}\right)}{4\pi r^2} .
\tag{14.74}
$$

Source of finite duration.   (*Wave system of finite spatial extent.*)
In this case both p and u (f and f') are zero ahead of and behind the wave, so the integral of f' (that is, p) through the wave is zero,

$$
\int_{-\infty}^{\infty} p(r,t)\, dt = 0 .
\tag{14.75}
$$

The area under the positive parts of the pressure disturbance is equal to that under the negative parts, and the total impulse is zero. The implications for the damaging effect of blast waves are important.

14.6   Cylindrical waves

For cylindrical waves the wave equation is simpler,

$$
\frac{1}{a_0^2} \frac{\partial^2 \phi}{\partial t^2} - \frac{1}{r} \frac{\partial}{\partial r}\left(r \frac{\partial \phi}{\partial r} \right) = 0 ,
\tag{14.76}
$$

but the solution is more complicated. It can be constructed by summing an array of spherical sources of uniform strength q aligned along the z-axis,

$$
\phi(r,t) = -\frac{1}{4\pi} \int_{-\infty}^{\infty} \frac{q\left(t - \frac{R}{a_0}\right)}{R}\, dz ,
\tag{14.77}
$$

where R is the distance from a source element at point $(0,0,z)$ to the observer in the x-y plane,

$$
\begin{aligned}
R^2 &= r^2 + z^2 \\
r^2 &= x^2 + y^2 .
\end{aligned}
\tag{14.78}
$$
$$
\tag{14.79}
$$

April 23, 2001

Grouping the contributions of pairs of points symmetric about $z = 0$ and rewriting the integral in terms of the retarded time

$$\tau = t - \frac{R}{a_0} , \tag{14.80}$$

such that

$$z^2 = a_0^2(t-\tau)^2 - r^2 , \tag{14.81}$$

gives

$$\phi(r,t) = -\frac{1}{2\pi} \int_{-\infty}^{t-\frac{r}{a_0}} \frac{q(\tau)}{\sqrt{(t-\tau)^2 - \frac{r^2}{a_0^2}}} \, d\tau . \tag{14.82}$$

The upper limit is the contribution from the nearest point on the z-axis ($z = 0$) and is retarded by the travel time. The lower limit shows that cylindrical waves have an infinite tail, even if the source is of finite duration. For example, if the source is only on for $0 < \tau < T$, then

$$\phi(r,t) = -\frac{1}{2\pi} \int_0^T \frac{q(\tau)}{\sqrt{(t-\tau)^2 - \frac{r^2}{a_0^2}}} \, d\tau . \tag{14.83}$$

and, for large time

$$\phi(r,t) \doteq -\frac{1}{2\pi} \frac{\int_0^T q(\tau) \, d\tau}{t} \tag{14.84}$$

$$p \doteq -\frac{\rho_0}{2\pi} \frac{\int_0^T q(\tau) \, d\tau}{t^2} . \tag{14.85}$$

The pressure dies off only algebraically at large time.

The integral in Eq. 14.82 has the unfortunate property that the integrand blows up at the upper limit, so the singular part must be removed. This is done most easily with the transformation

$$\tau = t - \frac{r}{a_0} \cosh \sigma$$

$$d\tau = -\frac{r}{a_0} \sinh \sigma \, d\sigma \tag{14.86}$$

$$= -\sqrt{(t-\tau)^2 - \frac{r^2}{a_0^2}} \, d\sigma .$$

After switching the limits of integration the solution becomes

$$\phi(r,t) = -\frac{1}{2\pi} \int_0^\infty q\left(t - \frac{r}{a_0} \cosh \sigma\right) d\sigma . \tag{14.87}$$

The singularity is removed and subsequent calculations are simplified. For example, the pressure turns out to be given simply by the differential of the source strength with respect to its argument, and the velocity yields a multiplicative term which is the r-derivative of the argument in the transformed equation,

$$p = \frac{\rho_0}{2\pi} \int_{-\infty}^{t-\frac{r}{a_0}} \frac{q'(\tau) \, d\tau}{\sqrt{(t-\tau)^2 - \frac{r^2}{a_0^2}}} \tag{14.88}$$

$$u = \frac{1}{2\pi r} \int_{-\infty}^{t-\frac{r}{a_0}} \frac{q'(\tau)(t-\tau) \, d\tau}{\sqrt{(t-\tau)^2 - \frac{r^2}{a_0^2}}} \tag{14.89}$$

14.7 General acoustic field from superposition of sources

Flow fields can in general be constructed by superposing distributions of point sources, such that the result satisfies the specified initial and boundary conditions. We first consider the simple case of point volume sources $f(\underline{r}, t)$. To conserve mass, they must be represented in the continuity equation, Eq. 14.13.

$$\frac{\partial \rho'}{\partial t} + \rho_0 \nabla \cdot \underline{u}' = \rho_0 \, q(\underline{r}, t) \, . \tag{14.90}$$

Eliminating ρ' from the first term with Eq. 6.40 and using the equations for $(p, \underline{u})$ in terms of the velocity potential, Eq. 14.35, there results a wave equation for ϕ,

$$\frac{1}{a_0^2} \frac{\partial^2 \phi}{\partial t^2} - \nabla^2 \phi = -q(\underline{r}, t) \, , \tag{14.91}$$

The solution is obtained by summing the effects observed by an observer at $\underline{r}$ of all the sources located at $\underline{\xi}$, where the separation distance is $\underline{R} = \underline{r} - \underline{\xi}$,

$$\boxed{\phi(\underline{r}, t) = -\frac{1}{4\pi} \int_{-\infty}^{\infty} \frac{q\left(\underline{\xi}, t - \frac{R}{a_0}\right)}{R} \, d\underline{\xi} \, ,} \tag{14.92}$$

(Born & Wolf, *Principles of Optics*, Pergammon, Ch. 2). ϕ is called the retarded potential.

From this solution, so-called fundamental solutions can be constructed for later superposition:

14.7.1 Impulsive point source.

An impulsive point source is

$$q(\underline{r}, t) = \delta(\underline{r}) \, \delta(t) \, , \tag{14.93}$$

where δ is the Dirac delta function. The solution g to the equation

$$\frac{1}{a_0^2} \frac{\partial^2 g}{\partial t^2} - \nabla^2 g = -\delta(\underline{r}) \, \delta t \tag{14.94}$$

is, from Eq. 14.92,

$$g(r, t) = -\frac{1}{4\pi} \int_{-\infty}^{\infty} \frac{\delta(\underline{\xi}) \, \delta\left(t - \frac{R}{a_0}\right)}{R} \, d\underline{\xi} \tag{14.95}$$

$$= -\frac{1}{4\pi} \frac{\delta\left(t - \frac{r}{a_0}\right)}{r} \, . \tag{14.96}$$

g is a Green's function. The Green's functions are spherically symmetric, *i.e.*, don't depend on the direction of $\underline{r}$.

The radial velocity induced by this source is

$$u = \frac{\partial g}{\partial r} = \frac{1}{4\pi} \left[\frac{\delta\left(t - \frac{r}{a_0}\right)}{r^2} + \frac{\delta'\left(t - \frac{r}{a_0}\right)}{a_0 r} \right] \, , \tag{14.97}$$

which, with[2]

$$\delta'(x) = -\frac{\delta(x)}{x} , \tag{14.98}$$

gives

$$u = \frac{\delta'\left(t - \frac{r}{a_0}\right)}{4\pi a_0 r} . \tag{14.99}$$

This equation has only one term, the $1/r$ term, and so exhibits far-field behavior *everywhere*, as would be expected of a point source.

14.7.2 General solution obtained from a distribution of impulsive point sources

. The solution to a general source distribution $f(\underline{r}, t)$ follows from

$$f(\underline{r}, t) = f(\underline{\xi}, \tau) \, \delta(\underline{r} - \underline{\xi}) \, \delta(t - \tau) , \tag{14.100}$$

by summing the corresponding Green's functions, namely,

$$\boxed{\phi(\underline{r}, t) = \iint_{-\infty}^{\infty} f(\underline{\xi}, \tau) \, g(|\underline{r} - \underline{\xi}|, t - \tau) \, d\underline{\xi} \, d\tau .} \tag{14.101}$$

Note that this is the convolution of the Green's function with the source distribution.

14.7.3 Harmonic point source.

The harmonic point source is

$$f(\underline{r}, t) = \delta(\underline{r}) e^{-i\omega t} , \tag{14.102}$$

the Green's function for which is, from Eq. 14.92,

$$g(r, t) = -\frac{1}{4\pi} \int_{-\infty}^{\infty} \frac{\delta(\underline{\xi}) \, e^{-i\omega\left(t - \frac{R}{a_0}\right)}}{R} \, d\underline{\xi} \tag{14.103}$$

$$= -\frac{1}{4\pi} \frac{e^{-i\omega\left(t - \frac{r}{a_0}\right)}}{r} = -\frac{1}{4\pi} \frac{e^{i(kr - \omega t)}}{r} , \tag{14.104}$$

where k is the wave number,

$$k = \frac{\omega}{a_0} . \tag{14.105}$$

---

[2]Properties of the delta function can be proven by operating on test functions, say $f(x)$. In this case it is convenient to expand $f(x)$ at the origin, $f(x) = f(0) + xf'(0) + \ldots$, and to consider the operation

$$\int_{-\infty}^{\infty} f(x) \frac{\delta(x)}{x} \, dx = f(0) \int_{-\infty}^{\infty} \frac{\delta(x)}{x} \, dx + f'(0) \int_{-\infty}^{\infty} \delta(x) \, dx + \ldots$$

$$= \int_{-\infty}^{\infty} f'(x) \delta(x) \, dx$$

$$= f(x) \delta(x) \Big|_{-\infty}^{\infty} - \int_{-\infty}^{\infty} f(x) \delta'(x) \, dx$$

The first term on the right side of the top equation is zero because $\delta(x)/x$ is an odd function, the second equation results from the definition $\int_{-\infty}^{\infty} f(x)\delta(x) \, dx = f(0)$, and the first term of the third equation is zero because $\delta(x)$ only has a contribution at $x = 0$. Thus, Eq. 14.98 is proven.

The acoustic velocity and pressure induced by the point harmonic source are

$$
\begin{aligned}
u &= \frac{\partial g}{\partial r} &= \frac{1}{4\pi r}\left(\frac{1}{r} - ik\right) e^{i(kr-\omega t)} \\
p &= -\rho_o \frac{\partial g}{\partial t} &= -\frac{\rho_0\, i\omega}{4\pi r} e^{i(kr-\omega t)} \; .
\end{aligned}
\tag{14.106}
$$

In the far field they are,

$$
\begin{aligned}
u &\doteq -\frac{1}{4\pi}\frac{ik}{r} e^{i(kr-\omega t)} \\
p &\doteq -\frac{\rho_0 a_0}{4\pi}\frac{ik}{r} e^{i(kr-\omega t)}
\end{aligned}
\tag{14.107}
$$

so, again, nearly plane-wave behavior results,

$$
p \doteq \rho_0 a_0\, u \; .
\tag{14.108}
$$

The acoustic energy flux is

$$
F = |pu| = \frac{1}{(4\pi)^2}\, \rho_0 a_0\, \frac{\omega^2}{r^2} \; .
\tag{14.109}
$$

14.7.4   General solution for harmonic waves

. The solution to a general source distribution,

$$
f(\underline{r},t) = f(\underline{r})\, e^{-i\omega t} \; ,
\tag{14.110}
$$

such that

$$
f(\underline{r},t) = f(\underline{\xi})\, \delta(\underline{r} - \underline{\xi})\, e^{-i\omega t} \; ,
\tag{14.111}
$$

is

$$
\boxed{\phi(\underline{r},t) = \int_{-\infty}^{\infty} f(\underline{\xi})\, g(|\underline{r} - \underline{\xi}|, t)\, d\underline{\xi} \; ,}
\tag{14.112}
$$

again, the convolution of the Green's function with the source distribution. Substituting from Eq. 14.104 yields the harmonic retarded potential,

$$
\boxed{\phi = -\frac{1}{4\pi} \int_{-\infty}^{\infty} f(\underline{\xi}) \frac{e^{i(kR-\omega t)}}{R}\, d\underline{\xi} \; .}
\tag{14.113}
$$

14.8   Harmonic dipoles and quadrupoles

In this section we construct higher-order singularities from simple ones.

14.8.1   Dipole source

A dipole can be constructed by superposing two point sources of equal magnitude A and opposite sign separated by an infinitesimal distance δ (Fig. 33).   For this calculation they are aligned with the z-axis. The acoustic field resulting from the superposition is

$$
\phi_d = \lim_{\delta \to 0} \frac{\left[Ag_{\frac{\delta}{2}} - Ag_{-\frac{\delta}{2}}\right]}{\delta}\, \delta = A'\frac{\partial g}{\partial z}\Big|_0 \; ,
\tag{14.114}
$$
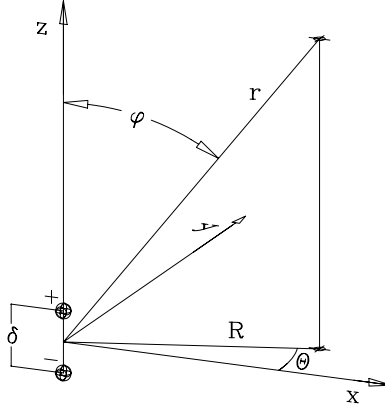
Figure 33. Schematic diagram for the construction of a dipole oriented with the z-axis.

where, in order to get a finite dipole strength A', the source strength must become infinite such that $A\delta \to A'$. Writing the z derivative

$$\frac{\partial}{\partial z} = \frac{z}{r}\frac{\partial}{\partial r} ; \qquad \frac{z}{r} = \cos\phi , \tag{14.115}$$

gives

$$\phi_d = -\frac{A'}{4\pi r} ik\cos\phi \left(1 + \frac{i}{kr}\right) e^{i(kr-\omega t)} . \tag{14.116}$$

Use of notation ϕ for both the velocity potential and an angle should cause no confusion because the angle always occurs in a trigonometric function. For a dipole aligned in any arbitrary direction, A' is assigned that direction, and

$$\boxed{\phi_d = -i\frac{A' \cdot k}{4\pi r}\left(1 + \frac{i}{kr}\right) e^{i(kr-\omega t)} .} \tag{14.117}$$

In the far field

$$\phi_d \doteq -\frac{A'}{4\pi}\frac{ik\cos\phi}{r}e^{i(kr-\omega t)} , \tag{14.118}$$

and

$$u \doteq \frac{A'}{4\pi}\frac{k^2\cos\phi}{r}e^{i(kr-\omega t)} \tag{14.119}$$

$$p \doteq \rho_0 a_0 \frac{A'}{4\pi}\frac{k^2\cos\phi}{r}e^{i(kr-\omega t)} , \tag{14.120}$$

showing once again the plane-wave behavior, and

$$F = |pu| = \rho_0 a_0 \left(\frac{A'}{4\pi}\right)^2 \frac{k^4\cos^2\phi}{r^2} . \tag{14.121}$$

14.8.2 Quadrupole source

A quadrupole is constructed from two dipoles displaced, say, in the x-direction (Fig. 34).

$$\phi_q = A'' \frac{\partial \phi_d}{\partial x} , \tag{14.122}$$

90   April 23, 2001
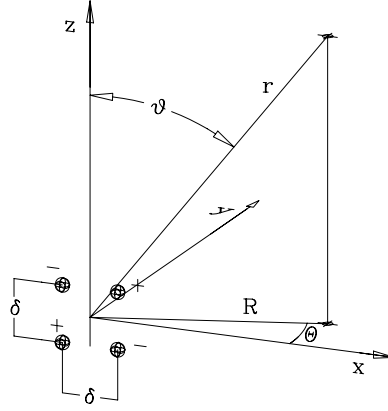
Figure 34. Schematic diagram for the construction of a quadrupole from two dipoles displaced along the x-axis.

where $A'\delta \to A''$. Writing

$$\frac{\partial}{\partial x} = \frac{x}{r}\frac{\partial}{\partial r} , \qquad (14.123)$$

gives

$$\phi_q = \frac{A''}{4\pi r}k^2\frac{xz}{r^3}\left[1 + \frac{3i}{kr} - \frac{3}{(kr)^2}\right]e^{(kr-\omega t)} . \qquad (14.124)$$

Now,

$$\frac{z}{r} = \cos\phi ; \qquad \frac{x}{R} = \cos\theta ; \qquad \frac{R}{r} = \sin\phi , \qquad (14.125)$$

so,

$$\boxed{\phi = \frac{A''}{4\pi r}\frac{k^2}{r}\sin\phi\cos\phi\cos\theta\left[1 + \frac{3i}{kr} - \frac{3}{(kr)^2}\right]e^{(kr-\omega t)} .} \qquad (14.126)$$

14.9 Radiation from a plane

A classic problem in acoustics is the sound generated by sources in a plane, with application to loudspeakers, transducers, etc. The geometry is shown in Fig. 35. The acoustic field at the point $\underline{r}$ generated by all the patches at $\underline{\rho}$ in the x-y plane, distance R from $\underline{r}$, is the summation of a distribution of spherical waves,

$$\phi = -\frac{1}{4\pi}e^{-i\omega t}\int f(\underline{\rho})\frac{e^{ikR}}{R}\,d\underline{\rho} . \qquad (14.127)$$

Now,

$$\rho^2 = \xi^2 + \eta^2 \qquad (14.128)$$
$$r^2 = x^2 + y^2 + z^2 \qquad (14.129)$$
$$R^2 = (x - \xi)^2 + (y - \eta)^2 + z^2 \qquad (14.130)$$
$$= r^2 + \rho^2 - 2(x\xi + y\eta) \qquad (14.131)$$
$$= r^2\left[1 + \frac{\rho^2}{r^2} - 2\frac{x\xi + y\eta}{r^2}\right] . \qquad (14.132)$$

From the sketch,

$$\frac{x\xi + y\eta}{r} = \frac{\widetilde{r}\cdot\underline{\rho}}{r} = \sin\phi\frac{\widetilde{r}\cdot\underline{\rho}}{\widetilde{r}} . \qquad (14.133)$$

91 April 23, 2001
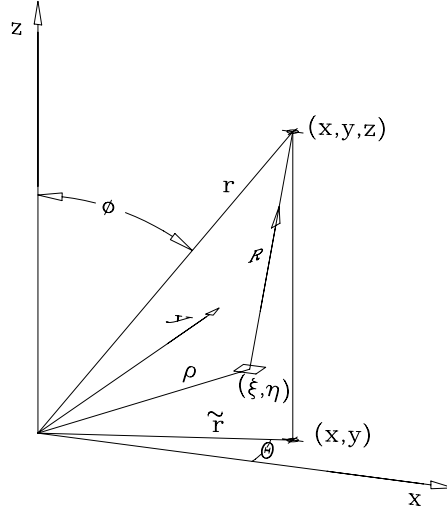
Figure 35. Geometry for radiation from a plane

For the purpose of approximating the phase kR, Eq. 14.132 is expanded as

$$R = r \left[1 + \underbrace{\frac{\rho^2}{2r^2}}_{\text{Fraunhofer}} - \frac{x\xi + y\eta}{r^2} - \underbrace{\frac{1}{2} \left(\frac{x\xi + y\eta}{r^2} \right)^2}_{\text{Fraunhofer}} \right] + \underbrace{\mathcal{O}\left(\frac{\rho^3}{r^2} \right)}_{\text{Fresnel}}, \tag{14.134}$$

where the underbraces denote the terms, and smaller, neglected for

$$\text{Fresnel Diffraction ;} \qquad \frac{k\rho^3}{r^2} \ll 2\pi \tag{14.135}$$

$$\text{Fraunhofer Diffraction ;} \qquad \frac{k\rho^2}{r} \ll 2\pi . \tag{14.136}$$

In the latter approximation, using Eq. 14.133,

$$kR \doteq kr - k \sin\phi \, \frac{\widetilde{r} \cdot \rho}{\widetilde{r}} . \tag{14.137}$$

Define the wave vector

$$\underline{k} \equiv k \, \frac{R}{R} \doteq k \, \frac{r}{r} . \tag{14.138}$$

It's projection in the x-y plane is

$$\underline{\kappa} = k \sin\phi \, \frac{\widetilde{\underline{r}}}{\widetilde{r}} , \tag{14.139}$$

so

$$kR \doteq kr - \underline{\kappa} \cdot \underline{\rho} . \tag{14.140}$$

Thus, the Fraunhofer approximation to Eq. 14.127 is

$$\phi = -\frac{e^{i(kr - \omega t)}}{4\pi r} \int_{-\infty}^{\infty} f(\underline{\rho}) \, e^{-i\underline{\kappa} \cdot \underline{\rho}} \, d\underline{\rho} . \tag{14.141}$$

April 23, 2001

This can be simplified by recognizing that the 2D spatial Fourier Transform is

$$\mathcal{F}(\underline{k}) \;=\; \frac{1}{2\pi} \int_{-\infty}^{\infty} f(\underline{\rho}) \, e^{-i\underline{k}\cdot\underline{\rho}} \, d\underline{\rho} \,, \tag{14.142}$$

so

$$\boxed{\phi \;=\; -\frac{e^{i(kr-\omega t)}}{2r} \, \mathcal{F}(\underline{\kappa}) \,.} \tag{14.143}$$

The resulting acoustic field consists of a spherical wave with a directional dependence which depends on the source distribution in the source plane. Acoustic propagation takes the Fourier transform of the distribution in the source plane. This result is the origin of the field called "Fourier optics."

Acoustically compact source If the extent a of the source in the transverse plane is small, in the sense that $ka \ll 1$, then the exponential evaluates to unity and

$$\mathcal{F}(\underline{k}) \;=\; \frac{S}{2\pi} \frac{1}{S} \int_{-\infty}^{\infty} f(\underline{\rho}) \, d\underline{\rho} \;=\; \frac{\overline{f}S}{2\pi} \,, \tag{14.144}$$

where S is the surface area of the volume occupied by the source and $\overline{f}$ is the mean source strength. The velocity potential is

$$\phi \;=\; -\overline{f}S \, \frac{e^{i(kr-\omega t)}}{4\pi r} \,. \tag{14.145}$$

14.10 Aero-acoustics

Aero-acoustics is the production of noise by nonsteady fluid flow, usually turbulent flow, but also periodically varying flows, *etc.* In the 1950's a model equation for generation of noise by flow was derived from the equations of motion by M. J. Lighthill. The advent of jet noise produced by modern jet-powered aircraft stimulated rapid growth of the field in the 1960's.

Allowing for mass sources in the continuity equation,

$$\frac{\partial \rho}{\partial t} + \nabla \cdot \rho \underline{u} \;=\; m \,, \tag{14.146}$$

and vector forces in the inviscid momentum equation,

$$\frac{\partial \rho \underline{u}}{\partial t} + \nabla \cdot \rho \underline{u}\underline{u} + \nabla p \;=\; \underline{F} \,, \tag{14.147}$$

eliminating the pressure by (6.40), differentiating the continuity equation w.r.t. t, taking the divergence of the momentum equation, and subtracting the latter from the former, yields a wave equation for ρ,

$$\boxed{\frac{1}{a_0^2} \frac{\partial^2 \rho}{\partial t^2} - \nabla^2 \rho \;=\; -\frac{1}{a_0^2}\left(-\frac{\partial m}{\partial t} + \nabla \cdot \underline{F} - \nabla \cdot \nabla \cdot \rho \underline{u}\underline{u}\right) \,.} \tag{14.148}$$

Treating the rhs as known, Eq. 14.148 is in the form of Eq. 14.91, so the solution is formally, say, Eq. 14.112,

$$\rho \;=\; \frac{1}{a_o^2} \int_{-\infty}^{\infty} (-\dot{m} + \nabla_{\underline{\xi}} \cdot \underline{F} - \nabla_{\underline{\xi}} \cdot \nabla_{\underline{\xi}} \cdot \rho \underline{u}\underline{u}) \; g(|\underline{r} - \underline{\xi}|, t) \, d\underline{\xi} \,. \tag{14.149}$$

The integral is over the entire source region, so if the surface containing the volume of integration is outside all sources, then by the divergence theorem

$$\int g \, \nabla \cdot \underline{F} \, d\underline{\xi} \;=\; -\int \underline{F} \cdot \nabla g \, d\underline{\xi} \,, \tag{14.150}$$

so the force term yields a dipole source. Similarly, the rate of strain tensor term transforms to a quadrupole source, and so in Cartesian tensor notation

$$\rho \;=\; \frac{1}{a_o^2} \int_{-\infty}^{\infty} \left(-\dot{m}g \;-\; F_i \frac{\partial g}{\partial \xi_i} \;+\; \rho u_i u_j \frac{\partial^2 g}{\partial \xi_i \partial \xi_j} \right) d\xi \;. \tag{14.151}$$

This equation is suggestive, and has been the basis for 4 decades of work on aerodynamic noise. However, the approach is not unique, and other possible models have not been thoroughly investigated.

14.10.1 *Scaling of jet noise*

To get an idea of the velocity dependence of jet noise, we model the dilatational effect of pressure perturbations in a turbulent jet as sources of mass. Consider a subsonic turbulent jet of velocity U as shown in Fig. 36. By dimensional reasoning, in turbulent flow pressure fluctuations are of order of the
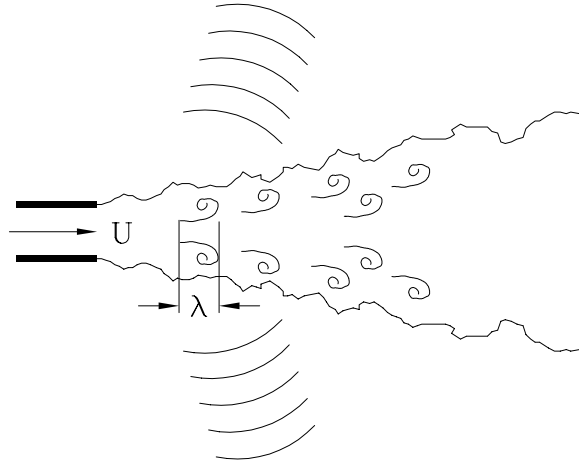
Figure 36. Model of the noise generated by a turbulent jet

turbulent energy,

$$\overline{p'} \;\sim\; \rho_0 \overline{u'^2} \;, \tag{14.152}$$

and a characteristic noise-producing scale of the turbulence is of the order of the diameter of the jet, or smaller, say, the so-called integral scale $\lambda \sim D$. The convection time,

$$\tau \;\sim\; \frac{\lambda}{U} \;, \tag{14.153}$$

fixes a typical period of the turbulence. The dilatational effect is obtained by transforming the pressure fluctuations to density fluctuations by Eq. 6.40,

$$\overline{\rho'} \;\sim\; \frac{\overline{p'}}{a_0^2} \;\sim\; \rho_0 \frac{\overline{u'^2}}{a_0^2} \;, \tag{14.154}$$

and the mass-flux fluctuation is a consequence of the density fluctuation ocurring for a time τ in a volume λ^3,

$$\dot{m}' \;\sim\; \frac{\rho' \lambda^3}{\tau} \;. \tag{14.155}$$

This in turn implies a volume source strength

$$q \sim \frac{\dot{m}'}{\rho_0} \,, \tag{14.156}$$

which finally gives us the forcing function for the acoustic waves,

$$q \sim \frac{\overline{u'^2}}{a_o^2} \frac{\lambda^3}{\tau} \,. \tag{14.157}$$

Propagation to the far field has, to order of magnitude, the effect of a point source, Eqs. 14.73, and differentiates the source strength. The acoustic pressure is given by the second of Eqs. 14.73, where $q' \sim q/\tau$, so

$$p \sim \rho_0 \frac{\overline{u'^2}}{a_o^2} \frac{\lambda^3}{\tau^2} \frac{1}{r} \,. \tag{14.158}$$

The acoustic energy flux (intensity) is therefore

$$F = |pu| = \frac{p^2}{\rho_0 a_0} \sim \rho_0 \frac{\left(\overline{u'^2}\right)^2}{a_0^5} \frac{\lambda^6}{\tau^4} \frac{1}{r^2} \,. \tag{14.159}$$

In jets, $\overline{u'} \sim U$. With Eq. 14.153, the total flux integrated over the entire sphere in the far field is

$$\boxed{F\, r^2 \sim \rho_0 \frac{\lambda^2 \, U^8}{a_0^5}} \,, \tag{14.160}$$

a very strong dependence on the jet velocity.

14.11 Geometrical acoustics

High-frequency limit. Geometrical acoustics is an intuitive way to treat wave-propagation in nonuniform media, and has application to the sonic boom problem. A plane wave in such a medium is taken to have amplitude and phase varying slowly, that is over distances large compared to the wavelength,

$$\phi(\underline{x}, t) = A(\underline{x}, t)\, e^{i\Psi(\underline{x}, t)} \,, \tag{14.161}$$

where Ψ is the phase function or eikonal. Over small distances and time the phase changes according to the Taylor expansion

$$\Psi = \frac{\partial \Psi}{\partial x} x_i + \frac{\partial \Psi}{\partial t} t \,. \tag{14.162}$$

Comparing with Eq. 14.35 for an outgoing wave, there results

$$\boxed{\begin{aligned} \underline{k} &= \nabla \Psi \\ \omega &= -\frac{\partial \Psi}{\partial t} \end{aligned}} \tag{14.163}$$

We consider problems in which

$$\frac{\partial \omega}{\partial t} = 0 \,, \tag{14.164}$$

so

$$\omega = f(\underline{k}, \underline{x}) = a_0(\underline{k}, \underline{x}) \, k \, . \tag{14.165}$$

That is,

$$-\frac{\partial \Psi}{\partial t} = f(\underline{k}, \underline{x}) \, . \tag{14.166}$$

Taking the gradient of (14.166) and changing the order of differentiation on the lhs,

$$-\frac{\partial k_i}{\partial t} = \frac{\partial f}{\partial k_j} \frac{\partial k_i}{\partial x_j} + \frac{\partial f}{\partial x_i} \, , \tag{14.167}$$

where also the order of differentiation of $\partial k_i / \partial x_j$ has been changed because

$$\frac{\partial k_j}{\partial x_i} = \frac{\partial^2 \Psi}{\partial x_i \partial x_j} = \frac{\partial^2 \Psi}{\partial x_j \partial x_i} \, . \tag{14.168}$$

Thus, in view of Eq. 14.165,

$$\frac{\partial k_i}{\partial t} + \frac{\partial \omega}{\partial k_j} \frac{\partial k_i}{\partial x_j} = -\frac{\partial \omega}{\partial x_i} \, . \tag{14.169}$$

This equation is in the form of a one-way wave equation where the propagation speed is

$$U = \frac{\partial \omega}{\partial k_j} \, , \tag{14.170}$$

the "group velocity." That is,

$$\boxed{\frac{d\underline{k}}{dt} = -\nabla \omega \qquad \text{along} \qquad \frac{d\underline{x}}{dt} = U = \frac{\partial \omega}{\partial \underline{k}} \, .} \tag{14.171}$$

This is the ray equation, prescribing how the rays of the wavefronts are traced.

In a nondispersive medium, $a_0 = a_0(\underline{x})$ and

$$\frac{d\underline{x}}{dt} = \frac{\partial \omega}{\partial \underline{k}} = a_0(\underline{x}) \frac{\underline{k}}{k} \, . \tag{14.172}$$

Uniform medium In a uniform dispersive medium dispersive $a_0 = a_0(\underline{k})$, so $\omega = f(\underline{k})$ and $\nabla \omega = 0$. Therefore,

$$\frac{d\underline{k}}{dt} = 0 \qquad \text{along} \qquad \frac{d\underline{x}}{dt} = \frac{\partial \omega}{\partial \underline{k}} \, . \tag{14.173}$$

In a nondispersive medium, Eq. 14.172 holds, so

$$\boxed{\frac{d\underline{k}}{dt} = 0 \qquad \text{along} \qquad \frac{d\underline{x}}{dt} = a_0 \frac{\underline{k}}{k} \, .} \tag{14.174}$$

In a uniform nondispersive medium the rays are straight and the direction of propagation is parallel to $\underline{k}$.

By tracing rays generated by accelerating and maneuvering aircraft according to the requirement that the ray angle to the flight path be $\frac{\pi}{2} - \beta$, where β is the Mach angle, one can show how the fronts tend to focus and form cusps at the foci. The first sketch shows the rays and one wavefront generated by an aircraft flying from left to right, initially at $M = 1$, and steadily accelerated until reaching the marked point with

April 23, 2001
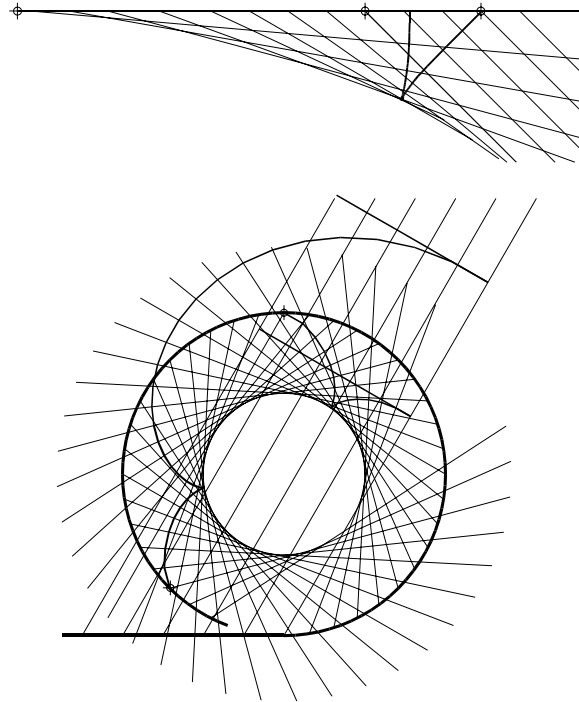
the emphasized ray, whereupon it maintains steady speed. A wavefront corresponding to a time near the end of the path is shown thickened. The second sketch above shows a map view of a supersonic aircraft which flies straight and then enters a left turn of constant radius at constant speed. Two wavefronts are shown, one half way through the maneuver and one near the end. It can be seen how the front folds twice, the first, proceeding from the aircraft, at a circular caustic and the second not at a crossing of rays, but owing to the fact that the post-focus wave joins with the unfocused wave from the straight-flying pre-maneuver trajectory. At the cusp a "super-boom" occurs. The figure below shows just one of many results obtained in French tests of aircraft maneuvers during the 1970's. The traces are pressure *vs.* time on an array of microphones. The incident shock starts at $t = 0$ with an N-wave (microphone 25) and the superboom occurs on microphone 15. Note the change of wave form on the post-focus fold of the front. On microphones 11–14 a "rumble" in the evanescent region is seen (see below).

Non-uniform non-dispersive medium. In a non-uniform non-dispersive medium

$$\omega(k, \underline{x}) \;=\; a_0(\underline{x})\, k \tag{14.175}$$

$$\nabla \omega \;=\; \nabla a_0 \, k \tag{14.176}$$

$$\frac{\partial \omega}{\partial \underline{k}} \;=\; a_0(\underline{x})\, \frac{\underline{k}}{k}\;, \tag{14.177}$$

so

$$\boxed{\frac{d\underline{k}}{dt} \;=\; -k\,\nabla a_0 \qquad \text{along} \qquad \frac{d\underline{x}}{dt} \;=\; a_0\, \frac{\underline{k}}{k}\;.} \tag{14.178}$$

Stratified atmosphere. A relatively simple non-uniform medium is a stratified atmosphere, $a_0 = a_0(y)$.

$$\omega \;=\; a_0(y)\, k \tag{14.179}$$

$$k^2 \;=\; \frac{\omega^2}{a_0^2(y)} \;=\; k_x^2 + k_y^2\;. \tag{14.180}$$

Therefore, from the ray equation,

$$\frac{dk_x}{dt} \;=\; 0\;;97 \qquad \boxed{k_x \;=\; k\sin\theta \;=\; \text{const}} \tag{14.181}$$
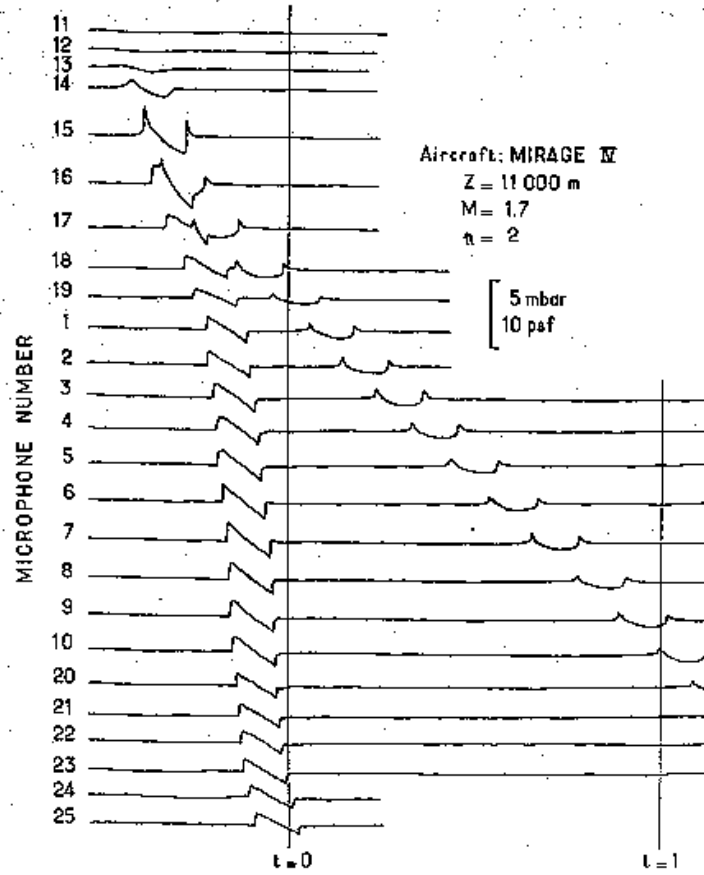
Wanner *et al.*, J. Acoust. Soc. Am., **52**, 13 (1972)

$$k_y = \pm\sqrt{\frac{\omega^2}{a_0^2(y)} - k_x^2} \, , \tag{14.182}$$

where θ is the angle between the k vector and the vertical, and the rays are

$$\frac{dx}{dt} = a_0(y)\frac{k_x}{k} \tag{14.183}$$

$$\frac{dy}{dt} = a_0(y)\frac{k_y}{k} \tag{14.184}$$

or,

$$\frac{dx}{dy} = \frac{k_x}{k_y} = \pm\sqrt{\frac{\omega^2}{a_0^2(y)k_x^2} - 1} \, , \tag{14.185}$$

The sketch shows the consequences for a point source in an atmosphere in which the sound-speed gradient points down vertically. The rays propagating upward have positive slope (the $+$ sign in Eq. 14.185) and experience a decreasing sound speed, so the slope increases. The rays propagating downward have negative slope (the $-$ sign in Eq. 14.185) and experience an increasing sound speed, so the slope decreases negatively, *i.e.*, it also increases. At the minima there is the possibility that the signs change to $+$, in which case the behavior is the same as in the positive half-plane (solid lines), or the sign does not change and k_y becomes

April 23, 2001
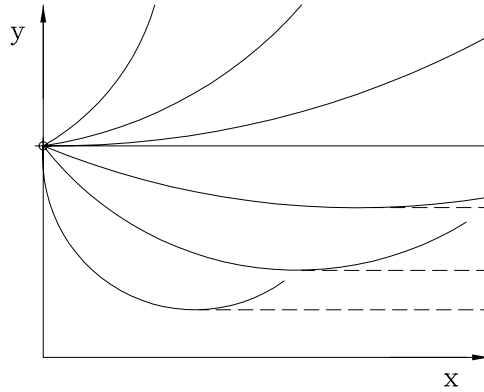
imaginary (dashed lines). The effect of this can be understood by considering what happens to a plane wave when k_y becomes imaginary,

$$\phi \;=\; A\,e^{i(k_x x + k_y y - \omega t)} \;=\; e^{i(k_x - \omega t)}\,e^{-k_y y} \;. \tag{14.186}$$

Thus, the wave decays rapidly in the y-direction. It is called an "evanescent" wave. The details of the geometrical acoustics of shadow regions and diffracted waves is elegantly described by the "geometrical theory of diffraction" (see for example Sekler & Keller, J. Acoust. Soc. Am. **31**, 192, 1952).

15 Potential Flow

Multi-dimensional nonsteady flow of an inviscid, non-heat conducting fluid.

15.1 Bernoulli equation for nonsteady flow

The Bernoulli equation for nonsteady flow is derived by introducing the definition of the velocity potential, $\underline{u} = \nabla\phi$ into the momentum equation, Eq. 2.16,

$$\frac{\partial \nabla\phi}{\partial t} + \frac{1}{2}\nabla(\nabla\phi)^2 + \frac{1}{\rho(p)}\nabla p = 0 . \tag{15.1}$$

How the second term was obtained can be understood in terms of Cartesian tensor notation. It is

$$u_j \frac{\partial u_i}{\partial x_j} = \frac{\partial \phi}{\partial x_j}\frac{\partial^2 \phi}{\partial x_i \partial x_j} \tag{15.2}$$

$$= \frac{1}{2}\frac{\partial}{\partial x_i}\left(\frac{\partial \phi}{\partial x_j}\frac{\partial \phi}{\partial x_j}\right) . \tag{15.3}$$

Differentiating (15.1) w.r.t. time gives

$$\frac{\partial^2 \nabla\phi}{\partial t^2} + \frac{1}{2}\frac{\partial}{\partial t}\nabla(\nabla\phi)^2 + \nabla\left(\frac{1}{\rho}\nabla p\right) = 0 , \tag{15.4}$$

where the last term is obtained by partially differentiating

$$\frac{\partial}{\partial t}\left(\frac{1}{\rho}\nabla p\right) = \frac{\partial 1/\rho}{\partial p}\nabla p \frac{\partial p}{\partial t} + \frac{1}{\rho}\nabla\frac{\partial p}{\partial t} \tag{15.5}$$

$$= \left(\nabla\frac{1}{\rho}\right)\frac{\partial p}{\partial t} + \frac{1}{\rho}\nabla\frac{\partial p}{\partial t} \tag{15.6}$$

$$= \nabla\left(\frac{1}{\rho}\frac{\partial p}{\partial t}\right) . \tag{15.7}$$

The ∇ can be taken outside every term of (15.4) and the equation integrated w.r.t. $\underline{x}$. The resulting arbitrary function of time is absorbed into ϕ. Thus

$$\frac{\partial^2 \phi}{\partial t^2} + \frac{1}{2}\frac{\partial}{\partial t}(\nabla\phi)^2 + \frac{1}{\rho}\frac{\partial p}{\partial t} = 0 . \tag{15.8}$$

This equation can then be integrated w.r.t. time to finally give the non-steady Bernoulli equation,

$$\boxed{\frac{\partial \phi}{\partial t} + \frac{(\nabla\phi)^2}{2} + \int \frac{dp}{\rho(p)} = \text{const} .} \tag{15.9}$$

15.2 The potential equation

The potential equation for this isentropic flow is derived from the mechanical energy equation Eq. 2.19 with $B = \tau = 0$, and Bernoulli's equation. The pressure gradient term in (2.19) can be written as part of a convective derivative, which can be converted to to the convective derivative of ρ by the definition of the

sound speed,

$$\frac{1}{\rho}\underline{u} \cdot \nabla p \;=\; \frac{1}{\rho}\frac{Dp}{Dt} - \frac{1}{\rho}\frac{\partial p}{\partial t} \tag{15.10}$$

$$=\; \frac{a^2}{\rho}\frac{D\rho}{Dt} - \frac{1}{\rho}\frac{\partial p}{\partial t} \tag{15.11}$$

$$=\; -a^2 \nabla \cdot \underline{u} - \frac{1}{\rho}\frac{\partial p}{\partial t} \;, \tag{15.12}$$

where the last equality is obtained by using the continuity equation. Thus the mechanical energy equation becomes

$$\frac{\partial u^2/2}{\partial t} + \underline{u} \cdot \nabla \frac{u^2}{2} - a^2 \nabla \cdot \underline{u} - \frac{1}{\rho}\frac{\partial p}{\partial t} \;=\; 0 \;. \tag{15.13}$$

Eq. 15.8 is used to eliminate the pressure from Eq. 15.13, with the result

$$\boxed{\frac{\partial^2 \phi}{\partial t^2} + \frac{\partial}{\partial t}(\nabla \phi)^2 + \frac{1}{2}\nabla \phi \cdot \nabla (\nabla \phi)^2 - a^2 \nabla^2 \phi \;=\; 0 \;.} \tag{15.14}$$

For steady flow, in terms of velocities in Cartesian tensor notation the equation is

$$\frac{1}{2}\,u_j\,\frac{\partial u_i^2}{\partial x_j} \;=\; a^2\,\frac{\partial u_i}{\partial x_i} \;. \tag{15.15}$$

Note that:

i. When $a \to \infty$ the equation becomes

$$\boxed{\nabla^2 \phi \;=\; 0 \;,} \tag{15.16}$$

the Laplace equation, valid for incompressible, nonsteady irrotational flow of an ideal (inviscid, non-heatconducting) fluid. The irrotationality follows from the existence of the velocity potential.

ii. For small amplitude motions, neglecting the nonlinear terms, the equation becomes

$$\boxed{\frac{\partial^2 \phi}{\partial t^2} - a_0^2\,\nabla^2 \phi \;=\; 0 \;,} \tag{15.17}$$

the wave equation.

iii. The dot-product nonlinear term in Cartesian tensor notation is, from the original form of the mechanical energy equation

$$\frac{1}{2}u_j\frac{\partial u_i^2}{\partial x_j} \;=\; u_i u_j \frac{\partial u_i}{\partial x_j} \tag{15.18}$$

so in these terms for steady flow, the equation becomes

$$\boxed{u_i u_j \frac{\partial u_i}{\partial x_j} \;=\; a^2\,\frac{\partial u_i}{\partial x_i} \;.} \tag{15.19}$$

This form illustrates how the coefficient of the nonlinear term "balances" a^2 to determine the super-sub-sonic behavior.

April 23, 2001

15.3 Small disturbance theory

We consider steady isentropic irrotational flow of a perfect gas, with uniform inflow from the left of velocity U and sound speed a_∞.

15.3.1 Energy equation for steady flow

In steady flow the total enthalpy is conserved,

$$a^2 + \frac{\gamma - 1}{2} u^2 = a_\infty^2 + \frac{\gamma - 1}{2} U^2 . \tag{15.20}$$

The velocity components are $(U + u, v, w)$. Substituting,

$$\boxed{a^2 = a_\infty^2 - \frac{\gamma - 1}{2} \left(2Uu - u^2 - v^2 - w^2\right) .} \tag{15.21}$$

15.3.2 The potential equation

Using this result in Eq. 15.19 and multiplying out gives

$$\left[a_\infty^2 - \frac{\gamma - 1}{2} \left(2Uu - u^2 - v^2 - w^2\right)\right] \left(\frac{\partial u}{\partial x} + \frac{\partial v}{\partial y} + \frac{\partial w}{\partial z}\right) \tag{15.22}$$

$$= (U+u)^2 \frac{\partial u}{\partial x} + v^2 \frac{\partial v}{\partial y} + w^2 \frac{\partial w}{\partial z} + (U+u)v \left(\frac{\partial v}{\partial x} + \frac{\partial u}{\partial y}\right)$$

$$+ (U+u)w \left(\frac{\partial w}{\partial x} + \frac{\partial u}{\partial z}\right) + vw \left(\frac{\partial v}{\partial z} + \frac{\partial w}{\partial y}\right) . \tag{15.23}$$

The above equations are exact. For small disturbances like those generated by slender bodies, $(u, v, w) \ll U$. If we now multiply out and keep terms of $\mathcal{O}(1)$ (lhs) and $\mathcal{O}(u)$ (rhs) in the coefficients of the velocity derivatives, we get

$$\left(1 - M_\infty^2\right) \frac{\partial u}{\partial x} + \frac{\partial v}{\partial y} + \frac{\partial w}{\partial z} = M_\infty^2 \left[(\gamma + 1)\frac{u}{U}\frac{\partial u}{\partial x} + (\gamma - 1)\frac{u}{U}\left(\frac{\partial v}{\partial y} + \frac{\partial w}{\partial z}\right)\right. \tag{15.24}$$

$$\left. + \frac{v}{U}\left(\frac{\partial v}{\partial x} + \frac{\partial u}{\partial y}\right) + \frac{w}{U}\left(\frac{\partial u}{\partial z} + \frac{\partial w}{\partial x}\right)\right] . \tag{15.25}$$

The terms on the rhs may become important when $M_\infty \to 1$, in particular the term in $\partial u/\partial x$. Thus, an equation valid for subsonic, transonic or supersonic flow is

$$\left(1 - M_\infty^2\right) \frac{\partial u}{\partial x} + \frac{\partial v}{\partial y} + \frac{\partial w}{\partial z} = M_\infty^2(\gamma + 1)\frac{u}{U}\frac{\partial u}{\partial x} , \tag{15.26}$$

or, in terms of the *perturbation* potential, $(u, v, w) = \nabla\phi$,

$$\boxed{\left(1 - M_\infty^2\right) \frac{\partial^2 \phi}{\partial x^2} + \frac{\partial^2 \phi}{\partial y^2} + \frac{\partial^2 \phi}{\partial z^2} = \frac{M_\infty^2(\gamma + 1)}{U} \frac{\partial \phi}{\partial x}\frac{\partial^2 \phi}{\partial x^2} .} \tag{15.27}$$

For subsonic and supersonic flow only,

$$\boxed{\left(1 - M_\infty^2\right) \frac{\partial^2 \phi}{\partial x^2} + \frac{\partial^2 \phi}{\partial y^2} + \frac{\partial^2 \phi}{\partial z^2} = 0 .} \tag{15.28}$$

April 23, 2001

In cylindrical polar coordinates,where

$$
\begin{aligned}
u_x &= \frac{\partial \phi}{\partial x} \\
u_r &= \frac{\partial \phi}{\partial r} \\
u_\theta &= \frac{1}{r} \frac{\partial \phi}{\partial \theta} ,
\end{aligned}
\tag{15.29}
$$

$$
\boxed{\left(1 - M_\infty^2\right) \frac{\partial^2 \phi}{\partial x^2} + \frac{1}{r} \frac{\partial}{\partial r}\left(r \frac{\partial \phi}{\partial r}\right) + \frac{1}{r^2} \frac{\partial^2 \phi}{\partial \theta^2} = 0 .}
\tag{15.30}
$$

15.3.3   Pressures.

The pressure coefficient is

$$
C_p = \frac{p - p_\infty}{\frac{1}{2} \rho_\infty U^2} = \frac{2}{\gamma M_\infty^2} \frac{p - p_\infty}{p_\infty} ,
\tag{15.31}
$$

where the last equality holds for a perfect gas. For isentropic flow,

$$
\frac{p}{p_\infty} = \left(\frac{a}{a_\infty}\right)^{\frac{2\gamma}{\gamma-1}} ,
\tag{15.32}
$$

which, with Eq. 15.21, gives

$$
\frac{p}{p_\infty} = \left[1 - \frac{\gamma-1}{2} M_\infty^2 \left(\frac{2u}{U} + \frac{u^2 + v^2 + w^2}{U^2}\right)\right]^{\frac{2\gamma}{\gamma-1}} .
\tag{15.33}
$$

Thus,

$$
C_p = \frac{2}{\gamma M_\infty^2} \left\{\left[1 - \frac{\gamma-1}{2} M^2 \left(\frac{2u}{U} + \frac{u^2 + v^2 + w^2}{U^2}\right)\right]^{\frac{\gamma}{\gamma-1}} - 1\right\}
\tag{15.34}
$$

From Eq. 15.21 we also have

$$
\frac{\rho}{\rho_\infty} = \left(\frac{T}{t_\infty}\right)^{\frac{1}{\gamma-1}} = \left[1 - \frac{\gamma-1}{2}\left(2Uu - u^2 - v^2 - w^2\right)\right]^{\frac{1}{\gamma-1}} .
\tag{15.35}
$$

Now, for small disturbances expand to quadratic terms. After some cancellations there results

$$
C_p \doteq -\left(\frac{2u}{U} + \left(1 - M_\infty^2\right)\frac{u^2}{U^2} + \frac{v^2 + w^2}{U^2}\right)
\tag{15.36}
$$

$$
\frac{\rho}{\rho_\infty} \doteq 1 - M_\infty^2 \frac{u}{U} + \frac{v^2 + w^2}{a_\infty^2} .
\tag{15.37}
$$

For plane flow it suffices to take just the linear term, but for axisymmetric flow because of the fact that u_r gets very large near the axis it turns out to be necessary to include the quadratic term in u_r (see below),

$$
\begin{aligned}
\text{Planar body}: \quad C_p &\doteq -2\frac{u}{U} \\
\text{Slender body of revolution}: \quad C_p &\doteq -2\frac{u}{U} - \frac{u_r^2}{U^2}
\end{aligned}
\tag{15.38}
$$

April 23, 2001

15.3.4 Boundary conditions – body.

The boundary condition on the body is that the flow be tangent to the body.

Plane Flow. For an airfoil with small surface deflections

$$\frac{v_b}{U + u_b} \doteq \frac{dy_b}{dx} \ , \tag{15.39}$$

so approximately

$$\frac{v_b}{U} \doteq \frac{dy_b}{dx} \ . \tag{15.40}$$

For a slender body the boundary conditions can be applied at $y = 0$,

$$\boxed{v(x, 0) \ = \ U \frac{d\, y_b(x)}{dx} \ .} \tag{15.41}$$

The result can be extended to nearly planar 3-dimensional flow, *i.e.*, for a slender wing, in which case the convention is to take y to be the spanwise coordinate and z to be vertical up,

$$\boxed{w(x, y, 0) \ = \ U \frac{\partial z_b(x, y)}{\partial x} \ .} \tag{15.42}$$

Axisymmetric Flow. Because the continuity equation must balance it implies an important scaling for u_r near $r = 0$,

$$\frac{1}{r} \frac{\partial u_r\, r}{\partial r} \ \sim \ \frac{\partial u}{\partial x} \ . \tag{15.43}$$

Since the last term must be well behaved we have that

$$u_r \ \sim \ \frac{1}{r} \quad \text{as} \quad r \longrightarrow 0 \ . \tag{15.44}$$

Therefore, the boundary condition should be multiplied by r and written

$$\boxed{(r\, u_r)_0 \ = \ U R \frac{dR(x)}{dx} \ .} \tag{15.45}$$

15.3.5 Solution – Plane slender body

The equations are

$$\text{Subsonic}: \quad \left(1 - M_\infty^2\right) \frac{\partial^2 \phi}{\partial x^2} + \frac{\partial^2 \phi}{\partial y^2} \ = \ 0$$

$$\tag{15.46}$$

$$\text{Supersonic}: \quad \left(M_\infty^2 - 1\right) \frac{\partial^2 \phi}{\partial x^2} - \frac{\partial^2 \phi}{\partial y^2} \ = \ 0$$

April 23, 2001

Supersonic case. By comparing the last equation with Eq. 14.21 we can immediately write down the solution from Eq. 14.33 by setting

$$\frac{x}{a_0} \quad \longrightarrow \quad \sqrt{M_\infty^2 - 1}\, y \;\equiv\; \lambda y \tag{15.47}$$

$$t \quad \longrightarrow \quad x \;, \tag{15.48}$$

i.e.,

$$\boxed{\phi \;=\; f\left(x - \sqrt{M_\infty^2 - 1}\, y\right) + g\left(x + \sqrt{M_\infty^2 - 1}\, y\right)} \tag{15.49}$$

The perturbation velocities and pressures are

$$u \;=\; \frac{\partial \phi}{\partial x} \;=\; f' + g' \tag{15.50}$$

$$v \;=\; \frac{\partial \phi}{\partial y} \;=\; -\lambda(f' - g') \tag{15.51}$$

$$\frac{v}{U} \;=\; -\frac{\lambda}{U}\left(f' - g'\right) \tag{15.52}$$

$$C_p \;=\; -2\frac{u}{U} \;=\; -\frac{2}{U}\left(f' + g'\right) \;. \tag{15.53}$$

Example. Diamond airfoil.
The surfaces of a slender diamond airfoil at angle of attack are
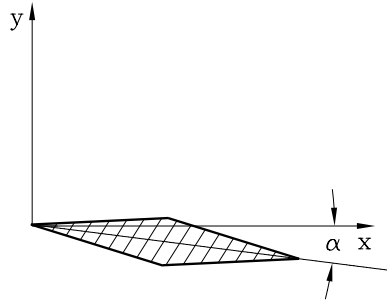
Figure 37. Diamond airfoil at angle of attack

$$
\begin{aligned}
y_u \;&=\; 2\delta\frac{x}{c} - \alpha x \;; & x &< \frac{c}{2} \\[2ex]
&=\; 2\delta\left(1 - \frac{x}{c}\right) - \alpha x \;; & x &> \frac{c}{2} \\[2ex]
y_l \;&=\; -2\delta\frac{x}{c} - \alpha x \;; & x &< \frac{c}{2} \\[2ex]
&=\; -2\delta\left(1 - \frac{x}{c}\right) - \alpha x \;; & x &> \frac{c}{2} \;.
\end{aligned}
\tag{15.54}
$$

Thus the boundary conditions $v/U = dy_b/dx$ are as follows, and their relationship to the pressure coefficient is established through Eqs. 15.52 and 15.53,

$$
\frac{v_u}{U} = \frac{dy_u}{dx} = \begin{array}{l} \dfrac{2\delta}{c} - \alpha \\[2ex] -\dfrac{2\delta}{c} - \alpha \end{array} = -\frac{\lambda}{U} f'(x - \lambda y_u) = \frac{\lambda}{U} \frac{U}{2} C_{pu} \quad \begin{array}{l} ; \quad x < \dfrac{c}{2} \\[2ex] ; \quad x > \dfrac{c}{2} \end{array}
$$
(15.55)

$$
\frac{v_l}{U} = \frac{dy_l}{dx} = \begin{array}{l} -\dfrac{2\delta}{c} - \alpha \\[2ex] \dfrac{2\delta}{c} - \alpha \end{array} = \frac{\lambda}{U} g'(x - \lambda y_l) = -\frac{\lambda}{U} \frac{U}{2} C_{pl} \quad \begin{array}{l} ; \quad x < \dfrac{c}{2} \\[2ex] ; \quad x > \dfrac{c}{2} \end{array} .
$$

Thus the pressure coefficients and their relations to lift and drag are

$$
C_{pu} = \begin{array}{l} \dfrac{2}{\lambda}\left(\dfrac{2\delta}{c} - \alpha\right) \\[2ex] -\dfrac{2}{\lambda}\left(\dfrac{2\delta}{c} + \alpha\right) \end{array} = \begin{array}{l} -dC_{Lu} \\[2ex] -dC_{Lu} \end{array} = \begin{array}{l} \dfrac{1}{\frac{2\delta}{c} - \alpha} dC_{Du} \\[2ex] -\dfrac{1}{\frac{2\delta}{c} + \alpha} dC_{Du} \end{array} \quad \begin{array}{l} ; \quad x < \dfrac{c}{2} \\[2ex] ; \quad x > \dfrac{c}{2} \end{array}
$$
(15.56)

$$
C_{pl} = \begin{array}{l} \dfrac{2}{\lambda}\left(\dfrac{2\delta}{c} + \alpha\right) \\[2ex] -\dfrac{2}{\lambda}\left(\dfrac{2\delta}{c} - \alpha\right) \end{array} = \begin{array}{l} dC_{Ll} \\[2ex] dC_{Ll} \end{array} = \begin{array}{l} \dfrac{1}{\frac{2\delta}{c} + \alpha} dC_{Dl} \\[2ex] -\dfrac{1}{\frac{2\delta}{c} - \alpha} dC_{Dl} \end{array} \quad \begin{array}{l} ; \quad x < \dfrac{c}{2} \\[2ex] ; \quad x > \dfrac{c}{2} \end{array} ,
$$

where the factors multiplying dC_D are the cosecants of the angles of the surface elements, i.e., their projections in the streamwise direction.

Integrating the lift we get

$$
C_{Lu} = -\frac{2}{\lambda}\left(\frac{2\delta}{c} - \alpha\right)\frac{c}{2} + \frac{2}{\lambda}\left(\frac{2\delta}{c} + \alpha\right)\frac{c}{2}
$$
(15.57)

$$
C_{Ll} = \frac{2}{\lambda}\left(\frac{2\delta}{c} + \alpha\right)\frac{c}{2} - \frac{2}{\lambda}\left(\frac{2\delta}{c} - \alpha\right)\frac{c}{2} ,
$$

so

$$
\boxed{C_L = \frac{4c}{\lambda}\alpha .}
$$
(15.58)

Of course there is no lift for $\alpha = 0$, and the lift is proportional to α.

The factors in $\left(\frac{2\delta}{c} \pm \alpha\right)$ in the drag multiply to give squares, which after multiplying out and canceling give

$$
\boxed{C_D = \frac{4c}{\lambda}\left[\left(\frac{2\delta}{c}\right)^2 + \alpha^2\right] .}
$$
(15.59)

April 23, 2001

Thus

- The drag is second order in δ.

- There is drag even for $\alpha = 0$. This is "wave drag" and is a consequence of the fact that the body makes first order disturbances far out into the fluid.

- The "drag due to lift" is of order α^2.

15.3.6 Solution – Slender body of revolution

The equations are

$$
\text{Subsonic}: \quad \left(1 - M_\infty^2\right) \frac{\partial^2 \phi}{\partial x^2} + \frac{1}{r} \frac{\partial}{\partial r} \left(r \frac{\partial \phi}{\partial r} \right) = 0
$$

$$
\text{Supersonic}: \quad \left(M_\infty^2 - 1\right) \frac{\partial^2 \phi}{\partial x^2} + \frac{1}{r} \frac{\partial}{\partial r} \left(r \frac{\partial \phi}{\partial r} \right) = 0
\tag{15.60}
$$

By comparing these equations with Eq. 14.76 we can immediately write down the solution from Eq. 14.82 by setting

$$
\frac{r}{a_0} \quad \longrightarrow \quad
\begin{cases}
\sqrt{M_\infty^2 - 1}\, r \;\equiv\; \lambda r \,; & \text{Supersonic case} \\[2ex]
\sqrt{1 - M_\infty^2}\, r \;\equiv\; mr \,; & \text{Subsonic case}
\end{cases}
\tag{15.61}
$$

$$
t \quad \longrightarrow \quad x
\tag{15.62}
$$

$$
\tau \quad \longrightarrow \quad \xi \,,
\tag{15.63}
$$

namely,

$$
\phi(x, r) = -\frac{1}{2\pi} \int_{-\infty}^{x - \lambda r} \frac{f(\xi)\, d\xi}{\sqrt{(\xi - x)^2 - \lambda^2 r^2}} \,; \qquad \text{Supersonic case}
\tag{15.64}
$$

$$
= -\frac{1}{4\pi} \int_{-\infty}^{\infty} \frac{f(\xi)\, d\xi}{\sqrt{(\xi - x)^2 + m^2 r^2}} \,; \qquad \text{Subsonic case} .
\tag{15.65}
$$

This is a solution for the velocity potential in terms of an as-yet undetermined source distribution f. For the subsonic case a form of Eq. 14.82 before the integration limits were changed to the semi-infinite range is used.

Supersonic case. This solution has the same structure as cylindrical acoustic waves, with the consequence that there is a disturbance (wake) downstream of the body, algebraically decaying to infinity. Again, the singular behavior of the integrand at the upper limit requires that the finite part of the integrals be determined. We use the same transformation as in acoustics,

$$
\xi = x - \lambda r \cosh \sigma \,,
\tag{15.66}
$$

so that

$$\lambda r \sinh \sigma = \sqrt{(\xi - x)^2 - \lambda^2 r^2} , \qquad (15.67)$$

and

$$d\xi = -\lambda r \sinh \sigma \, d\sigma \qquad (15.68)$$
$$= -\sqrt{(\xi - x)^2 - \lambda^2 r^2} \, d\sigma . \qquad (15.69)$$

We limit the range of integration by taking the body to start at $x = 0$. Then the solution transforms into

$$\phi = -\frac{1}{2\pi} \int_0^{\cosh^{-1} \frac{x}{\lambda r}} f(x - \lambda r \cosh \sigma) \, d\sigma . \qquad (15.70)$$

Now differentiation to get the velocities proceeds smoothly. We take that the body is sharp at the nose, $f(0) = 0$, so the term from the differential at the upper limit is zero. Then,

$$
\begin{aligned}
u &= \frac{\partial \phi}{\partial x} = -\frac{1}{2\pi} \int_0^{\cosh^{-1} \frac{x}{\lambda r}} f'(x - \lambda r \cosh \sigma) \, d\sigma \\[2mm]
&= -\frac{1}{2\pi} \int_0^{x - \lambda r} \frac{f'(\xi) \, d\xi}{\sqrt{(\xi - x)^2 - \lambda^2 r^2}} \\[2mm]
u_r \equiv v &= \frac{\partial \phi}{\partial r} = \frac{1}{2\pi} \int_0^{\cosh^{-1} \frac{x}{\lambda r}} \lambda \cosh \sigma f'(x - \lambda r \cosh \sigma) \, d\sigma \\[2mm]
&= \frac{1}{2\pi r} \int_0^{x - \lambda r} \frac{(\xi - x) f'(\xi) \, d\xi}{\sqrt{(\xi - x)^2 - \lambda^2 r^2}} .
\end{aligned}
\qquad (15.71)
$$

From the last equation it can be seen that

$$\lim_{r \to 0} 2\pi r v = f(x) , \qquad (15.72)$$

so we see that the source distribution is given in terms of the boundary condition applied at $r = 0$,

$$\boxed{f(x) = 2\pi U \left(\frac{rv}{U} \right)_0 .} \qquad (15.73)$$

In view of the boundary condition Eq. 15.45, the source strength can be written in terms of the cross-sectional area $S = \pi R^2$ of the body of revolution,

$$f(x) = U \frac{dS}{dx} . \qquad (15.74)$$

Example. Slender cone of half angle δ.
For the cone,

$$\frac{dR}{dx} = \delta \qquad (15.75)$$

$$\frac{dS}{dx} = 2\pi R \frac{dR}{dx} = 2\pi \delta^2 x , \qquad (15.76)$$

April 23, 2001

so

$$f(x) = 2\pi\,U\,\delta^2\,x \tag{15.77}$$
$$f'(x) = 2\pi\,U\,\delta^2\,, \tag{15.78}$$

and

$$\frac{u}{U} = -\delta^2 \int_0^{\cosh^{-1}\frac{x}{\lambda r}} d\sigma \tag{15.79}$$

$$= -\delta^2\,\cosh^{-1}\frac{x}{\lambda\,r} \tag{15.80}$$

$$= -\delta^2\,\ln\left(\frac{x}{\lambda\,r} + \sqrt{\frac{x^2}{\lambda^2\,r^2} - 1}\right)\,. \tag{15.81}$$

Similarly,

$$\frac{v}{U} = \delta^2\lambda \int_0^{\cosh^{-1}\frac{x}{\lambda r}} \cosh\sigma\,d\sigma \tag{15.82}$$

$$= \delta^2\lambda\,\sqrt{\cosh^2\sigma - 1}\,\Big|_0^{\cosh^{-1}\frac{x}{\lambda r}} \tag{15.83}$$

$$= \delta^2\lambda\sqrt{\left(\frac{x}{\lambda\,r}\right)^2 - 1}\,. \tag{15.84}$$

The solutions come out in terms of the "similarity" variable x/r, because there is no characteristic length in this problem. All flow quantities are constant along $x/r = $ const, rays from the origin. Clearly, the original equations could have been transformed to eliminate one of the independant variables and become ordinary differential equations for x/r and the solution obtained by solving the resulting equations. That is one approach for finding an exact solution to the cone problem.

Note that there is no change of flow deflection angle at the leading characteristic ($v/U(x/\lambda r = 1) = 0$), in contrast to the plane-flow case. This is because of azimuthal "leakage" in the flow over a body of revolution.

For the flow on or near the body, where r is small, for cases in which λ is not too large (supersonic but not hypersonic flow) $x/\lambda r \gg 1$, and the results can be simplified. In particular, on the body $x/\lambda r = 1/\lambda\delta$, so

$$\boxed{\begin{aligned}\frac{u}{U} &= -\delta^2\,\ln\frac{2}{\lambda\delta} \\[2mm] \frac{v}{U} &= \delta\,.\end{aligned}} \tag{15.85}$$

It was originally proposed that the quadratic term in Eq. 15.38 for bodies of revolution is necessary, and we now find that because $u \sim \delta^2$ while $v \sim \delta$ that is indeed the case

$$C_p = -2\frac{u}{U} - \frac{v^2}{U^2} \tag{15.86}$$

$$= \delta^2\left(2\ln\frac{2}{\lambda\delta} - 1\right)\,. \tag{15.87}$$

April 23, 2001

15.4 Similarity rules for compressible flow

Rules can be derived for converting results from one flow to another flow over a body of the same family of shapes at different Mach number and in a different perfect gas.

15.4.1 Plane flow – subsonic case

Consider flow 1, $\phi(x,y)$, at free-stream Mach number M_1 over a body characterized by a thickness ratio τ_1

$$\frac{y_b}{c} = \tau_1 f(\frac{x}{c}) . \tag{15.88}$$

The equation of motion is Eq. 15.28 written for plane flow, and the boundary conditions and pressures are

$$\left(\frac{\partial\phi}{\partial y}\right)_0 = U_1\tau_1 f'\left(\frac{x}{c}\right) \tag{15.89}$$

$$C_{p1} = -\frac{2}{U_1}\left(\frac{\partial\phi}{\partial x}\right)_0 . \tag{15.90}$$

Transform to flow 2, $\Phi(\xi,\eta)$, by

$$x = \xi \tag{15.91}$$

$$\sqrt{1 - M_1^2}\, y = \sqrt{1 - M_2^2}\, \eta \tag{15.92}$$

$$\phi(x,y) = A\frac{U_1}{U_2}\Phi(\xi,\eta) . \tag{15.93}$$

The arbitrary constant on the rhs of Eq. 15.93, which arises because the differential equation is homogeneous in ϕ, is chosen for convenience. The equation of motion transforms to the same form

$$\left(1 - M_2^2\right)\frac{\partial^2\Phi}{\partial x^2} + \frac{\partial^2\Phi}{\partial y^2} = 0 , \tag{15.94}$$

and the boundary condition transforms to

$$\left(\frac{\partial\phi}{\partial y}\right)_0 = \sqrt{\frac{1 - M_1^2}{1 - M_2^2}}\, A\frac{U_1}{U_2}\left(\frac{\partial\Phi}{\partial\eta}\right)_0 , \tag{15.95}$$

where

$$\left(\frac{\partial\Phi}{\partial\eta}\right)_0 = U_2\tau_2 f'\left(\frac{\xi}{c}\right) . \tag{15.96}$$

Thus, from Eq. 15.89 the boundary condition transforms unchanged if

$$\tau_2 = \tau_1\sqrt{\frac{1 - M_2^2}{1 - M_1^2}}\frac{1}{A} \tag{15.97}$$

and f' is the same. That is, the body shapes are the same though the thickness varies. The pressure coefficient transforms to

$$C_{p1} = -\frac{2}{U_1}\left(\frac{\partial\phi}{\partial x}\right)_0 = -\frac{2}{U_2}A\left(\frac{\partial\Phi}{\partial\xi}\right)_0 . \tag{15.98}$$

Comparing with Eq. 15.90 shows that

$$C_{p2} = \frac{1}{A}C_{p1} . \tag{15.99}$$

This scaling can be summarized in the following functional form,

$$\boxed{\frac{C_p}{A} = fnc\left(\frac{\tau}{A\sqrt{1-M_\infty^2}}\right) \cdot} \qquad (15.100)$$

A is an arbitrary parameter, various choices of which give commonly used similarity laws (see Table 3). For example, if we choose A to cancel the Mach numbers in Eq. 15.97, then we are comparing to different flows over the same body, $\tau_2 = \tau_1$. The first 3 entries are known as the Prandtl-Glauert similarity laws,

Table 3. Subsonic and Supersonic Compressible Flow Similarity Laws

	A	
1	1	$C_p = fnc\left(\dfrac{\tau}{\sqrt{1-M_\infty^2}}\right)$
2	$\dfrac{1}{\sqrt{1-M_\infty^2}}$	$C_p = \dfrac{1}{\sqrt{1-M_\infty^2}}\, fnc\,(\tau)$
3	τ	$C_p = \tau\, fnc\left(\sqrt{1-M_\infty^2}\right)$
4	$\dfrac{1}{1-M_\infty^2}$	$C_p = \dfrac{1}{1-M_\infty^2}\, fnc\left(\tau\sqrt{1-M_\infty^2}\right)$

and the last is the Göthert similarity law, applicable also to bodies of revolution (see below).

15.4.2 Supersonic flow

The same derivation goes through for the suppersonic form of the potential equation. One need only replace $(1-M_\infty^2)$ with (M_∞^2-1) in the results. Results valid for both cases can be written using $|(M_\infty^2-1)|$.

15.4.3 Axisymmetric flow – subsonic case

The equation of motion is Eq. 15.60. In this case it is necessary to be careful to avoid any problems that might arise from applying the boundary condition on the axis. In fact, to get the scaling laws it is easiest to simply apply the boundary conditions exactly *on the body*, $R/c = \tau_1 f(x/c)$. This will add another condition, which will fix A. The boundary condition is

$$\left(\frac{\partial\phi}{\partial r}\right)_b = U_1\tau_1\, f'\left(\frac{x}{c}\right) , \qquad (15.101)$$

and the pressure is

$$C_{p1} = -\frac{2}{U_1}\left(\frac{\partial\phi}{\partial x}\right)_0 - \frac{1}{U_1^2}\left(\frac{\partial\phi}{\partial r}\right)_0^2 . \qquad (15.102)$$

The transformation is

$$\phi = A\frac{U_1}{U_2}\Phi(\xi,\rho) \qquad (15.103)$$

April 23, 2001

$$x = \xi \tag{15.104}$$

$$\sqrt{1 - M_1^2}\, r = \sqrt{1 - M_2^2}\, \rho\,. \tag{15.105}$$

The boundary condition transforms to

$$\left(\frac{\partial \phi}{\partial r}\right)_{r=\tau_1 c f(x/c)} = \sqrt{\frac{1 - M_1^2}{1 - M_2^2}}\, A\, \frac{U_1}{U_2} \left(\frac{\partial \Phi}{\partial \rho}\right)_{\rho=\sqrt{\frac{1-M_1^2}{1-M_2^2}}\tau_1 c f(x/c)}, \tag{15.106}$$

where we require

$$\left(\frac{\partial \Phi}{\partial \rho}\right)_{\rho=\tau_2 c F(\xi/c)} = U_2 \tau_2\, F'\left(\frac{\xi}{c}\right)\,. \tag{15.107}$$

In order to have the radii at which the boundary conditions are applied comparable, the bodies must be of the same family, $F = f$ and

$$\tau_2 = \sqrt{\frac{1 - M_1^2}{1 - M_2^2}}\, \tau_1\,. \tag{15.108}$$

Substituting Eq. 15.107 into 15.106 and equating to Eq. 15.101 gives

$$A = \sqrt{\frac{1 - M_2^2}{1 - M_1^2}}\,. \tag{15.109}$$

Thus, for axisymmetric flow the arbitrary constant is fixed by the requirement that the boundary conditions transform. We know what the flow will be at a different Mach number only on a body whose thickness is determined by the new M_∞. Even though the pressures coefficients are given in terms of two terms, applying the transformation gives again Eq. 15.99. Thus the symmetry properties can be summarized by

$$\boxed{C_p\left(1 - M_\infty^2\right) = fnc\left(\sqrt{1 - M_\infty^2}\,\tau\right)\,,} \tag{15.110}$$

the Göthert similarity law, entry #4 in the table above.

16   Incompressible Flow

The transition from compressible flow to incompressible flow can be derived from our previous results by simply taking the limit $a_\infty \to \infty$, or $\lambda, m \to 1$. Here, in addition, we take a somewhat more general point of view.

Fluid flow is often constructed by superposing a distribution of singularities to satisfy boundary conditions, or to otherwise represent in simplified form bodies or sources of vorticity. From a mathematical point of view, this is because any vector field can be represented in terms of the gradient of a scalar potential ϕ and the curl of a vector potential $\underline{B}$; we will see that these represent volume and vorticity sources, respectively. In addition, in fluids there can exist a pure straining motion with no change of volume and no rotation, so this adds some additional flexibility in the flow which in general must be accounted for. In this chapter we construct velocity fields whose divergence and curl have specified values, and later in some examples we see how these can be translated to or from boundary conditions. Velocities $\underline{u}_e$ induced by expansion and velocities $\underline{u}_v$ induced by vorticity are given by

$$1) \qquad \nabla \cdot \underline{u}_e \; = \; f \; ; \qquad \nabla \times \underline{u}_e \; = \; 0 \tag{16.1}$$

$$2) \qquad \nabla \cdot \underline{u}_v \; = \; 0 \; ; \qquad \nabla \times \underline{u}_v \; = \; \underline{\omega} \tag{16.2}$$

In terms of the potentials the velocities are

$$\underline{u}_e \; = \; \nabla \phi \tag{16.3}$$

$$\underline{u}_v \; = \; \nabla \times \underline{B} \; . \tag{16.4}$$

The equations satisfied by ϕ and $\underline{B}$ are therefore

$$\nabla^2 \phi \; = \; f \tag{16.5}$$

$$\nabla \times \nabla \times \underline{B} \; = \; -\nabla^2 \underline{B} \; = \; \underline{\omega} \; . \tag{16.6}$$

The last equality of the second equation results if $\nabla \cdot \underline{B} = 0$, which is valid if the velocities go to zero at infinity and a suitable limiting procedure is adopted at boundaries (Batchelor 1967).

Now, getting back to the pure straining motion, if a velcity field $\underline{u}$ is consistent with *both* (16.1) and (16.2), then $\underline{v} = \underline{u} - \underline{u}_e - \underline{u}_v$ must be both divergence and curl free, and so in general is the purely straining motion satisfying

$$3) \qquad \nabla \cdot \underline{v} \; = \; 0 \; ; \qquad \nabla \times \underline{v} \; = \; 0 \; . \tag{16.7}$$

Flows driven by some simple, frequently utilized singularities are given later in this chapter. They in turn can be used to construct more complex structures by summing two equal and opposite elements spaced $2\underline{\delta}$ apart and then letting $\underline{\delta} \to 0$. In general, the limiting process is as follows (see Fig. 38). Given that

$$\phi \; = \; -A \, f(\underline{r}) \; , \tag{16.8}$$

summation of two such singularities gives

$$\phi \; = \; -A \; [f(\underline{r} - \underline{\delta}) - f(\underline{r} + \underline{\delta})] \; . \tag{16.9}$$

Multiplying and dividing by $\underline{\delta}$ and applying the limit $\underline{\delta} \to 0$; $A\underline{\delta} \to \underline{A}'$ gives

$$\phi \; = \; \underline{A}' \cdot \nabla f(\underline{r}) \; . \tag{16.10}$$

This result is used below.
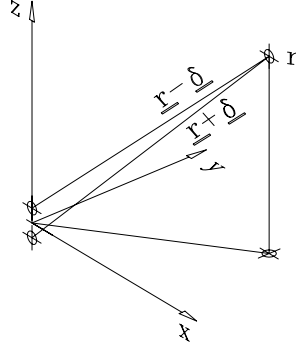
Figure 38. Construction of a higher-order singularity

16.1   The stream function

The stream function identically satisfies the continuity equation, so it has important physical significance. It arises in flows which have symmetries reducing the number of independent variables from 3 to 2, so that $\underline{B}$ has only one component, perpendicular to $\underline{u}$. That component is related to the stream function ψ. This section gives some examples. For completeness we also show the appropriate forms of the gradient of the velocity potential for obtaining the velocity components.

Cartesian coordinates (x, y, z)*: Plane flow;* $\frac{\partial}{\partial z} = 0$.   The vector potential is perpendicular to $\underline{u}$, so in 2D flow has only a z component, which we call ψ,

$$\underline{B} = (0, 0, \psi) . \tag{16.11}$$

Now from Eq. 16.4

$$\underline{u} = \underline{i}\,\frac{\partial \psi}{\partial y} - \underline{j}\,\frac{\partial \psi}{\partial x} , \tag{16.12}$$

so

$$\boxed{\begin{aligned} u &= \frac{\partial \psi}{\partial y} &= \frac{\partial \phi}{\partial x} \\[2mm] v &= -\frac{\partial \psi}{\partial x} &= \frac{\partial \phi}{\partial y} . \end{aligned}} \tag{16.13}$$

From Eq. 16.6, ψ satisfies a Poisson equation

$$\frac{\partial^2 \psi}{\partial x^2} + \frac{\partial^2 \psi}{\partial y^2} = \omega_z , \tag{16.14}$$

as does ϕ (Eq. 16.5)

$$\frac{\partial^2 \phi}{\partial x^2} + \frac{\partial^2 \phi}{\partial y^2} = f . \tag{16.15}$$

Cylindrical coordinates (r, θ, z)*: Plane flow;* $\frac{\partial}{\partial z} = 0$.   As before,

$$\underline{B} = (0, 0, \psi) . \tag{16.16}$$

From Eq. 16.4

$$\underline{u} = \underline{e}_r\,\frac{1}{r}\frac{\partial \psi}{\partial \theta} - \underline{e}_\theta\,\frac{\partial \psi}{\partial r} , \tag{16.17}$$

so

$$
\boxed{
\begin{aligned}
u_r &= \frac{1}{r}\frac{\partial \psi}{\partial \theta} = \frac{\partial \phi}{\partial r} \\[2mm]
u_\theta &= -\frac{\partial \psi}{\partial r} = \frac{1}{r}\frac{\partial \phi}{\partial \theta} \ .
\end{aligned}
}
\tag{16.18}
$$

The corresponding Poisson equations to be solved are

$$
\frac{\partial}{\partial r}\left(r\frac{\partial \psi}{\partial r}\right) + \frac{\partial}{\partial \theta}\left(\frac{1}{r}\frac{\partial \psi}{\partial \theta}\right) = -\omega_z \ .
\tag{16.19}
$$

$$
\frac{\partial}{\partial r}\left(r\frac{\partial \phi}{\partial r}\right) + \frac{\partial}{\partial \theta}\left(\frac{1}{r}\frac{\partial \phi}{\partial \theta}\right) = f \ .
\tag{16.20}
$$

Cylindrical coordinates (r, θ, z): *Axisymmetric flow;* $\frac{\partial}{\partial \theta} = 0$. In this case $\underline{B}$ has only a θ component which, to insure that ψ satisfies the continuity equation, we take to be

$$
\underline{B} = (0, \frac{\psi}{r}, 0) \ .
\tag{16.21}
$$

Then

$$
\underline{u} = -\underline{e}_r \frac{1}{r}\frac{\partial \psi}{\partial z} + \underline{e}_z \frac{1}{r}\frac{\partial \psi}{\partial r} \ ,
\tag{16.22}
$$

so

$$
\boxed{
\begin{aligned}
u_r &= -\frac{1}{r}\frac{\partial \psi}{\partial z} = \frac{\partial \phi}{\partial r} \\[2mm]
u_z &= \frac{1}{r}\frac{\partial \psi}{\partial r} = \frac{\partial \phi}{\partial z} \ ,
\end{aligned}
}
\tag{16.23}
$$

and, with the vorticity in the θ direction, ψ satisfies the equation

$$
\frac{1}{r}\frac{\partial}{\partial r}\left(r\frac{\partial \psi/r}{\partial r}\right) + \frac{\partial^2 \psi/r}{\partial z^2} = -\omega_\theta \ ,
\tag{16.24}
$$

and ϕ satisfies

$$
\frac{1}{r}\frac{\partial}{\partial r}\left(r\frac{\partial \phi}{\partial r}\right) + \frac{\partial^2 \phi}{\partial z^2} = f \ .
\tag{16.25}
$$

Spherical coordinates (r, ϕ, θ): *Axisymmetric flow;* $\frac{\partial}{\partial \theta} = 0$. Again $\underline{B}$ has only a θ component, in this case

$$
\underline{B} = (0, 0, \frac{\psi}{r \sin \phi}) \ .
\tag{16.26}
$$

In this case, ψ is called the *Stokes Stream Function.* Then

$$
\underline{u} = \underline{e}_r \frac{1}{r^2 \sin \phi}\frac{\partial \psi}{\partial \phi} - \underline{e}_\phi \frac{1}{r \sin \phi}\frac{\partial \psi}{\partial r} \ ,
\tag{16.27}
$$

April 23, 2001

so

$$
\begin{aligned}
u_r &= \frac{1}{r^2 \sin\phi} \frac{\partial \psi}{\partial \phi} = \frac{\partial \phi}{\partial r} \\
u_\phi &= -\frac{1}{r \sin\phi} \frac{\partial \psi}{\partial r} = \frac{1}{r} \frac{\partial \phi}{\partial \phi} ,
\end{aligned}
\tag{16.28}
$$

and, again with the vorticity in the θ direction,

$$
\frac{1}{r^2} \frac{\partial}{\partial r} \left(r^2 \frac{\partial \psi / r \sin\phi}{\partial r} \right) + \frac{1}{r^2 \sin\phi} \frac{\partial}{\partial \phi} \left(\sin\phi \frac{\partial \psi / r \sin\phi}{\partial \phi} \right) = -\omega_\theta .
\tag{16.29}
$$

while

$$
\frac{1}{r^2} \frac{\partial}{\partial r} \left(r^2 \frac{\partial \phi}{\partial r} \right) + \frac{1}{r^2 \sin\phi} \frac{\partial}{\partial \phi} \left(\sin\phi \frac{\partial \phi}{\partial \phi} \right) = -\omega_\theta .
\tag{16.30}
$$

Alternartively, for ψ

$$
\frac{1}{\sin\phi} \frac{\partial^2 \psi}{\partial r^2} + \frac{1}{r^2 \sin\phi} \frac{\partial}{\partial \phi} \left(\sin\phi \frac{\partial \psi / \sin\phi}{\partial \phi} \right) = -r\,\omega_\theta .
\tag{16.31}
$$

Physical interpretation of the stream function. The difference of the values of the stream function at two points in a flow is defined as being the volume flow between streamlines through the two points. From Fig. 39 it is seen that in a Cartesian system the incremental change of volume flux between the two points
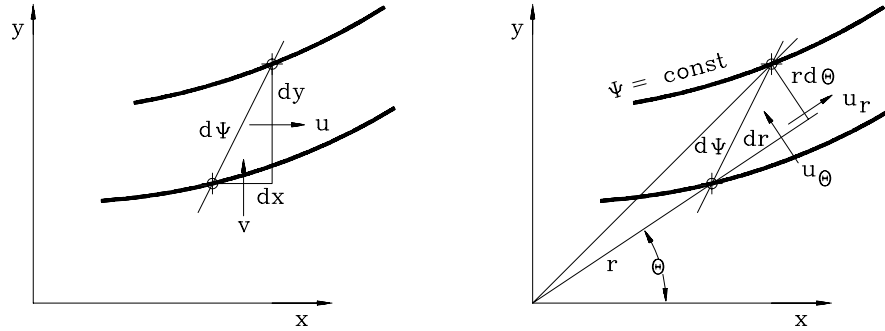
Figure 39. Geometry for computing volume fluxes from the stream function

is

$$
d\psi = -v\,dx + u\,dy
\tag{16.32}
$$

while in a polar coordinate system it is

$$
d\psi = -u_\theta\,dr + u_r\,r\,d\theta
\tag{16.33}
$$

Thus, as we have seen

$$
\begin{array}{ll}
\text{Cartesian Coords} & \text{Polar Coords} \\[4pt]
u = \dfrac{\partial \psi}{\partial y} & r u_r = \dfrac{\partial \psi}{\partial \theta}
\end{array}
\tag{16.34}
$$

$$
\begin{array}{ll}
v = -\dfrac{\partial \psi}{\partial x} & u_\theta = -\dfrac{\partial \psi}{\partial r} .
\end{array}
\tag{16.35}
$$

In the examples of simple flows given below, we derive the stream function from the velocity components for the appropriate symmetry as shown above.

April 23, 2001

16.2 Complex notation for plane flow

For plane flow, equations for the velocity components (u, v),

$$\frac{\partial \phi}{\partial x} = \frac{\partial \psi}{\partial y} \tag{16.36}$$

$$\frac{\partial \phi}{\partial y} = -\frac{\partial \psi}{\partial x}, \tag{16.37}$$

form Cauchy Riemann conditions establishing an analytic function

$$F(z) = \phi + i\,\psi \tag{16.38}$$

of the complex variable

$$z = x + i\,y = r\,e^{i\theta}, \tag{16.39}$$

such that its derivative

$$\frac{dF}{dz} = \frac{\partial \phi}{\partial x} + \frac{\partial \psi}{\partial y} \tag{16.40}$$

is the complex velocity w

$$w = u - i\,v. \tag{16.41}$$

In the examples of simple plane (2D) flows given below, we include expressions for the complex potential.

16.3 Flows with volume sources

Eq. 16.1 with 16.3 gives

$$\boxed{\nabla^2 \phi_e = f.} \tag{16.42}$$

We already have the solution for this equation by setting $a_0 = \infty$ ($k = \omega = 0$) in accoustics (Eq. 14.104) or $m = \lambda = 1$ in potential flow (Eq. 15.65),

$$\phi_e(\underline{r}) = -\frac{1}{4\pi} \int_{-\infty}^{\infty} \frac{f(\xi)\,d\underline{\xi}}{R} \tag{16.43}$$

$$u_e(\underline{r}) = \nabla \phi_e = -\frac{1}{4\pi} \int_{-\infty}^{\infty} \nabla \frac{1}{R}\, f(\xi)\,d\underline{\xi} \tag{16.44}$$

$$= \frac{1}{4\pi} \int_{-\infty}^{\infty} \frac{R}{R^3}\, f(\xi)\,d\underline{\xi}, \tag{16.45}$$

where $\underline{R} = \underline{r} - \underline{\xi}$. This gives the irrotational velocity field resulting from a distribution of volume sources. No dilatation occurs anywhere in the field except at the singularities.

Point source (3D). $\quad f(x) = q\delta(x).$

$$\boxed{\begin{aligned} \phi_e &= -\frac{q}{4\pi r} \\[2mm] \underline{u}_e &= \frac{q}{4\pi}\frac{\underline{r}}{r^3} \\[2mm] \psi &= -\frac{q}{4\pi}\cos\phi. \end{aligned}} \tag{16.46}$$

This is the near-field result (since $a_0 = \infty$) for a steady acoustic source.

Point source (2D).   3D point sources can be distributed along a straight line (z-axis) to form a line source. $\underline{R}$ is the distance from the sourcelet at $\xi = z$ on the z-axis to the observer at (r, θ) in the (x, y) plane, $R^2 = z^2 + r^2$. Thus

$$\underline{u}_e \;=\; \frac{q}{4\pi} \int_{-\infty}^{\infty} \frac{r}{R^3}\, dz \tag{16.47}$$

and there results

$$\boxed{\begin{aligned}
u_e &= \frac{q}{2\pi}\frac{r}{r^2} \\[2ex]
\phi_e &= \frac{q}{2\pi}\ln r \\[2ex]
\psi &= \frac{q}{2\pi}\theta \\[2ex]
F &= \frac{q}{2\pi}\ln z \;.
\end{aligned}} \tag{16.48}$$

Dipole (3D).   Summing two equal and opposite 3D point sources by the prescription given by Eq. 16.10 gives

$$\phi_e \;=\; \frac{1}{4\pi}\,\underline{\mu}\cdot\nabla\frac{1}{r}\;, \tag{16.49}$$

or

$$\boxed{\begin{aligned}
\phi_e &= -\frac{1}{4\pi}\,\underline{\mu}\cdot\frac{r}{r^3} \\[2ex]
\underline{u}_e &= \frac{1}{4\pi}\left(-\frac{\underline{\mu}}{r^3} + 3\frac{\underline{\mu}\cdot\underline{r}}{r^5}\,\underline{r}\right)\;.
\end{aligned}} \tag{16.50}$$

In spherical coordinates (r, ϕ, θ), <u>with the dipole oriented along the z-axis,</u>

$$\boxed{\begin{aligned}
\phi &= -\frac{\mu}{4\pi}\frac{\cos\phi}{r^2} \\[2ex]
u_r &= \frac{\mu}{2\pi}\frac{\cos\phi}{r^3} \\[2ex]
u_\theta &= \frac{\mu}{4\pi}\frac{\sin\phi}{r^3} \\[2ex]
\psi &= \frac{\mu}{4\pi}\frac{\sin^2\phi}{r}\;.
\end{aligned}} \tag{16.51}$$

Dipole (2D).   Summing two equal and opposite 2D point sources gives by Eq. 16.10

$$\phi_e \;=\; -\frac{1}{2\pi}\,\underline{\mu}\cdot\nabla\ln r\;, \tag{16.52}$$

April 23, 2001

or

$$\phi_e = -\frac{1}{2\pi}\,\underline{\mu}\cdot\frac{\underline{r}}{r^2}$$

$$\underline{u}_e = \frac{1}{2\pi}\left(-\frac{\underline{\mu}}{r^2}+2\frac{\underline{\mu}\cdot\underline{r}}{r^4}\,\underline{r}\right)\;. \tag{16.53}$$

In polar coordinates (r,θ), <u>with the dipole oriented along the x-axis,</u>

$$\phi = -\frac{\mu}{2\pi}\frac{\cos\theta}{r}$$

$$u_r = \frac{\mu}{2\pi}\frac{\cos\theta}{r^2}$$

$$u_\theta = \frac{\mu}{2\pi}\frac{\sin\theta}{r^2} \tag{16.54}$$

$$\psi = \frac{\mu}{2\pi}\frac{\sin\theta}{r}$$

$$F = -\frac{\mu}{2\pi z}\;.$$

If the dipole were oriented <u>along the y-axis</u> the complex potential would simply read

$$F = -i\,\frac{\mu}{2\pi z}\;. \tag{16.55}$$

The 2D dipole could also have been constructed by summing the *stream functions* of two sources,
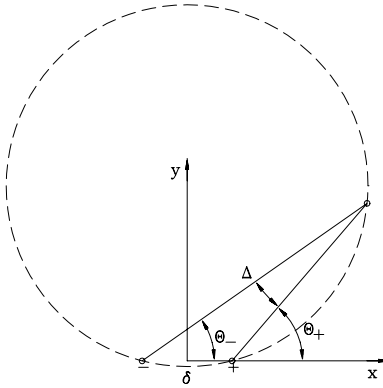
Figure 40. Construction of a 2D dipole by superposition

$$\psi = \frac{q}{2\pi}(\theta_+ - \theta_-) = \frac{q\Delta}{2\pi}\;, \tag{16.56}$$

and noting from the geometry of Fig. 40 that the curves $\psi = $ const. $(\Delta = $ const.$)$ are circles through both singularities such that

$$\sin\Delta = \frac{\delta}{d}\;, \tag{16.57}$$

119

where d is the diameter of the circle. In the limit $\delta \to 0$, we have

$$\theta_+ \approx \theta_- \equiv \theta \tag{16.58}$$

$$\frac{\delta}{\sin \Delta} \approx \frac{r}{\sin \theta} , \tag{16.59}$$

so,

$$\psi = \frac{\mu}{2\pi} \frac{\sin \theta}{r} \tag{16.60}$$

16.4 Flows with sources of vorticity

Formally, the solution of Eq. 16.6 is

$$\underline{B} = \frac{1}{4\pi} \int_{-\infty}^{\infty} \frac{\underline{\omega}(\xi)\, d\underline{\xi}}{R} \tag{16.61}$$

$$u_v(\underline{r}) = \nabla \times \underline{B} = \frac{1}{4\pi} \int_{-\infty}^{\infty} \nabla \times \frac{\underline{\omega}}{R}\, d\underline{\xi} \tag{16.62}$$

$$= -\frac{1}{4\pi} \int_{-\infty}^{\infty} \frac{\underline{R} \times \underline{\omega}}{R^3}\, d\underline{\xi} . \tag{16.63}$$

Applying the divergence theorem shows that in fact $\nabla \cdot \underline{B} = 0$ if $\underline{\omega} \cdot \underline{n} = 0$ on all boundaries of the fluid.

Point sources of vorticity do not exist because $\nabla \cdot \omega = 0$. Thus, as with magnetic fields, one thinks in terms of vortex lines or filaments, continuous lines everywhere parallel to $\underline{\omega}$. By the divergence theorem $\int \underline{\omega} \cdot \underline{n}\, dA$ on the area defined by any closed curve completely surrounding the same vortex lines must be the same. The closed curves and the vortex lines form a vortex tube. By Stokes theorem

$$\int \underline{\omega} \cdot \underline{n}\, dA = \oint \underline{u} \cdot d\underline{l} = \Gamma . \tag{16.64}$$

These results imply the

16.4.1 Helmholtz vortex theorems

1. The strength of a vortex filament is constant along its length.

2. A vortex filament can not end in a fluid; it must extend to the boundaries of the fluid or must form a closed path.

3. For an inviscid fluid,

   (a) In the absence of rotational external forces, a fluid that is initially irrotational remains irrotational.

   (b) In the absence of rotational external forces, if the circulation around a path enclosing a definite group of particles is initially zero, it will remain zero.

   (c) In the absence of rotational external forces, the circulation around a path that encloses a tagged group of elements is invariant.

April 23, 2001

16.4.2   Biot-Savart Law

A curved vortex is a singularity formed by shrinking a vortex tube to zero diameter such that

$$\int_{\delta\underline{\xi}} \underline{\omega}\, d\underline{\xi} \;=\; \Gamma\, \delta\underline{l}\,, \tag{16.65}$$

giving, from Eq. 16.63,

$$\boxed{\underline{u}_v \;=\; -\frac{\Gamma}{4\pi}\int \frac{\underline{R}\times d\underline{l}}{R^3}\,,} \tag{16.66}$$

the Biot-Savart Law.

Line vortex.   A line vortex (as distinct from a vortex line) is made by integrating the Biot-Savart law along a straight line, say the z-axis. From the geometry of Fig. 41, it is seen that $\underline{R}\times d\underline{l} = r\,dz,\ \ R^2 = r^2 + z^2$,
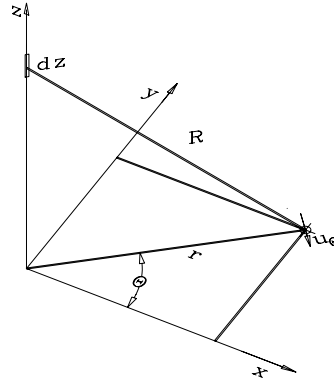
Figure 41. Effect in the x-y plane of a vortex element on the z-axis

and that the induced velocity is only in the θ direction. Thus, integrating Eg. 16.66,

$$u_\theta \;=\; -\frac{\Gamma}{4\pi}\int_{-\infty}^{\infty}\frac{r\,dz}{(r^2+z^2)^{3/2}} \tag{16.67}$$

$$=\; \frac{\Gamma}{4\pi}\frac{z}{r\,(r^2+z^2)^{1/2}}\Bigg|_{-\infty}^{\infty}, \tag{16.68}$$

so,

$$\boxed{\begin{aligned}
u_\theta &= \frac{\Gamma}{2\pi r}\\[2mm]
\phi &= \frac{\Gamma}{2\pi}\,\theta\\[2mm]
\psi &= -\frac{\Gamma}{2\pi}\,\ln r\\[2mm]
F &= -i\,\frac{\Gamma}{2\pi}\,\ln z\\[2mm]
w &= -i\,\frac{\Gamma}{2\pi z}\,.
\end{aligned}} \tag{16.69}$$

April 23, 2001

Vortex doublet. The vortex doublet is constructed by Eq. 16.10, where say, $\Gamma \underline{\delta} \to \underline{\lambda}$,

$$\psi = \frac{1}{2\pi} \underline{\lambda} \cdot \nabla \ln r , \tag{16.70}$$

so,

$$\psi = \frac{1}{2\pi} \frac{\underline{\lambda} \cdot \underline{r}}{r^2} . \tag{16.71}$$

In polar coordinates, with the doublet aligned along the *y*-axis,

$$
\boxed{
\begin{aligned}
\psi &= \frac{\lambda \sin\theta}{2\pi \, r} \\[2mm]
u_r &= \frac{\lambda}{2\pi} \frac{\cos\theta}{r^2} \\[2mm]
u_\theta &= \frac{\lambda}{2\pi} \frac{\sin\theta}{r^2} \\[2mm]
\phi &= -\frac{\lambda}{2\pi} \frac{\cos\theta}{r} \\[2mm]
F &= -\frac{\lambda}{2\pi z} .
\end{aligned}
}
\tag{16.72}
$$

Note that this field is identical to that induced by a 2D dipole oriented at $90°$ to the vortex doublet, Eqs. 16.54.

April 23, 2001

Infinite Vortex Sheet. An infinite vortex sheet can be constructed from the superposition of vortex lines of constant strength ω, as shown in Fig. 42. The circulation per unit length γ is defined from
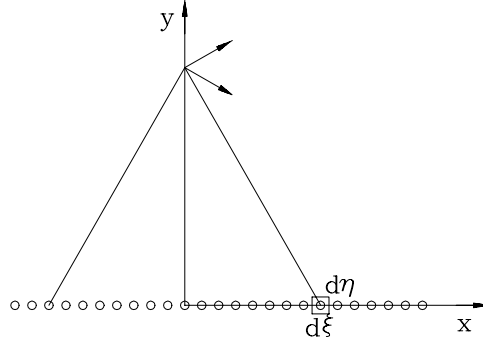
Figure 42. Construction of an infinite vortex sheet by superposition

$$d\Gamma = \underline{\omega} \cdot d\underline{S} = \omega \, d\eta \, d\xi = \gamma \, d\xi , \qquad (16.73)$$

where $\gamma \equiv \omega \, d\eta$. At each point $y > 0$ the contribution to the x-component of velocity from the two symmetric points shown is

$$du_+ = -2\frac{y}{r}\frac{d\Gamma}{2\pi r} = -\frac{\gamma}{\pi}\frac{y \, d\xi}{r^2} , \qquad (16.74)$$

while by symmetry $dv = 0$. Here, $r^2 = y^2 + \xi^2$. Integrating over $0 < \xi < \infty$, for $\gamma = $ const.,

$$u_+ = -\frac{\gamma}{\pi} \tan^{-1} \frac{\xi}{y}\bigg|_0^\infty = -\frac{\gamma}{2} \qquad (16.75)$$

For $y < 0$ we get the result $u_- = \gamma/2$, so across the sheet

$$\Delta u \equiv u_+ - u_- = -\gamma . \qquad (16.76)$$

Written in terms of the velocity potential, Eq. 16.75 is

$$\frac{\partial \phi_+}{\partial x} = -\frac{1}{2}\frac{d\Gamma}{dx} , \qquad (16.77)$$

A similar relation, with a change of sign, holds for ϕ_-, so if we take pairs of points above and below the vortex sheet

$$\frac{\partial \Delta\phi}{\partial x} = -\frac{d\Gamma}{dx} , \qquad (16.78)$$

where $\Delta\phi = \phi_+ - \phi_-$. If the vortex sheet is of finite extent, the total circulation Γ is finite and Eq. 16.78 can be integrated to yield

$$\boxed{\Gamma = -\Delta\phi .} \qquad (16.79)$$

16.4.3 General vortex sheet – Lift

Consider a 3-D (curved) vortex sheet of circulation γ per unit length in an otherwise uniform flow with velocity U_- below the sheet. The vorticity imposes a velocity change $u_+ = -\gamma/2$ on the top, and a change $u_- = +\gamma/2$ on the bottom thus causing velocity U_+ on the top (see Fig. 43). All of the vectors shown in the sketch lie in the tangent plane to the sheet. To accommodate a bound vortex sheet we allow for

April 23, 2001
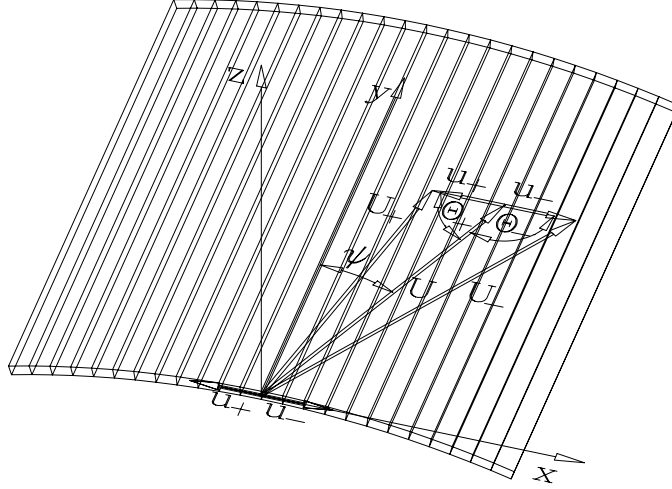
Figure 43. Vector diagram for a vortex sheet with convective velocity in the plane of the sheet

forces on it, namely, a pressure difference between the top p_+ and the bottom p_-. The mean velocity is $U = \frac{1}{2}(U_+ + U_-)$.

By Bernoulli's equation,

$$p_{0+} \;=\; p_+ + \frac{1}{2}\rho U_+^2 \;;\qquad p_{0-} \;=\; p_- + \frac{1}{2}\rho U_-^2 \;, \tag{16.80}$$

so,

$$\Delta p \;\equiv\; p_+ - p_- \;=\; \Delta p_0 + \frac{1}{2}\rho(U_-^2 - U_+^2) \;, \tag{16.81}$$

where $\Delta p_0 = p_{0+} - p_{0-}$. From the construction in the sketch, we have

$$U_-^2 - U_+^2 \;=\; -2U u_-(\cos\theta_- - \cos\theta_+) \tag{16.82}$$

$$=\; 4U u_+ \sin\frac{\theta_- + \theta_+}{2}\sin\frac{\theta_- - \theta_+}{2} \tag{16.83}$$

$$=\; 2U\gamma\sin\psi \;, \tag{16.84}$$

where $2\psi = \theta_- - \theta_+$. Thus, from Eq. 16.81 we have the result

$$\boxed{\Delta p \;=\; \Delta p_0 + \rho\, U \sin\psi\,\gamma \;,} \tag{16.85}$$

where $U\sin\psi = U_n$ is just the component of the convective velocity normal to the vorticity. We now apply Eq. 16.85 to three cases:

   i. *Trailing vortex sheet.*
      Typically behind a wing the flow on each side of the sheet has approximately the same total pressure so $\Delta p_0 = 0$. Since the sheet is free, it cannot support any pressure difference, so $\Delta p = 0$. Thus, $\psi = 0$, so any imposed "mean flow" U is aligned with γ, and the vortex sheet does not convect.

  ii. *Edge of a separated flow (bubble).*
      Dissipation acts in the recirculation region of a separated flow, so in general $\Delta p_0 \neq 0$. However, since the sheet is free, $\Delta p = 0$. Therefore, in this case $\psi \neq 0$, and the sheet is convected by the mean velocity.

iii. *Bound vortex sheet.*

In this case, a force must be present, $\Delta p \neq 0$, while for a thin wing $\Delta p_0 \approx 0$. We are free to choose U, and if we take it to be U_n, the free stream velocity of a flow over an airfoil swept at angle ψ, then

$$\Delta p = \rho U_n \gamma .\tag{16.86}$$

This is the **Kutta-Joukowski Theorem** for the lift force (actually the negative of lift). When integrated over the entire bound vortex sheet representing an airfoil, it gives the result

$$\boxed{L = -\rho U_n \Gamma ,}\tag{16.87}$$

where L is the force in the *positive z* direction.

16.5 Uniform flow, (x, y)

Uniform flow in the x-direction with velocity U is given by,

Plane flow

$$\phi = Ux \tag{16.88}$$
$$\psi = Uy \tag{16.89}$$
$$F = Uz . \tag{16.90}$$

In an incompressible fluid, if a body moves with constant velocity $\underline{U}$, and fluid particles move only as a consequence of the body motion, then

$$\frac{\partial}{\partial t} = -(\underline{U} \cdot \nabla) .\tag{16.91}$$

Axisymmetric flow   (Flow now in the z-direction.)
Polar coordinates, (r, θ, z), $\frac{\partial}{\partial \theta} = 0$.

$$\phi = Uz \tag{16.92}$$
$$\psi = \frac{Ur^2}{2} \tag{16.93}$$

Spherical coordinates, $(r, \phi.\theta)$, $\frac{\partial}{\partial \theta} = 0$.

$$\psi = \frac{U}{2} r^2 \sin^2 \phi \tag{16.94}$$
$$u_r = U \cos \phi \tag{16.95}$$
$$u_\theta = -U \sin \phi .\tag{16.96}$$

16.6 Flow over a lifting cylinder

Uniform flow + dipole + vortex.
To examine the flow over what is perhaps the simplest closed lifting body, consider the superposition of a

April 23, 2001

uniform flow U, a dipole oriented upstream $-\mu$, and a vortex Γ. The stream function is, from Eqs. 16.89, 16.54 and 16.69,

$$\Psi = Ur\sin\theta - \frac{\mu\sin\theta}{2\pi r} - \frac{\Gamma}{2\pi}\ln\frac{r}{a} \tag{16.97}$$

$$= Ur\sin\theta\left(1 - \frac{\mu}{2\pi Ur^2}\right) - \frac{\Gamma}{2\pi}\ln\frac{r}{a} , \tag{16.98}$$

where a is an arbitrary constant of integration which has been added for use in Eq. 16.100. Thus,

$$u_r = \frac{1}{r}\frac{\partial\Psi}{\partial\theta} = U\cos\theta\left(1 - \frac{\mu}{2\pi Ur^2}\right) . \tag{16.99}$$

Note that the radial velocity vanishes on a circle,

$$r = \sqrt{\frac{\mu}{2\pi U}} \equiv a , \tag{16.100}$$

and, since by the above choice the stream function is zero on $r = a$, we have derived the flow over a *cylinder of radius a and circulation* Γ. To summarize, the velocities in the field are

$$u_r = \frac{1}{r}\frac{\partial\Psi}{\partial\theta} = U\cos\theta\left(1 - \frac{a^2}{r^2}\right) , \tag{16.101}$$

$$u_\theta = -\frac{\partial\Psi}{\partial r} = -U\sin\theta\left(1 + \frac{a^2}{r^2}\right) + \frac{\Gamma}{2\pi r} . \tag{16.102}$$

On the cylinder the tangential velocity is

$$u_\theta = -2U\sin\theta + \frac{\Gamma}{2\pi a} . \tag{16.103}$$

The sense of the contributions of the first term is sketched on the left of Fig. 44 and of the second on the
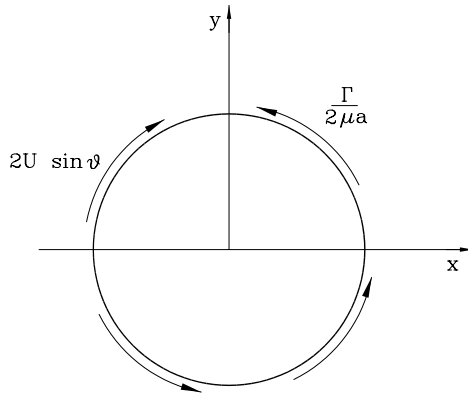
Figure 44. Sense of the contributions of terms in Eq. 16.103

right. These motions move the stagnation points $u_r = u_\theta = 0$ on the body. From Eq. 16.101 we see that $u_r = 0$ when $r = a$ or $\theta = \pm\pi/2$. In the first case, $u_\theta = 0$ when

$$\sin\theta = \Gamma/4\pi Ua . \tag{16.104}$$

Curves of constant ψ (streamlines) for one such case are shown in Fig. 45. When $\Gamma/4\pi Ua > 1$ there is

April 23, 2001
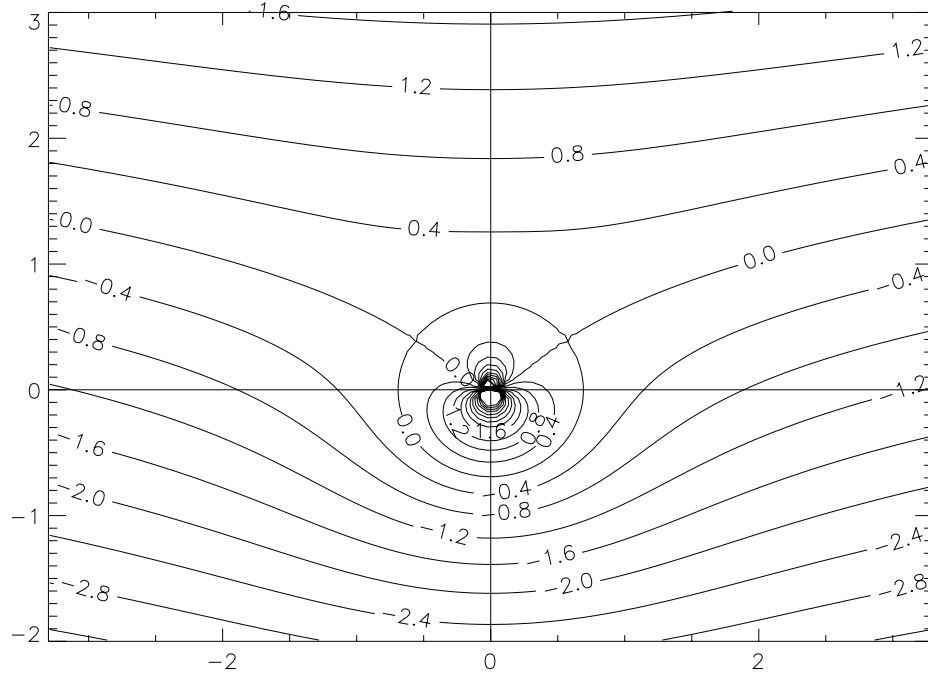
Figure 45. Streamlines around a circular cylinder for $U = 1$, $\mu = 3$ and $\Gamma = 5$ $(a = 0.691)$

a problem, because $\sin < 1$; the stagnation points move off the body and the condition $\theta = -\pi/2$ holds. Then, the zero of Eq. 16.102 is at

$$r = \frac{\Gamma}{4\pi U}\left[1 + \sqrt{1 - \left(\frac{4\pi Ua}{\Gamma}\right)^2}\right] . \tag{16.105}$$

Streamlines for one such case are shown in Fig. 46.

That the lift force on the cylinder satisfies the Kutta-Joukowski Theorem (Eq. 16.87) can be verified by integrating the pressure acting on the cylinder using Bernoulli's Equation:

$$p + \frac{\rho u^2}{2} = p_\infty + \frac{\rho U^2}{2} \tag{16.106}$$

$$p - p_\infty = \frac{\rho U^2}{2}\left[1 - \left(\frac{u}{U}\right)^2\right] \tag{16.107}$$

On the body, $u = u_\theta(r = a)$, so

$$p - p_\infty = \frac{\rho U^2}{2}\left[1 - 4\sin^2\theta - \left(\frac{\Gamma}{2\pi Ua}\right)^2 + \frac{2\Gamma}{\pi Ua}\sin\theta\right] . \tag{16.108}$$

The infinitesimal contributions to lift and drag are (Fig. 47)

$$dL = -(p - p_\infty)a\sin\theta\,d\theta \tag{16.109}$$

$$dD = -(p - p_\infty)a\cos\theta\,d\theta \tag{16.110}$$
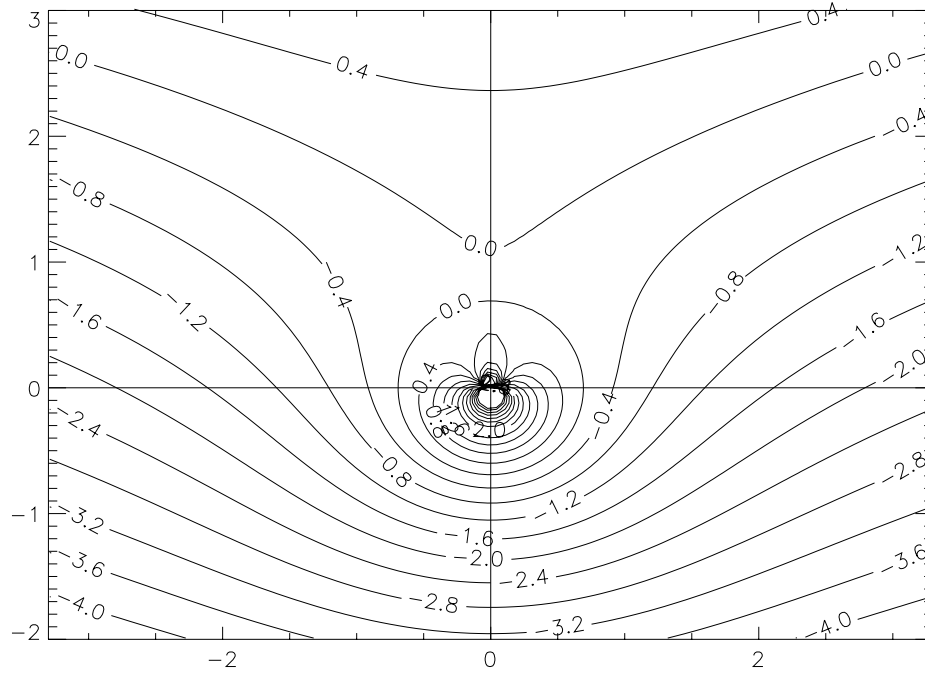
Figure 46. Streamlines around a circular cylinder for $U = 1$, $\mu = 3$ and $\Gamma = 9$ ($a = 0.691$)
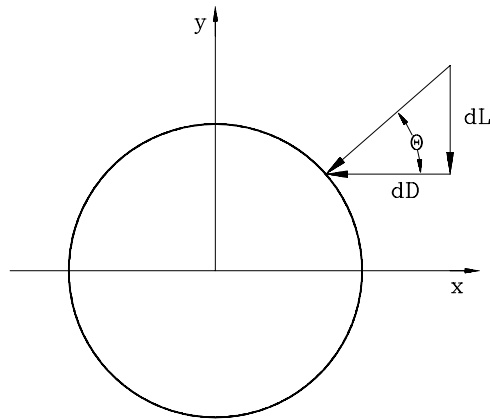
Figure 47. Orientation of lift and drag forces

The cosine multiplying every term in the drag formula insures that the integral from $\theta = 0$ to 2π of each term is zero. In the lift formula, the only contribution comes from terms with even powers of the sine, that is, only from the term with Γ. Integrating that term confirms that $L = -\rho U \Gamma$.

This example has not addressed how the cylinder might acquire circulation. In fact, attempts to realize this configuration, called the Flettner Rotor, have not met with total success. The key requirement is to control the location of separation, a very important example of *flow control*. In the next section we will see how an airfoil with a sharp trailing edge generates circulation. It then remains to calculate the circulation of a given shape airfoil. That is the subject of airfoil theory.

16.7   The Kutta condition

1. The way in which circulation is established about airfoils to generate lift is one of the great accomplishments of aerodynamic design, and one of the earliest successes in flow control. Of course, the magnitude of the accomplishment is somewhat mitigated by the fact that birds had developed the technology much earlier, and, to unlock the secret, all humans had to do was look up.

2. The Kutta condition states that the flow leaves the trailing edge of an airfoil smoothly, and that the velocity there is finite.

3. When an inviscid irrotational fluid is set into motion, the resulting flow is irrotational.

4. *Thus, the shape of a lifting body must be such that viscosity is forced to initially play a crucial role in establishing circulation, but later, after the flow is established, the effects of viscosity should be small.*
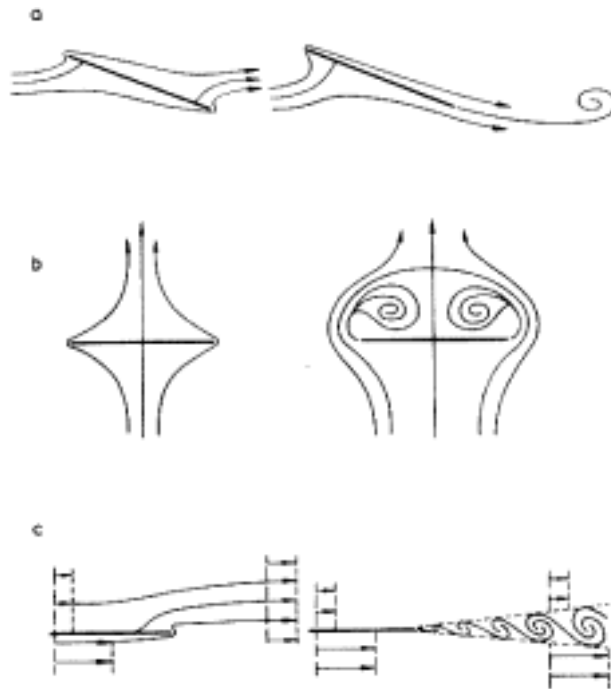
Figure 48. The consequences of adding viscous effects near a body, namely separation, to the global flow field

The left column of Fig. 48 shows three different flows as they would be established in a perfect (inviscid) fluid. They are;

1. flow over a flat plate at small incidence to the free stream,

2. flow normal to a flat plate,

3. two streams at different velocities and total pressure flowing parallel to a flat plate.

The common feature of all three flows is that the bodies have sharp edges.

In all cases there is no circulation, so both the lift and drag are zero.

Helmholtz (1868) first established that, in fact, vortex sheets trail downstream from sharp edges; that is, that sharp edges force separation. Kutta (1902) showed that if the flow leaves the trailing edge of a wing

smoothly *i.e.*, if the trailing edge is sharp (the **Kutta Condition**), then perfect-fluid theory (potential flow theory) can be used to calculate the lift.

The right column of Fig. 48 shows that the three flows manifest the effects of viscosity in three fundamentally different ways.

1. In the first one, at the initial instant the plate sheds a "starting vortex" which forces the Kutta condition on the flow. The trailing vortex sheet maintains the separation thereafter. The miracle of lift is that a starting vortex is generated of just the right strength Γ to provide the required force.

2. In flow normal to a plate a large vortex pair forms downstream of the plate and remains there forever, forcing the Kutta condition.

3. In order for the flow parallel to the plate to separate smoothly, it is necessary for vortices to be continually shed from the plate for all time.

April 23, 2001

17 Airfoil theory

17.1 Flat plate airfoil

The lift generated by a flat plate at angle of attack can be represented by a bound vortex sheet $\gamma(x)$, subject to the Kutta condition $\gamma(c) = 0$. If the angle of attack is small the vortex sheet can to an approximation be placed on the x-axis. The unknown vortex strength $\gamma(x)$ is determined by requiring that the flat plate be a streamline, that is, that the velocity normal to the plate be zero. From Eq. 16.69, the tangential velocity induced by an infinitesimal element $d\xi$ at point $(\xi, 0)$ is

$$du_\theta = \frac{\gamma\, d\xi}{2\pi\sqrt{(x-\xi)^2 + y^2}}\,. \tag{17.1}$$

On the axis the induced velocity is vertical,

$$dv = \frac{\gamma\, d\xi}{2\pi(x-\xi)}\,. \tag{17.2}$$

The component of the free stream normal to the plate is $U\sin\alpha$. Making the small angle approximation, and adding up the effects of all the elements and the free stream, we get

$$v = \frac{1}{2\pi}\int_0^c \frac{\gamma(\xi)}{x-\xi}d\xi + U\alpha\,. \tag{17.3}$$

Setting this expression to 0 to satisfy the requirement of streamline flow,

$$\boxed{\frac{1}{2\pi}\int_0^c \frac{\gamma(\xi)}{x-\xi}d\xi = -U\alpha\,.} \tag{17.4}$$

Integrals with singularities at $x = \xi$ appear often in wing theory, and in such cases it should always be understood that reference is to the principal value.

Using the transformation

$$\xi = \frac{c}{2}(1 - \cos\theta) \tag{17.5}$$

$$x = \frac{c}{2}(1 - \cos\phi)\,, \tag{17.6}$$

Eq. 17.4 and the Kutta condition become

$$\frac{1}{2\pi}\int_0^\pi \frac{\gamma(\theta)\sin\theta\, d\theta}{\cos\theta - \cos\phi} = -U\alpha \tag{17.7}$$

$$\gamma(\pi) = 0\,. \tag{17.8}$$

The distribution that satisfies Eqs. 17.7 and 17.8 is

$$\boxed{\gamma(\theta) = -2\alpha U\frac{1 + \cos\theta}{\sin\theta}} \tag{17.9}$$

Proof: In order to prove Eq. 17.9 it is necessary to show that

$$\int_0^\pi \frac{1 + \cos\theta}{\cos\theta - \cos\phi}d\theta = \pi\,. \tag{17.10}$$

April 23, 2001

First, consider the first term,

$$\int_0^\pi \frac{d\theta}{\cos\theta - \cos\phi} = \int_0^{\phi-\epsilon} \frac{d\theta}{\cos\theta - \cos\phi} + \int_{\phi+\epsilon}^\pi \frac{d\theta}{\cos\theta - \cos\phi} \tag{17.11}$$

$$= \frac{1}{\sin\phi} \ln \frac{\sin\frac{\phi+\theta}{2}}{\sin\frac{\phi-\theta}{2}} \Bigg|_0^{\phi-\epsilon} + \frac{1}{\sin\phi} \ln \frac{\sin\frac{\theta+\phi}{2}}{\sin\frac{\theta-\phi}{2}} \Bigg|_{\phi+\epsilon}^\pi \tag{17.12}$$

$$= \frac{1}{\sin\phi} \left[\ln\sin\left(\phi - \frac{\epsilon}{2}\right) - \ln\sin\frac{\epsilon}{2} - \ln\frac{\sin\frac{\phi}{2}}{\sin\frac{\phi}{2}} \right] \tag{17.13}$$

$$+ \frac{1}{\sin\phi} \left[\ln\frac{\sin\frac{\pi+\phi}{2}}{\sin\frac{\pi-\phi}{2}} - \ln\sin\left(\phi + \frac{\epsilon}{2}\right) + \ln\sin\frac{\epsilon}{2} \right] \tag{17.14}$$

$$= \frac{1}{\sin\phi} \left[\ln\frac{\sin\left(\phi - \frac{\epsilon}{2}\right)}{\sin\left(\phi + \frac{\epsilon}{2}\right)} \right] \longrightarrow 0 . \tag{17.15}$$

For the second term it follows that

$$\int_0^\pi \frac{\cos\theta}{\cos\theta - \cos\phi} d\theta = \int_0^\pi \left(1 + \frac{\cos\phi}{\cos\theta - \cos\phi}\right) d\theta = \pi . \tag{17.16}$$

Therefore, Eq. 17.10 is proven.

From Eqs. 17.9 and 17.6, the vortex distribution is

$$\gamma(x) = -2U\alpha \sqrt{\frac{c-x}{x}} , \tag{17.17}$$

and it is seen that the vortex distribution is singular at $x = 0$ and is zero at $x = c$. Fig. 49 shows the variation of $\gamma(x)$.
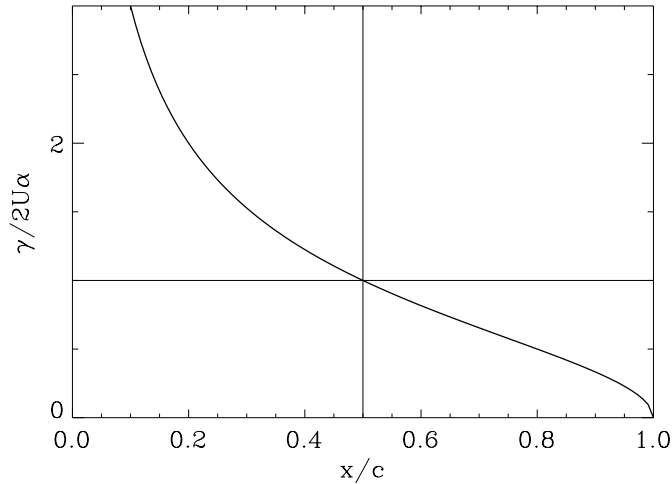
Figure 49. Vortex distribution for a flate plat airfoil

i) Lift. The lift is the integral of the pressure over the body, so, from Eqs. 16.86 and 17.5

$$L = -\int_0^c \Delta p(\xi) d\xi = -\frac{\rho U c}{2} \int_0^\pi \gamma(\theta) \sin\theta d\theta . \tag{17.18}$$

April 23, 2001

The non-dimensional lift is the *section lift coefficient*,

$$C_\ell = \frac{L}{\frac{1}{2}\rho U^2 c} \, , \tag{17.19}$$

so

$$C_\ell = -\int_0^\pi \frac{\gamma(\theta)}{U} \sin\theta \, d\theta \, . \tag{17.20}$$

From Eq. 17.9, for an uncambered thin airfoil we get

$$\boxed{C_\ell = 2\pi\alpha \, .} \tag{17.21}$$

The section lift coefficient slope is

$$\boxed{C_{\ell_\alpha} = 2\pi \, .} \tag{17.22}$$

The lift increases linearly with angle of attack with a slope of 2π.

ii) Moment. The clockwise moment about the leading edge of the airfoil ($x = 0$) is the moment of the pressure on the airfoil, so from Eqs. 16.86 and 17.5

$$M_0 = \int_0^c \Delta p \, \xi \, d\xi = \frac{\rho U c^2}{4} \int_0^\pi \gamma(\theta)(1 - \cos\theta)\sin\theta \, d\theta \, . \tag{17.23}$$

The non-dimensional moment, *the sectional moment coefficient*, is

$$C_{m_0} = \frac{M_0}{\frac{1}{2}\rho U^2 c^2} \, , \tag{17.24}$$

so,

$$C_{m_0} = \frac{1}{2}\int_0^\pi \frac{\gamma(\theta)}{U}(1 - \cos\theta)\sin\theta \, d\theta \, . \tag{17.25}$$

From Eq. 17.9, for an uncambered thin airfoil

$$\boxed{C_{m_0} = -\frac{\pi}{2}\alpha = -\frac{C_\ell}{4}} \tag{17.26}$$

iii) Center of pressure. The center of pressure $x_{c.p.}$ is centroid of the lift distribution, and, therefore, is the point about which the moment is zero

$$M_0 + L\, x_{c.p.} = 0 \, , \tag{17.27}$$

so

$$\boxed{x_{c.p.} = -\frac{cC_{m_0}}{C_\ell} = \frac{c}{4} \, .} \tag{17.28}$$

iv) Comment. Consistent with potential flow theory, we obtain a value for lift, the force perpendicular to the free-stream direction, while the drag is zero (Fig. 50). In this case the result is remarkable because it is known that the only force exerted on a body by an inviscid fluid is the normal pressure force P. Thus, in order to resolve the resultant force L, there must be a *thrust* $S \doteq L\alpha$ parallel to the plate. The source of this force is the infinite *leading edge suction pressure* caused by the infinite velocity at the infinitesimally thick leading edge!

Eqs. 17.21 and 17.26 are actually good first approximations to the performance of real thin uncambered airfoils, because by careful design of rounded leading edges it is possible to recover virtually all of the leading-edge suction.

April 23, 2001
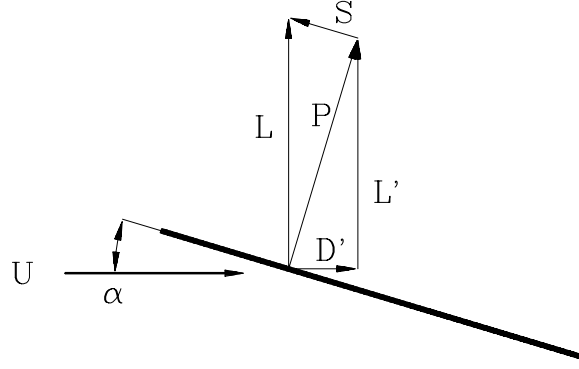
Figure 50. Vector diagram for the forces on a flate plate airfoil

17.2 The Joukowski Transformation

The earliest successful attempts to study airfoil sections analytically made use of the tools of complex analysis and conformal transformations. Joukowski experimented with the transformation which maps a circle of unit radius into a straight line,

$$\zeta = z + \frac{1}{z} . \tag{17.29}$$

The inverse transformation is

$$z = \frac{\zeta}{2} \pm \sqrt{\frac{\zeta^2}{2} - 1} . \tag{17.30}$$

The scale parameter of the transformation $d\zeta/dx = 1 - 1/\zeta^2$ shows that the points ± 1 map uncomformably; the unit circle maps to the line $\xi = 2\cos\theta$, $\eta = 0$. In terms of the real and imaginary parts (ξ, η) of ζ, Eq. 17.29 is

$$\xi = \left(r + \frac{1}{r} \right) \cos\theta \tag{17.31}$$

$$\eta = \left(r - \frac{1}{r} \right) \sin\theta . \tag{17.32}$$

This transformation is important because it maps the flow over a cylinder of unit radius, $F(z) = U(z + 1/z)$ into the flow over a flat plate at zero incidence $F(\zeta) = U\zeta$. The flat plate can be put at angle of attack α by first rotating the flow over the cylinder through the angle α

$$\zeta' = z e^{i\alpha} , \tag{17.33}$$

with the result that

$$F(\zeta') = U \cos\alpha \left(\zeta' + \frac{1}{\zeta'} \right) - iU \sin\alpha \left(\zeta' - \frac{1}{\zeta'} \right) , \tag{17.34}$$

and then using the inverse transformation Eq. 17.30 to write $\zeta'(\zeta)$, to obtain

$$F(\zeta) = U \cos\alpha \, \zeta \mp iU \sin\alpha \sqrt{\zeta^2 - 4} . \tag{17.35}$$

The signs in Eq. 17.35 apply to the upper and lower surfaces, respectively. This is an extension of the results of Sec. 17.1.

April 23, 2001

The Joukowski transformation maps circles with $r = r_0 > 1$ to ellipses

$$\frac{\xi^2}{(r_0^2 + 1)^2} + \frac{\eta^2}{(r_0^2 - 1)^2} = \frac{1}{r_0^2} \tag{17.36}$$

with foci at $\xi = \pm 2$. The sketch shows a graphical construction of the transformation. The circles ζ and


```
xc  =  .0
yc  =  .0
r   =  1.1
```
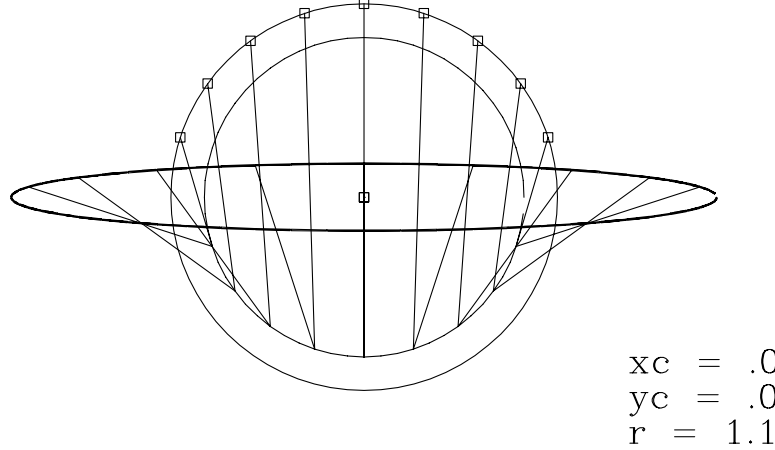
$1/\zeta$ are shown; representative points ζ (squares) and $1/\zeta$ and the points on the ellipse to which their sum maps are connected by straight-line segments. Joukowski used the fact that a short line segment through $(+1, 0)$ maps to a fold to devise shapes with sharp trailing edges. A circle of radius larger than unity with center at (x_c, y_c) which passes through the point $(+1, 0)$ transforms to a shape which has a nearly elliptical front edge and a sharp trailing edge. For $y_c = 0$ the resulting airfoil is symmetric and for $y_c > 0$ it is cambered (see next sketch).

A circle with center at $(0, y_c)$ which passes through *both* of the points $(\pm 1, 0)$ transforms to a circular arc (*i.e.*, it has two sharp ends and zero thickness; a flat plate which is bowed up) which forms the so-called 'skeleton' of the above airfoil. It results because of the property that the Joukowski Transformation, Eq. 17.29, has the alternative form

$$\frac{\zeta - 2}{\zeta + 2} = \frac{(z - 1)^2}{(z + 1)^2} . \tag{17.37}$$

The skeleton is an approximation to the camber line for small (x_c, y_c).

The next sketch shows the graphical construction for a circle with center at (-0.1, 0.1). Lift is generated by by applying circulation to the cylinder and rotating the flow to satisfy the Kutta condition at the trailing edge. When circulation is applied the stagnation point moves downward on the body (Fig. 44) to the position given by Eq. 16.104. The Kutta condition is satisfied by rotating the velocity vector counter clockwise until the rear stagnation point moves back up to the point $(+1, 0)$. From the geometry of the sketch $\alpha = \theta - \phi$. Therefore,

$$\Gamma = 4\pi U a \sin(\alpha + \phi) , \tag{17.38}$$

where

$$\phi = \tan^{-1} \frac{y_c}{1 - x_c} ; \qquad a = (1 - x_c) \sec \phi . \tag{17.39}$$

From Eq. 16.87 and Eq. 17.19, we have

$$C_\ell = 8\pi \frac{a}{c} \sin(\alpha + \phi) , \tag{17.40}$$

April 23, 2001

$$\text{xc} \;=\; -.1$$
$$\text{yc} \;=\; .1$$
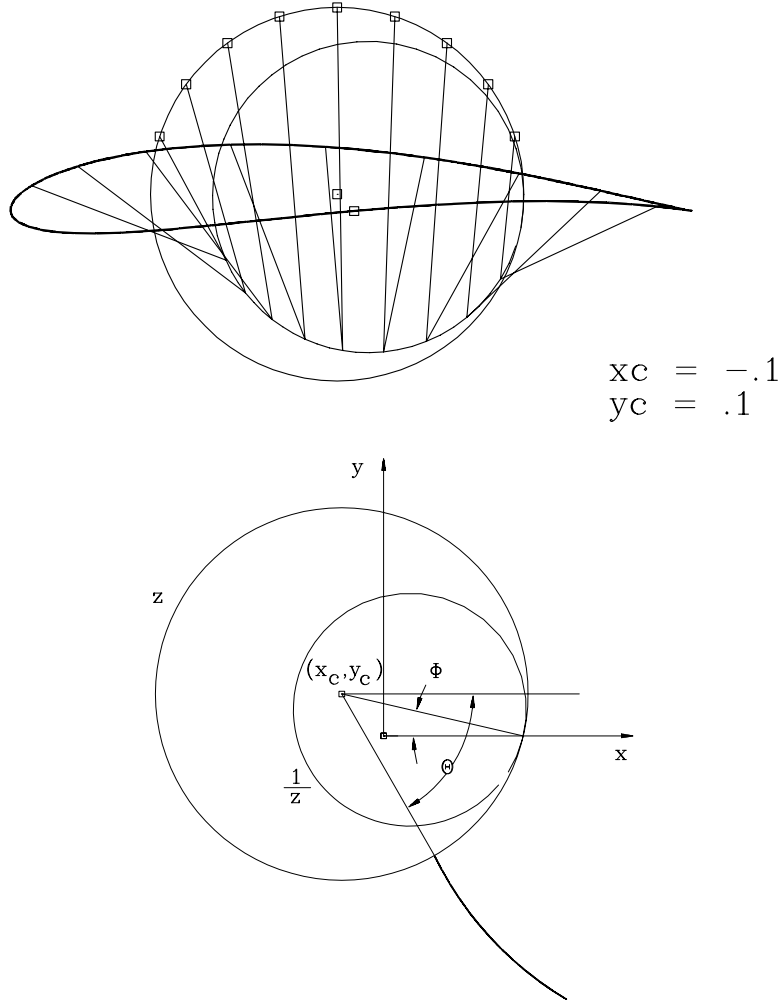
where, since for the transformation chosen $c = 4$,

$$\frac{a}{c} \;=\; \frac{1 - x_c}{4}\ \sec\phi\ . \tag{17.41}$$

Using the trigonometric addition formulas gives,

$$C_\ell \;=\; 2\pi(1 - x_c)\left(\sin\alpha + \frac{y_c}{1 - x_c}\cos\alpha\right)\ , \tag{17.42}$$

$$C_{\ell_\alpha} \;=\; 2\pi(1 - x_c)\left(\cos\alpha - \frac{y_c}{1 - x_c}\sin\alpha\right)\ . \tag{17.43}$$

In reality, lift is limited by stall, an effect of viscosity, rather than any limitations of the value of $\sin\alpha$ in Eq. 17.42 and Eq. 17.43, so it is valid to take the small angle approximation, with the result

$$\boxed{\begin{aligned}
C_\ell &= 2\pi(1 - x_c)\left(\alpha + \frac{y_c}{1 - x_c}\right)\ , \\[2ex]
C_{\ell_\alpha} &= 2\pi(1 - x_c)\left(1 - \frac{y_c}{1 - x_c}\alpha\right)\ .
\end{aligned}} \tag{17.44}$$

Finite camber ($y_c \neq 0$) gives a shape-dependent contribution to lift, and finite thickness ($x_c \neq 0$) modifies the lift curve slope from the thin-airfoil value of 2π.

18   Wing Theory

In this section we consider the modifications to airfoil theory that must be made to treat wings of finite span (see Fig. 51).   As with 2-dimensional sections, the Kutta condition establishes circulation around the
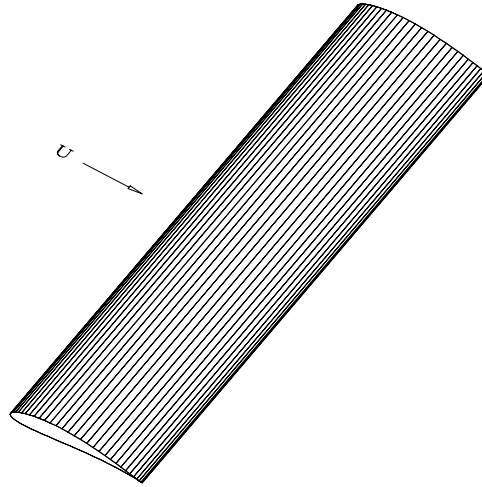
Figure 51. An airfoil of finite span is a wing

wing which can be represented as one or more bound vortex lines. With finite wings there is a problem with this model, because the Helmholtz vortex theorems state that vortex lines can not end in a fluid. The bound vorticity must connect to trailing free vortices at their ends. The simplest picture is a single horseshoe vortex, as indicated in the Fig. 52.   This model expresses the fact that the fluid on the bottom
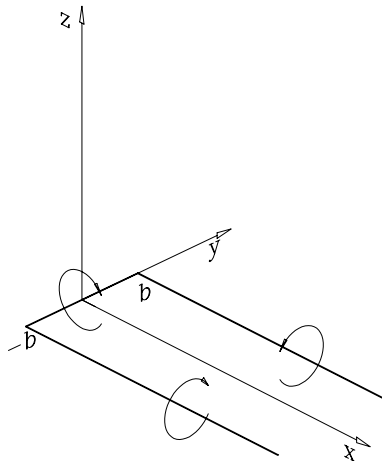
Figure 52. A single horseshoe vortex

high-pressure surface of the wing tends to wash up to the low-pressure top surface creating vorticity in the sense shown.

The loading at any section is $\Delta p \sim \gamma$, and we expect that it must go to zero smoothly at the wing tips. Thus, a more realistic model involves a continuous distribution of infinitesimal horseshoe vortices arranged so that the total strength is maximum at the wing centerline.

April 23, 2001

18.1 Induced Drag

The trailing vortices of a horseshoe vortex system contain kinetic energy. Work must be done to generate that energy, so it is reasonable to expect that drag will be connected with the kinetic energy of the wake. Treating the horseshoe vortex as a model of a finite-span wing, the downwash distribution induced by the vortices in the plane of the wing centerspan is shown schematically by the dashed line in Fig. 53. The incident flow apparent to the airfoil is inclined downward by the downwash, so the force
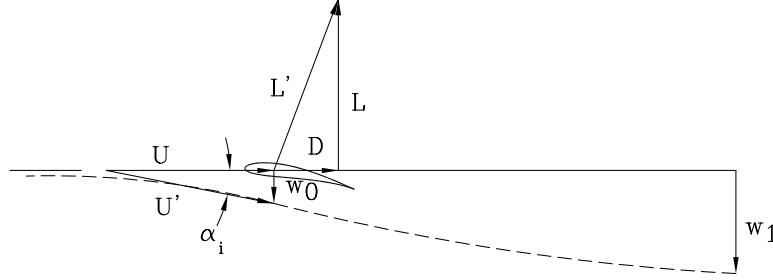
Figure 53. Notation for downwash and induced angle of attack

exerted by the bound vortex, which by the Kutta-Joukowski theorem is always at right angles to the incident flow, is now inclined backward. Since here we are taking Γ to be given, Fig. 53 does not show the angle of attack of the wing and other details about how Γ is generated, by the Kutta condition, *etc.* The figure is an "overlay" on such detail to show the effects of Γ. Note that

$$
\begin{aligned}
U &= U' \cos \alpha_i \\
w_0 &= U \sin \alpha_i \\
L &= L' \cos \alpha_i \\
D &= L' \sin \alpha_i .
\end{aligned}
\tag{18.1}
$$

The Kutta-Joukowski Theorem (incompressible flow) now gives for the lift

$$
L' = -\rho_\infty U' \Gamma , \tag{18.2}
$$

so,

$$
\begin{aligned}
L &= -\rho_\infty \, U' \, \Gamma \cos \alpha_i &= -\rho_\infty \, U \, \Gamma ; & \quad \perp \text{ to } \underline{U} \\
D &= -\rho_\infty \, U' \, \Gamma \sin \alpha_i &= -\rho_\infty \, w_0 \, \Gamma ; & \quad \parallel \text{ to } \underline{U} .
\end{aligned}
\tag{18.3}
$$

The lift remains perpendicular to the free-stream, and the drag is parallel to it. This is the *induced drag* D_i. From the above,

$$
\frac{D_i}{L} = \frac{w_0}{U} . \tag{18.4}
$$

Luckily for the airframe industry, which otherwise wouldn't exist, the drag is of smaller order than the lift. Because the fluid at the point where the lift and drag act ($x = 0$) sees only a semi-infinite vortex pair, while that far downstream sees an infinite one, w_0 is half of the downwash far downstream, w_1,

$$
w_0 = \frac{w_1}{2} . \tag{18.5}
$$

The same result holds if the vorticity is distributed across the span.

Table 5 summarizes the fundamental's that have been learned in this and the previous chapters.

April 23, 2001

Table 5. Summary of Airfol and Wing Theories

Airfoil:	α	$\xrightarrow{\text{Kutta}}$	Γ	$\longrightarrow$		$\begin{array}{c} L \\[4pt] D = 0 \end{array}$		(D'Alembert's Paradox)
Wing:	Γ	$\xrightarrow[\substack{\text{Trailing} \\ \text{vorticies}}]{}$	w_0	$\longrightarrow$	α_i	$\longrightarrow$	$\begin{array}{c} L \\[4pt] D_i \end{array}$	

18.2 Control Volume Analysis of the Forces on a Wing
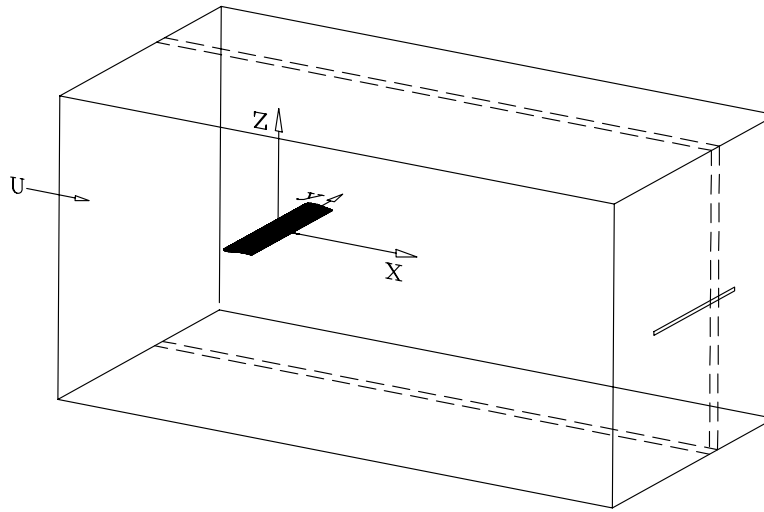
Figure 54. Control volume for calculating forces on a wing

In this section we calculate the forces acting on a wing by equating them to the momentum flux through the faces of a large control volume, as indicated in Fig. 54. The conservation of momentum Eq. 1.8 states that in steady flow the force on the airfoil (the negative of the force on the fluid) is

$$\underline{F} \;=\; -\int_S \Delta p\, dS \;-\; \int_S \rho(\underline{U} + \underline{u})\,(\underline{U} + \underline{u}) \cdot d\underline{S}\,, \tag{18.6}$$

where the surface S includes all 6 faces of the rectangular control volume. Velocities are represented as the sum of the undisturbed free-stream velocity $\underline{U}$, which, being constant, where it appears first in Eq. 18.6 integrates out to zero, and the disturbance velocities $\underline{u}$. The upstream plane normal to the flow direction is placed so far upstream that there are no disturbance velocities on it. The downstream plane normal to the flow direction, called the Trefftz plane (TP), is placed so far downstream that the disturbance velocities are vanishingly small except in the wake, but not so far downstream that the wake deviates much from planar; the vortex sheet is not rolled up. This may eliminate consideration of one class of wings, delta wings, where the vortices are rolled up right over the wing. However, the analysis is sufficiently general to include high-speed flight, where compressibility effects may be important.

We consider a body symmetric about the x-z plane, so there are no side forces. The vertical component

of the force in Eq. 18.6 is by definition the lift,

$$
\begin{aligned}
L &= -\int_{\mathrm{TP}} \underbrace{\rho w (U + u)}_{x=\infty} \, dy \, dz \\
&\quad - \int_{-\infty}^{\infty} dx \left(\int_{-\infty}^{\infty} \underbrace{\Delta p + \rho w^2}_{z=\pm\infty} \, dy + \int_{-\infty}^{\infty} \underbrace{\rho w v}_{y=\pm\infty} \, dz \right) ,
\end{aligned}
\tag{18.7}
$$

where $(x = \infty)$ indicates the TP, $(y = \pm\infty)$ denotes the two side faces of the control volume, and $(z = \pm\infty)$ denotes the top and bottom faces. The horizontal force is the drag,

$$
\begin{aligned}
D &= -\int_{\mathrm{TP}} \underbrace{\Delta p + \rho u (U + u)}_{x=\infty} \, dy \, dz \tag{18.8} \\
&\quad - \int_{-\infty}^{\infty} dx \left(\int_{-\infty}^{\infty} \underbrace{\rho u w}_{z=\pm\infty} \, dy + \int_{-\infty}^{\infty} \underbrace{\rho u v}_{y=\pm\infty} \, dz \right) ,
\end{aligned}
\tag{18.9}
$$

We take the surfaces of the control volume to be so far away that squares of the disturbance velocities are negligible. Furthermore, in the TP the only important disturbance velocities are those induced by the lift in the transverse direction; u is negligible. Then,

$$
L = -\int_{\mathrm{TP}} \underbrace{\rho U w}_{x=\infty} \, dy \, dz - \int_{-\infty}^{\infty} dx \int_{-\infty}^{\infty} \underbrace{\Delta p}_{z=\pm\infty} \, dy ,
\tag{18.10}
$$

$$
D = -\int_{\mathrm{TP}} \underbrace{\Delta p}_{x=\infty} \, dy \, dz .
\tag{18.11}
$$

18.3 Pressures

Using the Bernoulli equation, the pressures can be represented in terms of velocities. We take the fluid to be a perfect gas, and so treat compressible flow. From Eq. 15.36

$$
\Delta p \doteq -\rho_\infty U u - \frac{1}{2} \rho_\infty (u^2 + v^2 + w^2) .
\tag{18.12}
$$

From Eq. 15.37, in the TP, where $u = 0$, but not (v, w), to first order

$$
\rho_{TP} \doteq \rho_\infty .
\tag{18.13}
$$

18.4 Lift

Substituting Eqs. 18.12 and 18.13, evaluated to first order, into Eq. 18.10, gives

$$
L = \rho_\infty U \int_{-\infty}^{\infty} dy \left(-\int_{\mathrm{TP}} \underbrace{w}_{x=\infty} \, dz + \int_{-\infty}^{\infty} \underbrace{u}_{z=\pm\infty} \, dx \right) .
\tag{18.14}
$$

Now, $w = \partial\phi/\partial z$ and $u = \partial\phi/\partial x$, so the arguments in the last two integrals are perfect differentials. The z and x integrations are along the strip shown by dashed lines in Fig. 54. By symmetry, the only

April 23, 2001

contribution can come from the discontinuity in ϕ at the wake (see Eq. 16.79). Thus, the integral in y only has contributions from $-b < y < b$, where b is the semi-span, so

$$\boxed{L \;=\; \rho_\infty U \int_{-b}^{b} \Delta\phi(y)\,dy\;.}_{\text{TP}}$$

(18.15)

A major result is that both the lift (Eq. 18.15) and drag (Eq. 18.11) can be computed by considerations in the TP only. Of course, this does not make their determination any simpler, because the configuration of the wake in the TP may not be straightforward to determine.

18.5 Drag

In the Trefftz plane streamwise perturbations u and u^2 are taken to be smaller than lateral perturbations w^2 and v^2. Since for drag we are concerned with second-order quantities (energy), the Bernoulli equation Eq. 18.12 must be used correct to second order. Thus, as expected from the energy considerations of Sec. 18.1, the drag is a second-order quantity. Substituting Eq. 18.12 into Eq. 18.11, gives

$$D \;=\; \frac{1}{2}\rho_\infty \int_{\text{TP}} \left[\underbrace{\left(\frac{\partial\phi}{\partial y}\right)^2 + \left(\frac{\partial\phi}{\partial z}\right)^2}_{x=\infty} \right] dy\,dz\;.$$

(18.16)

Now, the further assumption that not only $u = 0$ but also $\partial u/\partial x = 0$ in the TP reduces the equation satisfied by the velocity potential for perfect-fluid flow to

$$\frac{\partial^2\phi}{\partial y^2} + \frac{\partial^2\phi}{\partial z^2} \;=\; 0\;.$$

(18.17)

Thus, the flow in the TP is two-dimensional. Then, using Green's Theorem to convert the surface integral to a line integral around the wake, with Eq. 18.17, gives

$$D \;=\; \frac{1}{2}\rho_\infty \oint \phi\frac{\partial\phi}{\partial n}\,ds\;.$$

(18.18)

The integral is along the strip $-b < y < b$. Taking pairs of points at $z = (0^+, 0^-)$ and the same y, gives

$$\boxed{D \;=\; \frac{1}{2}\rho_\infty \int_{-b}^{b} \Delta\phi\, w_1\,dy\;.}_{\text{TP}}$$

(18.19)

18.6 Constant Downwash

In oreder to proceed further, we consider a special case. A flat (untwisted) high-aspect-ratio wing produeces a uniform downwash distribution $w_1(y) = \text{const}$. Furthermore, it was shown by Munk in 1919 that this case yields minimum drag, so it is an important subcase. With constant downwash, w_1 in Eq. 18.19 comes out of the integral, so, with Eq. 18.15,

$$\boxed{D \;=\; \frac{1}{2}\frac{w_1}{U}L\;.}$$

(18.20)

It remains to determine the velocity potential ϕ in the wake. In this case the flow in the TP looks like the flow over a flat plate at $90°$ incidence with a *uniform* vertically upward free stream velocity w_1. Thus the velocity potential can be obtained directly from results for a flat plate airfoil with $U = w_1$ and $\alpha = \pi/2$.

$$\Delta\phi = 2w_1 b\sqrt{1 - \left(\frac{y}{b}\right)^2} . \tag{18.21}$$

Substituting into Eq. 18.15 gives

$$L = 2\rho_\infty U w_1 b \int_{-b}^{b} \sqrt{1 - \left(\frac{y}{b}\right)^2} \, dy , \tag{18.22}$$

The distribution of load on the wing is elliptic, and the total lift is

$$L = \pi\rho_\infty U w_1 b^2 . \tag{18.23}$$

With $C_L = L/\frac{1}{2}\rho U^2 S$, where S is the planform area, and $A\!R = 4b^2/S$,

$$\boxed{C_L = \frac{\pi}{2} A\!R \frac{w_1}{U}} \tag{18.24}$$

Eliminating w_1/U from Eqs. 18.24 and 18.20,

$$\boxed{C_D = \frac{1}{\pi A\!R} C_L^2} \tag{18.25}$$

Again, the drag is second order in the lift; a plot of $C_D(C_L)$ is a concave-up parabola. Only for two-dimensional airfoils ($A\!R \to \infty$) is the drag zero (d'Alembert's Paradox). Even when the lift is negative, the drag is positive; there's no way to avoid drag!

18.7 Vortex Distribution and Circulation on the Wing

From Eq. 16.78 we have in the Trefftz plane

$$\frac{\partial\phi_+}{\partial y} = -\frac{1}{2}\frac{d\Gamma}{dy} = -\gamma_{TP}(y) , \tag{18.26}$$

where $\Gamma(y)$ is the total circulation of the sheet, and $\gamma_{TP}(y)$ is the vorticity at point y. With Eq. 18.21 we get

$$\gamma_{TP} = 2w_1 \frac{y/b}{\sqrt{1 - (y/b)^2}} . \tag{18.27}$$

Helmholtz' Vortex Theorems state that the trailing vortex sheet contains the same vorticity as does the bound vortex on the wing, so they provide the mechanism for studying more about the actual flow over the wing. This is done most directly if $A\!R >> 1$ and the wing is untwisted, because in that case it can be assumed that the sheet is flat all the way from the wing to the TP. Then, in the TP

$$\Gamma(y) = -\Delta\phi(y) = -2w_1 b\sqrt{1 - \left(\frac{y}{b}\right)^2} , \tag{18.28}$$

and this result applies also to the wing. If we wish to apply it to the Kutta-Joukowski Theorem in order to determine the lift, we must apply the further restriction that the fluid is *incompressible*.

April 23, 2001

18.8 Spanwise Loading – Planform

The 'section lift' (lift per unit span) was treated in Section 17. In terms of the total lift, the section lift $\ell(y)$ is $\ell(y) = dL/dy$. The Kutta-Joukowski theorem is

$$\ell(y) \;=\; -\rho_\infty\, U\, \Gamma(y) \;=\; 2\rho_\infty U w_1 b \sqrt{1 - \left(\frac{y}{b}\right)^2} \,. \tag{18.29}$$

The section lift coefficient $C_\ell = l(y)/\frac{1}{2}\rho U^2 c(y)$ is,

$$C_\ell(y) \;=\; 4\frac{w_1}{U}\frac{b}{c(y)}\sqrt{1 - \left(\frac{y}{b}\right)^2} \,. \tag{18.30}$$

Using Eq. 18.24 ro eliminate w_1/U, the differential form of Eq. 18.22 is derived,

$$\boxed{C_\ell(y)\, c(y) \;=\; \frac{8b}{\pi \mathcal{R}}\, C_L \sqrt{1 - \left(\frac{y}{b}\right)^2}}\,. \tag{18.31}$$

This result exhibits the elliptic loading explicitly.

For large $\mathcal{R}$ wings, the flow over the wing can be treated as locally two-dimensional, except near the tips. In that case, for a wing with no twist and with constant section parameters the section lift is constant and approximately equal to C_L (see below),

$$C_\ell(y) \;=\; \text{const} \;=\; C_L \,. \tag{18.32}$$

For such a wing, from Eq. 18.31 the planform is elliptic,

$$\boxed{c(y) \;=\; \frac{8b}{\pi \mathcal{R}}\sqrt{1 - \left(\frac{y}{b}\right)^2}}\,. \tag{18.33}$$

The maximum chord $c_{\max}$ is at $y = 0$, and $c_{\max} = 8b/\pi\mathcal{R}$. This rather strange looking result is a consequence of the fact that for an elliptic wing

$$C_D \;=\; \frac{c_{\max}}{b}C_L^2 \tag{18.34}$$

As shown in Fig. 53, the *constant* downwash w_0 induces an angle of attack α_i,

$$\alpha_i \;=\; \frac{w_0}{U} \;=\; \frac{w_1}{2U} \,. \tag{18.35}$$

From Eq. 18.24,

$$\boxed{\alpha_i \;=\; \frac{C_L}{\pi \mathcal{R}}} \tag{18.36}$$

Approximating the behavior of large $\mathcal{R}$ wings by the linearized results of thin airfoil theory, we have

$$C_L \doteq C_\ell \;=\; C_{\ell_\alpha}\,\alpha_e \,, \tag{18.37}$$

April 23, 2001

where $\alpha_e = \alpha - \alpha_i$. Using Eqs. 18.37 and Eq. 18.36,

$$\alpha = \frac{C_L}{C_{\ell_\alpha}} \left(1 + \frac{C_{\ell_\alpha}}{\pi A\!\!R} \right) \,, \tag{18.38}$$

or,

$$C_{L_\alpha} = \frac{C_{\ell_\alpha}}{1 + \dfrac{C_{\ell_\alpha}}{\pi A\!\!R}} \,. \tag{18.39}$$

The wing lift curve slope is less than the section lift curve slope due to the effect of finite aspect ratio. For an *uncambered* thin airfoil, $C_{\ell_\alpha} = 2\pi$, so

$$\boxed{\frac{C_{L_\alpha}}{C_{\ell_\alpha}} = \frac{A\!\!R}{2 + A\!\!R} \,.} \tag{18.40}$$

In Eq. 18.40 $C_{\ell_\alpha} = 2\pi$.

19   Parallel Viscous Flows

The equations of motion for 2D plane, incompressible flow with $\mu = \mathrm{const}$ (and no body force) are

$$\frac{\partial u}{\partial x} + \frac{\partial v}{\partial y} = 0 \tag{19.1}$$

$$\frac{\partial u}{\partial t} + u\frac{\partial u}{\partial x} + v\frac{\partial u}{\partial y} = -\frac{1}{\rho}\frac{\partial p}{\partial x} + \nu\left(\frac{\partial^2 u}{\partial x^2} + \frac{\partial^2 u}{\partial y^2}\right) \tag{19.2}$$

$$\frac{\partial v}{\partial t} + u\frac{\partial v}{\partial x} + v\frac{\partial v}{\partial y} = -\frac{1}{\rho}\frac{\partial p}{\partial y} + \nu\left(\frac{\partial^2 v}{\partial x^2} + \frac{\partial^2 v}{\partial y^2}\right) \tag{19.3}$$

$$\frac{\partial \omega}{\partial t} + u\frac{\partial \omega}{\partial x} + v\frac{\partial \omega}{\partial y} = +\nu\left(\frac{\partial^2 \omega}{\partial x^2} + \frac{\partial^2 \omega}{\partial y^2}\right) \tag{19.4}$$

To study the basic physics of viscous flow, we first consider flows in which the velocity is in one direction only, $u(x, y, t)$, $v = 0$. From Eq. 19.1 $\partial u/\partial x = 0$, and it follows from Eq. 19.3 that $\partial p/\partial y = 0$

19.1   Viscous waves

Consider first a semi-infinite domain bounded by one solid surface.

Infinite flat plate oscillating parallel to itself.   The plate motion is

$$\begin{aligned} u(x, 0, t) &= u_0\, e^{int} \\ v(x, 0, t) &= 0\,, \end{aligned} \tag{19.5}$$

where in this section n is the frequency. As we will see, despite the fact that the fluid is assumed incompressible, this motion produces *transverse* waves.

In the x-momentum equation only the nonsteady term survives from the left hand side and, with constant viscosity, the only term from $\mu\nabla^2 u$ is $\mu\partial^2 u/\partial y$. The result is

$$\boxed{\frac{\partial u}{\partial t} = \nu\,\frac{\partial^2 u}{\partial y^2}}\,, \tag{19.6}$$

a diffusion equation. The vorticity $\omega = -\partial u/\partial y$ satisfies the same equation,

$$\boxed{\frac{\partial \omega}{\partial t} = \nu\,\frac{\partial^2 \omega}{\partial y^2}}\,. \tag{19.7}$$

We expect $u = f(\eta)e^{int}$, where η is the "similarity variable." Here we choose the characteristic time to be the period of the motion, and the corresponding similarity variable to be $\eta = y\sqrt{n/2\nu}$. As a consequence. the diffusion equation reduces to an o.d.e.

However, here we are trying to find waves, so we assume

$$u(y, t) = u_0\, e^{i(ky - nt)}\,, \tag{19.8}$$

and obtain a dispersion relation

$$k = \pm(1 + i)\sqrt{\frac{n}{2\nu}}\,. \tag{19.9}$$

April 23, 2001

To exclude exponentially growing solutions we select the $+$ sign. Thus

$$\boxed{u \; = \; u_0 \, e^{-\eta} \, e^{i(\eta - nt)} \,.}$$

(19.10)

This solution shows that the velocities die off exponentially away from the wall in distance $\delta = \sqrt{2\nu/n}$ and that the phase velocity $a = n/k$ is

$$a \; = \; \sqrt{2\nu n} \,,$$

(19.11)

while the group velocity $c = \partial n/\partial k$ is

$$c \; = \; 4\nu k \; = \; 2a \,.$$

(19.12)

The vorticity is

$$\omega(y, t) \; = \; -ik \, u(y, t)$$

(19.13)

and the circulation is

$$\Gamma \; = \; \int \omega \, dS \; = \; -\Delta x \int \frac{\partial u}{\partial y} \, dy$$
$$= \; \Delta x \, u(0, t)$$

(19.14)

$$\boxed{\Gamma \; = \; u_0 \, \Delta x \, e^{-int} \,.}$$

(19.15)

Since the circulation only depends on the wall motion, it is clear that the total vorticity only changes as the wall adds and subtracts vorticity from the fluid. The average circulation is null, because equal and opposite amounts of vorticity are added in each cycle.

A physically useful measure of the distance that the disturbance created by the plate extends into the fluid is the so-called *vorticity thickness*,

$$\omega(0, t) \, \delta_\omega(t) \; \equiv \; \int_0^\infty \omega(y, t) \, dy \; = \; -\int_0^\infty \frac{\partial u}{\partial y} \, dy$$

(19.16)

$$\delta_\omega \; = \; i(1 - i) \sqrt{\frac{\nu}{2n}}$$

(19.17)

Only the magnitude of δ is of interest, so

$$\boxed{\delta_\omega \; = \; \sqrt{\frac{\nu}{n}} \,.}$$

(19.18)

The disturbance is confined closer to the wall as the frequency increases. Compared to the amplitude of the plate motion,

$$\frac{\delta_\omega \, n}{u_0} \; \sim \; \frac{1}{\sqrt{Re_n}} \,,$$

(19.19)

where

$$Re_n \; = \; \frac{u_0^2}{\nu n} \,.$$

(19.20)

The layer is thin when the Reynolds number is large.

April 23, 2001

19.2 Rayleigh problem

The impulsive acceleration of a flat plate to velocity U parallel to itself in incompressible flow.

Here we take for the similarity variable

$$\eta = \frac{y}{2\sqrt{\nu t}} , \tag{19.21}$$

and substutute

$$\frac{u}{U} = f(\eta) \tag{19.22}$$

into the diffusion equation, giving the result

$$f'' + 2\eta \, f' = 0 ; \qquad \begin{array}{l} f(0) = 1 \\ f(\infty) = 0 \end{array} \tag{19.23}$$

The soution is

$$\boxed{f = \mathrm{erfc}\,\eta ,} \tag{19.24}$$

where $\mathrm{erfc}\,\eta = 1 - \mathrm{erf}\,\eta$, and

$$\mathrm{erf}\,\eta = \frac{2}{\sqrt{\pi}} \int_0^{\eta} e^{-x^2} \, dx . \tag{19.25}$$

The vorticity is

$$\omega = -U f' \frac{1}{2\sqrt{\nu t}} = U \frac{e^{-\eta^2}}{\sqrt{\pi \nu t}} , \tag{19.26}$$

so

$$\boxed{\omega(0,t) = \frac{U}{\sqrt{\pi \nu t}} .} \tag{19.27}$$

The vorticity thickness, defined in Eq. 19.16, is

$$\boxed{\delta_{\omega} = \sqrt{\pi \nu t} .} \tag{19.28}$$

If we normalize δ_{ω} with $L = Ut$, the distance the plate has traveled, then

$$\frac{\delta_{\omega}}{L} = \frac{1}{\sqrt{Re_L}} , \tag{19.29}$$

where $Re_L = UL/\nu$. The circulation is

$$\Gamma = \oint \underline{u} \cdot d\underline{\ell} = U\Delta x . \tag{19.30}$$

In this flow the total vorticity is constant for all time! All of the vorticity is deposited into the fluid by the plate at time $t = 0$ and all that happens after that is that the vorticity diffuses.

Arbitrary plate velocity. The motion induced by an arbitrary plate velocity $U(t)$ can be built up by the superposition of small impulsive motions. The motion at time t resulting from one such small impulse at time τ is

$$du(t) = dU(\tau) \, \mathrm{erfc} \frac{y}{2\sqrt{\nu(t-\tau)}} . \tag{19.31}$$

Therefore the complete flow is given by the Stieltjes integral

$$u(t) = \int_0^t \frac{dU(\tau)}{d\tau} \, \mathrm{erfc} \frac{y}{2\sqrt{\nu(t-\tau)}} \, d\tau . \tag{19.32}$$

　　　　　　　　　　　　　　　　April 23, 2001

19.3 Flows with Heat Transfer; Couette flow

Compressible, steady flow. (Liepmann & Roshko, 1957)

In Couette flow, the fluid is driven by a top plate moving parallel to itself, while the bottom plate is at rest. Now the simplifications are great enough that problems with heat transfer can easily be solved. From the problem specification, $\partial/\partial t = 0$ and $\partial/\partial x = 0$. The continuity equation gives $\rho v = $ const, which with the bottom plate boundary condition, and the requirement $\rho \neq 0$ again gives $v = 0$. The y-momentum equation gives the same result for p, while the entire lhs of the x-momentum equation is now 0, so

$$\begin{aligned} \frac{\partial \tau}{\partial y} &= 0 \\ \tau &= \tau_w \, . \end{aligned}$$
(19.33)

Because the lhs is gone, the density ρ does not appear (no inertia). The velocity profile follows from $\tau = \mu \partial u/\partial y$,

$$u(y) = \tau_w \int_0^y \frac{dy}{\mu(T(y))} \, ,$$
(19.34)

where T is the temperature. Compressibility in Couette flow appears only as variable viscosity $\mu(T)$. The velocity profile depends on the temperature distribution, which is determined by the energy equation.

The lhs of the energy equation (Eq. 2.24) similarly goes away, so all that remains is

$$\begin{aligned} \frac{d}{dy}(\tau_{xy} u - q) &= 0 \\ u\tau - q &= -q_w \, . \end{aligned}$$
(19.35)

With $\tau = \mu \, du/dy$ and $q = -k \, dT/dy$ this becomes

$$\frac{d\frac{u^2}{2}}{dy} + \frac{1}{Pr} \frac{dh}{dy} = -\frac{q_w}{\mu} \, ,$$
(19.36)

where $Pr = c_p \mu/k$ and $dh = c_p \, dT$ have been used. This equation can be integrated providing that Pr = const. Substituting Eq. 19.34 to eliminate the indefinite integral gives an exact integral of the energy equation

$$\boxed{h_w - h = Pr\left(\frac{u^2}{2} + \frac{q_w}{\tau_w} u\right) \, .}$$
(19.37)

This is the energy integral. It relates h and u. Note that h_w is the enthalpy of the fluid at the wall temperature, not the enthalpy of the wall. Assuming c_p = const permits evaluation of the temperature at the top wall, $(\ )_\infty$,

$$\boxed{T_w - T_\infty = \frac{Pr}{c_p}\left(\frac{U^2}{2} + \frac{q_w}{\tau_w} U\right) \, .}$$
(19.38)

Adiabatic wall. The wall temperature required to insure $q_w = 0$ is $T_w \equiv T_r$,

$$T_r = T_\infty + \frac{Pr}{2c_p} U^2 \, .$$
(19.39)

Assuming a perfect gas and using the perfect gas equation of state gives

$$\frac{T_r}{T_\infty} = 1 + Pr \frac{\gamma - 1}{2} M_\infty^2 \, ,$$
(19.40)

April 23, 2001

which looks something like Eq. 7.58. In fact, combining the two equations gives the *recovery factor*,

$$\frac{T_r - T_\infty}{T_t - T_\infty} \equiv r = Pr .$$ (19.41)

Another form of Eq. 19.38 is

$$\boxed{T_w = T_r + \frac{q_w}{c_p \tau_w} Pr \, U \, \tau_w ,}$$ (19.42)

which relates the heat flux to the wall shear,

$$q_w = \frac{c_p(T_w - T_r)}{U \, Pr} \tau_w .$$ (19.43)

Defining the Stanton number and skin friction coefficient

$$St \equiv \frac{q_w}{\rho_\infty U c_p (T_w - T_r)}$$ (19.44)

$$C_f \equiv \frac{\tau_w}{\frac{1}{2}\rho_\infty U^2} ,$$ (19.45)

Eq. 19.43 gives the *Reynolds Analogy*

$$\boxed{St = \frac{C_f}{2Pr} .}$$ (19.46)

19.4 Poiseuille flow

If the two parallel plates are fixed, distance h apart, a flow can nevertheless be driven if there is a pressure gradient dp/dx in the fluid. To generate a flow with positive velocity, the pressure gradient must be negative. The flow is assumed to be incompressible. In this parallel flow, as before, $\partial/\partial t = 0$, $\partial u/\partial x = 0$ and $\partial p/\partial y = 0$. In the x-momentum equation the entire lhs again goes away, and what's left is *two* terms on the rhs.

Channel flow – plane flow. The channel is of height $2h$, and $y = 0$ lies at mid-channel. For constant viscosity and plane flow

$$0 = -\frac{dp}{dx} + \mu\frac{\partial^2 u}{\partial y^2} ; \qquad \begin{array}{l} u(-h) = u(h) = 0 \\ \left(\frac{du}{dy}\right)_{h=0} = 0 \end{array}$$ (19.47)

This equation is easily integrated to give, first, the shear stress,

$$\tau = \mu\frac{du}{dy} = \frac{dp}{dx}y$$ (19.48)

$$\tau_w = -\frac{dp}{dx} h ,$$ (19.49)

where the constant of integration has been evaluated by the symmetry condition at $y = 0$. The shear stress on the wall determines the pressure drop in the pipe. For a control volume of length Δx and covering $0 < y < h$, the above equation gives

$$\tau_w \Delta x = -h \Delta p ,$$ (19.50)

April 23, 2001

which is just what would be derived from the integral form of the momentum equation. For the same area the circulation is

$$
\begin{aligned}
\Gamma &= \int \omega \, dS \\
&= -\Delta x \int_0^h \frac{du}{dy} \, dy \\
&= u_{max} \, \Delta x \, .
\end{aligned}
\tag{19.51}
$$

Next, the velocity profile can be calculated,

$$
u(y) = \frac{1}{\mu} \left(-\frac{dp}{dx} \right) \frac{h^2 - y^2}{2} \, .
\tag{19.52}
$$

The maximum velocity is

$$
u_{max} = \frac{1}{\mu} \left(-\frac{dp}{dx} \right) \frac{h^2}{2} \, ,
\tag{19.53}
$$

so the wall friction and velocity profile can be expressed as

$$
\tau_w = 2\mu \frac{u_{max}}{h}
\tag{19.54}
$$

$$
\frac{u}{u_{max}} = 1 - \left(\frac{y}{h} \right)^2 \, .
\tag{19.55}
$$

In nondimensional terms,

$$
C_f = \frac{4}{Re_h} \, ,
\tag{19.56}
$$

where here $C_f \equiv 2\tau_w / \rho u_m^2$ and $Re_h \equiv u_{max} h / \nu$.

Pipe flow. In this case,

$$
0 = -\frac{dp}{dx} + \mu \frac{1}{r} \frac{\partial}{\partial r} \left(r \frac{\partial u}{\partial r} \right) \, ; \qquad
\begin{array}{c}
u(-R) = u(R) = 0 \\
\left(\dfrac{du}{dr} \right)_{r=0} = 0
\end{array}
\tag{19.57}
$$

Again using the symmetry condition, one integration gives

$$
\tau = \mu \frac{du}{dr} = \frac{dp}{dx} \frac{r}{2}
\tag{19.58}
$$

$$
\tau_w = -\frac{dp}{dx} \frac{R}{2} \, ,
\tag{19.59}
$$

and a second gives

$$
u(r) = -\frac{dp}{dx} \frac{R^2 - r^2}{4\mu} \, .
\tag{19.60}
$$

The skin friction coefficient is conventionally defined with $\overline{u}$ the mean velocity, and the Reynolds number with $\overline{u}$ and the diameter d,

$$
C_f = \frac{\tau_w}{\frac{1}{2} \rho \overline{u}^2}
\tag{19.61}
$$

$$
Re = \frac{\rho \overline{u} d}{\mu} \, .
\tag{19.62}
$$

April 23, 2001

The volume flux is

$$Q = \int_0^R \int_0^{2\pi} ur \, dr \, d\theta \tag{19.63}$$

$$= -\frac{dp}{dx} \frac{\pi R^4}{8\mu} . \tag{19.64}$$

Thus the mean velocity is

$$\overline{u} \equiv \frac{Q}{\pi R^2} = -\frac{dp}{dx} \frac{R^2}{8\mu} , \tag{19.65}$$

so

$$C_f = \frac{8\mu}{\rho \overline{u} R} , \tag{19.66}$$

$$\boxed{C_f = \frac{16}{Re} .} \tag{19.67}$$

20 Thin-Layer Flows

In fluid mechanics there are situations in which the effects of viscosity are confined to very thin layers adjacent to the body, and the rest of the flow is given by irrotational considerations. In this section we derive what the conditions are for thin viscous layers to occur. For simplicity we consider plane flow of an incompressible fluid. Because the layer is thin, the coordinates are set up so that the x-coordinate follows the body surface, no matter what the body shape, and the y-coordinate is normal to the body surface. We scale the velocities and spatial coordinates as follows,

$$u \sim U \qquad v \sim V \tag{20.1}$$

$$x \sim x \qquad y \sim \delta . \tag{20.2}$$

If the layer is thin, then $\boxed{\delta/x \ll 1}$. Correspondingly, the velocity V must be small, and we take $\boxed{V/U \sim \delta/x}$.

x-momentum equation. The momentum equation, and the magnitude of the various terms are given below. The nonsteady term is assumed to scale with the convective ones, and the pressure is considered later.

$$\rho\frac{\partial u}{\partial t} + \underbrace{\rho u\frac{\partial u}{\partial x}}_{\dfrac{\rho U^2}{x}} + \underbrace{\rho v\frac{\partial u}{\partial y}}_{\dfrac{\rho UV}{\delta} = \dfrac{\rho U^2}{x}} = -\frac{\partial p}{\partial x} + \mu\left(\underbrace{\frac{\partial^2 u}{\partial x^2}}_{\dfrac{\mu U}{x^2}} + \underbrace{\frac{\partial^2 u}{\partial y^2}}_{\dfrac{\mu U}{\delta^2}}\right) \tag{20.3}$$

The last term on the right is much larger than the first. To balance the left side with the viscous term on the right, it must be that

$$\frac{Ux}{\nu}\left(\frac{\delta}{x}\right)^2 = \mathcal{O}(1) , \tag{20.4}$$

or

$$\boxed{\frac{\delta}{x} \sim \frac{1}{\sqrt{Re_x}} \ll 1} , \tag{20.5}$$

where $Re_x = Ux/\nu$. Thus the condition for thin viscous layers is $\boxed{Re_x \gg 1}$. The fact that Re must be large for these flows raises a question about the uniqueness of the solutions to be obtained. Laminar flow with thin layers holds in a limited Reynolds number regime between Stokes flow and turbulent flow.

y-momentum equation. Scaling of the y-momentum equation gives

$$\rho\frac{\partial v}{\partial t} + \underbrace{\rho u\frac{\partial v}{\partial x}}_{\dfrac{\rho UV}{x}} + \underbrace{\rho v\frac{\partial v}{\partial y}}_{\dfrac{\rho V^2}{\delta} = \dfrac{\rho UV}{x}} = -\frac{\partial p}{\partial y} + \mu\left(\underbrace{\frac{\partial^2 v}{\partial x^2}}_{\dfrac{\mu V}{x^2}} + \underbrace{\frac{\partial^2 v}{\partial y^2}}_{\dfrac{\mu V}{\delta^2}}\right) . \tag{20.6}$$

Every term in the y-momentum equation is smaller than in the x-momentum equation, so $\partial p/\partial y$ must be correspondingly small. In this approximation, it is

$$\frac{\partial p}{\partial y} = 0 ; \qquad \boxed{p(x) = p_\infty(x)} . \tag{20.7}$$

The pressure doesn't vary across the layer, and is "imposed" by whatever the behavior of the outer potential flow is. Thus, the x-momentum equation becomes, in the thin-layer approximation

$$\boxed{\rho\frac{\partial u}{\partial t} + \rho u\frac{\partial u}{\partial x} + \rho v\frac{\partial u}{\partial y} = -\frac{dp_\infty}{dx} + \mu\frac{\partial^2 u}{\partial y^2}} \tag{20.8}$$

April 23, 2001

Two important simplifications have resulted,

1. One higher order derivative has been removed, so the equations have been changed from elliptic-type to parabolic-type, the latter having diffusion-equation behavior. Parabolic equations can be solved by time-marching (x-marching) schemes.

2. The pressure field is now a given, not one of the unknowns.

Mechanical Energy equation.

$$\rho\frac{\partial u^2/2}{\partial t} + \rho u\frac{\partial u^2/2}{\partial x} + \rho v\frac{\partial u^2/2}{\partial y} \;=\; -u\frac{dp_\infty}{dx} + \mu u\frac{\partial^2 u}{\partial y^2}\;. \tag{20.9}$$

Energy equation. Thermal energy may diffuse at a different rate (k) than momentum (μ), so we allow for a separate thermal y-scale, δ_T. First, consider the dissipation in plane flow (Eq. 4.8),

$$\Phi \;=\; \left(\eta - \frac{2}{3}\mu\right)\underbrace{\left(\frac{\partial u}{\partial x} + \underbrace{\frac{\partial v}{\partial y}}_{\frac{\mu V^2}{\delta^2}=\frac{\mu U^2}{x^2}}\right)^2}_{\frac{\mu U^2}{x^2}} + \mu\left[\underbrace{2\left(\frac{\partial u}{\partial x}\right)^2}_{\frac{\mu U^2}{x^2}} - \underbrace{2\left(\frac{\partial v}{\partial y}\right)^2}_{\frac{\mu V^2}{\delta^2}=\frac{\mu U^2}{x^2}} + \underbrace{\left(\frac{\partial u}{\partial y} + \frac{\partial v}{\partial x}\right)^2}_{\frac{\mu U^2}{\delta^2}\quad\frac{\mu V^2}{x^2}}\right] \tag{20.10}$$

The largest term is $\mu U^2/\delta^2$, so in the thin-layer approximation

$$\boxed{\Phi \;=\; \mu\left(\frac{\partial u}{\partial y}\right)^2}\;. \tag{20.11}$$

The energy equation (Eq. 4.7) scales as

$$\frac{\partial T}{\partial t} + \underbrace{u\frac{\partial T}{\partial x}}_{\frac{UT}{x}} + v\frac{\partial T}{\partial y} \;=\; \underbrace{\frac{\alpha T}{\rho\,c_p}\left(\frac{\partial p}{\partial t} + u\frac{\partial p}{\partial x} + v\frac{\partial p}{\partial y}\right)}_{\frac{UT}{x}\;\frac{\alpha}{c_p\rho}\,x\frac{dp_\infty}{dx}} + \underbrace{\frac{\Phi}{\rho\,c_p}}_{\frac{\mu U^2}{c_p\rho\delta_T^2}} + \kappa\left(\underbrace{\frac{\partial^2 T}{\partial x^2}}_{\kappa\frac{T}{x^2}} + \underbrace{\frac{\partial^2 T}{\partial y^2}}_{\kappa\frac{T}{\delta_T^2}}\right) \tag{20.12}$$

The magnitude of the pressure-work term depends on $p_\infty(x)$. As before, the next to last term on the right side is small compared to the last. In order for this equation to balance, it must be that

$$\frac{\kappa}{\delta_T^2} \;\sim\; \frac{U}{x} \;=\; \frac{Ux}{\nu}\,\frac{\nu}{x^2} \;=\; \frac{\nu}{\delta^2}\;. \tag{20.13}$$

Therefore,

$$\boxed{\frac{\delta_T}{\delta} \;\sim\; \frac{1}{\sqrt{Pr}}}\;. \tag{20.14}$$

It remains to consider dissipation. The ratio of dissipation to heat conduction is

$$Pr\frac{U^2}{c_p\Delta T}\;. \tag{20.15}$$

April 23, 2001

For low velocities the dissipation is small. That large Pr may cause an increase of dissipation is often not a consideration because $Pr \gg 1$ usually also means high viscosity and therefore low Re, so the thin-layer assumption may not be appropriate in those problems. Thus, the thin-layer form of the energy equation is

$$\boxed{\frac{\partial T}{\partial t} + u\frac{\partial T}{\partial x} + v\frac{\partial T}{\partial y} \;=\; \frac{\alpha T}{\rho\, c_p}\left(\frac{\partial p}{\partial t} + u\frac{\partial p}{\partial x} + v\frac{\partial p}{\partial y}\right) + \frac{\Phi}{\rho\, c_p} + \kappa\frac{\partial^2 T}{\partial y^2}\;.}$$ (20.16)

The energy equation in terms of total enthalpy is

$$\rho u\frac{\partial h_t}{\partial x} + \rho v\frac{\partial h_t}{\partial y} \;=\; \frac{\partial}{\partial y}(\tau u - q) \;=\; \frac{\partial^2}{\partial y^2}\left(\mu\frac{u^2}{2} + kT\right)\;,$$ (20.17)

where the last equality holds, again, for constant μ and k.

20.1   Round Laminar Jet

Consider a steady round laminar jet (Fig. 55). At first we take the jet fluid to be compressible, because general results can easily be derived.   Assume that the thin layer approximation holds, and that the
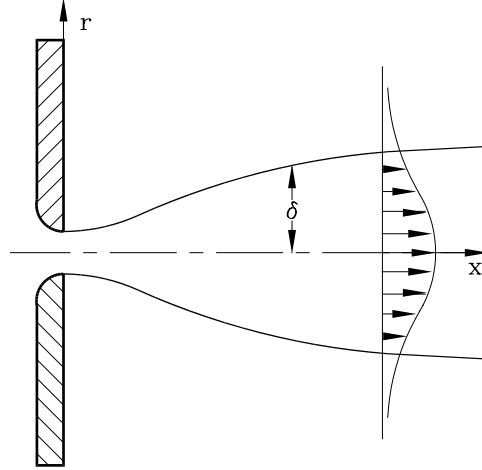
Figure 55. Schematic sketch of a round jet

ambient fluid is uniform, so $dp_\infty = \text{const}$. Then the continuity equation (Eq. 4.19) is

$$\frac{\partial \rho u}{\partial x} + \frac{1}{r}\frac{\partial \rho v r}{\partial r} \;=\; 0\;.$$ (20.18)

In the x-momentum equation (Eq. 4.20), the derivative of τ_{xx} is smaller in the thin layer approximation than first term in the derivative of $\tau_{rx} = \mu(\partial u/\partial r + \partial v/\partial x)$. Thus, written in conservation form which is convenient for integrating, the x-momentum equation is

$$\frac{\partial \rho u^2}{\partial x} + \frac{1}{r}\frac{\partial \rho u v r}{\partial r} \;=\; \frac{1}{r}\frac{\partial r\tau_{rx}}{\partial r}\;,$$ (20.19)

where

$$\tau_{rx} \;=\; \mu\frac{\partial u}{\partial r}\;.$$ (20.20)

April 23, 2001

20.1.1 Integral relations

To get the total x-momentum flux we multiply the momentum equation by $2\pi r\, dr$ and integrate with respect to r from $r = 0$ to $r = \delta$ (Fig. 55),

$$\int_0^{\delta(x)} \frac{\partial \rho u^2}{\partial x} 2\pi r\, dr + \int_0^{\delta(x)} \frac{\partial \rho uvr}{\partial r} 2\pi\, dr \; = \; \int_0^{\delta(x)} \frac{\partial r\tau}{\partial r} 2\pi\, dr \;. \tag{20.21}$$

The x-derivative can be taken outside, in accordance with the rules for partial differentiation of an integral, and the r integrations can be carried out,

$$\frac{d}{dx} \int_0^{\delta(x)} \rho u^2 2\pi r\, dr - (\rho u^2 2\pi r)_\delta \frac{d\delta}{dx} + 2\pi \rho uvr \Big|_0^\delta \; = \; 2\pi r\tau \Big|_0^\delta \;. \tag{20.22}$$

In order to evaluate the limits shown, the limit $\delta \to \infty$ is taken with the following requirements for how fast the velocity components must approach zero as $r \to \infty$,

$$\lim_{r\to\infty} \rho u^2 r \; = \; 0 \tag{20.23}$$

$$\lim_{r\to\infty} \rho uvr \; = \; 0 \tag{20.24}$$

$$\lim_{r\to\infty} r\tau \; = \; 0 \;. \tag{20.25}$$

Thus, the result is

$$\frac{dJ}{dx} \; = \; 0 \;; \qquad J \equiv 2\pi \int_0^{\delta(x)} \rho u^2 r\, dr \tag{20.26}$$

So, the total momentum flux in the jet remains constant, $\boxed{J = \text{const.}}$. Note that *all* fluid, including the ambient, is treated in this analysis; the jet extends to ∞. It does not exert a "drag" on the outer fluid, or vice versa; the momentum flux does not change.

However, there is a displacement effect; the jet entrains. This is shown by the continuity equation Eq. 20.18, Integrating as before,

$$\int_0^{\delta(x)} \frac{\partial \rho u}{\partial x} 2\pi r\, dr + \int_0^{\delta(x)} \frac{\partial \rho vr}{\partial r} 2\pi\, dr \; = \; 0 \tag{20.27}$$

$$\frac{d}{dx} \int_0^{\delta(x)} \rho u 2\pi r\, dr - (\rho u 2\pi r)_\delta \frac{d\delta}{dx} + 2\pi \rho vr \Big|_0^\delta \; = \; 0 \;. \tag{20.28}$$

In taking the limit $\delta \to \infty$, we now require

$$\lim_{r\to\infty} \rho ur \; = \; 0 \;, \tag{20.29}$$

but it is *not* possible to constrain ρvr at $r = \infty$, because the mass flux in the jet can not be constant if the momentum flux is. Thus,

$$\boxed{\frac{dm}{dx} \; = \; -2\pi(\rho vr)_\infty} \;; \qquad m \equiv 2\pi \int_0^{\delta(x)} \frac{\partial \rho u}{\partial x} r\, dr \tag{20.30}$$

The jet acts like a pump, pulling in fluid from far away, and continually increasing the mass flux.

20.1.2 Scaling

The x-dependence of the solution of the equations for a laminar jet can be deduced by scaling. Again, for the characteristic lengths and velocities we take (x, δ) and (U, V). From now on we consider incompressible flow with $\mu = \text{const.}$

From the thin-layer approximation,

$$\frac{V}{U} \sim \frac{\delta}{x}, \tag{20.31}$$

which is in conformity with the scaled continuity equation, Eq. 20.18. The r-momentum equation is Eq. 4.21 which scales as follows

$$\underbrace{u\frac{\partial v}{\partial x}}_{\frac{UV}{x}} + \underbrace{v\frac{\partial v}{\partial r}}_{\frac{V^2}{\delta}} = \nu \left[\underbrace{\frac{\partial}{\partial r}\left(\frac{2}{r}\frac{\partial rv}{\partial r}\right)}_{\frac{\nu V}{\delta^2}} + \underbrace{\frac{\partial^2 u}{\partial x \partial r}}_{\frac{\nu U}{x\delta}} + \underbrace{\frac{\partial^2 v}{\partial x^2}}_{\frac{\nu V}{x^2}} \right]. \tag{20.32}$$

The first and third terms on the rhs are of the same size, while the last term is smaller in the thin-layer approximation. Equating the second term on the lhs with the first on the rhs gives

$$\boxed{\frac{V\delta}{\nu} \sim 1}, \tag{20.33}$$

while equating the first and third terms gives

$$\boxed{\frac{\delta}{x} \sim \frac{1}{Re_\delta} \ll 1}, \tag{20.34}$$

where $Re_\delta = U\delta/\nu$. From Eq. 20.26

$$\boxed{\frac{J}{\rho} \sim U^2\delta^2}, \tag{20.35}$$

so, combining this result and Eq. 20.34 gives

$$\boxed{\begin{aligned} \delta &\sim \frac{\nu x}{\sqrt{J/\rho}} \\ U &\sim \frac{J/\rho}{\nu x} \\ V &\sim \frac{\sqrt{J/\rho}}{x} \\ \delta V &\sim \nu \end{aligned}} \tag{20.36}$$

The jet grows linearly with distance (in contrast to what Fig. 55 showed!), the axial velocity decreases as x^{-1}, the transverse velocity is independent of ν, and the rate of *mass* entrainment (the right hand side of Eq. 20.30) is simply proportional to μ.

April 23, 2001

20.1.3   Similarity.

Solutions to the equations of motion can be obtained by assuming a similarity form,

$$\frac{u}{U(x)} \;=\; F(\eta) \; ; \qquad \eta = \frac{r}{\delta(x)} \; . \tag{20.37}$$

U is now the maximum velocity (on the centerline). Similarity, as expressed in the above formula, is possible, when there is no characteristic length from the geometry of the problem, for example the orifice diameter. Therefore, the problem as expressed here is for a point source jet in a plane wall (point source of momentum). It is equivalent to a point force applied to the fluid. Put in other terms, the similarity solution is valid far downstream of the orifice. This reduces the equations to linear o.d.e.'s, which can solved analytically, as described by Schlichting (1955). A stream function is defined by

$$\psi \;=\; \nu x\, F(\eta) \; , \tag{20.38}$$

resulting after an integration in an o.d.e. of the form

$$\eta F'' + (F-1)F' \;=\; 0 \; , \tag{20.39}$$

which has the solution

$$F \;=\; \frac{\eta^2}{1 + \frac{1}{4}\eta^2} \; . \tag{20.40}$$

The streamlines $\psi = $ const are shown in Fig. 56. As a measure of the thickness of the jet the dashed lines trace approximately the points of closest approach of the streamlines to the axis of symmetry. Inside the dashed lines the streamlines diverge slightly as the jet grows.   The results for the parameters discussed

x
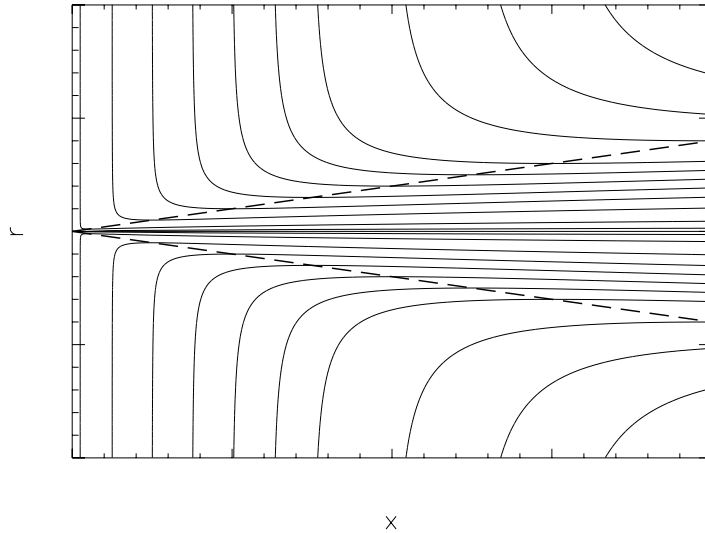
Figure 56. Streamlines of a round laminar jet

above are

$$\delta = \sqrt{\frac{16\pi}{3}} \frac{\nu x}{\sqrt{J/\rho}}$$

$$U = \frac{3}{8\pi} \frac{J/\rho}{\nu x}$$

$$m = 8\pi \, \mu x \qquad (20.41)$$

$$\frac{dm}{dx} = 8\pi \, \mu$$

$$(vr)_\infty = -4 \, \nu$$

The last of Eqs. 20.41 is proportional the volume entrainment rate. In fact, the pumping action of the jet is

$$\frac{d\dot{V}}{dx} = 8\pi \, \nu \, , \qquad (20.42)$$

independent of how large or small J is. This equation explains the extreme effectiveness of diffusion pumps for vacuum, which are nothing other than jets of low-vapor-pressure oil vapor. At extremely low pressure (low ρ), the volume rate is huge.

20.1.4 Point source of momentum

The above solution can be compared with another one for a point source of momentum in an infinite fluid (no wall) described by Batchelor (1973). In this case, the flow is an *exact* solution of the Navier-Stokes equations, and does not rely on the thin-layer approximation. Thus, in this flow the pressure varies through the jet. In spherical coordinates the stream function is written

$$\psi = r\nu \, f(\xi) \, , \qquad (20.43)$$

where $\xi = \cos\phi$, and after an integration the resulting o.d.e. is

$$f^2 - 2(1 - \xi^2)f' - 4\xi f = 0 \, . \qquad (20.44)$$

The solution is

$$f(\xi) = \frac{2(1 - \xi^2)}{1 + c - \xi} \, , \qquad (20.45)$$

where c is related to the momentum of the jet or the force applied to the fluid. The force F applied by the singularity at the origin to fluid contained in any sphere surrounding the origin is given by the difference between the momentum flux out of the sphere and stresses acting on the sphere. It turns out to be given solely in terms of c, or, equivalently, the spreading angle of the jet ϕ_0, defined as the locus of points of closest approach of the streamlines to the axis of symmetry. They are related by

$$\cos\phi_0 = \frac{1}{1 + c} \, . \qquad (20.46)$$

The force is given by

$$\frac{F}{2\pi\rho\nu^2} = \frac{32}{3} \frac{\cos\phi_0}{\sin^2\phi_0} + \frac{4}{\cos^2\phi_0} \ln\left(\frac{1 - \cos\phi_0}{1 + \cos\phi_0}\right) + \frac{8}{\cos\phi_0} \, . \qquad (20.47)$$

The streamlines are shown in Fig. 57, and the jet edge is indicated by dashed lines drawn at the angle ϕ_0.

159
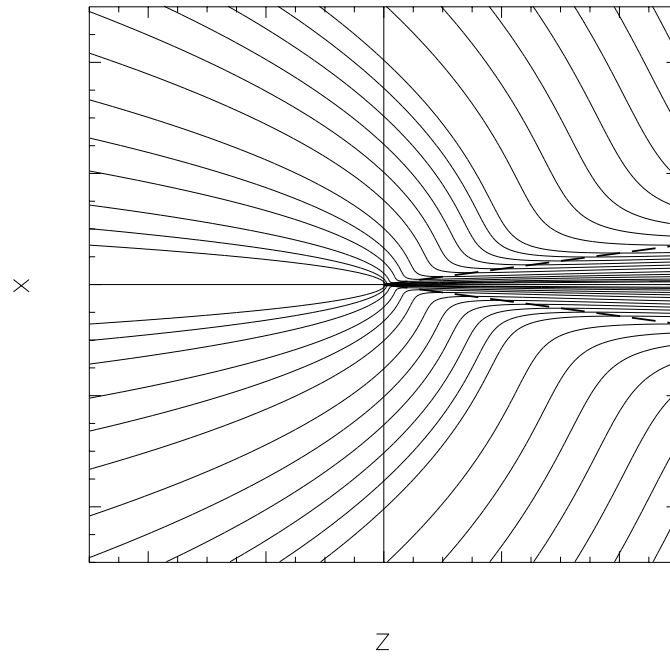
Figure 57. Streamlines of a point source of momentum

20.2   Plane Laminar Wake

The wake of a body is similarly caused by the force applied by the body on the fluid, in this case the drag D. This implies that drag can be measured by measuring the velocity profile of the wake, and *vice versa*, the wake profile depends on the drag. Fig. 58 shows a control volume for which surfaces 1–3 are far from the body. the fourth plane is a plane of symmetry, so there is no flux across it. Its (large) height is
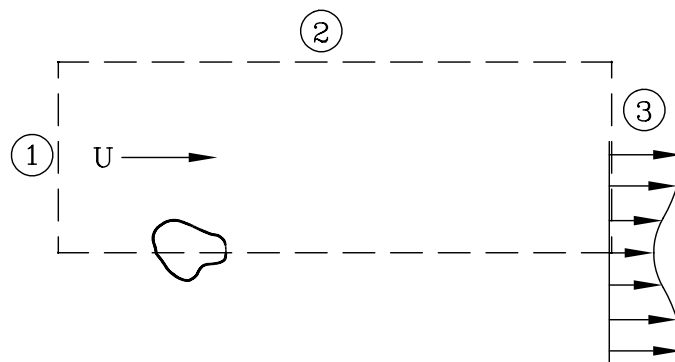
Figure 58. Control volume for the laminar wake

h. Far away from the body the departure u' of the velocity from U is small,

$$u' \; = \; U - u \; \ll \; U \; . \tag{20.48}$$

20.2.1 Drag.

There is a mass loss out of ② given by the difference between the fluxes through ① and ③,

$$\underbrace{\text{Mass Lost}}_{2} \;=\; \underbrace{\int_0^h \rho U \, dy}_{1} - \underbrace{\int_0^h \rho(U - u') \, dy}_{3} \tag{20.49}$$

$$=\; \underbrace{\int_0^h \rho u' \, dy}_{3} \;. \tag{20.50}$$

This mass flux carries its momentum ρU out ②. That momentum loss must balance the fluxes through the vertical surfaces, and half of the drag, since we are considering only the top half plane,

$$\frac{D}{2} \;=\; \underbrace{\int_0^h \rho U^2 \, dy}_{1} - \underbrace{\int_0^h \rho U u' \, dy}_{2} - \underbrace{\int_0^h \rho(U - u')^2 \, dy}_{3} \tag{20.51}$$

$$=\; U \underbrace{\int_0^h \rho u' \, dy}_{3} \;. \tag{20.52}$$

Taking the limit $h \to \infty$, and accounting for both half planes,

$$\boxed{D \;=\; U \int_{-\infty}^{\infty} \rho u' \, dy \;.} \tag{20.53}$$

This result holds for compressible fluids providing that the assumption of uniform flow at the boundaries (no shock waves) is satisfied. With multiplication by the appropriate $(2\pi r)$'s it holds for axisymmetric flow also.

20.2.2 Similarity.

From now on we consider plane incompressible flow. The x-momentum equation is written under the thin-layer assumption for ③, where it is assumed that the free-stream fluid is uniform ($p_\infty = \text{const.}$),

$$u\frac{\partial u}{\partial x} + v\frac{\partial u}{\partial y} \;=\; \nu\frac{\partial^2 u}{\partial y^2} \;. \tag{20.54}$$

Far downstream we take $u = U + u'$, where the velocity defect is small, $u' \ll U$, to give

$$U\frac{\partial u'}{\partial x} \;=\; \nu\frac{\partial^2 u'}{\partial y^2} \;. \tag{20.55}$$

Similarity in the form

$$u' \;=\; U\frac{f(\eta)}{\delta(x)} \;; \qquad \eta \;=\; \frac{y}{\delta} \;, \tag{20.56}$$

is assumed, where δ is the viscous length scale

$$\delta \;=\; \sqrt{\frac{\nu x}{U}} \tag{20.57}$$

and f has the dimensions of length. The scale of the body doesn't enter because only the far wake is being considered, where the body looks like a point. The unusual multiplicative factor $1/\delta$ in Eq. 20.56 is required to make the drag independent of x: From Eqs. 20.53 and 20.56,

$$D = \rho U^2 \int_{-\infty}^{\infty} f(\eta) \, d\eta \,, \tag{20.58}$$

which, as required, is constant. The derivatives of u' in Eq. 20.55 are obtained from the similarity form Eq. 20.56 as

$$\frac{\partial u'}{\partial x} = U \left(f \frac{d1/\delta}{dx} + \frac{1}{\delta} \frac{\partial f}{\partial x} \right) \,, \tag{20.59}$$

where

$$\frac{d1/\delta}{dx} = -\frac{1}{2\delta x} \tag{20.60}$$

$$\frac{\partial f}{\partial x} = -\frac{1}{2} \frac{\eta}{x} \frac{\partial f}{\partial \eta} \,, \tag{20.61}$$

so

$$U \frac{\partial u'}{\partial x} = -\frac{U^2}{2\delta x} (f + \eta f') \tag{20.62}$$

$$\nu \frac{\partial^2 u}{\partial y^2} = \frac{U\nu}{\delta} \frac{f''}{\delta^2} \,. \tag{20.63}$$

Combining and canceling gives the o.d.e.

$$f'' + \frac{\eta}{2} f' + \frac{f}{2} = 0 \,, \tag{20.64}$$

which can be integrated twice to give

$$f = K e^{-\frac{\eta^2}{2}} \,. \tag{20.65}$$

Now the integral in Eq. 20.58 can be evaluated to give

$$K = \frac{D}{2\sqrt{\pi} \rho U^2} = \frac{L}{4\sqrt{\pi}} C_D \,, \tag{20.66}$$

where now we have introduced the length scale L of the body to define the drag coefficient,

$$C_D \equiv \frac{D}{\frac{1}{2} \rho U^2 L} \,. \tag{20.67}$$

Finally, written out in terms of (x, y), the perturbation velocity is

$$\boxed{\frac{u'}{U} = \frac{C_D}{4\sqrt{\pi}} \sqrt{Re_L} \sqrt{\frac{L}{x}} \, e^{-\frac{y^2 U}{4\nu x}} \,.} \tag{20.68}$$
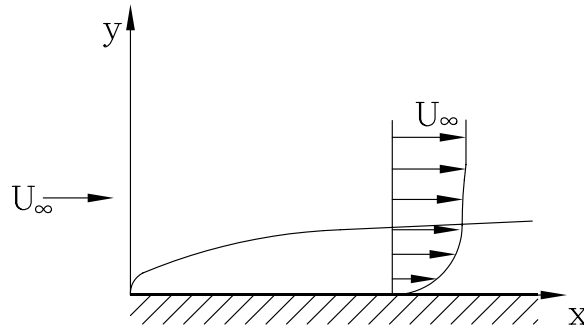
Figure 59. Schematic diagram of a flat plate boundary layer
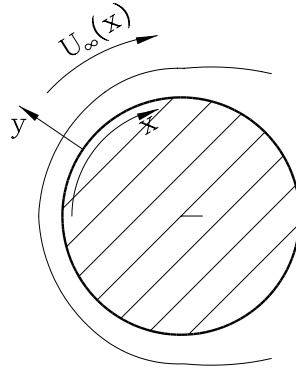
Figure 60. Thin boundary layer on a curved body

20.3 Boundary Layers

We now consider thin layers adjacent to bodies within which the effects of viscosity are confined, called boundary layers. The simplest case is the flat plate boundary layer (see Fig. 59).   For a thin flat plate, the flow far away is uniform, so $p_\infty = $ const. For a curved body, such as a cylinder or a sphere (Fig. 60), in general the pressure outside the boundary layer varies.   The flow there is inviscid, and to first order is parallel, so the x-momentum equation is, in the present notation,

$$\boxed{\frac{dp_\infty}{dx} \;=\; -\rho_\infty U \frac{dU}{dx} \,.}$$

(20.69)

The external pressure and velocity fields are related.

20.3.1 Integral relations

First we consider some integral properties, in particular, the behavior of the boundary-layer thickness. These analyses can be carried out for a general compressible fluid and an arbitrarily shaped body, but we limit consideration to steady flow.

Mass Thickness   (Displacement Thickness)
Integrating the continuity equation Eq. 4.4 from $y = 0$ to δ gives,

$$\rho_\delta v_\delta \;=\; -\int_0^\delta \frac{\partial \rho u}{\partial x} \, dy \,.$$

(20.70)

April 23, 2001

Add and subtract the x derivative of $\rho_\infty U$ to the integrand on the rhs,

$$\rho_\delta v_\delta \ = \ \int_0^\delta \frac{\partial(\rho_\infty U - \rho u)}{\partial x}\, dy - \int_0^\delta \frac{d\,\rho_\infty U}{dx}\, dy \ . \tag{20.71}$$

The x-derivative can be taken outside of the first term with no contribution from the derivative of the upper limit, because it has just been arranged that the integrand be zero at the upper limit as $\delta \to \infty$. The derivative in the second term on the right is not a function of y, so it integrates immediately,

$$\rho_\delta v_\delta \ = \ \frac{d\rho_\infty U \delta^*}{dx} - \delta \frac{d\,\rho_\infty U}{dx} \ , \tag{20.72}$$

where, taking the limit,

$$\boxed{\delta^* \ = \ \int_0^\infty \left(1 - \frac{\rho u}{\rho_\infty U}\right)\, dy \ .} \tag{20.73}$$

Now, far from the body, the fact that v_∞ is not zero (the "displacement effect") is expressed in the continuity equation,

$$\frac{d\,\rho_\infty U}{dx} \ = \ -\left(\frac{\partial \rho v}{\partial y}\right)_\infty \ . \tag{20.74}$$

This allows us to simplify Eq. 20.72 by "extrapolating" $\rho_\delta v_\delta$ to the wall,

$$\rho_\delta v_\delta \ \equiv \ \rho_0 v_0 + \delta \left(\frac{\partial \rho v}{\partial y}\right)_\infty \ . \tag{20.75}$$

This, together with Eq. 20.74, transforms Eq. 20.72 to

$$\boxed{\rho_0 v_0 \ = \ \frac{d\rho_\infty U \delta^*}{dx} \ .} \tag{20.76}$$

For the flat plate, $dU/dx = 0$, this becomes

$$\boxed{v_\infty \ = \ U\, \frac{d\delta^*}{dx} \ .} \tag{20.77}$$

The growth of the displacement thickness measures the velocity normal to the body induced by the presence of the boundary layer. The only effect of a thin viscous layer on the outer flow is a *displacement effect.* The effect of viscosity is to slightly displace the fluid outward from the body. Beyond that, there is no friction or heating exerted on the outer flow; as we shall see, only the fluid in the boundary layer feels the effects of friction and heating.

Momentum Thickness
The integrated momentum equation yields a connection between the velocity profile and wall friction in boundary layers. In Eq. 20.8, written in conservation form, U is subtracted and added on the l.h.s., as follows

$$\frac{\partial \rho u(u - U)}{\partial x} + \frac{\partial \rho v(u - U)}{\partial y} + \rho u \frac{dU}{dx} \ = \ \rho_\infty U \frac{dU}{dx} + \frac{\partial \tau}{\partial y} \ . \tag{20.78}$$

Integrating and taking the x-derivative out, as with the continuity equation, gives

$$\frac{d}{dx} \int_0^\delta \rho u(u - U)\, dy + \frac{dU}{dx} \int_0^\delta (\rho u - \rho_\infty U)\, dy \ = \ -\tau_w \ . \tag{20.79}$$

April 23, 2001

Thus, taking the limit $\delta \to \infty$,

$$\frac{d\rho_\infty U^2 \theta}{dx} + \rho_\infty U \frac{dU}{dx} \delta^* = \tau_w , \tag{20.80}$$

where the momentum thickness θ is

$$\theta = \int_0^\infty \frac{\rho u}{\rho_\infty U} \left(1 - \frac{u}{U} \right) dy . \tag{20.81}$$

Nondimensionalizing Eq. 20.80 by dividing through by $\rho_\infty U^2$, and differentiating out the first term, gives

$$\frac{C_f}{2} = \frac{d\theta}{dx} + \frac{\theta}{U} \frac{dU}{dx} \left(2 + \frac{\delta^*}{\theta} \right) . \tag{20.82}$$

$H = \delta^*/\theta$ is the "shape factor." The skin friction at any station x can be measured by measuring and integrating the velocity profile there. For a flat plate $(dU/dx = 0)$, the result is

$$\frac{C_f}{2} = \frac{d\theta}{dx} . \tag{20.83}$$

Mechanical Energy Thickness
Performing the now-familiar operations, this time on Eq. 20.9, leads one to subtract U^2 from the terms on the left-hand side,

$$\frac{\partial \rho u(u^2 - U^2)}{\partial x} + \frac{\partial \rho v(u^2 - U^2)}{\partial y} + \rho u \frac{dU^2}{dx} = \rho_\infty u \frac{dU^2}{dx} + 2u \frac{\partial \tau}{\partial y} . \tag{20.84}$$

Integrating, trading derivatives in the last term on the r.h.s. by partial differentiation, and taking the limit gives

$$\frac{d \, \rho_\infty U^3 \delta_{me}}{dx} = \rho_\infty U \frac{dU^2}{dx} \delta_\rho + \delta_\Phi , \tag{20.85}$$

where integrals have been represented by some pretty non-standard "thicknesses,"

$$\begin{aligned}
\delta_{me} &= \int_0^\infty \frac{\rho u}{\rho_\infty U} \left(1 - \frac{u^2}{U^2} \right) dy \\
\delta_\rho &= \int_0^\infty \left(\frac{\rho}{\rho_\infty} - 1 \right) \frac{u}{U} dy \\
\delta_\Phi &= \int_0^\infty \Phi \, dy .
\end{aligned} \tag{20.86}$$

For an incompressible fluid, $\delta_\rho = 0$, and δ_{me} measures the total dissipation in the boundary layer.

Energy Thickness
The energy thickness is obtained by integrating Eq. 20.17 in its general form (first equality). Subtracting h_{t_∞} from the terms on the l.h.s. and integrating gives

$$\int_0^\delta \frac{\partial \rho u(h_t - h_{t_\infty})}{\partial x} \, dy + \frac{dh_{t_\infty}}{dx} \int_0^\delta \rho u \, dy = -q_w . \tag{20.87}$$

165   April 23, 2001

The second term on the l.h.s. is troublesome because it doesn't integrate to a finite value in the limit $\delta \to \infty$. Therefore this analysis can only be carried out for $\boxed{dh_{t_\infty}/dx = 0}$. In that case,

$$\boxed{\frac{d\rho_\infty U h_{t_\infty} \delta_{h_t}}{dx} = q_w \,,}$$ (20.88)

where

$$\boxed{\delta_{h_t} = \int_0^\infty \frac{\rho u}{\rho_\infty} \left(1 - \frac{h_t}{h_{t_\infty}}\right) dy \,.}$$ (20.89)

20.3.2   Wall Fluxes

At the wall, the x-momentum equation gives

$$\begin{aligned}
\frac{dp_\infty}{dx} &= \left(\frac{\partial \tau}{\partial y}\right)_w \,; \qquad \tau = \mu \frac{\partial u}{\partial y} \\
&= \mu_w \left(\frac{\partial^2 u}{\partial y^2}\right)_w + \left(\frac{\partial \mu}{\partial y}\right)_w \left(\frac{\partial u}{\partial y}\right)_w \,.
\end{aligned}$$ (20.90)

Thus the curvature of the velocity profile near the wall is

$$\mu_w \left(\frac{\partial^2 u}{\partial y^2}\right)_w = \frac{dp_\infty}{dx} - \left(\frac{\partial u}{\partial y}\right)_w \left(\frac{\partial \mu}{\partial y}\right)_w \,.$$ (20.91)

It is affected by both the pressure gradient and any variation of the viscosity. For a flat plate and constant-viscosity fluid, the curvature is zero. Qualitative profiles are shown in Fig. 61.   Profiles with positive
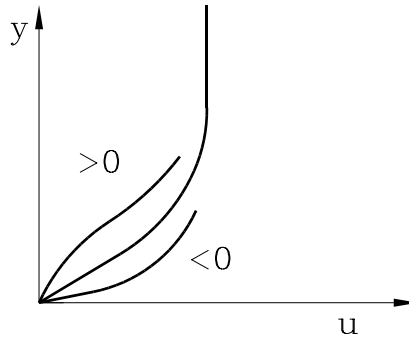
Figure 61. Schematic of velocity profiles for different pressure gradients

curvature have smaller shear, exhibit an inflection point, and tend to be less stable. The limit when the shear goes to zero is incipient separation (reverse velocities). So-called "adverse" pressure gradients ($dp_\infty/dx > 0$) induce positive curvature. Similarly, cooling the wall for a liquid or heating the wall for a gas is equivalent to an adverse pressure gradient. The subcases are indicated in the table.

Vorticity Flux
The diffusive flux of vorticity is

$$F_\omega = -\nu \frac{\partial \omega}{\partial y} \,,$$ (20.92)

which can be seen by writing the vorticity equation Eq. 3.17 in conservation form

$$\frac{D\omega}{Dt} + \frac{\partial F_\omega}{\partial y} = 0 \,.$$ (20.93)

April 23, 2001

$\partial^2 u/\partial y^2$	$F_{-\omega_w}$	τ_w	dp_∞/dx	$(\partial\mu/\partial y)_w$	Substance
> 0	< 0	low	> 0 (adverse)	< 0	liquid: cold wall gas: hot wall
< 0	> 0	high	< 0 (favorable)	> 0	liquid: hot wall gas: cold wall

In the thin layer approximation $\omega = -\partial u/\partial y$ and is negative in the boundary layer on the top of a body, so the flux of negative vorticity is

$$F_{-\omega} = -\nu\frac{\partial^2 u}{\partial y^2} \,. \tag{20.94}$$

Near the wall, using Eq. 20.91

$$F_{-\omega_w} = -\frac{1}{\rho_w}\frac{dp_\infty}{dx} + \frac{1}{\rho_w}\left(\frac{\partial u}{\partial y}\right)_w\left(\frac{\partial\mu}{\partial y}\right)_w \,. \tag{20.95}$$

The vorticity flux behaves just the same as the curvature, except for the sign, and has been included in the table above. For a flat plate, there is no flux of vorticity from the wall! It is all deposited at the leading edge, and simply diffuses as the flow progresses downstream. On the other hand, a favorable pressure gradient adds further negative vorticity to the fluid in the downstream flow, while an adverse gradient adds vorticity of the opposite sign.

20.3.3 Energy equation

Flows with Heat Transfer.

The thin-layer energy equation in the form of Eq. 20.17 describes flows with heat transfer. Written in conservation form for non-constant density and viscosity, it is

$$\frac{\partial\rho u h_t}{\partial x} + \frac{\partial\rho v h_t}{\partial y} = \frac{\partial}{\partial y}(u\tau - q) \tag{20.96}$$

$$= \frac{\partial}{\partial y}\mu\left(\frac{\partial u^2/2}{\partial y} + \frac{1}{Pr}\frac{\partial h}{\partial y}\right) \,. \tag{20.97}$$

For $Pr = 1$, which we henceforth assume, the equation simplifies to

$$\frac{\partial\rho u h_t}{\partial x} + \frac{\partial\rho v h_t}{\partial y} = \frac{\partial}{\partial y}\mu\frac{\partial h_t}{\partial y} \,. \tag{20.98}$$

Adiabatic Wall.   One immediate solution of Eq. 20.98 is $h_t = $ const. A consequence from Eq. 20.17 and the boundary conditions at $y = \infty$ is

$$\boxed{u\tau = q \,.} \tag{20.99}$$

Dissipation is balanced by heat flux everywhere through the boundary layer. This is the same result as in Couette flow, but that result was for any constant Pr, while here it is restricted to $Pr = 1$. For $Pr = 1$, by scaling the two layers have the same thicknes, $\delta_T = \delta$.

The solution obtained is

$$h + \frac{u^2}{2} = h_w = h_\infty + \frac{U^2}{2} \,. \tag{20.100}$$

April 23, 2001

Differentiating shows that

$$\left(\frac{\partial h}{\partial y}\right)_w = \left(c_p \frac{\partial T}{\partial y}\right)_w = 0 , \tag{20.101}$$

that is, $\boxed{q_w = 0}$. There is no heat flux to the wall. Hence the name "adiabatic wall." By definition, the wall temperature with $q_w = 0$ is the recovery temperature. $T_w = T_r$, with the corresponding enthalpy $h_w = h_r$.

Crocco Integral. Another simple solution is $h_t \sim u$, that is, $h_t = h_w + Cu$, where C is a constant of integration. Again differentiating at $y = 0$

$$\left(\mu \frac{\partial h}{\partial y}\right)_w = Pr \left(k \frac{\partial T}{\partial y}\right)_w = C \left(\mu \frac{\partial u}{\partial y}\right)_w , \tag{20.102}$$

so for $Pr = 1$

$$C = -\frac{q_w}{\tau_w} . \tag{20.103}$$

Thus, the *Crocco Integral*, valid for $Pr = 1$, is

$$\boxed{h + \frac{u^2}{2} = h_w - \frac{q_w}{\tau_w} u .} \tag{20.104}$$

It can be verified that this solution satisfies the energy equation by substituting it into Eq. 20.98. The resulting equation rfeduces to the momentum equation! Evaluating the Crocco Integral at $y = \infty$ provides another useful relation

$$\boxed{h_w = h_r + \frac{q_w}{\tau_w} U ,} \tag{20.105}$$

which then suggests rewriting the Crocco Integral as

$$\boxed{h + \frac{u^2}{2} = h_w + (h_r - h_w) \frac{u}{U} .} \tag{20.106}$$

Furthermore, it gives

$$q_w = (h_w - h_r) \frac{\tau_w}{U} , \tag{20.107}$$

which can be nondimensionalized with the Stanton number and the skin-friction coefficient to give

$$\boxed{St = \frac{C_f}{2} ; \qquad Pr = 1 .} \tag{20.108}$$

This Reynolds Analogy is the same as the one obtained for Couette flow (assuming $Pr = $ const) in the case $Pr = 1$.

An empirical relation for arbitrary Pr that is often used is (see below)

$$St = \frac{C_f}{2 \, Pr^{\frac{2}{3}}} . \tag{20.109}$$

April 23, 2001

20.3.4   Lighthill's formula

The fact that integrals are generally insensitive to slight inaccuracies of the integrand can often be exploited to derive powerful analytical approximations to general, complex nonlinear behavior[3]. The integral of the energy equation can be used to express the dependence of the wall heat flux on the parameters of the flow under rather general circumstances. The case considered here is that studied by Liepmann (JFM **3**, 357 1950);

i. $Pr = \mathrm{const} \neq 1$.

ii. $h_\infty = \mathrm{const}$, for simplicity

iii. Subsonic compressible flow; neglect dissipation, and $u^2/2$ in h_t.

iv. Variable $T_w(x)$, ρ, μ.

Then the enrgy equation simplifies to

$$\frac{\partial \rho u h}{\partial x} + \frac{\partial \rho v h}{\partial y} = -\frac{\partial q}{\partial y} \ . \tag{20.113}$$

Multiplying by dy and integrating over the boundary layer, having manipulated terms to avoid problems at the upper limit, and taking the limit $\delta \to \infty$ gives

$$\frac{d}{dx} \int_0^\infty \rho u (h - h_w) \, dy = q_w \tag{20.114}$$

$$\boxed{\begin{aligned} \frac{d}{dx}(\rho U h_\infty \theta_h) &= -q_w \\ \theta_h &= \int_0^\infty \frac{\rho u}{\rho_\infty U} \left(1 - \frac{h}{h_\infty}\right) dy \end{aligned}} \tag{20.115}$$

Now, the strategy is to consider the velocity profile in Eq. 20.114 to be a function of h, $u(h)$. Then the integrand becomes a universal function which integrates to a constant. $u(h)$ can be expressed with enough accuracy for substitution into the integral, which by its averaging property is insensitive to any small inaccuracies, by evaluating near the wall,

$$\begin{aligned} u &\doteq \left(\frac{\partial u}{\partial y}\right)_w y = \frac{\tau_w}{\mu_w} y \\ h - h_w &\doteq \left(\frac{\partial h}{\partial y}\right)_w y = -\frac{c_p q_w}{k_w} y \\ h - h_w &= -Pr \frac{q_w}{\tau_w} u \end{aligned} \tag{20.116}$$

---

[3]For example, *Weyl's method* can be used to estimate the Blasius function (Sec. 20.3.5). It approximates the exact first integral of the Blasius equation Eq. 20.143

$$f'' = f''(0) \exp\left(-\int_0^\eta f \, d\eta\right) \tag{20.110}$$

by substituting a Taylor series expansion of f at the wall, $f = f(0) + f'(0) + f''(0)\eta^2/2$, which after satisfying the wall boundary conditions yields

$$\int_0^\eta f \, d\eta = f''(0)\frac{\eta^3}{6} \tag{20.111}$$

with the result

$$f'(\eta) = f''(0) \int_0^\eta e^{-\frac{f''(0)\eta^3}{6}} \, d\eta \ . \tag{20.112}$$

April 23, 2001

This looks like the Crocco integral without u^2 terms, but *with* the Prandtl number. Substituting into (20.114) gives

$$-\frac{1}{Pr}\frac{d}{dx}\frac{\tau_w}{q_w}\int_0^\infty \rho(h-h_w)(h-h_\infty)\,dy = q_w \,, \tag{20.117}$$

which, after dividing by $dh/dy = -\frac{c_p}{k}q$, becomes

$$\frac{1}{Pr}\frac{d}{dx}\frac{\tau_w}{q_w}\int_{h_w}^{h_\infty}\frac{\rho\mu}{Pr}\frac{(h-h_w)(h-h_\infty)}{q}\,dh = q_w \,. \tag{20.118}$$

This rewritten into the following universal form

$$\frac{1}{Pr^2}\frac{d}{dx}\underbrace{\frac{\rho_w\mu_w\tau_w(h_\infty-h_w)^3}{q_w^2}}_{f(x)}\underbrace{\int_0^1\frac{\rho\mu}{\rho_w\mu_w}\frac{\frac{h-h_w}{h_\infty-h_w}\frac{h-h_w+h_w-h_\infty}{h_\infty-h_w}}{q/q_w}\,d\frac{h-h_w}{h_\infty-h_w}}_{\frac{1}{\alpha}} = q_w \,, \tag{20.119}$$

such that α integrates to a constant and the equation for f is

$$\frac{2}{3}\frac{df^{\frac{3}{2}}}{dx} = \frac{Pr^2}{\alpha}\sqrt{\rho_w\mu_w\tau_w(h_\infty-h_w)^3}\,. \tag{20.120}$$

The equation can easily be integrated. After re-expanding the result, we get Lighthill's formula for the heat flux

$$q_w = \left(\frac{2}{3}\right)^{\frac{1}{3}}\sqrt{\rho_w\mu_w\tau_w(h_\infty-h_w)^3}\frac{\alpha^{\frac{1}{3}}}{Pr^{\frac{2}{3}}}\left(\int_0^x\sqrt{\rho_w\mu_w\tau_w(h_\infty-h_w)^3}\,dx\right)^{-\frac{1}{3}}\,. \tag{20.121}$$

In terms of nondimensional coefficients, where St is now conveniently normalized with $(h_\infty-h_w)$,

$$St = \frac{q_w}{\rho_\infty U(h_\infty-h_w)} \tag{20.122}$$

it is

$$\boxed{St = \left(\frac{2}{3}\alpha\right)^{\frac{1}{3}}Pr^{-\frac{2}{3}}\sqrt{\frac{\rho_w\mu_w}{\rho_\infty\mu_\infty}\frac{C_f}{2}\Delta h}\left(\int_0^{Re_x}\sqrt{\frac{\rho_w\mu_w}{\rho_\infty\mu_\infty}\frac{C_f}{2}\Delta h^3}\,dRe_x\right)^{-\frac{1}{3}}\,.} \tag{20.123}$$

This is the Reynold's Analogy, showing explicitly the dependence on Pr, the $\rho\mu$ product, and the enthalpy difference $\Delta h = h_\infty - h_w$.

20.3.5 *Flat-plate boundary layer*

We now seek the solution of the equations of motion for $dp/dx = 0$. For simplicity we assume ρ, μ = const. ('Compressible' boundary layers can be treated by similar methods, and, in the case of $\mu \sim T$, exactly as here.) The flow is a plane flow so the equations to be solved are

$$\text{Mass}: \quad \frac{\partial u}{\partial x}+\frac{\partial v}{\partial y} = 0 \tag{20.124}$$

$$x-\text{momentum}: \quad u\frac{\partial u}{\partial x}+v\frac{\partial u}{\partial y} = \nu\frac{\partial^2 u}{\partial y^2}$$

$$\tag{20.125}$$

The continuity equation is satisfied by using the stream function,

$$u = \frac{\partial \psi}{\partial y} \tag{20.126}$$

$$v = -\frac{\partial \psi}{\partial x} \,. \tag{20.127}$$

The momentum equation becomes

$$\frac{\partial \psi}{\partial y} \frac{\partial^2 \psi}{\partial x \partial y} - \frac{\partial \psi}{\partial x} \frac{\partial^2 \psi}{\partial y^2} = \nu \frac{\partial^3 \psi}{\partial y^3} \,. \tag{20.128}$$

Similarity is assumed in the form

$$\psi \equiv U \delta(x) \, f(\eta) \tag{20.129}$$

$$\eta = \frac{y}{\delta(x)} \tag{20.130}$$

$$\delta(x) = \sqrt{\frac{2\nu x}{U}} \,. \tag{20.131}$$

Differentiating to get u gives

$$u = \frac{\partial \psi}{\partial y} = U f' \,, \tag{20.132}$$

or,

$$\boxed{f' = \frac{u}{U} \,; \quad \begin{array}{c} f'(0) = 0 \\[2mm] f'(\infty) = 1 \end{array}} \tag{20.133}$$

Other derivatives that are needed are

$$\frac{\partial}{\partial y} = \frac{1}{\delta} \frac{\partial}{\partial \eta} \tag{20.134}$$

$$\frac{d\delta}{dx} = \frac{1}{2} \frac{\delta}{x} \tag{20.135}$$

$$\frac{\partial \eta}{\partial x} = -\frac{\eta}{\delta} \frac{d\delta}{dx} = -\frac{\eta}{2x} \tag{20.136}$$

$$\frac{\partial \psi}{\partial x} = U \left(f \frac{d\delta}{dx} + \delta f' \frac{\partial \eta}{\partial x} \right) \tag{20.137}$$

$$= U \frac{\delta}{2x} (f - \eta f') \tag{20.138}$$

$$\frac{\partial^2 \psi}{\partial x \partial y} = -\frac{U}{2x} \eta f'' \tag{20.139}$$

$$\frac{\partial^2 \psi}{\partial y^2} = U \frac{f''}{\delta} \tag{20.140}$$

$$\frac{\partial^3 \psi}{\partial y^3} = U \frac{f'''}{\delta^2} \,. \tag{20.141}$$

Substituting in to Eq. 20.128 gives

$$-U f' \frac{U}{2x} \eta f'' - \frac{U\delta}{2x} (f - \eta f') U \frac{f''}{\delta} = \nu U f''' \frac{U}{2\nu x} \,. \tag{20.142}$$

After cancelations the *Blasius Equation* results

$$f''' + f f'' = 0 ; \qquad \begin{cases} f'(0) = 0 \\ f(0) = 0 \\ f'(\infty) = 1 \end{cases} \tag{20.143}$$

This nonlinear equation can be compared to the linear ones derived for the Rayleigh problem Eq. 19.23 and the wake Eq. 20.64, which have similarities. Note that $f'''(0) = 0$; the curvature of the velocity profile at the wall is zero, as we have already seen.

The system of equations and boundary conditions comprises a two-point boundary-value problem. It can be solved as an initial-value problem by the shooting method, which converges by trial and error on a value $f''(0)$ assuring the boundary condition at ∞. The result is $\boxed{f''(0) = 0.46952}$ and the solution, labeled $n = 0$, is shown in Fig. 62. The shear stress at the wall is given by
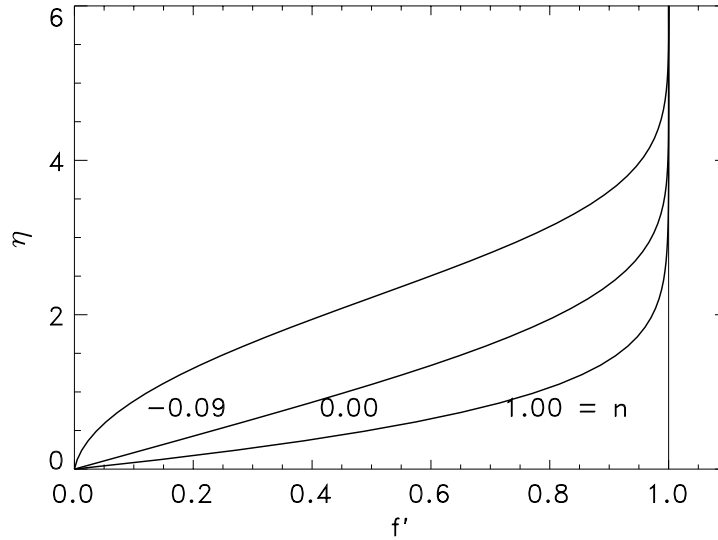
Figure 62. Velocity profiles for different pressure gradients

$$\tau_w = \mu \left(\frac{\partial u}{\partial y} \right)_w = \mu U \sqrt{\frac{U}{2\nu x}} \, f''(0) . \tag{20.144}$$

In terms of the skin friction coefficient, it is

$$C_f = \frac{\tau_w}{\frac{1}{2} \rho U^2} = \sqrt{\frac{2\nu}{Ux}} \, f''(0) \tag{20.145}$$

$$\boxed{C_f = \frac{0.66411}{\sqrt{Re_x}}} . \tag{20.146}$$

20.3.6   Boundary Layers on Curved Bodies

The x-momentum boundary-layer equation for a general body is

$$u\frac{\partial u}{\partial x} + v\frac{\partial u}{\partial y} = U\frac{dU}{dx} + \nu\frac{\partial^2 u}{\partial y^2} \; . \tag{20.147}$$

In terms of the stream function the momentum equation is

$$\frac{\partial \psi}{\partial y}\frac{\partial^2 \psi}{\partial x \partial y} - \frac{\partial \psi}{\partial x}\frac{\partial^2 \psi}{\partial y^2} = U\frac{dU}{dx} + \nu\frac{\partial^3 \psi}{\partial y^3} \tag{20.148}$$

In order to calculate such a boundary layer it is first necessary to solve the outer potential flow and determine the velocity history $U(x)$ at the surface. Simple plane flows can be solved by complex variable mapping techniques. Otherwise, CFD numerical solution methods are used. In incompressible flow a stagnation point gives, $U \sim x$. Incompressible flow over an infinite wedge of half angle $\frac{n}{n+1}\pi$ gives $U \sim x^n$.

It turns out that the power-law behavior $U \sim x^n$ admits similarity of the form,

$$\psi = U(x)\delta(x)\,f(\eta) \tag{20.149}$$

$$\eta = \frac{y}{\delta(x)} \tag{20.150}$$

$$\delta(x) = \sqrt{\frac{2}{n+1}\frac{\nu x}{U(x)}} \tag{20.151}$$

$$U(x) = K\,x^n \tag{20.152}$$

Substituting into the momentum equation results in the following nonlinear ordinary differential equation for f:

$$f''' + ff'' + \frac{2n}{n+1}\left(1 - f'^2\right) = 0\;; \qquad \mathrm{Faulkner - Skan\ Equation} \tag{20.153}$$

Results:

$$\delta(x) \quad \sim \quad \sqrt{\frac{\nu x}{U(x)}} \sim x^{\frac{1-n}{2}} \tag{20.154}$$

$$C_f = \sqrt{\frac{2(n+1)}{Re_x}}\,f''(0) \sim x^{-\frac{n+1}{2}} \tag{20.155}$$

$$f'''(0) = -\frac{2n}{n+1} \tag{20.156}$$

$$n = -0.0904 \implies f''(0) = 0 \tag{20.157}$$

Velocity profiles for 3 different values of n are given in Fig. 62.

21 Turbulent boundary layers

We describe the effort that has been made over many decades to origanize a purely emprical science, the study of incompressible turbulent boundary layers. Experiments show that the velocity profile $u(y)$ has two regions, an inner and an outer. Fig. 63 shows the latest experimental data for the velocity profile of a pipe boundary layer measured to better than 5% accuracy over a very large range of Reynolds number in the same facility (Zagarola et al. 1997). Data upon which earlier interpretations and evaluation of
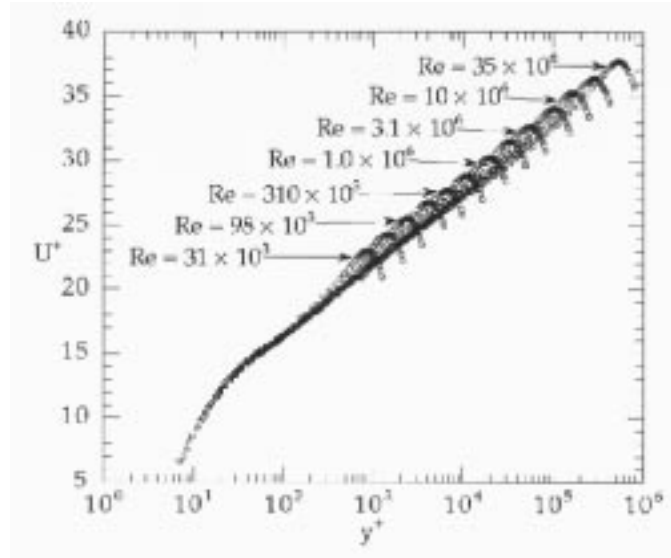
Figure 63. Data of Zagarola et al. 1997

the coefficients to be derived are shown in Fig. 64. The variables at a given streamwise station x that
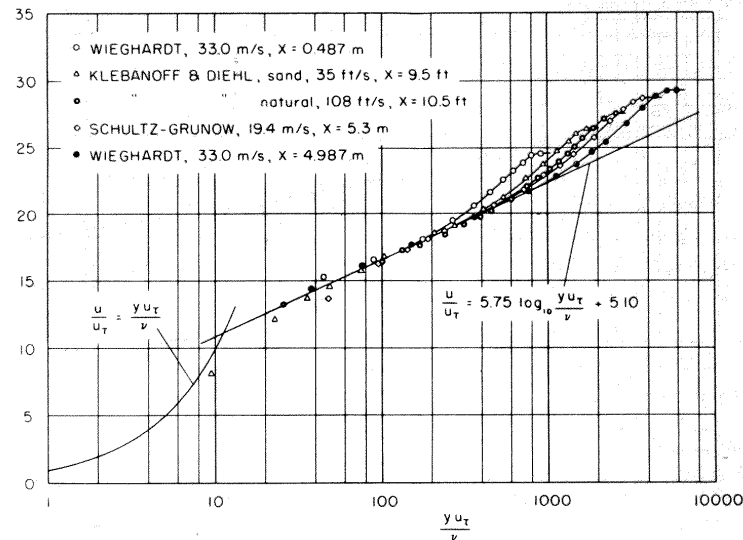
Figure 64. Compendium of early data on turbulent boundary layers

characterize the flow are:

1. the velocity profile $u(y)$

2. the free-stream velocity U
3. the boundary layer thickness $\delta(x)$
4. the wall stress $\tau_w(x)$
5. the fluid properties ρ, η, and $\nu = \eta/\rho$
6. the independent variable y.

In the inner region the velocity depends only on y the distance from the wall, the shear stress and the fluid properties,

$$u = \mathrm{fnc}(y, \tau_w, \rho, \nu) . \tag{21.1}$$

In order to nondimensionalize, the characteristic velocity in the near-wall region is the *friction velocity*,

$$u_\tau = \sqrt{\frac{\tau_w}{\rho}} , \tag{21.2}$$

and the corresponding length is the friction length ν/u_τ. Defining

$$u^+ = \frac{u}{u_\tau} ; \qquad y^+ = \frac{y u_\tau}{\nu} , \tag{21.3}$$

the nondimensional form of the inner behavior is

$$\boxed{u^+ = f(y^+) ; \qquad y^+ \longrightarrow 0 .} \tag{21.4}$$

This is the *Law of the Wall*, which is associated with the names Prandtl, von Karman and Nikuradse, who obtained the experimental data on which the classical form is based. Note that *at* the wall

$$u \doteq \frac{\tau_w}{\mu} y , \tag{21.5}$$

so

$$u^+ = y^+ ; \qquad y^+ \to 0 . \tag{21.6}$$

In the outer region the effect of the wall is to cause a velocity defect, as in a wake, which does not depend on the viscosity. The characteristic length there is the boundary layer thickness δ (R for a pipe) and we take again as the characteristic velocity u_τ ($\overline{u}$ for a pipe). Thus,

$$U - u = \mathrm{fnc}(y, \delta, u_\tau) . \tag{21.7}$$

The nondimensional distance from the wall is $\eta = y/\delta$, so

$$\boxed{\frac{U - u}{u_\tau} = F(\eta) ; \qquad \begin{array}{c} y \sim \delta \\ y \not\longrightarrow 0 \end{array}} \tag{21.8}$$

This is the *Defect Law*, and is due to von Karman.

The objective is to deduce a universal law for the velocity profile in a region of overlap where both Eqs. 21.4 and 21.8 are applicable. The derivation is due to Millikan (1938). For each region there is an appropriate Reynolds number based on the boundary layer thickness,

$$Re^+ = \frac{\delta u_\tau}{\nu} \tag{21.9}$$

$$Re = \frac{\delta U}{\nu} , \tag{21.10}$$

April 23, 2001

so y^+ and η are related by

$$y^+ \;=\; \frac{y u_\tau}{\nu} \;=\; Re^+ \eta \,. \tag{21.11}$$

In the overlap region, we expect

$$\frac{u}{u_\tau} \;=\; G\left(y^+,\eta\right) \;=\; G(Re^+\eta,\eta) \,. \tag{21.12}$$

At $y = \delta$ this becomes

$$\frac{U}{u_\tau} \;=\; G_1(Re^+) \,. \tag{21.13}$$

This is an implicit equation for $\tau_w(U,\delta,\rho,\nu)$, so it is the skin friction law for turbulent boundary layers. Note that $C_f = 2/G_1^2$. From Fig. 63 it can be seen that the overlap region is larger at higher Reynolds number. In the above-defined notation, the Law of the Wall and the Defect Law become

$$\frac{u}{u_\tau} \;=\; f(Re^+\,\eta)\,; \qquad \eta \longrightarrow 0 \tag{21.14}$$

$$\frac{u}{u_\tau} \;=\; G_1(Re^+) - F(\eta) \;\equiv\; h(Re^+,\eta)\,; \qquad \eta \nrightarrow 0 \,. \tag{21.15}$$

"Overlap" implies the following equality

$$f(Re^+\eta) \;=\; G_1(Re^+) - F(\eta) \,, \tag{21.16}$$

suggesting that in some sense the variables are separable. To make this precise, differentiate f in two different ways and use Eq. 21.16,

$$\frac{\partial f}{\partial Re^+} \;=\; f'\eta \;=\; G_1'$$

$$\frac{\partial f}{\partial \eta} \;=\; f'Re^+ \;=\; -F' \,. \tag{21.17}$$

The primes denote differentiation with respect to the arguments, which are different for each function. Solving for f' gives

$$\underbrace{G_1'\,Re^+}_{\text{fnc}(Re^+)} + \;=\; \underbrace{-F'\eta}_{\text{fnc}(\eta)} \;=\; \text{const} \;\equiv\; \frac{1}{\kappa} \,. \tag{21.18}$$

κ is the *Karman constant*. Integrating G_1 and F separately in Eq. 21.18 gives

$$G_1(Re^+) \;=\; \frac{1}{\kappa}\ln Re^+ + C \tag{21.19}$$

$$F(\eta) \;=\; -\frac{1}{\kappa}\ln\eta + D\,; \qquad \eta \nrightarrow 0 \,, \tag{21.20}$$

where C and D are constants of integration. These two equations are of completely different natures, because the first involves only constants at each x location, while the second deals with y variations. Because of that fact, C is strictly constant and the friction law Eq. 21.13 becomes

$$\boxed{\frac{U}{u_\tau} \;=\; \frac{1}{\kappa}\ln Re^+ + C \,.} \tag{21.21}$$

On the other hand, because of the limited range of the result (21.20), D may not in general be constant for all η, so set

$$D = -g^*(\eta) . \tag{21.22}$$

Now, to determine what f and h are, we try a simple sum which will be forced to behave properly at the wall and at the edge,

$$\frac{u}{u_\tau} = G(Re^+\eta, \eta) = f(Re^+\eta) + h(Re^+, \eta) . \tag{21.23}$$

That is, it is required that

$$\lim_{\eta \to 0} h(Re^+, \eta) = 0 . \tag{21.24}$$

From Eqs. 21.19 and 21.20 we have for the Defect Law (Eq. 21.15)

$$\frac{u}{u_\tau} = \frac{1}{\kappa} \ln Re^+ + C + \frac{1}{\kappa} \ln \eta + g^*(\eta) \tag{21.25}$$

$$= \frac{1}{\kappa} \ln Re^+\eta + C + g^*(\eta) . \tag{21.26}$$

Thus, the required behavior results if we separately take f and h to be

$$f(Re^+\eta) = \frac{1}{\kappa} \ln Re^+\eta + C \quad +g^*(0) \tag{21.27}$$

$$h(Re^+, \eta) = g^*(\eta) \quad -g^*(0) , \tag{21.28}$$

where the last terms in each equation have been added and subtracted to insure Eq. 21.24. In Eq. 21.27 we let $E = C + g^*(0)$. Simplifying the results, we get

$$
\begin{aligned}
\text{Overlap} \qquad & \frac{u}{u_\tau} & = & \quad \frac{1}{\kappa} \ln Re^+\eta + \phi(\eta) \\
\text{Wall} \qquad & u^+ & = & \quad \frac{1}{\kappa} \ln y^+ + \phi(0) \\
\text{Friction} \qquad & \frac{U}{u_\tau} & = & \quad \frac{1}{\kappa} \ln Re^+ + \phi(1) \\
\text{Overlap} \qquad & \frac{U-u}{u_\tau} & = & \quad -\frac{1}{\kappa} \ln \eta - \phi(\eta) + \phi(1) ,
\end{aligned}
\tag{21.29}
$$

where $\phi(\eta) = g^*(\eta) - g^*(0) + E$. Zagarola et al. (1997) fitted their data in the wall region to get

$$u^+ = \frac{1}{0.436} \ln y^+ + 6.13 . \tag{21.30}$$

Thus the Karman constant is $\boxed{\kappa = 0.436}$. In terms of the primitive variables, the results are

$$
\boxed{
\begin{aligned}
\text{Overlap} \qquad & \frac{u}{u_\tau} & = & \quad \frac{1}{\kappa} \ln\left(\frac{yu_\tau}{\nu}\right) + \phi\left(\frac{y}{\delta}\right) \\
\text{Wall} \qquad & \frac{u}{u_\tau} & = & \quad \frac{1}{\kappa} \ln\left(\frac{yu_\tau}{\nu}\right) + \phi(0) \\
\text{Friction} \qquad & \frac{U}{u_\tau} & = & \quad \frac{1}{\kappa} \ln\left(\frac{u_\tau \delta}{\nu}\right) + \phi(1) \\
\text{Overlap} \qquad & \frac{U-u}{u_\tau} & = & \quad -\frac{1}{\kappa} \ln\left(\frac{y}{\delta}\right) - \phi\left(\frac{y}{\delta}\right) + \phi(1) ,
\end{aligned}
}
\tag{21.31}
$$

The thickness δ is not well defined, so it is better to express, say, the Friction Law in terms of integral definitions of thickness, such as the momentum thickness Θ (Coles, 1954),

$$\Theta = \int_0^\delta \frac{u}{U}\left(1 - \frac{u}{U}\right) dy , \tag{21.32}$$

and the displacement thickness,

$$\delta^* = \int_o^\delta \left(1 - \frac{u}{U}\right) dy . \tag{21.33}$$

Then

$$\frac{U - u}{u_\tau} = -\frac{1}{\kappa} \ln \frac{R_\Theta}{c_1 - c_2(u_\tau/U)} + \phi(1) , \tag{21.34}$$

where R_Θ is the Reynolds number

$$R_\Theta = \frac{U\Theta}{\nu} , \tag{21.35}$$

and c_1 and c_2 are

$$
\begin{aligned}
c_1 &= \frac{U}{u_\tau}\frac{\delta^*}{\delta} &= \frac{U}{u_\tau}\int_0^1 \left(1 - \frac{u}{U}\right) d\eta &= \int_0^1 F(\eta)\, d\eta \\
c_2 &= \left(\frac{U}{u_\tau}\right)^2 \left(\frac{\delta^* - \Theta}{\delta}\right) = \left(\frac{U}{u_\tau}\right)^2 \int_0^1 \left(1 - \frac{u}{U}\right)^2 d\eta &= \int_0^1 F^2(\eta)\, d\eta
\end{aligned}
\tag{21.36}
$$

$c_{1,2}$, which are functions of the unknown u_τ, are evaluated from the first integral, where the experimental profile data are integrated using a consistent definition of the upper limit δ.

22 Low Reynolds Number Flow

22.1 Stokes flow – Creeping flow

Low Reynolds number, incompressible flow.
The Navier Stokes equation for incompressible flow (constant viscosity), Eq. 3.28, becomes in the limit of low Re,

$$\nabla p \;=\; \mu \, \nabla \underline{u}^2 \,, \tag{22.1}$$

with the continuity equation

$$\nabla \cdot \underline{u} \;=\; 0 \,. \tag{22.2}$$

Because

$$\nabla^2 \underline{u} \;=\; \nabla(\nabla \cdot \underline{u}) - \nabla \times (\nabla \times \underline{u}) \,, \tag{22.3}$$

the momentum equation is

$$\nabla p \;=\; -\mu \, \nabla \times \omega \,. \tag{22.4}$$

Note that these equations do not depend on the density of the fluid. Inertia, and therefore the density, play no role in Stokes flow. Thus, if L is a characteristics size of the body, and U is the free-stream velocity, by dimensional reasoning the drag must go as

$$D \;\propto\; \mu U L \,. \tag{22.5}$$

Because the Laplacian is interchangable with both the grad and curl operators, when the divergence of Eq. 22.1 is taken, there results

$$\nabla^2 p \;=\; 0 \,, \tag{22.6}$$

(having used $\nabla \cdot u = 0$), and when the curl is taken the result is

$$\nabla^2 \omega \;=\; 0 \tag{22.7}$$

(having used curl grad $= 0$).

The classical solution for Stokes flow, which we now outline, is for the motion of a sphere of radius R moving at constant velocity U in the z direction in a uniform fluid (see Fig. 65). Various derivations of the solution can be found in standard fluid mechanics texts, such as Batchelor (1973), Landau & Lifshitz (1959) and Lamb (1945). The vorticity generated by the motion of the sphere is azimuthal, in the form of vortex rings with axes falling on the z-axis, $\underline{\omega} = \omega_\theta$. In spherical symmetry the pressure and vorticity can be expressed in terms of spherical harmonics, and the only one with the required symmetry about the z axis is the dipole aligned with the z axis,

$$\frac{p - p_\infty}{\mu} \;=\; C \frac{U \cdot r}{r^3} \,. \tag{22.8}$$

The vorticity is an axial vector, and the only way this can be constructed from the two polar vectors available, $\underline{U}$ and $\underline{r}$, is by crossing them,

$$\underline{\omega} \;=\; C \frac{U \times r}{r^3} \,. \tag{22.9}$$

An axisymmetric velocity field in spherical coordinates (r, ϕ, θ) is expressed in terms of the Stokes Stream Function Eq. 16.27, while the vorticity, with the symmetry $\partial/\partial\theta = 0$, is

$$\omega_\theta \;=\; \frac{1}{r}\frac{\partial rv}{\partial r} - \frac{1}{r}\frac{\partial u}{\partial \phi} \,. \tag{22.10}$$
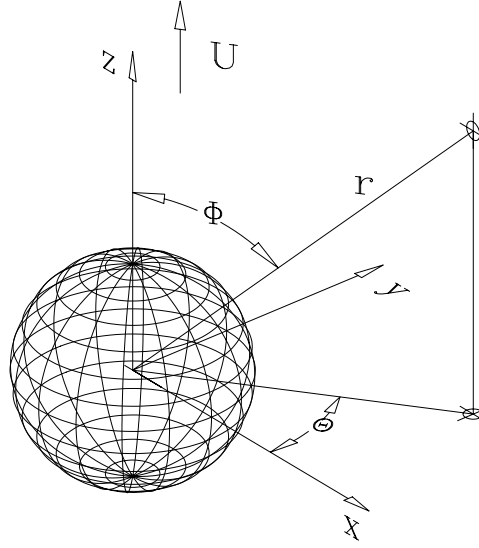
Figure 65. Schematic sketch of a sphere moving at velocity U in the z-direction, with the spherical polar co-ordinate system defined.

Eqs. 22.9 and 22.10 give

$$\frac{\partial^2 \psi}{\partial r^2} + \frac{\sin\phi}{r^2}\frac{\partial}{\partial\phi}\left(\frac{1}{\sin\phi}\frac{\partial\psi}{\partial\phi}\right) = C\frac{U\sin^2\phi}{r} \ . \tag{22.11}$$

In view of the rhs, trying the solution

$$\psi = U\sin^2\phi \, f(r) \tag{22.12}$$

gives

$$f'' - \frac{2f}{r^2} = -\frac{C}{r} \ , \tag{22.13}$$

the solution of which is

$$f(r) = \frac{C}{2}r + \frac{L}{r} + Mr^2 \ . \tag{22.14}$$

The normal-velocity boundary condition $u(R) = U\cos\phi$ requires $f(R) = R^2/2$. At $r \to \infty$, the velocity (stream function) is zero $\frac{f}{r^2} \to 0$. These two conditions determine L and M. The no-slip tangential-velocity condition leads to $C = \frac{3}{2}R$. This immediately gives the pressure

$$p - p_\infty = -\frac{3}{2}\mu R\frac{U\cdot r}{r^3} \ , \tag{22.15}$$

and the stream function is (Batchelor, 1973)

$$\boxed{\psi = \frac{UR^2\sin^2\phi}{4}\left(3\frac{r}{R} - \frac{R}{r}\right)} \tag{22.16}$$

Note that the stream function does not depend on μ. The streamlines at the instant the sphere is at the origin are shown in Fig. 66. At every instant before and after, the instantaneous streamlines are different, following the body as it moves. The pathlines differ from the instantaneous streamlines, and tend to close on themselves. The "flow" inside the sphere is of course fictitious, but interesting. The flow is symmetric fore and aft owing to the linearity. Thus, there is no "wake;" the vorticity diffuses equally in all directions.

April 23, 2001
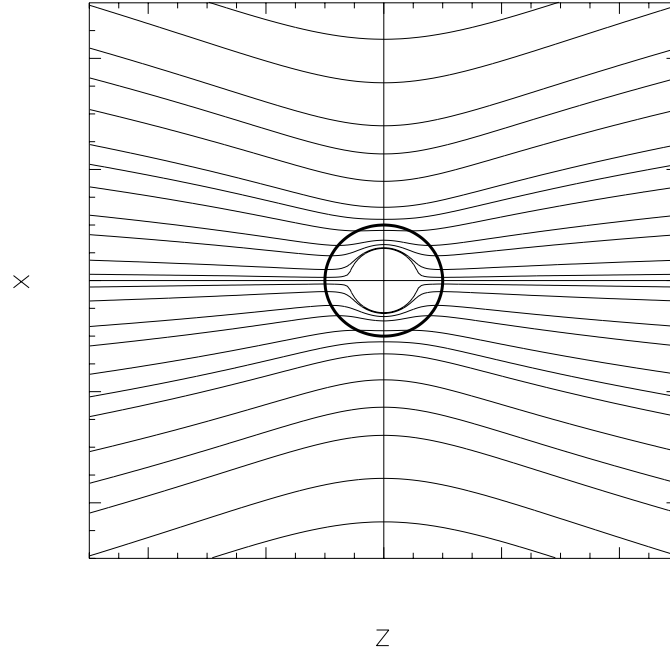
Figure 66. Streamlines for moving sphere in low Reynolds number (Stokes) flow.

The steady stream lines in the system in which the sphere is fixed and the velocity in the free stream is $U\underline{k}$ is shown in Fig. 67.

In the latter system the r and ϕ components of the velocity are (Landau & Lifshitz, 1959)

$$u = U\cos\phi\left(1 - \frac{3R}{2r} + \frac{R^3}{2r^3}\right) \tag{22.17}$$

$$v = -U\sin\phi\left(1 - \frac{3R}{4r} - \frac{R^3}{4r^3}\right). \tag{22.18}$$

In vector notation the velocity field is given by (Lagerstrom, 1964)

$$\underline{u} = U\underline{k} - \frac{3}{2}\frac{UR}{r}\underline{k} + \frac{UR}{4}\nabla\left(R^2\frac{\partial 1/r}{\partial z} + 3\frac{z}{r}\right), \tag{22.19}$$

where $\underline{k}$ is the unit vector in the z-direction. The first term is the free-stream velocity. The second is the only rotational contribution, and therefore is the only term which contributes to the viscous stress and the drag. It gives the $1/r$ term in Eq. 22.17 and twice the $1/r$ term in Eq. 22.18. The first and third terms are irrotational.

The drag is calculated by integrating the z-component of the normal pressure and viscous stresses and the tangential viscous forces,

$$D = \int(-p\cos\phi + \tau_{rr}\cos\phi - \tau_{r\phi}\sin\phi)\,dS. \tag{22.20}$$
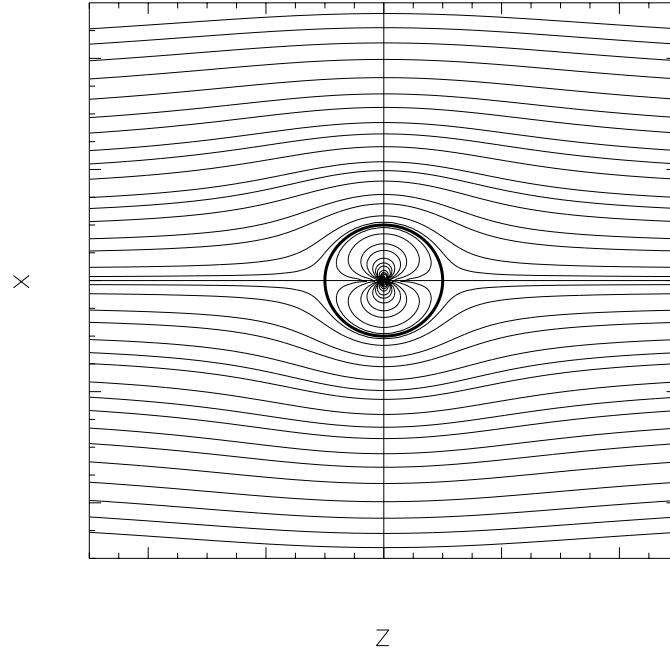
Figure 67. Streamlines for fixed sphere in low Reynolds number (Stokes) flow with freestream velocity U.

It turns out that the pressure integrates out, and the viscous stresses give a force in the z direction that is at every point the same,

$$\tau_w = \frac{3\mu U}{2R}\underline{k}\,, \tag{22.21}$$

so the total drag results from simply multiplying by the surface area,

$$\boxed{D = 6\pi\,R\,\mu\,U}\,, \tag{22.22}$$

or, defining $C_D = D/\frac{1}{2}\rho U^2 A$, with the frontal area $A = \pi R^2$,

$$\boxed{C_D = \frac{24}{Re}\,; \qquad Re = \frac{UD}{\nu}\,.} \tag{22.23}$$

A comparison of flow visualization of a sphere moving in a tube at $Re = 0.1$, and the stream function of the body-fixed system is given in Fig. 68. The streamlines near the body agree very well, but far from the body the constraint of the tube limits the curvature of the flow.

Stokes flow over a cylinder is impossible.   Repeating the above analysis in a cylindrical polar coordinate system appropriate for low Reynolds number flow over a cylinder, *i.e.*, assuming the form of the solution analogous to Eq. 22.12,

$$\psi = U\sin^2\phi\,f(r)\,, \tag{22.24}$$

gives, instead of Eq. 22.13

$$f'' + \frac{f'}{r} - \frac{f}{r^2} = -\frac{C}{r}\,, \tag{22.25}$$

April 23, 2001
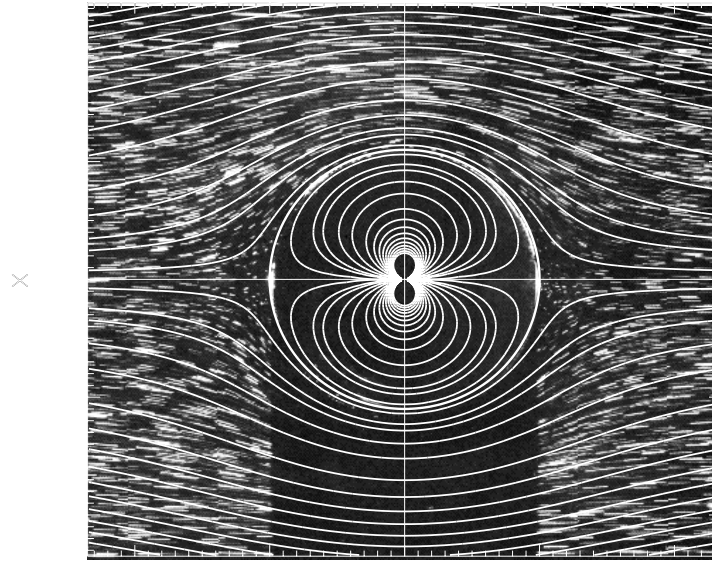
Figure 68. Calculated streamlines in Stokes flow overlaid on a streak photograph of a sphere in a tube, the latter from Van Dyke, 1982.

and, for the velocity field,

$$\underline{u} \;=\; \underline{U} + C\underline{U}\left(-\frac{1}{2}\ln\frac{r}{R} - \frac{1}{4} + \frac{R^2}{4r^2}\right) + C\underline{r}\frac{\underline{U}\cdot 2\underline{r}}{r^2}\left(1 - \frac{R^2}{r^2}\right)\;, \tag{22.26}$$

where the constant C would have to be evaluated from the boundary condition at $r \to \infty$. But this can't be carried out because of the logarithmic term. Thus, there is no solution for Stokes flow over a cylinder. Because the flow over a cylinder doesn't "escape" around the ends, as with a sphere, the very large extent of the perturbation induced by Stokes flow just becomes impossibly large for a cylinder.

Integration of the forces on the body gives the drag in terms of C,

$$D \;=\; 2\pi\mu U\,C\;. \tag{22.27}$$

Other bodies. The drag for bodies of other shapes has been calculated. For example, a disk aligned perpendicular, or parallel, to the direction of motion has drag

$$C_D \;=\; 16\,\mu\,U\,R \tag{22.28}$$

$$C_D \;=\; \frac{32}{3}\,\mu\,U\,R\;, \tag{22.29}$$

respectively. Thus, in creeping flow the drag does not depend much on the shape or orientation of the body.

Balance between inertial and viscous forces. In the coordinate system in which the body is stationary, the velocity far away from the origin can be approximated by the linearizing assumption

$$\underline{u} \;=\; U\underline{k} + \underline{u}'\;, \tag{22.30}$$

April 23, 2001

where $u' \ll U$. From the solution the order of magnitude of the velocity components is

$$u' \sim \frac{UR}{r} . \tag{22.31}$$

Thus in the solution the size of the inertial and vicous terms are

$$\rho \underline{u} \cdot \nabla \underline{u} \sim \rho \underline{U} \cdot \nabla \underline{u}' \sim \rho U^2 \frac{R}{r^2} \tag{22.32}$$

$$\mu \nabla^2 \underline{u}' \sim \mu \frac{UR}{r^3} , \tag{22.33}$$

and their ratio is

$$\frac{\text{Inertia}}{\text{Viscous}} \sim Re \frac{r}{R} . \tag{22.34}$$

This result says that in low Reynolds number flow the effect of the body is felt very far from the body, and, in fact, the solution is not uniformly valid over the entire domain. Thus, though the solution is good close to the body (in particular, the drag), far away it is erroneous. Corrections can be made as described later.

22.2   The Oseen equations

The Stokes equations are linear, and, as such, can be considered as linearizations of the Navier-Stokes equations about $\underline{u} = 0$. An improvement can be made for the behavior in the far field if, instead, the equations are linearized about the velocity $\underline{U}$. The resulting solution will not be as good near the body, but for low Re flow the intertial terms there will be negligible anyway. This approach also make it possible to obtain a solution for low Reynolds number flow over a cylinder, not possible in the Stokes approximation. In the system in which the sphere is moving, providing the motion is steady, Eq. 16.91 holds for the nonsteady inertial term, and the convective term is quadratic and smaller, the Oseen equations become

$$\boxed{-\rho \underline{U} \cdot \nabla \underline{u} = -\nabla p + \mu \nabla^2 \underline{u} .} \tag{22.35}$$

This equation is linear, and as yet no restrictions on Re have been made. However, a closed-form solution is not available, and only approximate solutions for small Re can be found, which is what was desired, anyway. Because of the linearization about the free-stream velocity, the solution should not be very good near the body where, in fact, in the body-fixed coordinate system the velocity must go to zero. However, for low Re it turns out that the solution there is almost as good as the Stokes solution. The stream function resulting from an analysis similar to that above for Stokes flow about a sphere is (Batchelor, 1973)

$$\psi = UR^2 \left\{ -\frac{R}{4r} \sin^2 \phi + \frac{3(1 - \cos \phi)}{Re} \left[1 - e^{-Re \frac{r}{4R}(1 + \cos \phi)} \right] \right\} , \tag{22.36}$$

where $Re = UD/\nu$. In this solution, the fore-and-aft symmetry of Stokes flow is lost, and the beginnings of a "wake" appear. The distortion of the instantaneous steamlines is shown in Fig. 69, in which a body is moving from right to left with velocity U. The instantaneous streamlines follow the body as it moves. Note that the fluid appears to be convecting through the body, apparently an artifact of the approximate nature of the solution near the body, where the convection isn't quite right. In Fig. 70, a uniform velocity U from the left has been added, which fixes the sphere. In both views the "wake" on the right is seen.

The problem of computing the flow over a cylinder can now be resolved by taking the Oseen solution for the cylinder, which is valid far away from the body, and requiring it to match with the Stokes solution

April 23, 2001
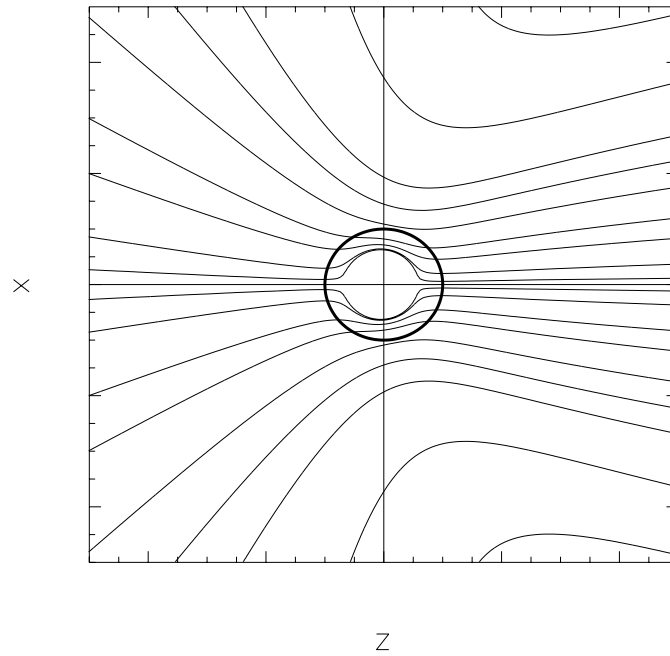
Figure 69. Oseen flow over a moving sphere.

Eq. 22.26 near the body. The result is that (Lamb, 1945)

$$C = \frac{2}{\frac{1}{2} - \gamma - \ln\left(\frac{Re}{8}\right)} \, , \tag{22.37}$$

where γ is Euler's constant $= 0.57722$, so (Batchelor, 1973)

$$\boxed{C_D = \frac{8\pi}{Re\ln\left(\frac{7.4}{Re}\right)}} \tag{22.38}$$

22.3 Drag at higher Reynolds numbers $-$ D $vs.$ Re.

Eq. 22.23 gives the drag for low Re, but that covers only a small part of the range of Re that is important for fluid mechanics applications. The remainder can only be treated by experimental measurement. Figure 71 gives the drag coefficient over a large range of Re, obtained from both theory and experiment (Lagerstrom, 1964, Fig. B,16b). The so-called "drag-crisis" at about $Re = 3 \times 10^5$ is a notable effect unpredictable by any theory, which has important applications in technology, such as baseball and cricket.

22.4 Lubrication theory

The objective of a mechanical bearing is to support a large load with minimal losses. To understand the mechanisms of lubrication theory we consider the simple linear geometry of a pad bearing (see Fig. 72).

High pressures are developed by the fundamentally important fact that the slot through which the lubricating fluid flows is not of unifom width, $h = h(x)$. We consider a long pad, $L \gg h$, inclined at a

April 23, 2001
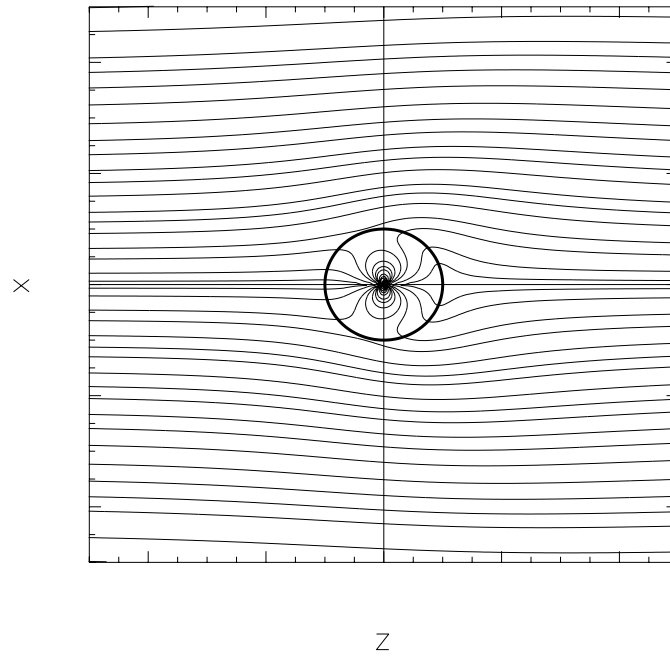
Figure 70. Oseen flow as seen in a body-fixed coordinate system.
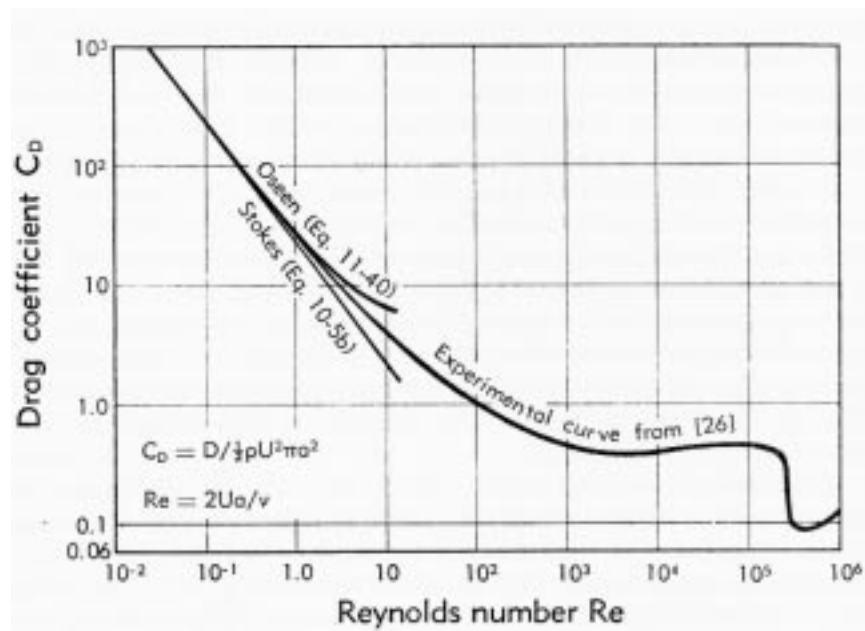
Figure 71. Sphere drag over eight orders of magnitude in Reynolds Number.

small angle $\alpha \ll 1$. The combination of a moving block plus a confined channel yields a superposition of
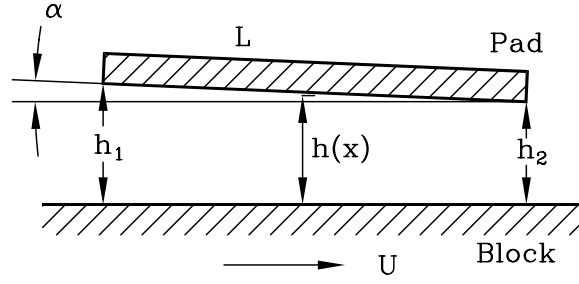
Figure 72. A pad bearing in plane geometry

Poiseuille and Couette flows,

$$u(x, y) = -\frac{1}{\mu}\left(-\frac{dp}{dx}\right)\frac{y(h-y)}{2} + U\frac{h-y}{h} \ . \tag{22.39}$$

This solution can be written in terms of the volume flux

$$Q = \int_0^h u \, dy = -\frac{dp}{dx}\frac{h^3}{12\mu} + \frac{Uh}{2} \ , \tag{22.40}$$

yielding for the pressure gradient,

$$\frac{dp}{dx}(x) = 6\mu\left(\frac{U}{h^2(x)} - \frac{2Q}{h^3(x)}\right) \ . \tag{22.41}$$

With

$$\alpha = -\frac{dh}{dx} \tag{22.42}$$

the pressure integrates to

$$p - p_1 = \int_{h_1}^{h_2}\frac{dp}{dx}\frac{dx}{dh} \, dh = \frac{6\mu}{\alpha}\left[U\left(\frac{1}{h} - \frac{1}{h_1}\right) + Q\left(\frac{1}{h^2} - \frac{1}{h_1^2}\right)\right] \ . \tag{22.43}$$

To evaluate the load-carrying pressure that is developed in the bearing, it is necessary to complete the flow loop. The flow connects over the top where the flow area is large, so there is little resistance, and $p_1 = p_2$. Using this in Eq. 22.43 evaluated at p_2 gives

$$Q = U\frac{h_1 h_2}{h_1 + h_2} \ . \tag{22.44}$$

Substituting for Q in Eq. 22.43 gives

$$\boxed{p - p_1 = \frac{6\mu U}{\alpha}\frac{(h_1 - h)(h - h_2)}{h^2(h_1 + h_2)}} \ . \tag{22.45}$$

As drawn above, $\boxed{h_1 > h > h_2, \text{ so } p > p_1}$. But $p_1 = p_2$, so there must be a maximum pressure. From Eqs. 22.41 and 22.44, it occurs at

$$h = \frac{2h_1 h_2}{h_1 + h_2} \ , \tag{22.46}$$

with the result

$$(p - p_1)_{max} = \frac{6\mu U}{\alpha} \frac{(h_1 - h_2)^2}{4h_1 h_2 (h_1 + h_2)} . \tag{22.47}$$

An optimal bearing design generates a large bearing pressure, so in general

$$\frac{\Delta h}{h_1} = \mathcal{O}(1) , \tag{22.48}$$

and

$$\alpha = \frac{\Delta h}{L} \sim \frac{h_1}{L} . \tag{22.49}$$

Thus

$$\Delta p_{max} \sim \frac{\mu U L}{h_1^2} . \tag{22.50}$$

An effective bearing runs with large μ, U and L, and small h_1. However, more important is its "efficiency," that is the bearing load versus the frictional force. The total normal force supported is

$$F_n = \int_{h_1}^{h_2} \frac{\Delta p}{\alpha} \, dh \sim \frac{\mu U L}{h_1^2} , \tag{22.51}$$

while the tangential forces are of order

$$F_t = \int_0^L \mu \frac{du}{dy} \, dx \sim \frac{\mu U L}{h_1} . \tag{22.52}$$

Therefore,

$$\frac{\text{Tangential}}{\text{Normal}} \sim h_1 , \tag{22.53}$$

so the relative frictional forces are reduced as the bearing gap is reduced. This explains why bearings must be machined very accurately to remove roughness and ensure that the surfaces can be very close without touching.

April 23, 2001

23 Turbulence

23.1 Reynolds Averaging

In this section we discuss the equations for incompressible turbulent shear flow, for simplicity, with a steady mean flow. In an attempt to get managable equations, the flow is decomposed into mean and fluctuating components

$$\underline{u} = \overline{\underline{u}} + \underline{u}' \,; \qquad \overline{\underline{u}'} = 0 \tag{23.1}$$

$$\overline{\left(\frac{\partial \underline{u}}{\partial x} \right)} = \frac{\partial \overline{\underline{u}}}{\partial x} \,, \tag{23.2}$$

etc. We use Cartesian tensor notation.

The continuity equation is

$$\frac{\partial(\overline{u_i} + u_i')}{\partial x_i} = 0 \,, \tag{23.3}$$

which, when averaged gives

$$\boxed{\frac{\partial \overline{u_i}}{\partial x_i} = 0} \quad \Longrightarrow \quad \boxed{\frac{\partial u_i'}{\partial x_i} = 0} \,. \tag{23.4}$$

The mean and fluctuating components are separately incompressible.

The momentum equation, in conservation form, is

$$\frac{\partial(\overline{u_i} + u_i')}{\partial t} + \frac{\partial(\overline{u_i} + u_i')(\overline{u_j} + u_j')}{\partial x_j} = -\frac{\partial \overline{(p + p')}}{\partial x_i} + \nu \frac{\partial^2(\overline{u_i} + u_i')}{\partial x_j{}^2} \,. \tag{23.5}$$

When averaged, the first term gives nothing, because the mean flow is steady. The second term is

$$\frac{\partial \overline{u_i}\,\overline{u_j}}{\partial x_j} + \frac{\partial \overline{u_i}u_j'}{\partial x_j} + \frac{\partial \overline{u_j}u_i'}{\partial x_j} + \frac{\partial \overline{u_i'u_j'}}{\partial x_j} \,. \tag{23.6}$$

When averaged, only the first and last terms contribute. Thus, the momentum equation becomes

$$\frac{\partial \overline{u_i}\,\overline{u_j}}{\partial x_j} + \frac{\partial \overline{u_i'u_j'}}{\partial x_j} = -\frac{1}{\rho}\frac{\partial \overline{p}}{\partial x_i} + \nu \frac{\partial^2 \overline{u_i}}{\partial x_j{}^2} \,. \tag{23.7}$$

A new term and new mechanism for momentum transport arises. When moved to the r.h.s., it becomes a stress, the *Reynolds stress*,

$$\overline{\tau_{ij}} = \overline{u_i'u_j'} \,. \tag{23.8}$$

Thus, using the averaged continuity equation,

$$\boxed{\overline{u_j}\frac{\partial \overline{u_i}}{\partial x_j} = -\frac{1}{\rho}\frac{\partial \overline{p}}{\partial x_i} - \frac{\partial \overline{u_i'u_j'}}{\partial x_j} + \nu \frac{\partial^2 \overline{u_i}}{\partial x_j{}^2}} \,. \tag{23.9}$$

$\overline{u_i'u_j'}$ is an unknown quantity involving the product of velocities. An equation for the first moment of velocity (the momentum) is expressed in in terms of an unknown second moment (velocity^2). It can now be seen that this procedure leads to an endless chain: Each equation, when averaged, will be in terms of unknown higher-order products. The only recourse is to at some stage make an assumption which closes the system (or to solve the full Navier-Stokes equations from the outset!).

April 23, 2001

A shear flow producing positive vorticity is expected to result in a positive correlation $\overline{u_i' u_j'}$, because fluctuation flux upward $v' > 0$ will carry momentum from high-velocity to low-velcocity regions, $u' > 0$. This is analogous to the way molecules with random thermal velocities convect momentum in shear flows by molecular diffusion. Splitting the 'viscous Bernoulli equation' (Eq. 3.30), in Cartesian tensor notation there results,

$$\frac{\partial \overline{u_i}}{\partial t} \;=\; -\frac{\partial}{\partial x_j}\left(\frac{p}{\rho} + \frac{u^2}{2} + \frac{\overline{u'^2}}{2}\right) + \epsilon_{ijk}\left(\overline{u_j}\,\overline{\omega_k} + \overline{u_j'\omega_k'}\right) + \nu\frac{\partial^2 \overline{u_i}}{\partial x_j^2} \;, \tag{23.10}$$

where ϵ_{ijk} is the permutation operator, so that

$$\epsilon_{ijk}\,\overline{u_j}\,\overline{\omega_k} \;=\; (\underline{u} \times \underline{\omega})_i \;. \tag{23.11}$$

The cross-product terms $\overline{u_j'\omega_k'}$ represent the cross-stream derivatives of the Reynolds stress. For example, in 2-D flow with 3-D turbulence, they are

$$\overline{v'\omega_z'} - \overline{w'\omega_y'} \;\dot{=}\; -\frac{\partial \overline{u'v'}}{\partial y} \;, \tag{23.12}$$

where the $\dot{=}$ means that we neglect normal stress (turbulent 'pressure') in favor of shear (Reynolds) stress. In 2D flow $\overline{v'\omega_z'}$ could be represented in terms of a mixing length and the gradient $\partial \overline{u}/\partial y$ (a 'mixing length theory of vorticity transfer', Tennekes & Lumley, p80), but $\overline{w'\omega_y'}$ would have to be represented by some out-of-plane gradient, which is impossible in 2D. By differentiating the rhs of Eq. 23.12, represented in terms of a mixing length, $u'\ell\partial\overline{u}/\partial y$, it can be seen that the ω_y' term must be associated with $\partial\ell/\partial y$, i.e., with a change of scale, or vortex stretching. This is called the 'vortex stretching force' (because the term is on the rhs of the momentum equation!) (Tennekes & Lumley, p. 80).

Splitting Eq. 2.57 gives the turbulent vorticity equation,

$$\overline{u_j}\frac{\partial \overline{\omega_i}}{\partial x_j} \;=\; -\overline{u_j'\frac{\partial \omega_i'}{\partial x_j}} + \frac{1}{2}\overline{\omega_j'\epsilon_{ij}'} + \frac{1}{2}\overline{\omega_j}\,\overline{\epsilon_{ij}} + \nu\frac{\partial^2 \overline{\omega_i}}{\partial x_j^2} \tag{23.13}$$

$$\;=\; -\frac{\partial \overline{u_j'\omega_i'}}{\partial x_j} + \frac{\partial \overline{\omega_j'u_i'}}{\partial x_j} + \frac{1}{2}\overline{\omega_j}\,\overline{\epsilon_{ij}} + \nu\frac{\partial^2 \overline{\omega_i}}{\partial x_j^2} \;, \tag{23.14}$$

where the second form follows because, since (div curl) $= 0$, the vorticity, both mean and fluctuating, is divergence free. The first term on the right is analogous to the Reynolds stress, and the second term is the gain of mean vorticity due to the stretching of fluctuating vorticity by fluctuating strain.

To study vorticity interactions, one needs equations equivalent to the mean and fluctuationg kinetic energy equations,

$$\overline{u_j}\frac{\partial \frac{1}{2}\overline{\omega_i}^2}{\partial x_j} \;=\; -\underbrace{\frac{\partial \overline{\omega_i}\,\overline{\omega_i'u_j'}}{\partial x_j}}_{\text{transport}} + \underbrace{\overline{u_j'\omega_i'}\frac{\partial \overline{\omega_i}}{\partial x_j}}_{\text{production}} + \underbrace{\overline{\omega_i}\,\overline{\omega_j\epsilon_{ij}}}_{\text{stretching}} + \underbrace{\overline{\omega_i}\,\overline{\omega_j'\epsilon_{ij}'}}_{\text{stretching}} \tag{23.15}$$

$$\;+\; \underbrace{\nu\frac{\partial^2 \frac{1}{2}\overline{\omega_i}^2}{\partial x_j^2}}_{\substack{\text{viscous}\\\text{transport}}} - \underbrace{\nu\left(\frac{\partial \overline{\omega_i}}{\partial x_j}\right)^2}_{\substack{\text{viscous}\\\text{dissipation}}} \;.$$

April 23, 2001

$$\overline{u_j}\frac{\partial\frac{1}{2}\overline{\omega_i'^2}}{\partial x_j} \;=\; -\; \underbrace{\overline{u_j'\omega_i'}\frac{\partial\overline{\omega_i}}{\partial x_j}}_{\text{production}} \;+\; -\frac{1}{2}\; \underbrace{\frac{\partial\overline{u_j'\omega_i'^2}}{\partial x_j}}_{\text{transport}} \;+\; \underbrace{\overline{\omega_i'\omega_j'\epsilon_{ij}'}}_{\text{stretching}} \;+\; \underbrace{\overline{\omega_i'\omega_j'}\,\overline{\epsilon_{ij}}}_{\text{stretching}} \;+\; \underbrace{\overline{\omega_j}\,\overline{\omega_i'\epsilon_{ij}'}}_{\text{stretching}} \quad (23.16)$$

$$+\; \underbrace{\nu\frac{\partial^2\frac{1}{2}\overline{\omega_i'^2}}{\partial x_j{}^2}}_{\substack{\text{viscous}\\\text{transport}}} \;-\; \underbrace{\nu\,\overline{\left(\frac{\partial\overline{\omega_i'}}{\partial x_j}\right)^2}}_{\substack{\text{viscous}\\\text{dissipation}}} \;.$$

23.2 Closure – Turbulence Models

We outline the ideas behind two historical simple models.

23.2.1 Eddy Viscosity Model.

The idea behind the eddy viscosity is that, as with molecular transport, turbulent transport is driven by the mean velocity gradient. This was the first of many *gradient-transport models*. Thus, in a plane shear flow,

$$\overline{u'v'} \;=\; \nu_T\,\frac{\partial\overline{u}}{\partial y}\;. \tag{23.17}$$

Clearly, ν_T must be determined empirically, and, unfortunately, it turns out to be far from constant. For example, it must go to zero at any wall, where $(u',v')=0$.

23.2.2 Prandtl's Mixing Length Theory.

Prandtl exploited the analogy between molecular and turbulent transport, representing the interaction between two fluid particles as the interaction between two molecules. In a plane shear flow, kinetic theory states that a molecule moving downward one mean-free-path Λ in its thermal motion from a high-speed region $u+\Delta u$ at $y+\Delta y$ to a low-speed region u at y transports excess momentum $m\Delta u$, where m is its mass. The number of molecules doing so per unit time per unit area, on average, is $n\bar{c}/4$. Thus, molecular transport of momentum gives

$$\tau \;\sim\; m\,\Delta u\,\frac{n\bar{c}}{4}\;. \tag{23.18}$$

The density is $\rho=mn$, and $\Delta u=\Lambda\partial u/\partial y$, so

$$\tau \;\sim\; \frac{\rho\bar{c}\Lambda}{4}\,\frac{du}{dy}\;. \tag{23.19}$$

Therefore, the molecular kinetmatic viscosity is

$$\nu \;=\; \frac{\bar{c}\Lambda}{4}\;. \tag{23.20}$$

Note that, using the relation between *collision cross section* σ and Λ

$$\Lambda \;=\; \frac{1}{n\sigma}\;, \tag{23.21}$$

April 23, 2001

the temperature dependence of μ can be exhibited

$$\mu \sim \frac{m\overline{c}(T)}{4\sigma(T)} \,. \tag{23.22}$$

The application to turbulence comes in associating the vertical thermal velocity with v' and the mean free path with a "mixing length" l,

$$\boxed{\nu_T = k\overline{v'}l \,.} \tag{23.23}$$

23.2.3 Other closure schemes

Another approach to closing the Reynolds averaged equations is to develop equations for higher-order moments, which can be used to evaluate the Reynolds stress. These equations will, in turn, have even higher moments, which must be modeled. The hope is that with more equations, and with models for only very high order correlations, the physics might be represented more accurately. Intuitively, the idea is that the approximations are being pushed to smaller and smaller scales.

Some of the equations that provide fuel for this activity are given below.

Mean Kinetic Energy

$$\rho\frac{D\overline{u^2}/2}{Dt} + \rho\,\overline{u_j}\frac{\partial\overline{u^2}}{\partial x_j} = \frac{\partial}{\partial x_j}\Big(\underbrace{-p\overline{u_j}}_{\substack{\text{pressure}\\\text{work}}} + \underbrace{\eta\,\epsilon_{ij}\overline{u_i}}_{\substack{\text{viscous}\\\text{transport}}} - \underbrace{\rho\,\overline{u_i'u_j'}\,\overline{u_i}}_{\substack{\text{Reynolds}\\\text{stress}\\\text{transport}}}\Big) - \underbrace{\Phi}_{\text{dissipation}} + \underbrace{\rho\,\overline{u_i'u_j'}\,\frac{\epsilon_{ij}}{2}}_{\substack{\text{turbulence}\\\text{production}}}$$

$$\tag{23.24}$$

Turbulent Kinetic Energy – Steady Flow

$$\rho\,\overline{u_j}\frac{\partial\overline{u'^2}}{\partial x_j} = -\frac{\partial}{\partial x_j}\Big(\underbrace{-\overline{p'u_j}}_{\substack{\text{pressure}\\\text{work}}} + \underbrace{\frac{1}{2}\rho\,\overline{u_i'^2 u_j}}_{\substack{\text{turbulent}\\\text{transport}}} - \underbrace{\eta\,\overline{u_i'\epsilon_{ij}'}}_{\substack{\text{viscous}\\\text{transport}}}\Big) - \underbrace{\rho\,\overline{u_i'u_j'}\,\frac{\epsilon_{ij}}{2}}_{\substack{\text{turbulence}\\\text{production}}} - \underbrace{\frac{\eta}{2}\,\overline{\epsilon_{ij}'\epsilon_{ij}'}}_{\substack{\text{viscous}\\\text{dissipation}}} \tag{23.25}$$

$$\text{Turbulent dissipation} \equiv \epsilon = \frac{\eta}{2}\,\overline{\epsilon_{ij}'\epsilon_{ij}'} \tag{23.26}$$

Energy Equation

$$\frac{\partial\overline{T}}{\partial t} + \overline{u_j}\frac{\partial\overline{T}}{\partial x_j} = -\frac{\partial\overline{u_j'T'}}{\partial x_j} - \kappa\frac{\partial^2\overline{T}}{\partial x_j^2} \tag{23.27}$$

$$q_j = c_p\rho\,\overline{u_j'T'} - k\frac{\partial\overline{T}}{\partial x_j} \tag{23.28}$$

23.3 Turbulent Scales

The important scales of turbulence are defined in this section. **Integral scale,** ℓ
(Example: transport scale transverse to the free-stream)
Size of the "'eddies," at which turbulent convection balances inertia ($\ell/L = u'/U$).

$$\ell = \frac{1}{\overline{v'^2}} \int_0^\infty \overline{v'(y+\eta)\, v'(y)}\, d\eta \tag{23.29}$$

Kolmogorov scale, μ
The smallest (rapidly adjusting) scale of turbulence, at which dissipation occurs.
Dimensional analysis: 2 variables (ν, ϵ) to make a length (ϵ = turbulent dissipation; Eq. 23.26).

$$\mu = \left(\frac{\nu^3}{\epsilon}\right)^{\frac{1}{4}}, \tag{23.30}$$

from which,

$$\tau = \left(\frac{\nu}{\epsilon}\right)^{\frac{1}{2}} \tag{23.31}$$

$$u = (\nu\epsilon)^{\frac{1}{4}} \tag{23.32}$$

$$Re \equiv \frac{\mu u}{\nu} = 1 \tag{23.33}$$

Taylor microscale, λ
Time scale of strain-rate fluctuations (τ_T).
Take

$$\epsilon = \frac{1}{\rho}\left(\frac{\eta}{2}\,\overline{\epsilon'_{ij}\epsilon'_{ij}}\right) \sim \nu\,\overline{\left(\frac{\partial u'}{\partial x}\right)^2} \equiv \nu\,\frac{u'^2}{\lambda^2}, \tag{23.34}$$

where u' is a typical velocity fluctuation scale. There is actually no reason to associate the velocity scale u' with ϵ, but the corresponding time,

$$\tau_T \sim \frac{\lambda}{u'}, \tag{23.35}$$

is well defined.

April 23, 2001

24 Buoyancy Effects

The study of buoyancy effects often specializes to approximations more applicable to atmospheres (gases) than to oceans (liquids). Thus in this section we talk mostly about gases, but from time to time write equations applicable also to liquids.

24.1 Hydostatic compressible gas

In a neutrally stable atmosphere with no motion

$$\frac{ds}{dz} = 0 \,. \tag{24.1}$$

Thus for a perfect gas,

$$p \sim \rho^\gamma \sim T^{\frac{\gamma}{\gamma-1}} \,, \tag{24.2}$$

or, in terms of a reference state $(p_o, \rho_\theta, \theta)$,

$$\frac{p}{p_o} = \left(\frac{\rho}{\rho_\theta}\right)^\gamma = \left(\frac{T}{\theta}\right)^{\frac{\gamma}{\gamma-1}} \,. \tag{24.3}$$

$$\theta = T \left(\frac{p}{p_0}\right)^{-\frac{\gamma-1}{\gamma}} \tag{24.4}$$

$$\rho_\theta = \rho \left(\frac{p}{p_0}\right)^{-\frac{1}{\gamma}} \tag{24.5}$$

ρ_θ and θ are the *potential density and temperature*, respectively, and are the density and temperature of the fluid at pressure p_0. In a neutrally stable atmosphere they remain constant when a fluid particle moves upward or downward (a more precise statement will be made later).

Differentiating Eqs. 24.4 and 24.5, and using the perfect gas equation of state $(d\rho/\rho = dp/p = -dT/T)$,

$$\frac{d\theta}{\theta} = \frac{dT}{T} - \frac{\gamma-1}{\gamma}\frac{dp}{p} \tag{24.6}$$

$$\frac{d\rho_\theta}{\rho_\theta} = \frac{d\rho}{\rho} - \frac{1}{\gamma}\frac{dp}{p} \tag{24.7}$$

$$= -\left(\frac{dT}{T} - \frac{\gamma-1}{\gamma}\frac{dp}{p}\right) \,, \tag{24.8}$$

so

$$\boxed{\frac{1}{\theta}\frac{d\theta}{dz} = -\frac{1}{\rho_\theta}\frac{d\rho_\theta}{dz} = \frac{1}{T}\frac{dT}{dz} - \frac{\gamma-1}{\gamma}\frac{1}{p}\frac{dp}{dz} \,.} \tag{24.9}$$

The z-momentum equation for a stationary fluid gives $dp/dz = -\rho g$, so

$$\boxed{\frac{1}{\theta}\frac{d\theta}{dz} = \frac{1}{T}\left(\frac{dT}{dz} + \frac{g}{c_p}\right) \,.} \tag{24.10}$$

April 23, 2001

For a neutrally stable atmosphere, $ds/dz = d\theta/dz = 0$, so

$$\frac{dT}{dz} = -\frac{g}{c_p} . \tag{24.11}$$

This is the so-called *adiabatic lapse rate*. However, note that the stipulation was that the *entropy* be constant. That is a stronger requirement than that any changes be adiabatic (no heat transferred from outside the system). Constant entropy means that the process be adiabatic and reversible, so the motions introduced to test the stability must be made reversibly.

For the neutrally stable atmosphere, the temperature profile is

$$T = T_0 - \frac{gz}{c_p} . \tag{24.12}$$

The density profile is given by

$$\frac{1}{\rho}\frac{d\rho}{dz} = \frac{1}{\gamma p}\frac{dp}{dz} = -\frac{g}{\gamma R T(z)} = \frac{g}{a^2} , \tag{24.13}$$

where a is the sound speed. The charcteristic depth a^2/g is called the scale height,

$$\Lambda = \frac{a^2}{g} . \tag{24.14}$$

Small amplitude long wavelength gravity waves travel at a speed c given by Froude number based on depth (Λ) unity,

$$Fr = \frac{c}{\sqrt{g\Lambda}} = \frac{c}{a} = M = 1 , \tag{24.15}$$

so the waves also travel at Mach 1 and are therefore also acoustic waves. Substituting the temperature variation Eq. 24.12 into Eq. 24.13 and integrating gives

$$\rho = \rho_0 \left(\frac{gz}{1 - c_p T_0}\right)^{\frac{1}{\gamma-1}} . \tag{24.16}$$

24.2 Boussinesq approximation (Spiegel &Veronis, 1960)

The Boussinesq approximation applies to a thin layer (much thinner than the scale height of the system) of compressible fluid within which density fluctuations are no larger than the change of density due to gravitational effects. Dissipation in a gas scales as M^2/Re and so is small for atmospheric motions.

The pressure, density and temperature are represented by sums of the spatial mean value, the hydrostatically varying component, and the flow-driven component,

$$p = \overline{p} + p_s(z) + p'(x, y, z, t) \tag{24.17}$$
$$\rho = \overline{\rho} + p_s(z) + \rho'(x, y, z, t) \tag{24.18}$$
$$T = \overline{T} + T_s(z) + T'(x, y, z, t) \tag{24.19}$$

The scale height for each is, for example,

$$\Lambda_p = \left|\frac{1}{\overline{p}}\frac{dp_s}{dz}\right|^{-1} . \tag{24.20}$$

The Boussinesq approximation is:

1. The layer thickness D is very small compared to the scale height Λ

$$D \ll \Lambda_\rho \tag{24.21}$$

$$\frac{D}{\overline{\rho}}\frac{d\rho_s}{dz} \ll 1 . \tag{24.22}$$

Integrating this over the layer gives for the gravitational density changes there,

$$\frac{\Delta\rho_s}{\overline{\rho}} \ll 1 . \tag{24.23}$$

2. The perturbation density is no larger than the gravitational changes

$$\frac{\rho'}{\overline{\rho}} \leq \frac{\Delta\rho_s}{\overline{\rho}} . \tag{24.24}$$

24.2.1 Equation of State

$\rho(p, t)$ is expanded in a Taylor series about its mean value

$$\rho = \overline{\rho} + \overline{\left(\frac{\partial\rho}{\partial T}\right)_p}(T - \overline{T}) + \overline{\left(\frac{\partial\rho}{\partial p}\right)_T}(p - \overline{p}) + \dots \tag{24.25}$$

$$= \overline{\rho}\left[1 + \overline{k}_T(p - \overline{p}) - \overline{\alpha}(T - \overline{T})\right] + \dots , \tag{24.26}$$

where the isothermal compressibility and the coefficient of thermal expansion are

$$\overline{k}_T = \frac{1}{\overline{\rho}}\overline{\left(\frac{\partial\rho}{\partial p}\right)_T} \tag{24.27}$$

$$\overline{\alpha} = -\frac{1}{\overline{\rho}}\overline{\left(\frac{\partial\rho}{\partial T}\right)_p} . \tag{24.28}$$

Collecting terms of equal magnitude in the resulting equation,

$$1 + \frac{\rho_s + \rho'}{\overline{\rho}} = 1 + \overline{k}_T(p_s + p') - \overline{\alpha}(T_s + T') , \tag{24.29}$$

gives

$$\rho_s = \overline{\rho}\left(\overline{k}_T\,p_s - \overline{\alpha}\,T_s\right) \tag{24.30}$$

$$\rho' = \overline{\rho}\left(\overline{k}_T\,p' - \overline{\alpha}\,T'\right) , \tag{24.31}$$

24.2.2 Continuity Equation

The continuity equation (2.13) expands to

$$\frac{\partial\rho'}{\partial t} + \underline{u} \cdot \nabla(\rho_s + \rho') + \rho\nabla \cdot \underline{u} = 0 \tag{24.32}$$

$$\frac{\left(\frac{\partial}{\partial t} + \underline{u} \cdot \nabla\right)(\rho_s + \rho')}{\overline{\rho}} + \frac{\rho}{\overline{\rho}}\nabla \cdot \underline{u} = 0 . \tag{24.33}$$

From the inequalities Eqs. 24.23 and 24.24 the first term is small, so there results

$$\nabla \cdot \underline{u} = 0 \tag{24.34}$$

24.2.3 Momentum Equation

For no motion, the vertical component of the momentum equation is

$$\frac{dp_s}{dz} = -g\overline{\rho} - g\rho_s . \tag{24.35}$$

Thus, in the full momentum equation Eq. 3.19,

$$\nabla p = \nabla p_s + \nabla p' \tag{24.36}$$

$$= -g\overline{\rho} - g\rho_s + \nabla p' , \tag{24.37}$$

where $\underline{g}$ points in the z-direction. Therefore,

$$-\nabla p - \underline{g}\rho = -\nabla p' - \underline{g}\rho' . \tag{24.38}$$

Using Eqs. 24.34 and 24.38, the momentum equation becomes

$$\overline{\rho}\frac{D\underline{u}}{Dt} = -\nabla p' - \rho'\underline{g} + \mu\nabla^2\underline{u} , \tag{24.39}$$

The gravity term in the momentum equation is actually of a smaller order than the others, but it must be kept, or there would be no buoyancy effect. It means that the acceleration of gravity is always much larger than the acceleration of fluid driven by gravity effects.

The vertical component of the pressure and gravity terms in Eq. 24.39 are

$$-\frac{1}{\overline{\rho}}\frac{\partial p'}{\partial z} - \frac{\rho'}{\overline{\rho}}g$$

$$= -\frac{1}{\overline{\rho}}\left[\frac{\partial p'}{\partial z} + \overline{\rho}\overline{k}_T g\, p'\right] - \overline{\alpha}g\, T' . \tag{24.40}$$

Now

$$\overline{\rho}\overline{k}_T g \equiv \frac{1}{H} = \mathcal{O}\left(\frac{1}{\Lambda_\rho}\right) \tag{24.41}$$

is the inverse of a characteristic length, of the order of the scale height. Therefore,

$$\frac{\partial p'}{\partial z} \sim \frac{p'}{D} \gg \frac{p'}{H} , \tag{24.42}$$

so the vector momentum equation reduces to

$$\boxed{\frac{D\underline{u}}{Dt} = -\frac{\nabla p'}{\overline{\rho}} - \alpha T'\underline{g} + \nu\nabla^2\underline{u} .} \tag{24.43}$$

24.2.4 Energy equation

Eq. 3.13 is expanded, as above. For no flow it is

$$k\nabla^2 T_s + \overline{\rho}Q_s = 0 . \tag{24.44}$$

Subtracting this from the full equation gives

$$\overline{\rho}c_v\left(\frac{\partial T'}{\partial t} + \underline{u} \cdot \nabla T\right) = -p\nabla \cdot \underline{u} + k\nabla^2 T' + \overline{\rho}Q' , \tag{24.45}$$

April 23, 2001

where $Q' = Q - Q_s$, and the dissipation has been neglected. From Eqs. 24.23 and 24.24 we take in the first term on the right $p = \overline{p} + p_s + p' \doteq \overline{p}$. To the same approximation, Eq. 24.31 is

$$\rho' \;=\; -\overline{\rho}\,\overline{\alpha}\,T' \;. \tag{24.46}$$

Using that and Eq. 24.30 in 24.32 gives

$$p\nabla \cdot \underline{u} \;=\; -\overline{p}\frac{D}{Dt}\left[\overline{k}_T p_s - \overline{\alpha}(T_s + T')\right] \;. \tag{24.47}$$

Now, since $p_s = p_s(z)$,

$$\frac{D\overline{k}_t p_s}{Dt} \;=\; \overline{k}_T w\frac{dp_s}{dz} \;=\; -\overline{k}_T wg\overline{\rho} \;, \tag{24.48}$$

where the first approximation to Eq. 24.35 has been used for the last equality. The result is

$$-p\nabla \cdot \underline{u} \;=\; -\overline{p}\frac{D}{Dt}\left[\overline{\alpha}(T_s + T')\right] + \overline{p}\overline{k}_T wg\overline{\rho} \;, \tag{24.49}$$

and Eq. 24.45 becomes

$$\boxed{\overline{\rho}\left(c_v + \frac{\overline{p}\,\overline{\alpha}}{\overline{\rho}}\right)\left(\frac{\partial T'}{\partial t} + \underline{u}\cdot\nabla T\right) + \overline{p}\overline{k}_T wg\overline{\rho} \;=\; k\nabla^2 T' + \overline{\rho}Q'} \;, \tag{24.50}$$

For gases $\overline{\alpha} = 1/\overline{T}$ and $\overline{k}_T = 1/\overline{p}$, so the first parentheses is c_p, and the result can be written

$$\boxed{\frac{DT'}{Dt} + w\left(\frac{dT_s}{dz} + \frac{g}{c_p}\right) \;=\; \kappa\nabla^2 T' + \frac{Q'}{c_p}} \;. \tag{24.51}$$

Note that the adiabatic lapse rate emerges as an important parameter in the dynamical equations.

24.3 Axisymmetric Buoyant Plumes

The simplest plume is generated by a steady point source of heat. We analyze plumes making the Boussinesq approximation, and assuming constant transport properties, constant ambient temperature T_∞ (but at the same time neutrally buoyant atmosphere), and thin-layer approximation.

The scales of the velocity and thermal fields will in general be different, because the diffusivities of momentum (viscosity) and heat (conductivity) or mass (diffusion coefficient) are different. In this treatment we attempt to distinguish these scales as δ and δ_T, respectively, and also the corresponding entrainment velocities V and V_T. The scale that is largest, δ or δ_T, will in general set the scale of the flow. Thus for large Pr (viscous liquids) the scale will be δ and for small Pr (liquid metals) the scale will be δ_T,

24.3.1 Laminar Plumes

The equations of motion, and their order of magnitude scaling, are then

$$\underbrace{\frac{\partial ru}{\partial x}}_{\frac{U}{x}} + \underbrace{\frac{\partial rv}{\partial r}}_{\frac{V}{\delta}} \;=\; 0 \tag{24.52}$$

April 23, 2001

$$u\frac{\partial u}{\partial x} + v\frac{\partial u}{\partial r} \;=\; \underbrace{g\alpha(T - T_\infty)}_{g\alpha T} + \underbrace{\frac{\nu}{r}\frac{\partial}{\partial r}\left(r\frac{\partial u}{\partial r}\right)}_{\frac{\nu U}{\delta^2}} \qquad (24.53)$$

where under the left side: $\underbrace{\phantom{u\frac{\partial u}{\partial x}}}_{\frac{U^2}{x}} \quad \underbrace{\phantom{v\frac{\partial u}{\partial r}}}_{\frac{UV}{\delta}}$

$$\underbrace{u\frac{\partial T}{\partial x}}_{\frac{UT}{x}} + \underbrace{v\frac{\partial T}{\partial r}}_{\frac{V_T T}{\delta_T}} \;=\; \underbrace{\frac{\kappa}{r}\frac{\partial}{\partial r}\left(r\frac{\partial T}{\partial r}\right)}_{\frac{\kappa_T T}{\delta_T^2}} \;. \qquad (24.54)$$

x is vertical, as is the gravity vector, and r is the transverse coordinate. Note that separate lateral scales δ and δ_T, and corresponding lateral velocities V and V_T, have been assumed for viscous and thermal effects. The boundary conditions are

$$\begin{aligned} r &= 0 \;; \quad v = \frac{\partial}{\partial r} = 0 \\ r &\longrightarrow \infty \;; \quad u \longrightarrow 0 \\ & \qquad\qquad T \longrightarrow T_\infty \end{aligned} \qquad (24.55)$$

The *buoyancy flux* (here the heat flux) is defined as

$$Q \equiv \underbrace{\int_0^\infty \rho c_p (T - T_\infty) u \, 2\pi r \, dr}_{\rho c_p T U \delta_T^2} \;. \qquad (24.56)$$

It is the constant heat input driving the plume.

The consequences of scaling are:
As with jets, from the continuity equation, the thin-layer scaling,

$$\frac{U}{x} \;\sim\; \frac{V}{\delta} \;; \qquad (24.57)$$

from the first and fourth terms in the momentum equation the requirement for high Reynolds number,

$$\frac{U\delta}{\nu} \;\sim\; \frac{x}{\delta} \;; \qquad (24.58)$$

and a new result from the gravitational term,

$$g\alpha T \;\sim\; \frac{\nu^2 x}{\delta^4} \;; \qquad (24.59)$$

from the first and third terms in the energy equation,

$$\delta_T \;\sim\; \sqrt{\frac{\kappa x}{U}} \;\sim\; Pr^{-\frac{1}{2}}\delta \;; \qquad (24.60)$$

and from the second and third terms,

$$V_T \;\sim\; \frac{\kappa}{\delta_T} \;\sim\; Pr^{-\frac{1}{2}}V \;. \qquad (24.61)$$

199   April 23, 2001

It is useful to simplify the bookeeping for distinguishing between the large and small Pr cases by introducing simple interpolation formulas so only one scale need be considered. This is accomplished by inserting a factor $1 + Pr/Pr$ at appropriate locations.

$$
\begin{aligned}
\delta &\sim \left(\frac{\nu x}{U}\frac{1+Pr}{Pr}\right)^{\frac{1}{2}} \\
V &\sim \frac{\nu}{\delta}\frac{1+Pr}{Pr} .
\end{aligned}
\tag{24.62}
$$

Combining Eqs. 24.56, 24.58 and 24.60 gives

$$
\frac{Q}{c_p\rho} \sim TU\delta_T^2 \sim TU\delta^2\frac{1+Pr}{Pr} \sim T\nu x\frac{1+Pr}{Pr} .
\tag{24.63}
$$

Thus,

$$
\boxed{T \sim \frac{Q}{c_p\rho\,\nu\,x}\frac{Pr}{1+Pr} .}
\tag{24.64}
$$

The temperature perturbation decreases as $1/x$. Continuing by applying Eqs. 24.59 to 24.63,

$$
\frac{Q}{c_p\rho} \sim \frac{\nu^3}{g\alpha}\frac{x^2}{\delta^4}\frac{1+Pr}{Pr} ,
\tag{24.65}
$$

so

$$
\boxed{\frac{\delta}{x} \sim \left(\frac{c_p\rho}{Q\alpha}\frac{\nu^3}{g}\frac{1+Pr}{Pr}\right)^{\frac{1}{4}}x^{-\frac{1}{2}} .}
\tag{24.66}
$$

The plume diameter increases with the expected parabolic behavior. Now, the Grashof number is

$$
Gr_x \equiv \frac{\alpha Tg x^3}{\nu^2} .
\tag{24.67}
$$

Using the scaling for T, we have, for plumes,

$$
\boxed{Gr_x = \frac{g\alpha Q}{c_p\rho}\frac{x^2}{\nu^3}\frac{Pr}{1+Pr} .}
\tag{24.68}
$$

Thus, Eq. 24.66 is the same thing as

$$
\boxed{\frac{\delta}{x} \sim (Gr_x)^{-\frac{1}{4}} .}
\tag{24.69}
$$

It remains to determine the dependence of $U(x)$ and the momentum flux $J(x)$,

$$
J = \underbrace{\int \rho u^2\, 2\pi r\, dr}_{\rho U^2\delta^2} .
\tag{24.70}
$$

Putting Eq. 24.66 in 24.58 gives

$$
\boxed{U \sim \left(\frac{g\alpha Qg}{c_p\mu}\frac{Pr}{1+Pr}\right)^{\frac{1}{2}} .}
\tag{24.71}
$$

April 23, 2001

The characteristic (e.g., centerline) velocity is constant. Thus, the momentum must increase as the plume grows. Eq. 24.70 gives

$$\boxed{J \sim \left(\frac{g\alpha Q\mu}{c_p}\frac{Pr}{1+Pr}\right)^{\frac{1}{2}} x \,,}$$

(24.72)

so the momentum flux increases linearly with x.

A comparison of the behaviors of momentum-driven laminar jets and buoyancy-driven laminar plumes is given in the table below.

	Plume	Jet
Conserved	Q	J
U	$\left(\dfrac{g\alpha Qg}{c_p\mu}\dfrac{Pr}{1+Pr}\right)^{\frac{1}{2}}$	$\dfrac{J/\rho}{\nu x}$
Entrainment $\dfrac{dm}{dx} \sim \rho V\delta$	$\mu\dfrac{1+Pr}{Pr}$	μx
J	$\left(\dfrac{g\alpha Q\mu}{c_p}\dfrac{Pr}{1+Pr}\right)^{\frac{1}{2}} x$	const
Q	const	—

Similarity.
Define the similarity variable

$$R = \frac{r}{\delta(x)}\,,$$

(24.73)

the stream function

$$\psi(x,r) = \nu x f(R)\,,$$

(24.74)

the nondimensional temperature

$$\theta(R) = \frac{T - T_\infty}{T_0(x) - T_\infty}\,,$$

(24.75)

and assume the behavior of $T_0(x) - T_\infty$ given in Eq. 24.64. Then the buoyancy flux becomes (see Eqs. 16.23)

$$Q = 2\pi\rho c_p(T_0(x) - T_\infty)\nu x \int_0^\infty \theta f'\, dR\,,$$

(24.76)

and the momentum and energy equations reduce to two coupled ordinary differential equations,

$$f''' + (f-1)\left(\frac{f'}{R}\right)' + R\theta = 0$$

(24.77)

$$(R\theta')' + Pr\,(f\theta)' = 0\,.$$

(24.78)

Since $Pr = $ const, the energy equation can be integrated twice to give

$$\theta(R) = e^{-Pr\int_0^R \frac{f}{R}dR}\,.$$

(24.79)

When this is substituted into the momentum equation there results an ordinary integro-differential equation. After the solution for f is obtained, the lateral velocity is given by

$$v = \frac{\nu}{\delta(x)}\left(\frac{f'}{2} - \frac{f}{R}\right)\,.$$

(24.80)

The solutions will yield the numerical constants multiplying the results of the previous section.

April 23, 2001

24.3.2 Buoyancy driven by density variations (e.g., concentration)

Buoyancy can equally well be induced by variations of the concentration of different fluids or constituents. In this case transport of momentum by viscous diffusion is important as above, but replacing the smoothing of temperature by diffusion of heat, there now arises concentration smoothing by mass diffusion. The corresponding equation to replace the energy equation is mass conservation of one of the constituents. If written in terms of the density perturbation $\rho_\infty - \rho$ that equation can be written down by analogy to the energy equation, which is what we do here. The only fundamental change is that the diffusivity changes from κ to D, the diffusion coefficient. The equations in conservation form are,

$$\frac{\partial ru}{\partial x} + \frac{\partial rv}{\partial r} = 0 \tag{24.81}$$

$$\frac{\partial u^2}{\partial x} + \frac{1}{r}\frac{\partial ruv}{\partial r} = g\frac{\rho_\infty - \rho}{\rho_0} + \frac{\nu}{r}\frac{\partial}{\partial r}\left(r\frac{\partial u}{\partial r}\right) \tag{24.82}$$

$$\frac{\partial(\rho_\infty - \rho)u}{\partial x} - u\frac{d\rho_\infty}{dx} + \frac{1}{r}\frac{\partial r(\rho_\infty - \rho)v}{\partial r} = \frac{D}{r}\frac{\partial}{\partial r}\left(r\frac{\partial(\rho_\infty - \rho)}{\partial r}\right) . \tag{24.83}$$

The buoyancy flux is

$$F = \int_0^\infty g\frac{\rho_\infty - \rho}{\rho_0}u\, 2\pi r\, dr \tag{24.84}$$

24.3.3 Laminar plumes in stratified atmospheres (Morton 1967)

A stratified atmosphere adds sufficient complexity that similarity can no longer be expected. Thus, the problem is treated by analyzing the integrated equations of motion (see Sec. 20.1). Plumes involve both viscous diffusion and thermal diffusion, so, as discussed in Sec. 24.3, it is necessary to account for two lateral scales, δ and δ_T. In this section we consider the case $Pr \geq 1$, so we take $\delta_T \sim \delta/\sqrt{Pr}$. Multiplying the continuity equation by $r\, dr$ and integrating across the plume gives (see Eq. 20.18),

$$\frac{d}{dx}\int_0^\delta ur\, dr = -(rv)_\infty . \tag{24.85}$$

The term on the lhs can be written in terms of the stream function $\psi = \nu x\, f(R)$, where $R = r/\delta$,

$$\int_0^\delta ur\, dr = \nu x f_\infty , \tag{24.86}$$

so the entrainment is

$$-(rv)_\infty = \nu f_\infty . \tag{24.87}$$

f_∞ is thought of as the *entrainment coefficient.*

Integrating Eq. 24.53, cast into conservation form, gives

$$\frac{d}{dx}\int_0^\delta u^2 r\, dr = \int_0^{\delta_T} g\alpha(T - T_\infty)r\, dr . \tag{24.88}$$

In the energy equation 24.54 T is the perturbation temperature, which here we write explicitly as $T(x, r) - T_\infty(x)$. It is necessary to account for the fact that here the base temperature $T_\infty(x)$ is a function of x; doing so, and then using the continuity equation to put in conservation form, Eq. 24.54 becomes

$$\frac{\partial u(T - T_\infty)}{\partial x} + u\frac{dT_\infty}{dx} + \frac{1}{r}\frac{\partial rv(T - T_\infty)}{\partial r} = \frac{\kappa}{r}\frac{\partial}{\partial r}\left(r\frac{\partial T}{\partial r}\right) . \tag{24.89}$$

April 23, 2001

In integrating this equation we adopt the case $dT_\infty/dx = $ const, so it comes out of the integral of the second term, and Eq. 24.86 can be used. Thus,

$$\frac{d}{dx}\int_0^{\delta_T} u(T-T_\infty)r\,dr + \frac{dT_\infty}{dx}f_\infty\nu x = 0 . \tag{24.90}$$

This equation can be integrated wrt x to obtain

$$\int_0^{\delta_T} u(T-T_\infty)r\,dr = \frac{Q}{2\pi c_p\rho} - \frac{dT_\infty}{dx}f_\infty\nu\frac{x^2}{2} , \tag{24.91}$$

where the first term on the right is the constant of integration evaluated using Eq. 24.56.

24.3.4 Approximate Integral Method

Approximate solutions to Eqs. 24.85, 24.88 and 24.91 can be obtained by assuming a form of the velocity profile $u(r)$ and carrying out the integrations. The simplest profile is the top-hat profile, which gives for the differential form,

$$\frac{d}{dx}\frac{u\delta^2}{2} = f_\infty\nu \tag{24.92}$$

$$\frac{d}{dx}u^2\delta^2 = g\alpha(T-T_\infty)\delta_T^2 \tag{24.93}$$

$$\frac{d}{dx}\frac{u(T-T_\infty)\delta_T^2}{2} = -\frac{dT_\infty}{dx}f_\infty\nu x , \tag{24.94}$$

and after integrating wrt x,

$$u\frac{\delta^2}{2} = f_\infty\nu x \tag{24.95}$$

$$\frac{d}{dx}u^2\delta^2 = g\alpha(T-T_\infty)\frac{\delta^2}{Pr} \tag{24.96}$$

$$u(T-T_\infty)\frac{\delta^2}{Pr} = \frac{Q}{\pi c_p\rho} - \frac{dT_\infty}{dx}f_\infty\nu x^2 , \tag{24.97}$$

where δ_T^2 has been replaced by δ^2/Pr, i.e., $Pr > 1$. Substituting the third equation into the second equation to eliminate $T-T_\infty$, using the first to eliminate δ, and multiplying by ux, gives

$$ux\frac{dux}{dx} = \frac{g\alpha}{2f_\infty\nu}\left(\frac{Q}{\pi c_p\rho} - \frac{dT_\infty}{dx}f_\infty\nu x^2\right)x , \tag{24.98}$$

which integrates to

$$\boxed{u^2 = g\alpha\left(\frac{Q}{2\pi c_p\rho f_\infty\nu} - \frac{1}{4}\frac{dT_\infty}{dx}x^2\right)} \tag{24.99}$$

This confirms that similarity is lost, but it has the interesting result that the plume stops at a finite altitude x_m

$$x_m = \left(\frac{2Q}{\pi c_p\rho f_\infty\nu\frac{dT_\infty}{dx}}\right)^{\frac{1}{2}} . \tag{24.100}$$

$u(x)$ then becomes

$$u^2 = u_0^2\left[1-(x/x_m)^2\right] , \tag{24.101}$$

where

$$u_0 = \left(\frac{g\alpha Q}{2\pi f_\infty c_p \mu} \right)^{\frac{1}{2}} \tag{24.102}$$

is the constant velocity of plumes in a uniform atmosphere. Putting $u(x)$ into the continuity equation and solving for δ gives

$$\delta^2 = \delta_0^2 \frac{x/x_m}{[1 - (x/x_m)^2]^{\frac{1}{2}}} \; ; \qquad \frac{\delta_0^2}{x_m} = \frac{2f_\infty \nu}{u_0} \; . \tag{24.103}$$

Finally, the temperature is given by

$$T - T_\infty = \frac{1}{2} \frac{dT_\infty}{dx} x_m \left(\frac{x_m}{2x} - \frac{x}{x_m} \right) \tag{24.104}$$

The behavior of these parameters is shown in Fig. 73. In the limit when the atmosphere becomes uniform,
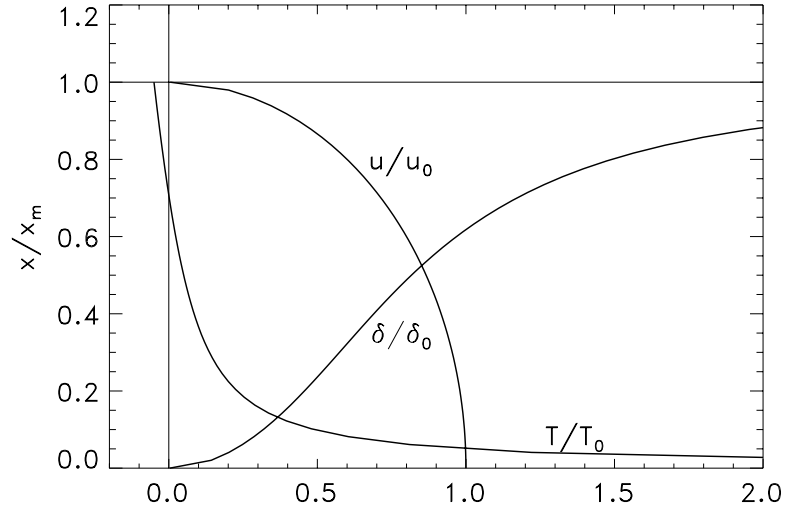

Figure 73. Variation of the velocity, radius and temperature of a laminar plume in a stratified atmosphere

$x_m \to \infty$, and the results approach those obtained in Sec. 24.3.1.

24.4 Turbulent Plumes (Morton et al. 1956)

At high enough Reynolds numbers plumes become unstable and transition to turbulence. At very high Re when the turbulence is strong molecular diffusivity is unimportant and is replaced by turbulent transport. If an eddy viscosity model, or some other possibly more sophisticated gradient-transport model, us used, the equations integrate to give the same form as in the laminar case. In the laminar case ν and κ do not appear in the momentum and energy integral equations, only ν in the continuity equation. With turbulence, it's the same, so it becomes necessary to model the entrainment term.

After the same procedure as was used above is applied to Eqs. 24.81–24.84, the equations for a top-hat profile plume are,

$$\frac{d\,u\delta^2}{dx} = -2(rv)_\infty = 2\alpha\delta u \tag{24.105}$$

$$\frac{d\,u^2\delta^2}{dx} = g\frac{\rho_\infty - \rho}{\rho_0}\delta^2 \tag{24.106}$$

$$\frac{d\,(\rho_\infty - \rho)u\delta^2}{dx} = \frac{d\,\rho_\infty}{dx}u\delta^2 \ , \tag{24.107}$$

The last equality in Eq. 24.105 is the *entrainment hypothesis*, namely, that $(rv)_\infty$ is proportional, with proportionality constant α, to the volume flux per unit length of the plume. This hypothesis is based on dimensional reasoning and the idea that fluid is ingested into the plume at a rate dependent on the axial velocity.

24.4.1 Uniform atmosphere

For a uniform atmosphere the term on the right of Eq. 24.107 is zero, so

$$F = g\frac{\rho_\infty - \rho}{\rho_0}u\delta^2 = \text{const} = F_0 \ . \tag{24.108}$$

Thus Defining

$$\begin{aligned} V &= u\delta \\ W &= u\delta^2 \ , \end{aligned} \tag{24.109}$$

The continuity and momentum equations equations become

$$\frac{dW}{dx} = 2\alpha V \tag{24.110}$$

$$\frac{dV^2}{dx} = \frac{F_0}{u} = F_0\frac{W}{V^2} \ . \tag{24.111}$$

Eliminating W from the momentum equation by differentiation gives

$$\frac{d^2V^4}{dx^2} = 4F_0\alpha V \ . \tag{24.112}$$

This equation can be solved by letting $v = V^4$ and $p = dv/dx$, resulting in

$$\frac{dp}{dx} = p\frac{dp}{dv} = 4F_0\alpha v^{\frac{1}{4}} \ . \tag{24.113}$$

Integrating once to get $p(v) = dv/dx$ and again to get $v(x)$ gives finally for $V(x)$ (and by integration $W(x)$)

$$V = \left(\frac{9}{10}F_0\alpha\right)^{\frac{1}{3}} x^{\frac{2}{3}} \tag{24.114}$$

$$W = \frac{3\alpha}{5}\left(\frac{9}{10}F_0\alpha\right)^{\frac{1}{3}} x^{\frac{5}{3}} \ . \tag{24.115}$$

The original unknowns follow immediately

$$\boxed{\begin{aligned} \delta &= \frac{3\alpha}{5}x \\ u &= \frac{5}{3\alpha}\left(\frac{9}{10}F_0\alpha\right)^{\frac{1}{3}} x^{-\frac{1}{3}} \\ g' = g\frac{\rho_\infty - \rho}{\rho_0} &= \frac{5F_0}{3\alpha}\left(\frac{9}{10}F_0\alpha\right)^{\frac{1}{3}} x^{-\frac{5}{3}} \ . \end{aligned}} \tag{24.116}$$

Because of the entrainment term, the turbulent plume behaves very differently than the laminar plume. δ grows much more rapidly and so the velocity decreases rather than being constant.

April 23, 2001

24.4.2   Nonuniform atmosphere

For a nonuniform atmospher there is one more unknown, $F(x)$. The equations become

$$\frac{dW}{dx} = 2\alpha V \tag{24.117}$$

$$\frac{dV^2}{dx} = \frac{F_0}{u} = F_0 \frac{W}{V^2} \tag{24.118}$$

$$\frac{dF}{dx} = -WG \ . \tag{24.119}$$

Defining the nondimensional variables

$$\xi = \alpha^{\frac{1}{2}} F_0^{-\frac{1}{4}} G^{\frac{3}{8}} x \tag{24.120}$$

$$v = F_0^{-\frac{1}{2}} G^{\frac{1}{4}} V \tag{24.121}$$

$$w = \alpha^{-\frac{1}{4}} F_0^{-\frac{3}{4}} G^{\frac{5}{8}} W \tag{24.122}$$

$$f = \frac{F}{F_0} \ , \tag{24.123}$$

the equations become

$$\frac{dw}{d\xi} = v \tag{24.124}$$

$$\frac{dv^4}{d\xi} = fw \tag{24.125}$$

$$\frac{df}{d\xi} = -w \ , \tag{24.126}$$

which are in the form for numerical computaion. The numerical solution yields the behavior with ξ, and therefore $u(x)$, $\delta(x)$, $g'(x)$ and $F(x)$. The numerical value of ξ_m at which the velocity vanishes is also a result of the numerical computation. The dimensional height x_m of the plume is given in terms of the strength F_0 of the plume, the atmospheric lapse rate G, and a fundamental fluid mechanical property, the entrainment coefficient α. Morton et al. (1956) conducted laboratory experiments to determine α, with the result $\alpha = 0.093$. Then the computed height of the plume was found to be

$$\boxed{x_m = 3.79\, F_0^{\frac{1}{4}} G^{-\frac{3}{8}} \ .} \tag{24.127}$$

24.5   Stratified Flows

24.5.1   Shallow water waves

The theory of shallow water waves describes the motion of a stably stratified thin layer of dense fluid. "Shallow" means that the layer depth $h(x,t)$ is small compared to the lateral scale of the flow λ. A consequence is that vertical accelerations must be very small

$$\frac{Dw}{Dt} = 0 \ . \tag{24.128}$$

April 23, 2001

Here we take the fluid to be incompressible (*e.g.*, water), and for simplicity consider a two-dimensional plane flow (x, z). Also, the fluid is inviscid. We first consider the simple case in which the light overlying fluid is of zero density. Thus the equations of motion for the dense layer are

$$\nabla \cdot \underline{u} = 0 \tag{24.129}$$

$$\rho \frac{D\underline{u}}{Dt} = -\nabla p - \rho \underline{g} . \tag{24.130}$$

or

$$\frac{\partial u}{\partial x} + \frac{\partial w}{\partial z} = 0 \tag{24.131}$$

$$\rho \frac{Dw}{Dt} = -\frac{\partial p}{\partial z} - \rho g \tag{24.132}$$

$$\rho \frac{Du}{Dt} = -\frac{\partial p}{\partial x} . \tag{24.133}$$

The boundary conditions are

$$\left. \begin{array}{rcl} p & = & 0 \\ \dfrac{\partial h}{\partial t} + u\dfrac{\partial h}{\partial x} & = & w \end{array} \right\} \quad z = h \tag{24.134}$$

$$w = 0 \} \quad z = 0 \tag{24.135}$$

Because the layer is thin, the lhs of Eq. 24.132 is zero so the pressure is hydrostatic,

$$\frac{\partial p}{\partial z} = -\rho g \tag{24.136}$$

$$\boxed{p(x, z, t) = \rho g(h(x,t) - z) .} \tag{24.137}$$

Thus $\partial p/\partial x$ (and $\partial p/\partial y$) does not depend on z, so neither does Du/Dt. We conclude that if $\underline{u}(x, z, t)$ is initially not a function of z, then it never is, so $u = u(x,t)$. Thus integrals of the equations over depth are easy; they just account for variations of depth $h(x,t)$. Consequently, to get equations for the behavior of depth $h(x,t)$, we integrate the above equations. For continuity,

$$\int_0^h \frac{\partial u}{\partial x}\, dz + w\Big|_0^h = 0 \tag{24.138}$$

$$\frac{\partial}{\partial x} \int_0^h u\, dz - u(h)\frac{dh}{dx} + w(h) = 0 , \tag{24.139}$$

so,

$$\frac{\partial uh}{\partial x} + \frac{\partial h}{\partial t} = 0 , \tag{24.140}$$

where u is now the mean velocity, and the last term in the last equation has been obtained from the boundary conditions. Thus

$$\boxed{\frac{\partial h}{\partial t} + \frac{\partial uh}{\partial x} = 0 .} \tag{24.141}$$

The x-momentum equation is

$$\frac{\partial u}{\partial t} + u\frac{\partial u}{\partial x} + g\frac{\partial h}{\partial x} = 0 . \tag{24.142}$$

Multiplying it through by h, and using the continuity equation, puts it in conservation form

$$\boxed{\frac{\partial uh}{\partial t} + \frac{\partial u^2 h}{\partial x} + \frac{1}{2}\frac{\partial gh^2}{\partial x} = 0 .} \tag{24.143}$$

April 23, 2001

24.6   Small Amplitude Motions

Linearizing the continuity and momentum equations for small changes of depth and small velocities gives

$$\frac{\partial h}{\partial t} + h\frac{\partial u}{\partial x} = 0 \tag{24.144}$$

$$\frac{\partial u}{\partial t} + g\frac{\partial h}{\partial x} = 0. \tag{24.145}$$

Cross differentiating and subtracting to eliminate u gives the wave equation for h

$$\frac{\partial^2 h}{\partial t^2} - gh\frac{\partial^2 h}{\partial x^2} = 0. \tag{24.146}$$

Solutions have the form

$$h = f(x - ct) + g(x + ct), \tag{24.147}$$

where $c = \sqrt{gh}$ is the wave speed.

24.7   Hydraulic Jump

The above equations can be directly used to describe the hydraulic jump and the dam break problem. A jump is a transition of unspecified structure between two uniform states, and so is analogous to a shock wave. The jump conditions can be derived by a) a control-volume analysis of the above equations, or b) by integrating them across the jump (wrt x). Integrating the continuity equation through the jump gives

$$uh = \text{const} \tag{24.148}$$

and evaluating at the two uniform states (1) and (2) gives

$$u_2 h_2 = u_1 h_1. \tag{24.149}$$

Similarly, the momentum equation gives

$$u^2 h + \frac{gh^2}{2} = \text{const} \tag{24.150}$$

through the jump and thus

$$u_2^2 h_2 + \frac{gh_2^2}{2} = u_1^2 h_1 + \frac{gh_1^2}{2}. \tag{24.151}$$

Using the continuity equation to eliminate u_2 from the momentum equation gives

$$\left(\frac{h_2}{h_1}\right)^2 - 1 - \frac{2u_1^2}{gh_1}\left(1 - \frac{h_2}{h_1}\right) = 0. \tag{24.152}$$

Setting $F_1 = u_1/\sqrt{gh_1}$, a given quantity, and $H \equiv h_2/h_1$ the unknown, gives

$$(H - 1)(H^2 + H - 2F_1) = 0 \tag{24.153}$$

Beside the trivial solution $H = 1$, the solution is

$$\boxed{H = \frac{\sqrt{1 + 8F_1} - 1}{2}.} \tag{24.154}$$

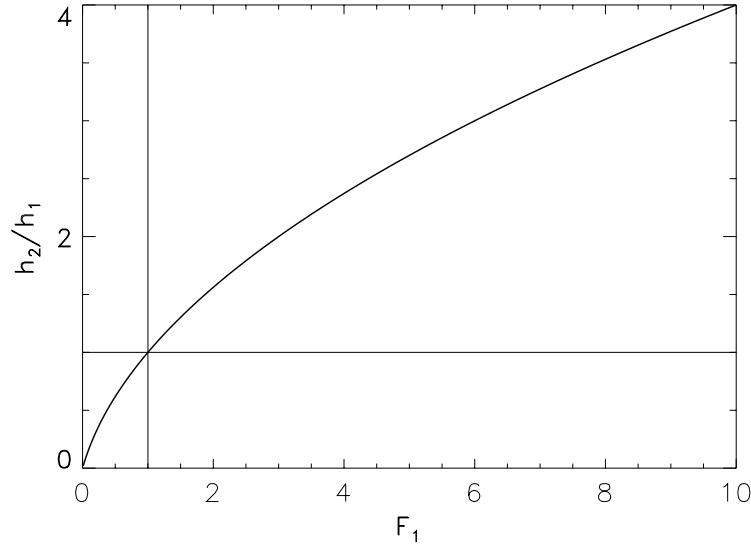April 23, 2001

Figure 74. Hydraulic jump

Then the downstream velocity is given by

$$\frac{F_2}{F_1} \;=\; \frac{1}{H^3} \;=\; \frac{8}{\left(\sqrt{1 + 8F_1} - 1\right)^3} \;.$$

(24.155)

The variation of h_2 with F_1 is shown in Fig. 24.7. In this derivation, the energy equation has not been used. In fact, the kinetic energy flux is not conserved. The fact that energy must be dissipated is shown by breaking and turbulence at the front, or, with weak waves, a system of waves that radiates downstream from the front.

24.8   Flows With No Losses

To describe flows in which no losses occur (because the wave fronts are smooth) requires use of the Bernoulli equation, which from Eq. 3.30, with $\omega = 0$, is

$$\frac{\partial \underline{u}}{\partial t} + \nabla \left(\frac{u^2}{2} + \frac{p}{\rho} + G \right) \;=\; 0 \;.$$
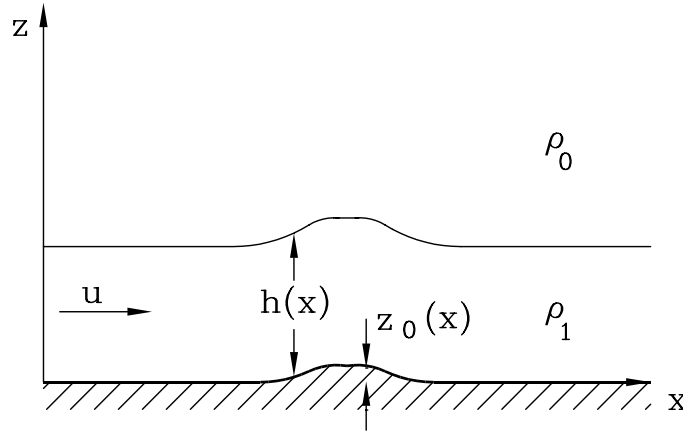
(24.156)

We have $\nabla G = \underline{g}$, so $G = gz+$ const. Also, for inviscid, incompressible, irrotational flow, $\underline{u} = \nabla \phi$. Integrating gives

$$\boxed{\frac{\partial \phi}{\partial t} + \frac{u^2}{2} + \frac{p}{\rho} + gz \;=\; \text{const} \;.}$$

(24.157)

24.8.1   Steady flow

For steady flow the Bernoulli equation is Eq. 2.25,

$$\frac{u^2}{2} + \frac{p}{\rho} + gz \;=\; H \;.$$

(24.158)

Consider a steady inflow from the left of a layer of density $\rho_1 = \rho_0 + \rho'$ and thickness $h(x)$ which flows over an obstacle of shape $z_0(x)$ and is overlain by a very thick stagnant layer of density ρ_0 (sketch). The Bernoulli equation applied to each layer on the stream line $z = h + z_0$ (that is, on the interface) is

$$\frac{p_0}{\rho_0} + g(h + z_0) = H_0 \tag{24.159}$$

$$\frac{u^2}{2} + \frac{p_1}{\rho_1} + g(h + z_0) = H_1 . \tag{24.160}$$

The continuity equation is

$$uh = Q . \tag{24.161}$$

On the interface $p_1 = p_0$. Eliminating p_0 using the Bernoulli equation for the top layer, and u using the continuity equation gives

$$\frac{Q^2}{2gh^2} + (h + z_0)\left(1 - \frac{\rho_0}{\rho_1}\right) = H_1 - \frac{\rho_0}{\rho_1}H_0 . \tag{24.162}$$

Dividing through by $1 - \rho_0/\rho_1 = \rho'/\rho_1$, and defining

$$g' = \frac{\rho'}{\rho_1} g , \tag{24.163}$$

gives

$$\boxed{\frac{Q^2}{2g'h^2} + h = H - z_0(x) ,} \tag{24.164}$$

where H is a redefined Bernoulli constant. The left hand side is plotted in the sketch. It can be shown that the minimum occurs at $F = 1$, and to the left is "supercritical" flow, while to the right is "subcritical." For any given inflow condition (Q, H), where at inflow $z_0 = 0$, the flow can be in zero or two states, shown by the square points. As the flow encounters the obstruction, $z_0(x) > 0$, according to Eq. 24.164 the flow is driven toward critical. It can never pass critical unles *just* at that point the obstruction reaches its maximum height and begins to decrease.
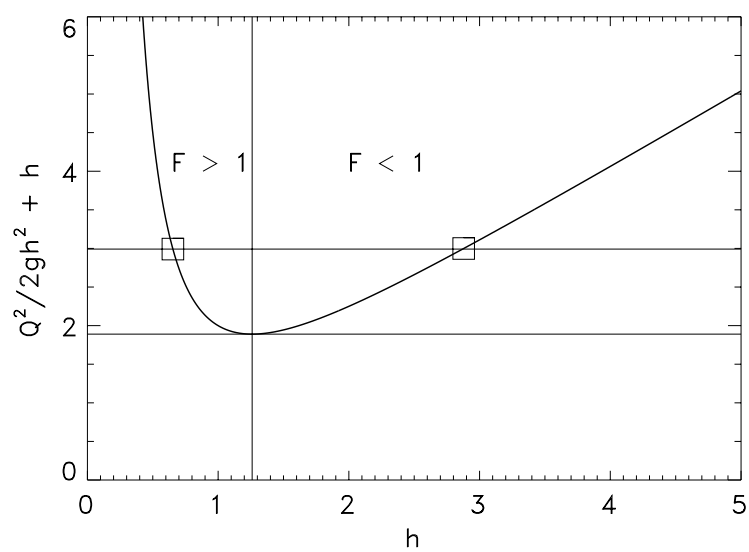
25   Rotating Flows
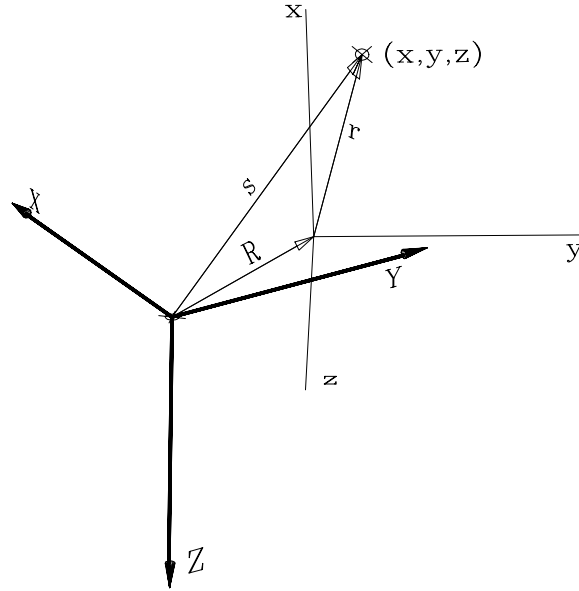
25.1   Coordinate Systems

Figure 75.

We treat two coordinate systems; an inertial system (X, Y, Z) and a non-inertial system (x, y, z), which may be accelerating or rotating relative to the inertial system. The distance between the origin of the inertial axes and the origin of the moving, rotating system is $\underline{R}$, and the distance between the origin of the inertial axes and a point in the rotating system distance $\underline{r}$ from its origin is $\underline{s}$. Thus,

$$\underline{s} \;=\; \underline{R} + \underline{r} \,, \tag{25.1}$$

and, differentiating,

$$\underline{u} \;=\; \underline{U} + \underline{u}' \,, \tag{25.2}$$

where $\underline{u} = d\underline{s}/dt$, $\underline{U} = d\underline{R}/dt$, $\underline{u}' = d\underline{r}/dt$.

Some important results are:

1. *The angular velocity ω of the rotating system is unique.* It is always possible to decompose any motion into a translation plus a rotation,

$$d\underline{s} \;=\; d\underline{R} + d\underline{\phi} \times \underline{r} \,. \tag{25.3}$$

Dividing by dt, there results

$$\boxed{\underline{u} \;=\; \underline{U} + \underline{\omega} \times \underline{r} \,.} \tag{25.4}$$

The motion consists of the velocity $\underline{U}$ of the origin (center of mass) plus the *rotational velocity $\underline{\omega} \times \underline{r}$* perpendicular to $\underline{\omega}$.

For a *second* rotating system $()'$ with origin distance $\underline{a}$ away but the same point $\underline{s}$, such that $\underline{r} = \underline{r}' + \underline{a}$,

$$\underline{u} \;=\; \underline{U} + \underline{\omega} \times (\underline{r}' + \underline{a}) \,, \tag{25.5}$$

April 23, 2001

At the same time, formally,

$$\underline{u} = \underline{U}' + \underline{\omega}' \times \underline{r}' . \tag{25.6}$$

It follows that,

$$\boxed{\underline{U}' = \underline{U} + \omega \times \underline{a}} \tag{25.7}$$

and

$$\boxed{\underline{\omega}' = \underline{\omega} .} \tag{25.8}$$

Thus, the angular velocity is unique to each rotating system (body). Furthermore, *it is always possible to find an origin which is instantaneously fixed (or at worst translating along the axis of rotation) such that the "instantaneous axis of rotation" passes through it.*

2. *For a fixed point in the rotating system, $d\underline{r}$ as seen in the inertial system is nonzero only because of rotation.* Then for any vector $\underline{A}$ changing as $d'\underline{A}/dt$ in the rotating system, the changes seen in the inertial system are

$$\frac{d\underline{A}}{dt} = \frac{d'\underline{A}}{dt} + \underline{\omega} \times \underline{A} . \tag{25.9}$$

In particular,

$$\frac{d}{d\underline{r}}t = \frac{d'\underline{r}}{dt} + \underline{\Omega} \times \underline{r} , \tag{25.10}$$

or,

$$\boxed{\underline{u} = \underline{u}\prime + \underline{\Omega} \times \underline{r} .} \tag{25.11}$$

$$\boxed{\frac{d\underline{u}}{dt} = \frac{d'\underline{u}}{dt} + \underline{\omega} \times \underline{u} .} \tag{25.12}$$

Also, for an angular velocity $\underline{\omega}$ which is itself in a system rotating with angular velocity $\underline{\Omega}$,

$$\frac{d\underline{\omega}}{dt} = \frac{d'\underline{\omega}}{dt} + \underline{\Omega} \times \underline{\omega} . \tag{25.13}$$

Substituting Eq. 25.11 into the right hand side of Eq. 25.12 and expanding gives

$$\boxed{\frac{d\underline{u}}{dt} = \frac{d'\underline{u}}{dt} + \underbrace{2\underline{\Omega} \times \underline{u}'}_{\substack{\text{Coriolis} \\ \text{acceleration}}} + \underbrace{\underline{\Omega} \times (\underline{\Omega} \times \underline{r})}_{\substack{\text{centripetal} \\ \text{acceleration}}} + \frac{d'\underline{\Omega}}{dt} \times \underline{r} .} \tag{25.14}$$

In geophysics the last term is zero.

The centripetal acceleration (centrifugal force) can be absorbed into the body force $\underline{B}$.

25.2 Momentum equation

The momentum equation was derived in an inertial system. Gradients are unchanged in a rotating system. Therefore, in a rotating system,

$$\rho \left(\frac{D\underline{u}}{Dt} + 2\underline{\Omega} \times \underline{u} \right) = -\nabla p + \nabla \cdot \tau \tag{25.15}$$

$$\rho \frac{D\underline{u}}{Dt} = -\nabla p - \rho \underbrace{2\underline{\Omega} \times \underline{u}}_{\substack{\text{Coriolis} \\ \text{force}}} + \nabla \cdot \tau \tag{25.16}$$

25.3 Vorticity equation

The vorticity equation was derived in an inertial system. Now,

$$\underbrace{\underline{\omega}}_{\substack{\text{absolute} \\ \text{vorticity}}} = \underbrace{\underline{\omega}'}_{\substack{\text{relative} \\ \text{vorticity}}} + \underbrace{2\underline{\Omega}}_{\substack{\text{planetary} \\ \text{vorticity}}} . \tag{25.17}$$

But $D\underline{\omega}/Dt = D\underline{\omega}'/Dt$, so, in the rotating system (see Eq. 2.64),

$$\rho \frac{D\underline{\omega}'/\rho}{Dt} = (\underline{\omega} \cdot \nabla)\,\underline{u} - \nabla \frac{1}{\rho} \times \nabla p + \nabla \times \left(\frac{1}{\rho} \nabla \cdot \tau \right) . \tag{25.18}$$

Differentiating the LHS and using the continuity equation yields another form of the vorticity equation,

$$\frac{D\underline{\omega}'}{Dt} = (\underline{\omega} \cdot \nabla)\,\underline{u} - \underline{\omega} \nabla \cdot \underline{u} - \nabla \frac{1}{\rho} \times \nabla p + \nabla \times \left(\frac{1}{\rho} \nabla \cdot \tau \right) . \tag{25.19}$$

25.3.1 Potential vorticity

The potential vorticity $\underline{\underline{\Pi}}$ is defined by,

$$\underline{\underline{\Pi}} = \frac{\underline{\omega}' + 2\underline{\Omega}}{\rho} \cdot \nabla \lambda , \tag{25.20}$$

where λ is a scalar which may have a source Ψ,

$$\frac{D\lambda}{Dt} = \Psi . \tag{25.21}$$

To learn about the conservation of Π, take the dot product of $\nabla \lambda$ with $1/\rho$ times the vorticity equation (Eq. 25.18), and use the last term of the identity

$$\frac{\underline{\omega}}{\rho} \cdot \frac{D\nabla \lambda}{Dt} = \left(\frac{\underline{\omega}}{\rho} \cdot \nabla \right) \frac{D\lambda}{Dt} - \left[\left(\frac{\underline{\omega}}{\rho} \cdot \nabla \right) \underline{u} \right] \cdot \nabla \lambda \tag{25.22}$$

to substitute for the dot product of $\nabla\lambda$ with the vortex-stretching term on the RHS of 25.18. (Eq. 25.22 can be proven by using Cartesian tensor notation.) The result is,

$$\frac{D\underline{\Pi}}{Dt} \;=\; \left(\frac{\underline{\omega}}{\rho}\cdot\nabla\right)\frac{D\lambda}{Dt} \;-\; \frac{\nabla\lambda}{\rho}\cdot\left(\nabla\frac{1}{\rho}\times\nabla p\right) \;+\; \frac{\nabla\lambda}{\rho}\cdot\left(\nabla\times\frac{1}{\rho}\nabla\cdot\tau\right) \tag{25.23}$$

The three terms on the RHS of Eq. 25.23 are zero, respectively, when

1. λ is conserved ($\Psi = 0$),
2. (a) the flow is barotropic, *or*
   (b) $\lambda = \mathrm{fnc}(p,\rho)$ only,
3. the fluid is inviscid.

In case 2b,

$$\nabla\lambda \;=\; \frac{\partial\lambda}{\partial p}\nabla p \;+\; \frac{\partial\lambda}{\partial\rho}\nabla\rho \,, \tag{25.24}$$

so $\nabla\lambda$ has no component parallel to the perpendicular of ∇p and $\nabla\rho$.

When 1–3 hold, the potential vorticity is a conserved quantity,

$$\boxed{\frac{D\underline{\Pi}}{Dt} \;=\; 0 \,.} \tag{25.25}$$

25.4   Small Rossby number

Small Rossby number $Ro = U/\Omega L$ implies that velocities induced by the applied forces are small compared to the rotation velocity. Thus

$$\underline{\omega}' \;\ll\; \underline{\omega} \,, \tag{25.26}$$

so $\underline{\omega} \doteq \underline{\Omega}$. The ratio of the LHS of Eq. 25.19 to the vortex stretching and tilting terms on the RHS is Ro, so for $Ro \ll 1$ and $E \ll 1$, where $E = \nu/\Omega L^2$ is the Ekman number, Eq. 25.19 becomes

$$\boxed{(2\underline{\Omega}\cdot\nabla)\underline{u} \;-\; 2\Omega\,\nabla\cdot\underline{u} \;=\; \nabla\frac{1}{\rho}\times\nabla p \,.} \tag{25.27}$$

This equation expresses a (delicate) balance between baroclinic vorticity production and vortex stretching and tilting, and provides for the maintanance of long-lived motions which otherwise would change in time Ω^{-1}. In component form Eq. 25.27 is

$$2\Omega\frac{\partial u}{\partial z} \;=\; -\frac{1}{\rho^2}\left(\frac{\partial p}{\partial z}\frac{\partial\rho}{\partial y} - \frac{\partial p}{\partial y}\frac{\partial\rho}{\partial z}\right) \tag{25.28}$$

$$2\Omega\frac{\partial v}{\partial z} \;=\; \frac{1}{\rho^2}\left(\frac{\partial p}{\partial z}\frac{\partial\rho}{\partial x} - \frac{\partial p}{\partial x}\frac{\partial\rho}{\partial z}\right) \tag{25.29}$$

$$2\Omega\left(\frac{\partial u}{\partial x} + \frac{\partial v}{\partial y}\right) \;=\; \frac{1}{\rho^2}\left(\frac{\partial p}{\partial x}\frac{\partial\rho}{\partial y} - \frac{\partial p}{\partial y}\frac{\partial\rho}{\partial x}\right) \;\doteq\; 0 \,, \tag{25.30}$$

April 23, 2001

where a coordinate system with $\underline{\Omega}$ aligned with the z-axis has been used. Eqs. 25.28–25.29 describe the *thermal wind.* The RHS of Eq. 25.30 is small because of the thin-layer approximation.

For low Rossby and Ekman numbers, the momentum equation (Eq. 25.16 including the body force term) is

$$\rho\, 2\underline{\Omega} \times \underline{u} \;=\; -\nabla p + \rho \underline{B} \tag{25.31}$$

25.5   Taylor-Proudman Theorem

For constant-density flow ($\nabla \cdot \underline{u} = 0$) Eq. 25.30 gives that

$$\frac{\partial w}{\partial z} \;=\; 0\,. \tag{25.32}$$

Thus if the flow is bounded by a solid bottom, where $w = 0$, then $w = 0$ everywhere and the flow is two-dimensional. The result of towing a body (sphere) horizontally through the rotating fluid is a Taylor column which moves along with the sphere, deflecting the fluid as though the body were a cylinder.

25.6   Geostrophic Motion

This treatment is slightly different than that carried out in class.

To get the geostrophic equations we subtract out the hydrostatic balance and make the thin layer approximation. In the coordinate system (r, θ, ϕ), that is, (altitude, latitude, longitude), with velocities
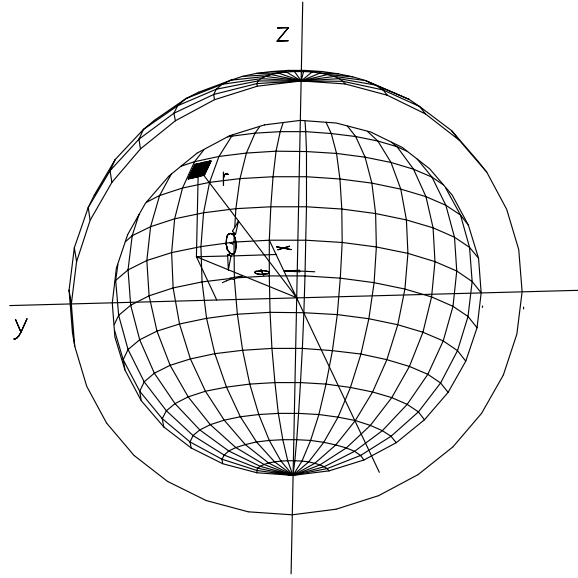

Figure 76.

(w, v, u) (vertical, north-south, east-west), respectively, Eq. 25.31 written out in component form is

$$\rho\left(-2\Omega\, v \sin\theta + 2\Omega w \cos\theta\right) \;=\; -\frac{1}{r\cos\theta}\frac{\partial p}{\partial \phi} \tag{25.33}$$

$$\rho\, 2\Omega\, u \sin\theta \;=\; -\frac{1}{r}\frac{\partial p}{\partial \theta} \tag{25.34}$$

$$-\rho\, 2\Omega\, u \cos\theta \;=\; -\frac{\partial p}{\partial r} - \rho g\,. \tag{25.35}$$

April 23, 2001

With

$$p = p_s(r) + p'(r, \theta, \phi) \tag{25.36}$$

$$\rho = \rho_s(r) + \rho'(r, \theta, \phi) , \tag{25.37}$$

where $()_s$ refers to the static (no motion) case, such that

$$-\frac{\partial p_s}{\partial r} = \rho_s g , \tag{25.38}$$

the equations become

$$(\rho_s + \rho')\left(-2\Omega\, v \sin\theta + 2\Omega w \cos\theta\right) = -\frac{1}{r\cos\theta}\frac{\partial p'}{\partial \phi} \tag{25.39}$$

$$(\rho_s + \rho')\, 2\Omega\, u \sin\theta = -\frac{1}{r}\frac{\partial p'}{\partial \theta} \tag{25.40}$$

$$-(\rho_s + \rho')\, 2\Omega\, u \cos\theta = -\frac{\partial p'}{\partial r} - \rho' g . \tag{25.41}$$

we have in the thin layer approximation, $D/L \ll 1$,

$$w \sim U\frac{D}{l} \tag{25.42}$$

$$p' \sim \rho 2\Omega U L \tag{25.43}$$

$$\frac{\partial p'}{\partial r} \sim \rho 2\Omega U \frac{L}{D} \tag{25.44}$$

$$\rho' \sim \frac{p'}{gD} \sim \frac{\rho 2\Omega U L}{gD} \tag{25.45}$$

$$\frac{\rho'}{\rho} \sim Ro\,\frac{4\Omega^2 L^2}{gD} , \tag{25.46}$$

so Eqs. 25.39–25.41 become,

$$fv = \frac{1}{\rho_s r_0 \cos\theta}\frac{\partial p}{\partial \phi} \tag{25.47}$$

$$fu = -\frac{1}{\rho_s r_0}\frac{\partial p}{\partial \theta} \tag{25.48}$$

$$\rho g = -\frac{\partial p}{\partial z} , \tag{25.49}$$

or,

$$\boxed{\underline{u_H} = \frac{1}{f\rho_s}\underline{k} \times \nabla p ,} \tag{25.50}$$

where $f = 2\Omega \sin\theta$ and $z = r - r_0$. The primes have been dropped from the first two equations because $p_s = p_s(r)$.

In another form,

$$fv = \frac{1}{r_0 \cos\theta}\, g\left(\frac{\partial z}{\partial \phi}\right)_{\theta,p} \tag{25.51}$$

$$fu = -\frac{1}{r_0}\, g\left(\frac{\partial z}{\partial \theta}\right)_{\phi,p} , \tag{25.52}$$

April 23, 2001

or,

$$\underline{u_H} = \frac{g\underline{k}}{f} \times (\nabla z)_p \,, \tag{25.53}$$

Differentiating Eqs. 25.47–25.48, gives the equations for the thermal wind in this coordinate system and approximation,

$$\frac{\partial v}{\partial z} = -\frac{g}{f\rho\,r_0\cos\theta}\left(\frac{\partial\rho}{\partial\phi}\right)_p \tag{25.54}$$

$$\frac{\partial u}{\partial z} = \frac{g}{f\rho\,r_0}\left(\frac{\partial\rho}{\partial\theta}\right)_p \,, \tag{25.55}$$

or

$$\frac{\partial\underline{u_H}}{\partial z} = \frac{g\underline{k}}{\rho f} \times (\nabla\rho)_p \,, \tag{25.56}$$

26   References

Batchelor, G. K.,   1973   *An Introduction to Fluid Dynamics*, Cambridge University Press.

Coles, D.   1954   The problem of the turbulent boundary layer. *J. App. Math. Phys. (ZAMP)* **5**, 181-203.

Lagerstrom, P.A.,   1964   *Laminar Flow Theory*, Princeton University Press.

Lamb, H.,   1945   *Hydrodynamics*, Dover.

Landau, L. D., Lifshitz, E. M.,   1959   *Fluid Mechanics*, Addison-Wesley.

Liepmann, H. W., Roshko, A.,   1957   *Elements of Gasdynamics*, Wiley.

Millikan, C. B.,   1938   A critical discussion turbulent flows in channels and circular tubes. *Proc. 5th Int. Cong. App. Mech.*, 386-392.

Morton, B. R.   1967   Entrainment models for laminar jets, plumes and wakes. *Phys. Fluids* **10**, 2120-2127.

Morton, B. R., Taylor, G. & Turner, J. S.   1956   Turbulent Gravitational Convection from Maintained and Instantaneous Sources. *Proc. Roy. Soc. A* **234**, 1.

Schlichting, H.,   1955   *Boundary Layer Theory*, McGraw-Hill.

Spiegel, Veronis,   1960   *Astrophys. J.* **131**, 442-447.

Thompson, P.A.,   1972   *Compressible Fluid Dynamics*, McGraw-Hill.

Van Dyke, M.   1982   *An Album of Fluid Motion*, Parabolic Press.

Zagarola, M. V., Perry, A. E. & Smits, A. J.   1997   Log laws or power laws: The scaling in the overlap region. *Phys. Fluids* **9**, 2094-2100.

April 23, 2001